ELUCIDATION AND OPTIMIZATION OF MOLECULAR FACTORS FOR DENDRITIC CELL RESPONSES TO SURFACE PRESENTED GLYCANS

A Dissertation

Presented to

The Academic Faculty

by

Nathan Alexander Hotaling

In Partial Fulfillment

of the Requirements for the Degree

Doctor of Philosophy in Bioengineering

From the Department of Biomedical Engineering

Georgia Institute of Technology

AUGUST 2013

ELUCIDATION AND OPTIMIZATION OF MOLECULAR FACTORS FOR DENDRITIC CELL RESPONSES TO SURFACE PRESENTED GLYCANS

Approved by:

Dr. Julia E. Babensee, Advisor
School of Biomedical Engineering
Georgia Institute of Technology

Dr. Andres J. Garcia
School of Mechanical Engineering
Georgia Institute of Technology

Dr. Richard D. Cummings
Department of Biochemistry
Emory University

Dr. Daniel M. Ratner
Department of Bioengineering
University of Washington

Dr. Thomas Barker
School of Biomedical Engineering
Georgia Institute of Technology

Dr. John S. Kauh, MD
Department of Hematology and Medical Oncology
Emory University

Date Approved: May 20th, 2013

To my friends and family; whose belief and support made all of this possible.

ACKNOWLEDGEMENTS

I would like to acknowledge my Mother and Father, Helene and Gene Hotaling, for their constant love, support, and encouragement over the years and the role it has played in shaping who I am today. I have always known that whatever decisions I make my parents cared most for my happiness and so as long as I followed my passion they would support me. I have always been able to rely on their love which has formed the foundation from which I have been able to stand and overcome all the trials in my life. Their love of educating has instilled in me a deep respect for education which led me to attain its highest degree. Additionally, both of my parents inspired me to choose a career path that I loved and was passionate about via leading by example. Both of my parents have chosen careers not based on money or convenience but by what they loved, respected, and enjoyed. This example has been invaluable to me as I have looked at what I would like to do with my life. Nothing that I have accomplished could have been done without them and I am grateful for everything they have done for me.

I would also like to acknowledge the influence, support, and inspiration that I have received from the rest of my family including my grandparents, sisters, and nieces and nephews. My grandfather, Alan Hotaling, came from a line of machinists and was the first in our family to become a mechanical engineer. Throughout my childhood his stories about what he did, where he traveled and how he did the things he'd done inspired me to become an engineer. His and my grandmother's, Louise Hotaling, love and support over the years helped prepare me for my future and made me into the man I am today. My sisters, Lauren Ortiz and Thea Hotaling, deserve acknowledgement for never letting me take myself too seriously and for always keeping me humble. Their light-

hearted harassment helped me stay rooted in what matters and the unquestionable love of their little brother has served as a model for all of my friendships. Also, I would like to acknowledge my nephew and niece Ashton and Coralei Deriso for reminding me of the importance of wonder and seeing the world through new eyes.

I would like to thank and acknowledge Doctor Julia Babensee for her continued support, mentorship and advice. I would have never of been as successful or as sure of myself, and where I want to go in my life, if it was not for her consistent and exemplary example. My project took many turns and she stayed with me every step of the way and continued to offer me support and encouragement even when I had given up myself. I had many side projects during my PhD and took many detours along the road to its completion and Julie's patience with me was almost limitless. Her allowing me to find my own way and explore every avenue I wanted was unprecedented and I am so grateful to of had her as my advisor. I would also like to acknowledge my committee members, Drs Daniel Ratner, Andres Garcia, Richard Cummings, Thomas Barker, and John Kauh for their mentorship, advice, and help over the years. My project sprang from a fortitous donation of reagents by Dr. Ratner and thus my PhD project would literally of never of happened if it wasn't for him. I would like to acknowledge Drs Garcia and Cummings for their ability to always get me to think more deeply about not just my project but my life and where it was headed and for giving what seemed to be just the right advice at just the right time consistently throughout my PhD. Finally, I'd like to acknowledge Drs Barker and Kauh for their ability to make me see the bigger picture of my project and helping me to see beyond the scope of my project.

I believe that no one can accomplish anything of significance without being taught by teachers of significance. To that end five teachers have been instrumental in how I view the world, the choices I have made, and the fields I have chosen. First, was an elementary school teacher, Ms. Atkinson, who was the first teacher to make me believe that I could accomplish anything I wanted with my life. Her unabashed belief in me led me to believe in myself and set me on the path to where I am today. Next, came my middle school gifted teacher, Ms. Ann Rushing. Her love of education, acceptance of different learning styles, and unconventional curriculum helped me to not only realize that learning can be fun but that I didn't need to be embarrassed of my intelligence. Additionally, I would like to acknowledge two of my high school teachers Ms. Gwynn Pealer and Mr. Frank Evans. Their love of education and science inspired me to get a minor in chemistry as an undergraduate and pursue a biomedical engineering doctorate degree. Without their passion for STEM, inspiring lectures, and excitement for education I would never have chosen to get the degrees in the fields that I have today. I cannot express the depth of impact they have had on the underlying career path I have taken in my life and how grateful I am for their passion in education. Finally, I would like to acknowledge Dr. Yongho Sohn from the University of Central Florida for seeing potential in me that others missed and giving me the opportunity to do research in his lab. He inspired me to go to graduate school and his guidance and mentorship are a model for how I would like to mentor students one day. His support is in large part the reason why I was able to get into graduate school and I cannot thank him enough for all of the opportunities that he provided me during my undergraduate carrier.

A large part of my time at Georgia Tech has been devoted to TAing and teaching engineering design courses. I have loved that experience and have even gotten a publication from the experience. I would like to acknowledge Dr. Alexander Leonessa who was my mentor when I took capstone design and inspired me to love engineering design. Additionally, I would like to acknowledge Franklin Bost, James Rains, Mark McJunkin, Marty Jacobson, Dr. Barbara Fasse, and Dr. Wendy Newstetter from the design and education departments at Tech for their help, support, and expertise over my entire time at Georgia Tech. Finally, I would like to acknowledge Dr. Craig Forest for his friendship, advice, and assistance in design and publications.

I would like to acknowledge my best and oldest friends: Colby Nealis, John Ketcham, Gary Licquia, Andy Oswald, Jane Smith, and Chrissy Garton. This group of people has been friends with me for well over half of my life and has accepted me for who I am every step along the way. Each deserves a paragraph and there are too many things that I love them for to be specific and maintain a reasonable page count for the acknowledgements. Each of these individuals has profoundly impacted my life and I would not be who I am today without them. Their unwavering friendship has been a large source of strength, comfort, and love over the years and there is no way I could have made it to this point without their love and faith in me. Too often their belief in me was what kept me going when I didn't think I could complete the next step of my life. Their respect and acceptance of my eccentricities is limitless and I cannot fathom how they have put up with me for all of these years. I cannot imagine my life without them and I look forward to many years of memories to come.

I have heard that the greatest friends you will make in your life are found when you are in college. While I cannot compare the magnitude of their friendship to those friends mentioned above I would like to acknowledge Kyle Hallenbeck, Daniel Simone, Nancy Beady, Keith Bartholomew, Susan Bartholomew, George Hatzistavridis, Jake Schellack, Julian Sanchez, Benjamin Overstreet, and Dani Cleveland for being some of the greatest friends imaginable. Kyle Hallenbeck for being one of the few people on the planet that I can talk with equal ease about non-linear flow and why pot stickers are called pot stickers when they don't actually stick to pots, or are even cooked in pots. Daniel Simone for always being the friend I wish I could be. Nancy Beady for always providing a girls perspective while not judging me for being brutally honest and natural around her. Keith Bartholomew who taught me how to win any argument and to never approach a problem via its most obvious solution. Susan Bartholomew who cares for me and all of her friends more than she cares for herself and is the most giving person I have ever met. George Hatzistavridis for all the soccer, car talk, mechanical discussion, deep conversations on friends and life, and general understanding and acceptance of me and all of our friends. Jake Schellack who I could always count on to be a slacker with me but to have it together in every way that matters. Julian Sanchez for always calling me out when I needed it and for never being offended at jokes at his expense. Benjamin Overstreet for showing me that nice guys don't finish last. And Dani Cleveland for breaking my table, general insanity, and most importantly for being happy and free with me when everyone else just couldn't understand.

Graduate school occurred over the majority of my 20s and the friends I have made there are undoubtedly ones that I will have for the rest of my life. I would like to

acknowledge Jonathan Vernon, Lindsey Goodman, Rolando Gittens, Kimberly Portmess, Seth Gazes, Reggie Paxton, Sarah Marske, James Wade, Reyhaan Chaudhri, Douglas White, and Catherine Rivet for all that they have done with/for me during my time at Georgia Tech. Jonathan Vernon for being a kindred spirit in engineering, life, recreation, and they gym. Lindsey Goodman for accepting my friendship even when it wasn't easy and I didn't deserve it. Rolando Gittens for understanding what being on time actually means and for being one of the few people who I can actually completely relax around. Kimberly Portmess and the Portmess family for being some of the most incredible people I've ever met. Seth Gazes who taught me how to have a better work/life balance by example and whose sage advice has often been insightful and helpful. Reggie Paxton for her limitless patience with Seth and I and whose book taste is impeccable. Sarah Marske for loving and accepting me for who I am. James Wade who I met later in graduate school but whom I have deep respect for both academically and athletically. Reyhaan Chaudhri who completed the MSCR program with me and has been a great friend since. Douglas White for all the time in the gym and all the fantastic memories outside of Tech. And finally, I would like to acknowledge Catherine Rivet who has patiently dealt with me and my thesis for my final time at Tech; her understanding, forgiveness, and support have meant more to me than I ever expressed and I owe her my sanity for these last months.

This dissertation could not have occurred without the combined work of many other graduate and undergraduate students. To that end I would like to acknowledge Peng Meng Kou, Todd Rogers, Lori Norton, Jae Hyung Park, Matthew Ho, Andrew Acevado, Jamie Heimburg-Molinaro, Xuezheng Song, Nina Prasanphanich, Anthony

Luyai, and Connie Arthur for their help and support during my project. Peng Meng Kou for developing the assay my entire dissertation is based on; Todd Rogers for showing me the ropes in the Babensee lab; Lori Norton for her passion for science and indefatigable positive attitude; and Jae Hyung Park for taking the time to train me when he was so close to graduating. I would like to acknowledge and thank all of the undergraduates who worked for me but most specifically Andrew Acevado and Matt Ho for their diligent work and dedication to my project. Finally, I worked extensively with Dr. Cummings' lab and received extensive advice, knowledge, and time from Jamie Heimburg-Molinaro, Xuezheng Song, Nina Prasanphanich, Anthony Luyai, and Connie Arthur. I'd like to thank Dr. Xuezheng Song for his patience in teaching me glycoconjugation chemistry, purification, and characterization; Jamie Heimburg-Molinaro for making me feel accepted and helping integrate me into the Cummings' lab, Anothony Luyai for his help in trouble shooting my project and coming up with interesting future directions; Nina Prasanphanich for her friendship and experimental help; and Connie Arthur for her help with the glycobiology side of my project.

Last but not least I would like to acknowledge all of the people who donated blood to my project and the phlebotomists who collected blood for me. I have collected over two gallons of blood from over 40 different donors over the past 6 years. Each has made my project possible and I appreciate their donations. Additionally, I'd like to acknowledge the entire administrative staff of Georgia Tech, both financial and not, who has had to deal with my various grants, programs, incorrectly filled out, or late submissions over my time at Tech. Specifically, Susan Bowman, Chris Ruffin, Colly Mitchell, Meg McDevitt, Penelope Pollard, Tracie Dinkins, Sally Gerrish, Shannon

Sullivan, Floyd Wood II, Alyceson Andrews were all critical people to my success at Georgia Tech and I give them my thanks for all that they have done for me over the past year.

In conclusion I would like to acknowledge my funding sources, the NIH Cell and Tissue Training Grant, the MSCR translational research master's program from Emory University, the Johnson & Johnson GT Healthcare Innovation Award, and the Wallace H. Coulter GT/Emory-PKU BME Collaborative Research Seed Grant.

TABLE OF CONTENTS

LIST OF TABLES

LIST OF FIGURES

LIST OF SYMBOLS AND ABBREVIATIONS

Abbreviation	Description
28AHAC	28vol% ammonium hydroxide solution saturated with ammonium carbonate
Ab	Antibody
AEAB	2-Amino-N-(2-amino-ethyl)-benzamide – Fluorescent glycan linker
AF647	Alexa Fluor 647 – Fluorophore with Excitation/Emission 650/668
Alpha	Variable representing terminal α1-2 terminal linked mannose structures
ANOVA	Analysis of Variance
AP-1	Activator Protein 1
APC	Antigen Presenting Cell
Asn	Asparagine
BCA	Bicinchoninic acid assay used from quantifying protein content
BDCA-2	Blood dendritic cell antigen 2: a lectin on DCs
Branch	Variable representing terminal α1-3Man, α1-6Man branched trimannose structures
BSA	Bovine Serum Albumin
cBSA	Bovine Serum Albumin cationized with an excess of EDA
CD86	Cluster Designation 86, a pro-inflammatory costimulatory molecular expressed on DCs.
CDS	Cell Disassociation Solution
CHO	Chinese Hamster Ovary
CLEC	C-type lectin-like receptor
CLR	C-Type Lectin Receptor
ConA	Concanavalin A: A plant lectin
CR3	Compliment Receptor 3
cSA	Streptavidin cationized with an excess of EDA
CTL	Cytotoxic T Lymphocyte
DAMP	Danger Associated Molecular Patterns
DAP12	Adapter protein used in Siglec signaling
DC	Dendritic Cell
DCAL-1	Dendritic Cell Associated Lectin-1: Lectin expressed on DC cell membrane
DCIR	Dendritic cell immunoreceptor: Lectin expressed on DC cell membrane
DC-SIGN	Dendritic Cell-Specific Intercellular adhesion molecule-3-Grabbing Non-integrin: Lectin expressed on DC cell membrane
Density_cat	Variable Representing the categorical density variable where glycoconjugates were grouped into four levels of density0
DHC	Diammonium hydrogen citrate

DMSO	Dimethylsufoxide
DNA	Deoxyribonucleic Aced
DNGR-1	DC, NK lectin group receptor-1: Lectin expressed on DC cell membrane
Dol-P	Starting residue for building block of N-linked glycans
Dol-P-P-GlcNAc	GlcNAc intermediary used as building block for N-glycan formation
D-PBS	Dulbecco's Phosphate buffered saline
DST	Disuccinimidyl tartrate
ECM	Extracellular matrix
EDA	Ethylenediamine
EDC	1-Ethyl-3-(3-dimethylaminopropyl) carbodiimide: active linker for covalent linkage to amines.
EDTA	Disodium Ethylenediaminetetraacetic acid
ELLA	Enzyme Linked Lectin Assay
ER	Endoplasmic Reticulum
ERK	Extracellular signal-regulated kinases
FcRγ	An immunoreceptor tyrosine-based activation motif
FDA	Food and Drug Administration
FITC	Fluorescein isothiocyanate a green fluorophore
Fuc	Fucose
Gal	Galactose
GalNAc	N-acetylgalactoseamine
GFP	Green Fluorescent Protein
Glc	Glucose
GlcNAc	N-Aceytlglucosamine
GM-CSF	N-Aceytlgalactosamine
gMFI	Geometric Mean Fluorescent Intensities
H-BSA	Highly cationized BSA with no ligand attached to its maleimide groups.
H-BSA-Glc100	Highly cationized BSA with Glc-OEG2-SH attached to its maleimide groups, reacted at a 100:1 ratio of glycan to BSA.
HBSA-Man100	Highly cationized BSA with Man-OEG2-SH attached to its maleimide groups, reacted at a 100:1 ratio of glycan to BSA.
H-BSA-OEG100	Highly cationized BSA with OEG3-SH attached to its maleimide groups, reacted at a 100:1 ratio of glycan to BSA.
HEMA	Hydroxyethylmethacrylate
HIV	Human immunodeficiency Virus
HMGB1	High mobility group 1
HPLC	High Pressure Liquid Chromatography
HRP	Horse Radish Peroxidase
HSA	Human Serum Albumin

HTP	High Throughput
iDC	Untreated primary human dendritic cells
IFN	Interferon
IgG	Immunoglobulin G
IKK	IκB kinase
IL-#	Interleukin- any number. Cytokines that have diverse effects on DC phenotype and that are secreted by DCs
ILT-3	Immunoglobulin Like Transcript-3, surface marker associated with tolerogenic DC phenotype
IMF	Inflammatory Maturation Factor, CD86/DCSIGN
IRF3	Interferon regulatory transcription factor 3
ITAM	Immunoreceptor tyrosine-based activation motif
ITIM	Immunoreceptor tyrosine-based inhibition motif
IUPAC	International Union of Pure and Applied Chemistry
JAK	Janus Kinase: Tyrosine kinase based enzyme for phosphorylation of proteins
L-BSA	BSA cationized with 0.05M EDA with no ligand attached to its maleimide groups
LNT	Lacto-N-tetrose
LPS	Lipopolysaccharide
LSECtin	A type II transmembrane lectin that is related to CD23 and DC-SIGN
MALDI	Matrix Assisted Laser Desorption-Ionization
Man	Mannose
MAPK	Mitogen-activated protein kinases
M-BSA	BSA cationized with 0.15M EDA with no ligand attached to its maleimide groups
MCL	Macrophage C-type lectin
mDC	Primary human DCs treated with 1 ug/ml of LPS for 24hrs
MDL-1	Myeloid DAP12-associating lectin
MGL	Macrophage galactose lectin
MHC	Major Histocompatability Complex
MICL	Myeloid C-type lectin-like receptor
MLR	Mixed Lymphocyte Reaction
MMPs	Matrix Metalloproteases
MMR	Macrophage Mannose Receptor
mod-SLA	Acid-etched hydrophilicly modified titanium
MOI	Multiplicity of Infection
mol	Molecules of a given ligand
MS	Mass spectrometry
MUC	Mucin
MyD88	Myeloid differentiation primary response 88
NC-BSA	Natively Charged BSA

ND	Not Determined
NeuAc	Neuraminic Acid
NF-kB	Nuclear Factor- kB
NHS	N-hydroxysuccinimide
N-linked	Nitrogen Linked
NPA	Narcissus pseudonarcissus: A plant lectin
nm	Nanometer
OEG	Oligoethyleneglycol
O-linked	Oxygen linked
OVA	Ovalbumin
PAMP	Pathogen Associated Molecular Patterns
PBMC	Peripheral Blood Mononuclear Cell
PBS	Phosphate buffered saline
PCA	Principle component analysis
PE	Polyethylene
PEG	Polyethyleneglycol
pHEMA	Poly(2-hydroxyethyl methacrylate)
pI	Isoelectric Point
pIBTMA	Poly(Isobutyl-triethylene glycol methyl ether methacrylate)
PLGA	Poly Lactic-co-Glycolic Acid
PLL	Poly-L-lysine
PNGase F	Peptide -N-Glycosidase F
ppGalNAcT	Glycosyltransferase critical to O-glycosylation
PRR	Pattern Recognition Receptor
PT	Pure titanium
RAF1	Gene provides instructions for making a protein that is part of a signaling pathway called the RAS/MAPK pathway
RCF	Relative centrifugal force
RGD	Arginylglycylaspartic acid is a tripeptide composed of L-arginine, glycine, and L-aspartic acid.
rhDC-SIGN-Fc	Recombinant human DC-SIGN chimera with an Fc portion of an antibody.
rhDectin-1	Recombinant human Dectin-1
RNA	Ribonucleic Acid
RNase B	Ribonuclease B
ROS	Reactive Oxygen Species
RPM	Rotations per minute
SA	Streptavidin
SAMP	Self-associated molecular pattern
SDS	Sodium dodecyl sulfate
SDS-PAGE	Dodium dodecyl sulfate polyacrylamide gel electrophoresis

SEC	Size Exclusion Chromatography
Ser	Serine
SHP	A Cytoplasmic protein tyrosine phosphatases
siRNA	Small interfering RNA
SLA	Acid-etch of titanium surface
STAT	Signal Transducer and Activator of Transcription
TCPS	Tissue Culture Polystyrene
TCR	T-Cell Receptor
tDC	Primary human DCs treated with IL10 and IFNα at 3500 units/ml and 35000 units/ml respectively
TFP ester	Tetrafluoro phenol ester
TGF-β	Tumor Growith Factor
Th_1	CD4+ T helper cells that stimulate other T cells
Th17	T cells that mediate tumor grown and autoimmunity
Th_2	CD4+ T helper cells that stimulate B cell proliferation
Thr	Threonine
TLR	Toll-Like Receptor
TMB	3,3',5,5'-tetramethylbenzidineperoxide substrate for HRP
TMF	Tolerogenic Maturation Factor, ILT3/CD86
TNF-α	Tumor Necrosis Factor α
TRAF	TNF receptor associated factors
T_{reg}	T Regulatory Cell
TRIF	TNF receptor inhibitory factors
Tris	Trisaminomethane
TWEEN20	Polysorbate 20, surfactant
U	Units
UDP	Uridine diphosphate
UV	Ultraviolet
µm	Micrometer

SUMMARY

The implications for glycan and glycoprotein presentation from a biomaterial surface in mediating immune cell interactions and responses are incompletely understood. The goal of this dissertation was to obtain critically needed data in glycomics relevant to the next generation of biomaterials and combination products. To do this required a deeper understanding of how human immune cells interact with glycans and glycoproteins presented from material surfaces. Dendritic cells (DCs) are the most potent antigen presenting cells (APCs) and provide a bridge between the innate, non-specific, immune response toward external signals such as foreign pathogens and the adaptive immune response directed toward specific antigens. C-type lectin receptors (CLRs) are a class of pattern recognition receptors (PRRs) found on DCs and their recognition of glycans have been shown to have immunomodulatory (both tolerogenic and pro-inflammatory) effects.[1–3] CLRs have been shown to be key regulators of pathogen-induced innate immunity, antigen processing for adaptive immune responses, immune system evasion by pathogens and tumors, and in recognition of self-proteins.[3–7] Given that DCs use CLRs to recognize characteristic pathogen and tumor glycan structures, and that this recognition leads to functional immunomodulatory effects, we hypothesized that DCs use these CLRs to recognize and respond to biomaterials, through glycan structures in the adsorbed protein layer (or inherent in the biomaterial structure) to direct immune responses. Thus, with an understanding of this interaction, immunomodulatory combination products could be designed to direct the DC response toward a pro-inflammatory vaccine delivery system or induction of tolerogenic phenotype for tissue engineered constructs.

The **primary objectives** of this dissertation were to (1) analyze and optimize molecular factors of importance in recognition of surface presented glycans for recognition and promotion of both pro- and anti-inflammatory DC phenotypes and (2) to

elucidate the effect of presentation modality (i.e. soluble, phagocytosable, and non-phagocytosable delivery of glycans) on DC phenotype. The **overall hypothesis** was that distinct molecular presentations of glycans/glycoproteins to DCs are able to controllably modulate their phenotype with functional immunological consequences. **Specific Aim 1** was to develop a carrier for glycans that was able to show a differential DC phenotype across similar glycan structures and that had optimal molecular characteristics i.e. charge and ligand valency, for maximal modulation of DC phenotype from a non-phagocytosable display. **Specific Aim 2** was to identify how glycan presentation modality alters DC phenotype and how these display strategies can be harnessed to drive DCs toward a desired phenotype. Throughout both of these aims multivariate linear regression was used to quantify claims made and to provide predictive results that could possibly be applied to systems other than those developed herein. .

To accomplish Aim 1 a suitable carrier for glycans that could modulate DC phenotype when displaying glycans from a non-phagocytosable surface had to be identified. To do this, five different carriers were assessed for their efficacy. Cationized bovine serum albumin (BSA) modified with polymannose structures and adsorbed to a tissue culture polystyrene (TCPS) well was found to modulate DC phenotype to the greatest extent. Thus, further optimization of cationized BSA, was performed to help optimize the DC response to surface adsorbed glycans.

The charge and number of glycans covalently bound to BSA was varied and the subsequent DC phenotype to these adsorbed conjugates was determined. It was found that highly cationized (pI above 9.75) BSA with an average of more than 20 carbohydrates per protein modulated DC phenotype to the greatest extent in response to the presented glycan. Furthermore, this presentation context was shown to be able to modulate DC phenotype across multiple glycan structures indicating its use as a platform for surface presentation of glycans to DCs. The results from these studies were then modeled and it was found that the most important factors for a pro-inflammatory DC

response were having a high density (>20 glycans/BSA) and then to a lesser extent having a pI above 9.75. No significant trends were found for the tolerogenic reporter from DCs when doing this modeling, however, an inverse trend in density and charge was shown for the tolerogenic reporter than for that of the pro-inflammatory response.

The interaction of the DCs with the carbohydrates was confirmed to be via receptors that utilize calcium or manganese, thus implicating CLRs in their use, by treating DCs with EDTA and looking at internalization of beads by DCs and subsequent DC phenotype in response to these adsorbed conjugates in the presence of EDTA. Finally, the modulation of DC phenotype was found to also be carbohydrate structure-dependent, even when comparing similar structures, and thus the conjugates were further validated as a platform for use in presenting carbohydrates from a non-phagocytosable surface to DCs. The results from the comparison between sugar structures were then analyzed in a model and it was found that distinct terminal structures of glycans were able to be predicative of DC phenotype.

The optimization studies from Aim I discovered that single mannose presented in a high density (>20 sugars per BSA) from highly cationized BSA (isoelectric point>9.75) was able to modulate DC phenotype to an equal extent as other more complex glycan structures. Thus, for the determination of presentation modalities' effect on DC phenotype only the monosaccharides mannose and glucose were used. Glucose was chosen as a control for mannose because of its structural similarity to mannose and because, in its monosaccharide form, no known CLR on DCs binds to glucose. The high density and cationic glycoconjugates were then adsorbed to the wells of 384 well plates, delivered in a range of soluble concentrations, or adsorbed to 1 μm and 50 μm of polystyrene beads and delivered to DCs to examine modality of display effects. The subsequent DC phenotype was then assessed. However, prior to assessment of DC phenotype an indicator of which receptors DCs were using to respond to these conjugates was desired. Thus, enzyme linked lectin assays were performed with recombinant human

lectins, Dectin-1 and DC-SIGN, on the adsorbed conjugates. It was found that DC-SIGN bound the mannose conjugates with high affinity and that the glucose conjugates were not bound by Dectin-1 to a greater extent than that of the negative control.

Mannose glycoconjugates adsorbed to a non-phagocytosable surface modulated DC phenotype to the greatest extent. Interestingly, glycoconjugates delivered in a soluble form to DCs did not alter DC phenotype to a statistically significant level over untreated cells, even at high (100 μg/ml) concentrations, and conjugates adsorbed to phagocytosable polystyrene beads produced an effect that is in between those two extremes. The results from these studies were then run in a multivariate general linear model and it was found that the presentation modalities were statistically different from each other, even when controlling for ligand and donor variances. Also, using an interaction model between modalities and ligands it was found that adsorbed and soluble mannose conjugates were statistically different from each other, indicating a receptor specific response from the cells toward these conjugates. Thus, antibody blocking and EDTA treatment of DCs was performed and phagocytosis of coated microbeads in the presence of these inhibitors was assessed via flow cytometry. It was found that for the mannose conjugates anti-DC-SIGN and anti-Dectin-1 both statistically decreased phagocytosis of the beads by DCs. Additionally, EDTA also statistically decreased the amount of internalization of beads by DCs. This provided further evidence for CLR mediated response to the adsorbed conjugates. Finally, an indication of what the fate of the adsorbed conjugates was upon interaction with the DCs was desired. Thus, conjugates were fluorescently modified and adsorbed to wells, DCs were then incubated with the adsorbed fluorescent conjugates for 24 hours and the subsequent DC fluorescence was measured. It was found that DCs were removing glycans from the surface of the wells and that this removal was increased for the mannose conjugates. Again, indicating a specific receptor mediated response to the adsorbed mannose conjugates.

In summary, this report identifies molecular factors of importance for non-phagocytosable display of glycans to DCs. It uses modeling to statistically prove these associations and provides indications for future researchers in the design of glycan microarrays. Furthermore, this study statistically shows that glycan presentation to DCs is dependent upon the modality of the display and that this differential response is at least in part due to CLRs and more specifically DC-SIGN and Dectin-1.

However, this research has led to additional new questions that require study. Why is the response to the cationized adsorbed conjugates by DCs so much higher than that of the non-cationized conjugates? What signaling and specific receptors are mediating this response? How do the cells treated with these adsorbed conjugates affect the systemic immune system, i.e. Th_1, Th_2, T_{reg} proliferation, cytokine production, MHC presentation of co-delivered antigen, etc.? Is an analogous response to other disparate glycan structures not tested herein similar to those found here? Are models used here able to be used with other classes of glycan or CLRs? What other molecular factors are of importance for phenotypic modulation of DCs by adsorbed conjugates that were not tested or varied herein, i.e. ligand length and lability? What molecular signaling mechanism is involved in the differential response to different display modalities? What is the mechanism of recognition and activation of DCs to adsorbed high density glucose presented from highly cationic BSA conjugates which should not be recognized by a specific CLR? Finally, the results showed that adsorbed conjugates were being internalized by DCs. Whether this internalization is necessary for DC activation and to what extent the internalization of conjugates plays in the phenotype modulation of DCs is an important and unanswered question. All of these are future directions for the work proposed herein and could each provide valuable insight for the understanding of DC interaction with glycans and more importantly how to harness that interaction to exploit DCs immunomodulatory ability.

CHAPTER 1 INTRODUCTION

Dendritic cells are seen as the link between innate and adaptive immunity. They have an array of pattern recognition receptors that can see and respond to pathogen, danger, and self-associated molecular patterns.[8] One class of these receptors, known as CLRs, can bind to and recognize glycan structures. These receptors have only recently begun to be studied on DCs and thus many of their signaling mechanisms, ligand specificities, and downstream ligation effects are not known. These receptors have not been as intensively studied as other receptor classes in large part due to the limited supply of glycan structures that are able to be obtained via natural or synthetic means. Glycosylation of proteins is not template driven like DNA and protein synthesis and thus obtaining large amounts of homogenous glycan structures from cells or bacteria is not challenging. Additionally, using carbohydrate chemistries currently available to create large arrays of diverse structures is not economically feasible. Thus, glycan microarrays have been created to determine ligands for recombinantly expressed CLRs. Many different approaches for these arrays have been created but all are generally non-phagocytosable display of glycans. Few studies have been conducted with whole cells and these arrays because only adhesion and cell death can be easily assessed from these arrays. Furthermore, DC response to any of the arrays has not yielded positive results in the past due to the "loosely" adherent nature of DCs and because of the complex surface marker and soluble factor release that constitutes different DC phenotypes. Thus, two fronts for improving the current state of the field for DCs were studied herein. The first was to design an optimized carrier for non-phagocytosable surface display of glycans to DCs for use as an indicator of properties necessary for DC response to glycan microarrays. The second was to determine if the cell response to these adsorbed conjugates was relatable across display modalities. This is of interest because if cell response to the adsorbed conjugates was identical to that of the cell response when

delivered in a microbead or in a soluble form then cell response to microarrays should become an area of intensive research for all glycobiology. If, however, cell response was not relatable between these display modalities then more diverse efforts would be needed on the part of glycobiologists to assess cell response to a variety of carbohydrates in a variety of display modalities.

1.1 Research Significance

Fibrous encapsulation is pervasive and has been shown to have deleterious effects in orthopedic prostheses, biosensors, electrodes, and cardiovascular implants.[9–13] For example, in the United States alone, dental implants fail in ~50,000 people/year and ~15% of all total knee arthroplasties fail due to fibrous encapsulation.[14,15] To limit this effect, a tolerogenic, anti-inflammatory, wound healing immune response to the implant is critically needed.[7,16–18] Conversely vaccines require a pro-inflammatory and/or immunostimulatory response.[3,5,19] However, few clinically approved combination products, biologics, or materials have shown an ability to elicit a large and controllable effect that changes the ultimate fate of implants or increases efficacy of vaccines over that of current clinical adjuvants.

Dendritic cells and their interaction with carbohydrates through CLRs have been shown to play critical roles in both immune acceptance and activation and thus are seen as an ideal target for modulating the responses discussed above. However, carbohydrates can only be exploited with a more complete understanding of host immune interaction with carbohydrates and glycoproteins. This dissertation builds part of the carbohydrate foundation onto which future implanted devices and vaccine conjugates can be designed. The information uncovered has direct implications in development of glycan-based surfaces/biomaterials which stimulate DC maturation as effective adjuvants for vaccines or inhibit DC maturation to minimize immune responses in tissue engineering and implanted medical devices. Additionally, the work herein shows that glycan display

modality is an important factor for consideration of DC response to glycoconjugates which has implications across the field of glycobiology. Modality of display, has not been accessed across the field and thus, while not studied in this report, it is possible that other immune cells and indeed any cells, respond differentially to different modalities of display of glycan. Furthermore, this dissertation lays the groundwork for creating a template for modeling of immune interaction with glycans. Modeling has the potential to play an instrumental role in the elucidation of cell response to glycan structures because extremely limited amounts of purified complex carbohydrate sugars are capable of being synthesized. Due to this shortcoming, extensive cellular studies cannot easily be performed and modeling can be used to overcome this limitation. It is hypothesized that the information obtained from modeling will offer new avenues and approaches in immune modulation and potentially lead to new types of combination products utilizing CLR ligands. These could have the potential to modulate the immune response toward clinically efficacious vaccines and implants/coatings and thus improve clinical outcomes.

1.2 Innovation:

Soluble and phagocytosable glycan presentation to APCs has been studied but little direct comparative data between the two and no comparison to well surface displayed glycans has been seen.[20,21] Furthermore, due to the extremely limited supply of well-defined oligosaccharides capable of being obtained via synthetic or biological means surface interaction with recombinant CLRs or other lectins to glycan microarrays has been used as a proxy for direct cellular response for glyco-conjugate creation and therapeutic approaches.[22,23] Additionally, the non-phagocytosable surface display of glycans to cells has not undergone a thorough analysis. Thus, the critical molecular factors for display of glycans to DCs so that the cells can respond to the glycans with high efficacy from biomaterial surfaces are unknown. The experiments herein addressed these issues by use of a novel high throughput (HTP) methodology. This method allowed

for an order of magnitude less glycan to be used than previous functional assays, evaluate both pro- and anti-inflammatory immune responses from DCs, and allowed for the testing of multiple surface display modalities simultaneously. The work completed herein challenged the conventional view in the literature that it is glycan structure, density, and context of presentation alone that determine phenotypic modulation of DCs and cells in general. This was done by first optimizing single molecular factors and combinations of factors in concert to obtain a foundation of non-phagocytosable display parameters that were then used to show quantitative difference in DC response across display modalities. Finally, the creation and validation of predictive models for DC activation in response to CLR stimulation via adsorbed synthetic glycoproteins was performed. It is hypothesized that this modeling approach can now be used as a template for future glycan studies performed across multiple classes of glycan ligands. This has not been seen in the literature previously and has a large value to the field of glycobiology because modeling has the ability to isolate and predict factors of importance to glycan display which ultimately means that less glycan will be needed to complete the necessary studies for clinically efficacious treatments.

CHAPTER 2 SPECIFIC AIMS AND HYPOTHESES

The role that glycans play in systemic immune response is still largely unexplored and the DC response to diverse glycan motifs across various presentation contexts has not been assessed. Because of the critical role that DCs play in the coordination of both innate and adaptive immune responses to foreign pathogens, this is a major limitation for the intelligent design of biomaterials, coatings, and combination products that utilize glycans. Elucidation of the fundamentals factors of glycan display important for the immune response to these conjugates will be critical for determining how to overcome fibrous encapsulation of implants, impotent vaccine conjugates, and to develop therapeutics targeting cancers and parasitic infections. Furthermore, understanding optimal presentation modalities for glycans to engineer immune response toward a desired outcome is critical for the design of future therapeutics. Due to the extremely rare nature of complex glycan structures, this understanding can currently only be had if computational models are employed to predict the DC response to glycans. These models have not been seen in the literature and thus must be developed in order to move to the next phase of therapeutic development.

Aim 1: Identify molecular factors in the non-phagocytosable display of glycans to dendritic cells that are important for phenotypic modulation. *Hypothesis: Molecular characteristics (density, charge, and glycan structure) of both the carrier and glycan can significantly modulate DCs toward a pro- or anti-inflammatory phenotype*. The purpose of this Aim was to permutate molecular factors of the carrier and glycan to determine which factors lead to altered DC phenotypes when the DC is cultured with glycans displayed from a non-phagocytosable surfaces. Molecular characteristics of vaccine and biomaterial conjugates have been shown to drastically alter the immunogenicity of conjugates.[24–28] However, this has not been shown in relation to DCs and non-

phagocytosable glycan presentation. Assessment of DC phenotype modulation by glycans via a thorough analysis of carrier charge, density of presentation, and glycan structure as well as combinations therein were performed. We examined the effect on DC phenotype of two monosaccharides at multiple densities, four levels of carrier charge, and six distinct mannose structures. Assessment of DC phenotype was performed via the High throughput (HTP) technique developed in house. After assessment of charge and density multivariate modeling was used to statistically isolate and predict which molecular factors carried the most weight in phenotypic modulation. These factors were then used to create an optimized carrier that was used with more complex glycan structures. The DC phenotype was then assessed in response to the conjugates and the structural motifs necessary for DC phenotype modulation were uncovered via multivariate modeling.

Aim 2: Identify how glycan presentation modality alters DC phenotype and how these display strategies can be harnessed to drive DCs toward a desired phenotype. *Hypothesis: Displaying carbohydrates to dendritic cells in a soluble, phagocytosable, and non-phagocytosable form will cause a differential DC phenotype.* The purpose of this Aim is to determine how DC phenotype is modulated by a limited set of simple proteoglycan conjugates displayed in three presentation modalities. The immune response to non-phagocytosable glycans has been implicated in the body's innate response to implanted materials and biofilms. However, a correlative relationship between the two has not been established. Furthermore, a comprehensive study of the DC response to non-phagocytosable glycans versus other display modalities has not been performed. In this aim we measured the DC response to simple proteoglycan conjugates displayed in a soluble form, from a phagocytosable bead, and from a well surface to explicitly define this relationship. The optimized proteoglycan conjugates from Aim 1 were used so that maximal DC response could be seen and to better mimic the display of glycans found in nature. Assessment of DC phenotype in response to these structures was

performed via the same HTP technique as in Aim 1. The DC phenotype in response to the altered modality of display for identical conjugates was then modeled using a multivariate linear model to show that different display modalities had differential effects on DC phenotype. Proof that DCs were interacting with the conjugates from these studies via CLRs was desired. Thus, antibody blocking studies were performed with conjugates adsorbed onto 1 μm beads to determine if blocking antibodies were able to inhibit phagocytosis of the beads by DCs. Finally, an indication of what the fate of the adsorbed conjugates was upon interaction with the DCs was desired. Thus, conjugates were fluorescently modified and adsorbed to wells, and DC internalization of the fluorescent conjugates was assessed.

CHAPTER 3 LITERATURE REVIEW

3.1 Dendritic Cells in Immunology

Dendritic cells play a pivotal role in the host immune response to a variety of foreign entities.[29,30]. Dendritic cells are distributed in almost every tissue and organ in the body and are considered APCs. Dendritic Cells are of hematopoietic origin and are specialized for the non-specific uptake, transport, processing and presentation of antigens to T cells.[31–33] While several other cell types are defined as APCs, macrophages and B cells, only DCs are able to efficiently stimulate naïve T cells.[34] DCs are derived from monocytes in vivo and are differentiated form monocytes using ganulocyte-macrophage colony stimulating factor (GM-CSF) and interluken-4 (IL-4).[35,36]. However, differentiation of monocytes into DCs is not guaranteed as monocytes have been shown to differentiate into macrophages, osteoblasts and osteoclasts.[37] Interestingly, in the presence of IL-6 secreting fibroblasts, monocytes will not differentiate into DCs even when cultured with GM-CSF and IL-4.[38]

Dendritic cells are the most potent APCs of the immune system. These cells have evolved to have a myriad of pattern recognition receptors that can distinguish characteristic pathogenic structures and signal the cell to respond. Dendritic cells reside in almost every tissue in the body and their primary function is to sample the local microenvironment for pathogenic or foreign molecules, uptake these structures, and present them to other leukocytes. How the antigen is processed, the extent of activation of the DC, the phenotypic outcome of that stimulation, and the extent of the downstream immune response can all be regulated by the context in which the DC encounters the antigen and the subsequent response to that antigen. The DC constantly samples the surrounding environment with its PRRs. Once a pathogen is detected the pathogen is phagocytized, killed, processed, and its peptides displayed on the Major histocompatibility complex (MHC) of the DC. If the pathogen has infected the DC

(viruses or mycobacteria) the DC has no need to capture the pathogen but instead process the pathogens' peptides and present them on the MHC. While the antigen is being processed the DC is also going through a process known as maturation. During maturation the DC up regulates co stimulatory molecules, increases cytokine production, and down regulates phagocytosis receptors and begins to migrate toward the lymph node. Once the antigen is processed, displayed, and the DC has up-regulated all costimulatory molecules the DC is said to be a mature DC (mDC). When the mDC reaches the lymph node it encounters naïve T cells which sample the peptides displayed on the DC surface. If the T-cell receptor (TCR) is specific for the peptide the T cell matures and begins to clonally expand.

The maturation process is key in the development of an immune response not only because it signals the DC to migrate to the lymph where it will encounter naïve T cells but because it enables the DC to activate those T cells and cause them to clonally expand. This process is not necessarily linked to a pro-inflammatory response as DC maturation can lead to proliferation of tolerogenic T cells (T_{regs}).[39,40] The exact mechanism of DC recognition and processing after initial contact with the pathogen or foreign material is heavily dependent upon what receptors are activated. For instance if the CLR, Dectin-1, is stimulated via the delivery of β-glucans to DCs the DC is able to prime Th1 and Th17 responses as well as cytotoxic T-lymphocyte (CTL) responses.[41] In a study done by Leibundgut-Landmann et al. Dectin-1 stimulation was also shown to be an adjuvant for CTL cross-priming *in vivo*. This ability to promote cross-priming of antigen led to potent CTL responses that protected the treated mice from developing tumors.[41] In contrast stimulation of the CLR Dec205, DC‑SIGN, or macrophage mannose receptor (MMR) by antibodies without co-stimulation of toll-like receptors (TLRs) efficiently induces a tolerogenic state in DCs.[42–44] Thus, elucidating which PRRs stimulate the desired response from DCs can be of enormous benefit in not just vaccine

delivery but also in implantation of tissue engineered constructs and other medical devices.

3.1.1 Mechnisms by which DCs respond to biomaterials

Dendritic cells have been shown by the Babensee lab to undergo maturation upon biomaterial contact depending on the biomaterial used.[45–47] The form of the biomaterial microparticles, scaffold or film[48] has been shown to influence the DC response as well as the effect of surface contact and area.[45,49] Thus, that DC interaction with biomaterials is an important factor in tissue engineering is clear. However, in combination products, materials that utilize both a synthetic and biological component, the effect of the biomaterial adjuvant effect has been demonstrated to influence downstream effectors of DC maturation such as humoral IgG production and .[50,51] Thus, elucidating how the presence of biomaterials alters the host immune response to co-delivered biologics and discovering the optimal ways in which to tailor those biomaterials shows great promise for the improved modulation of host response against combination products.

Biomaterials have been shown to have an adjuvant effect that enhances the immunogenicity of ovalbumin (OVA). OVA adsorbed to phagocytosable microparticles, co-delivered in poly(lactic-co-glycolic acid) (PLGA) microparticles, or delivered in PLGA scaffolds, was found to support a moderate humoral immune response that was able to be maintained for over four months and was seen to be primarily a Th2 response as indicated by IgG1 antibody titers.[50] Interestingly, the PLGA scaffold delivery induced a larger and longer lasting humoral response than did the two microparticle counterparts.[52] Such enhanced immune response was hypothesized to be due to the danger signals released from tissue damage at the implant site due to the fact that HMGB1 a potent danger signal, was found in higher concentrations in exudates from subcutaneously implanted PLGA scaffolds in comparison to naïve control.[53] This result suggested the possible role of danger signal biomaterial-induced adjuvant effect.

Furthermore, different biomaterials have been found to induce differential DC maturation. PLGA and chitosan films were shown to induce DC maturation with alginate and agarose did not.[54] Mixed lymphocyte reactions showed that DCs treated with PLGA and chitosan films supported higher levels of T-cell proliferation as compared to that of untreated DCs, and DCs treated with hyaluronic acid films induced lower levels of T-cell proliferation. Additionally, agarose and alginate showed no change in T cell proliferation as compared to that untreated cells. Furthermore, surface processing of titanium surfaces has been shown to drastically alter DC phenotype as measured by both cytokine secretion and surface marker expression of costimulatory molecules by DCs.[46] Specifically that hydrophobic surface modification in combination with high roughness increases activation marker CD86 in DCs.[46] A complex cytokine release profile was determined in which DC surface marker expression did not couple with historically expected cytokines, thus implicating a new hybrid phenotype for the DCs. Principle Component Analysis (PCA) was performed on the data to draw more clear correlations between the soluble factors and DC phenotype and it was found that pure titanium and SLA modification of titanium surface pushed DCs toward a pro-inflammatory phenotype, while modified SLA surface treatment was associated with non-inflammatory DC response.[46] Additionally, it was found that for titanium surfaces hydrophobicity/philicity was heavily associated with IL10 production in DCs. Interestingly, from this work it was also shown that increased DC adhesion was not sufficient to induce DC maturation as surfaces that showed statistically different CD86 expression showed equivalent adhesion to surfaces.[46]

The study above clearly indicates the importance of biomaterial surface properties and DC maturation however, material properties for the tested biomaterials were not completely controlled. Thus, very controlled surface presentation of defined surface chemistries has also been studied using self-assembled monolayers and with distinct terminal groups (CH_3, OH, COOH, and NH_2).[55] Based on cell morphology,

allostimulatory capacity, and expression of maturation markers each SAM surface elicited modest DC maturation in comparison to untreated DCs. Methylated surfaces were found to be the least activating in terms of surface marker expression but released the largest amounts of pro-inflammatory cytokines TNF-α an IL-6. It was found that this was due to the fact that cell viability on the methylated surfaces was lower than that of the other SAMs.

Further study was given to DC response to controlled polymeric surfaces in a recent study that looked at a library of polymethacrylates (pMAs).[47] It was found that pMAs induced differential DC responses. Specifically that several of the the pMAs increased the maturation factor of DCs to a greater extent than that of the positive control LPS, and each of the pMA treatments produced a unique cytokine profile from the DCs with HEMA showing strong anti-inflamamtory response and nbutyl-cyclohexyl-undecyl methacrylate and isobutyl-benzyl-THFF methacrylate producing the most inflammatory phenotype. Also of interest was that when these factors were modeled alongside the material properties it was found that based off of polymer composition one could predict DC phenotype using a PCA model. Furthermore, it was found that DCs were morphologically distinct on different polymer surfaces and that pHEMA and not pIBTMA was able to induce a significant amount of DC apoptosis. pIBTMA was consistently shown to low levels of inflammatory cytokines and chemokines as compared to untreated cells and rounded cell morphologies.

Finally, the exact mechanisms by which DCs recognize and respond to biomaterials remains to be elucidated. Complement and adsorption of danger signals from plasma proteins have both been implicated in the response.[56] However, recent research using MyD88 and TLR knockout mice demonstrated that DCs use TLR2, TLR4, and TLR6 for the responses to a diverse set of biomaterials.[57] Also recently, β integrins were shown to play a role in mediating DC adhesion and response to biomaterials.[58] These studies implicate extracellular matrix (ECM) proteins adsorbed to biomaterial

surfaces as being integral to DC response to these proteins. DCs cultured on collagen or vitronectin substrates released higher levels of IL-12p40 while DCs cultured on albumin or serum coated plates generated higher amounts of IL10.[59] Based off of these results, intelligently engineered biomaterials may guide the presentation, orientation, or conformation of adsorbed proteins in such a way that these combination products will either induce DC tolerance or activation to co-delivered antigen. The utility of using biomaterials over natural, heterogeneous, ligands is that biomaterials can induce a controllable and tunable response from the immune system that can be tailored for any level or phenotype desired. The experiments listed above begin to uncover the factors necessary for this control and it is expected that future works will further uncover novel factors for modulation of DC response to biomaterials.

3.2 Pattern Recognition Receptors

The two most heavily studied and diverse PRR classes on DCs are TLRs and CLRs (CLRs). Toll-like receptors, the most characterized of the PRRs, are membrane bound proteins containing varying amounts of leucine-rich repeats in their extracellular domains that are involved in the ligand-recognition.[60] Currently, twelve TLR receptors have been discovered in humans.[60] These TLRs recognize a variety of bacterial and viral pathogen associated molecular patterns PAMPs and several injury molecular motifs, danger associated molecular patterns (DAMPS).[60–62] Examples of microbial or viral ligands for TLRs include lipopolysaccharide (LPS) (TLR4), lipopeptides and lipoproteins (TLR2), double-stranded viral RNA (TLR3), and bacterial flagellin (TLR5). [60,63–68]. Most TLR's signaling propagation occurs through MyD88, a cytoplasmic adapter protein common for all TLRs (except TLR3). TLR4 is also able to signal in a MyD88 independent manner [69]. Upon ligation TLRs can stimulate three independent signaling pathways: the IKK complex (inhibitor of nuclear factor-κB), mitogen-activated protein kinase (MAPK), and toll/IL-1R domain-containing adapter molecule (Trif). Activation

of the IKK pathway results in the release and activation of nuclear factor- κB (NF-κB) transcription factor family (p65, p50, p52, RelB, and cRel). Activation of the MAPK family (c-Jun N-terminal kinase, JNK; p38, and extracellular-signal-regulated kinase, ERK) results in the subsequent phosphorylation/activation of activator protein (AP)-1 transcription factor family (cJun, cFos, FosB, Fra-1, Fra-2, JunB, JunD). Activation of the Toll/IL-1R domain-containing adapter molecule (Trif), a MyD88 independent pathway, leads to the activation of interferon regulatory factor 3 (IRF3) transcription factor to induce interferon production [60]. The above pathways can be stimulated singly or in an overlapping fashion depending on the availability of ligand for a particular TLR. Co stimulation through NF-κB and AP-1 has been shown to yield a more potent inflammatory response [70]. The up-regulation of the transcription factors above can have diverse effects on DC maturation and phenotypic outcome of the DC. However, most of the above transcription factors when activated via the TLR pathway lead to pro-inflammatory mediators.

3.2.1 C-Type Lectin Receptors on Dendritic Cells

C-type lectin receptors are calcium dependent carbohydrate binding receptors that represent a unique class of signaling receptors that has only begun to be studied. In DCs these receptors are conically thought to recognize carbohydrate moieties present on pathogens but they have also been found to bind to altered carbohydrate structures found on apoptotic, cancerous and necrotic cells.[1,42,71–74] Table 1 shows all of the currently known lectins present on DCs. Of note is that for many of the lectins many ligand specificities are unknown or signaling pathway have not been uncovered.[42] What Table 1 makes apparent is that while CLRs have not been as well characterized as TLRs they do play an important role in the DC interaction with a variety of intercellular mediators and pathogens.[1,40,42,74–78] Also of note from Table 1 is the redundancy of these receptors; seven CLRs have been shown to bind to mannosylated structures while ten sialic acid

binding proteins are found on DCs. This redundancy can be explained in part by the fact that *in vivo* CLRs are often expressed on specific subsets of DCs. For instance, MR is highly expressed on myeloid DCs, whereas Langerin expression is restricted to Langerhans cells.[42] Another good example is DC-SIGN which is widely expressed on dermal DCs, as well as DCs in lymph nodes and mucosal tissues but MGL is only seen in a subset of dermal DCs.[79,63] Thus, multiple lectins are needed to produce distinct outcomes in each subset depending on the DC microenvironment and function. It has also been postulated that the redundancy of CLRs on specific DC subsets could be present to create diverse, highly regulatable, and specific phenotypic responses from DCs.[4,5,42,80] This is supported by comparing the adapter protein each receptor signals through, seen in Table 1, which shows that drastically different outcomes would be possible when different lectins bound an identical pathogen even within the same DC subset.[81]

Table 1: List of lectins on DCs. For each CLR signaling motifs and pathways, functional effects of ligation, ligand specificity, endocytic activity, calcium dependence and reference if known is listed.

Lectin	Other Names	Signaling Motifs	Signaling Pathways	Functional Effects	Ligand Specficities	Endocytic Activity	Ca+ Dependent	Refer.
DC-SIGN	CLEC4L, CLEC4L, CD209	YxxL, LL, EEE	ManLAM: LSP1, KSR1, CNK, RHOA, LARG, RAS, Src kinases, PAKs, Raf-1. Salp15: MEK-Raf-1. Fucose: LSP1. Abs: Ca2+, PLCγ, PI3K, Akt, ERK1/2	ManLAM: TLR-stimulated IL10, IL8, IL6, IL12 Salp15: Decreased TLR-induced IL-6, IL-12, TNFα Fucose: Increased IL10, decreased IL6, and IL12	High mannose, Mannan Fucosylated Glycans (Lewis Structures)	Yes	Yes	82–89
LSECtin	CLEC4G	YxxV/L, EE	ND	Negative regulation of T-Cells	Mannan, Fucose	Yes	Yes	90,91
BDCA-2	DLEC, CD303, CLECSF7, CLEC4C	Tmb K, EEE	FcRγ chain- ITAM Syk, LYN, BTK, BLNK, PLCγ2. Abs: Src, Ca2+	Decrease TLR induced Type 1 IFN and TRAIL secretion. TLR induced Increase IL10	gp120, mannose	Clatherin Dependent	Yes	92–96
DCIR	CLECS-F6 LLIR, CLEC4A	I/Vx, Yxx V/L	SHP-1, SHP-2	Decreases IL12, TNFα, IFNα	ND	Clatherin Dependent	Yes	97–101
Dectin-2	CLEC6A	Tmb R	FcRγ chain- ITAM Syk, CARD9, Src Kinases	Increased TNFα,IL-1RA, IL6, IL-1β, IL23, ROS, NALP3, IL4, IL10, Cysteinyl leukotrienes	High mannose, Mannan	Yes	Yes	102–107

Table 1 continued

MCL	CLECS-F8, CLEC4D	ND	ND	ND	ND	Yes	Yes	108
Mincle	CLEC4E	Tmb R	FcRγ chain- ITAM Syk, CARD9, Src Kinases	Increased TNFα, IL6, CXCL2, CXCL1	α-mannose, glycolipids, SAP-130	ND	Yes	109–113
Langerin	CLEC4K, CD207	Proline Rich	ND	Endocytosis	High mannose, mannan, Lewis Y, Lewis B, GlcNAc	Yes, via Birbeck Granules	Yes	114,115
MGL	CD301, CLEC10A	YxxF, LL	ND	Inhibits T cells via CD45 binding	Terminal GalNAc	Yes	Yes	116,117
MMR	MR, CD206, MRC1	FxxxxY, LL	CDC42, RHOB, PAKs, ROCK1	Increased CD80, CD86, IL10, IL1RA, TNFα. With TLR Signaling decreased TNFα, IL-1β, and IL-6. With apoptotic cells increased TNFα decreased IL10	High mannose, mannan, sLeX, GlcNAc	Yes	Yes	118–123
Dec-205	CD205, LY75	FxxxxY, EDE	ND	Increased MHC Presentation	PLA, K12, mannose	Yes	Yes	124–129

Table 1 continued

DCAL-1	CLECL1	Tmb K	Abs: JNK, p44/42 MAPK	Increased HLA-DR, T cell prolifaration/costimulation	ND	ND	130,131
MICL	DCAL-2, KLRL1, CLL1	VxYxxV	SHP-1, SHP-2. Abs: ERK, p38	Abs: Increase CCR7, IL6, IL10, MIP3β, TNF, IL12. If TLR mediated decrease IL12 and TNF.	ND	Yes	No	132 133 134
CLEC-2	CLEC1B	Yxxl, LL	HemITAM-Syk, Src and Tec kinases, PLCγ2, Lat, SLP-76, Rac1, VAV-1/3	Increase TNFα	Podoplanin, Rhodocytin	Yes	No	135 136 137 138 139
DNGR-1	CLEC9A	YxxL	HemITAM-Syk	Increases Cross Presentation of Necrotic Signals	ND	Yes	No	140 141 142 143
CLEC12B	MAH	VxYxxL	SHP-1, SHP-2	Inhibits Activation caused by ITAMs	ND	ND	No	40
CLEC-1	CLEC1A	YxxT, DDD, TmbR	FcRγ chain	ND	ND	ND	No	136 144
Dectin-1	βGR, CLECSF12, CLEC7A	YxxL, DED	HemITAM-Syk, Bcl10-Malt-1-CARD9, PLCγ2, ERK, p38, JNK, RAF-1	Increased IL10, IL2, IL6, IL23, ROS, NALP3, TNF, IL12	β-glucans	Yes	Both	72,76,145–153
Siglec-1	Sialoadhesin	V/L		Attenuate cDC function, Increase IL-10	α2-6Neu5Ac, α2-3Neu5Ac	Yes	No	154–160

Table 1 continued

Siglec-2	CD22	ND	ITIM - SHP-1/2 ITIM like motif, Grb2	Apoptosis of B-Cells, Attenuation of B-Cell activation	α2-6Neu5Ac	ND	No	160
Siglec-3	CD33	I/Vx, Yxx V/L	ITIM, ITIM-like, SHP-1	ND	α2-3Neu5Ac	ND	No	161
Siglec-4	MAG	ND	Tyrosine	ND	α2-6Neu5Ac, α2-3Neu5Ac	ND	No	161
Siglec-5	CD33 Related	I/Vx, Yxx V/L	ITIM, ITIM-like, SHP-1	Increase IL-10, IL12P70	α2-3Neu5Ac	Yes	No	155,162–164
Siglec-6	CD33 Related	I/Vx, Yxx V/L	ITIM, ITIM-like, SHP-1	ND	α2-6Neu5Ac	ND	No	161
Siglec-7	CD33 Related	I/Vx, Yxx V/L	ITIM, ITIM-like, SHP-1	Attenuation of NK cells, signal attenuation in NK cells,	α2-8diNeu5Ac, α2-6Neu5Ac, α2-3Neu5Ac	ND	No	159,160
Siglec-9	CD33 Related	I/Vx, Yxx V/L	ITIM, ITIM-like, SHP-1	Attenuation of neutrophils and macrophage, neutrophil apoptosis, attenuate cDC function, IL10 production	α2-3Neu5Ac, α2-6Neu5Ac	ND	No	159,165–167
Siglec-10	CD33 Related	ND	Grb2 binding tyrosine, ITIM, ITIM-like	Attenuated signaling in response to DAMPs	α2-3Neu5Ac, α2-6Neu5Ac	ND	No	168,169
Siglec-11	CD33 Related	I/Vx, Yxx V/L	Grb2 binding tyrosine, ITIM, ITIM-like	Attenuating microglia mediated inflammation	α2-8Neu5Ac	ND	No	170,171

ND means not determined.

3.2.1.1 Signaling by CLRs on Dendritic Cells

Based on cytoplasmic signaling motifs and signaling potential, shown in Table 1 myeloid CLRs can be grouped independently of structure into the following broad categories: Syk-coupled CLRs, CLRs with immunoreceptor tyrosine-based inhibitory motif (ITIM) domains, and CLRs without a clear immunoreceptor tyrosine-based activating motif (ITAM) or ITIM motif. Each of these groups can then be further divided into receptor classes based on calcium dependence, seen in Table 1, and by glycan ligand able to be bound.

Syk has emerged as a major tyrosine kinase involved in the early signaling by a subset of CLRs. CLR coupling to Syk can be indirect, often occurring through the Fc receptor γ chain (FcRγ) or DAP12, which are classical Syk-recruiting ITAM motifs.[82] However, lectins in Table 1 with a hemITAM signaling molecule possess the ability to directly signal Syk through a single tyrosine-based motif found in the cytoplasmic domain.[83] For these receptors phosphorylation of the tyrosine in the ITAM or hemITAM motifs generates docking sites for the SH2 domains of Syk, which undergoes a conformational change that allows auto-phosphorylation and activation of the Syk pathway.[82] Active Syk can then signals through a variety of intermediaries to PI3K or PLCγ, which in turn coordinates many downstream signaling pathways that lead to myeloid cell activation.[42] This class of receptors is most easily divided by the hemITAM-based CLRs (Dectin-1, CLEC-2, DNGR-1, and SIGN-R3) and the ITAM-coupled CLRs (Dectin-2, BDCA-2, Mincle, and MDL-1). Though functional downstream activation effects of stimulation of both of these classes are similar ultimate phenotypes have been found to be disparate depending on stimulation.[82,84]

Lectins with ITIM domains are a distinct group of CLRs that express ITIM motifs that recruit phosphatases and thereby negatively regulate signaling through kinase-associated receptors, notably the Syk-coupled CLRs and TLRs.[84] ITIM-bearing CLRs

modulate myeloid cell activation when they are triggered together with receptors known to stimulate pro-inflammatory responses from DCs such as TLRs and compliment receptors. Myeloid CLRs included in this group are DCIR, MICL and the Siglecs. Of these receptors the Siglecs are the most heavily studied and well understood. Within the Siglecs there are generally three groups based on features of the transmembrane and cytoplasmic tails of individual Siglecs that reflect the major mechanisms by which they mediate their biological functions. The first group is made up of Siglec-1 and Siglec-4 lectins that lack inhibitory signaling cytosolic motifs and possess neutral transmembrane domains.[84] These Siglecs have been shown to primarily mediate adhesion events between immune cells and endothelium and are known to be critical in the arrest of cell rolling on the endothelium wall.[84]

The second group of Siglecs in this type of functional classification is the largest and includes members in which the major biological function is immune-inhibitory, mediated by cytosolic ITIMs. In this family of Siglecs, ligand recognition results in phosphorylation of the ITIM tyrosine and the ITIM-like tyrosine to Src family kinases such as Lyn. These kinases can phosphorylate cytosolic ITIM tyrosines, which then in turn recruit tyrosine phosphatases such as SHP-1 or SHP-2 that can attenuate signal transduction.[85,86] Human Siglecs that contain ITIM motifs include Siglec-2, -3, and -5 through 12. A general view of ITIM-containing Siglecs is that they maintain a constitutive inhibitory signal when bound to their cognate sialoglycoconjugates in the same cell in which they are expressed.[87] Exposure of the host to a pathogen, even if the pathogen lacks surface sialoglycans, may either alter Siglec expression or alter cellular levels of Siglec ligands.[84] Pathogens that do express surface sialic acid may engage cognate Siglecs to attenuate inflammation as part of immune evasion, but innate immune cell activation may also be modulated in order for the host to generate specific protective responses.[87]

The third category of Siglecs, members contain a positively charged residue in the transmembrane anchor region. These Siglecs associate with a disulfide-linked homodimer of DAP12 which contains an aspartate transmembrane residue and a cytosolic ITAM motif. On the basis of data from other DAP12-containing receptors whose ligands are known, it is hypothesized that ligation of these ITAM-linked Siglecs leads to a conformational change that results in enhanced accessibility of the cytosolic tyrosine containing motifs of either DAP12 or DAP10 to non-receptor tyrosine kinases.[84] This enhanced accessibility further results either in tyrosine phosphorylation of the ITAM of DAP12 to facilitate Syk family tyrosine kinase recruitment and activation or in phosphorylation of DAP10, resulting in phosphatidylinositol-3 kinase recruitment and activation. In humans, Siglecs with positively charged residues in the transmembrane region include Siglec-14 through 16.[88–91] Primarily in the context of the biology of pDCs, it is hypothesized that DAP12 ITAMs contribute to the attenuation of TLR signaling in an uncharacteristic role for the ITAM motif. [84] Although ITAMs that shut off signaling pathways have sometimes been referred to as inhibitory ITAMs[92,93], the concept of ITAMs mediating unique inhibitory signals has long been studied in the immune context. B cell anergy and T cell anergy both involve antigen receptor–linked ITAM activation, but the biochemical pathways induced inhibit lymphocyte activation.

Finally, CLRs without a clear ITAM or ITIM motif, including MR, DEC-205, DCSIGN, Langerin, MGL, CLEC-1, DCAL-1, MCL, and LSECtin. These CLRs can engage the endocytic machinery and mediate the capture of antigenic cargo for processing and presentation to T cells.[94] Nevertheless, triggering of these receptors in isolation has not been seen to induce obvious signs of myeloid cell activation without interaction with other PRRs. As can be seen in Table 1, some of this group of CLRs (e.g., DC-SIGN), has the signaling pathway involved in modulation elucidated, but for most it is unknown. From Table 1 it is clear that depending on the ligand delivered to the lectins in this class the downstream effectors of its ligation can vary drastically. Thus, this class

of lectins shows a more complex and nuanced phenotypic modulation of DC phenotype as compared to the other two classes in which signaling from ligation is more direct.

Targeting of CLRs on Dendritic cells

Development in the glycoimmunology field will take considerable expenditure of resources and time from a diverse range of specialties and thus a large value to this research must be shown to justify this expenditure. To this end, many implications for CLRs have been seen in studies with antibody binding of the CLRs to simulate ligand engagement.[44,95–99] These studies have led to clinical therapies that are just beginning to enter the market.[5,100] Also, many studies have been done showing that receptors expressed on DCs, in their recombinant form, can bind, with high prejudice, glycan structures immobilized in micro arrays.[101–106] These assays can lead to potent ligand identification for use in treating a range of pathologies. A plethora of studies have shown altered DC behavior across soluble, phagocytosable, and non-phagocytosable presentation of glycans which has potential in vaccine and implant development; which has implications across the entire medical community.[107–111] Additionally, CLRs found on DCs have been expressed in non-DCs and their ability to bind and uptake carbohydrates has been assessed and show implications for a mechanistic understanding of what these isolated receptors are capable of inducing.[112–114] Furthermore, many studies have optimized particle and dendrimeric polymer carriers of carbohydrates to increase phagocytosis or intercellular transport of ligands.[115–117] Finally, several studies have also shown enhanced or abrogated migration of DCs due to glycan ligand immobilization to non-phagocytosable sufaces.[20,118,119] In combination these studies showed that a variety of immune responses, both pro-inflammatory and tolerogenic in origin, were possible through CLR stimulation and thus this group of PRRs warrants further study.

3.2.1.2 Antibodies against CLRS

Recent studies suggest that antibodies against C-type lectins such as MMR, DEC-205/ CD205, or DC-SIGN/CD209 can be used as antigen-delivering vehicles to induce immune tolerance, T cell proliferation, or cytokine release.[120–126] In these studies non-traditional phenotypes, where typical maturation markers such as CD80 and CD86 were not up regulated, were identified.[95,127,128] In the study by Meyer-Wentrup et al. DCs showed a reduction in their pro-inflammatory cytokine profile when the DCs were stimulated with TLR8 agonists but were first treated with Abs against DCIR. However, traditional anti-inflammatory or tolerogenic cytokine profiles (IL-10, TGFβ, and IL-6) were not found to be up-regulated. Another study involving CLEC9A show that murine DCs expressing CLEC9A are capable of producing potent CD4+ and CD8+ T cell proliferation without increasing the typical activation markers expressed by DCs (surface markers MHC class II, CD80, CD86, and CD40) when the CLEC9A receptor was stimulated.[128] While the exact natural ligand for CLEC9A is unknown this receptor has been shown to be a critical player in clearing necrotic tissue without activation associated surface markers being up-regulated but with an increase in IFN-γ.[129] Furthermore, in a study by Meyer-Wentrup et al. DCIR cross-linking selectively inhibited TLR8-mediated IL-12 and TNF-α production in DCs. DCIR triggering with Abs showed that it also inhibits TLR-induced cytokine production and leaves TLR-induced CD80 and CD86 expression unaffected.[95] Recently, a DCIR peptide containing the phosphorylated ITIM domain has been shown to bind to the protein tyrosine phosphatases SHP-1 and SHP-2, thus further substantiating an immune-inhibitory role for DCIR.[130] Bonifaz et Al. showed that injection of anti–DEC-205 mAb coupled with ovalbumin alone induced regulatory T cells and leads to suppression of OVA-specific T-cell proliferation.[122,123] However, simultaneous injection of anti–DEC-205 OVA conjugates with an agonistic anti-CD40 Ab significantly enhanced host immune responses against an OVA-expressed tumor and infection by an OVA expressing vaccina virus.[123,126] Similarly, anti–DC-SIGN mediated targeting of antigen-induced, specific T-cell proliferation even without the presence of

other DC maturation stimuli. [120,126] Again in this study the DCs that were observed to promote T cell proliferation did not display typical maturation markers for mature DCs (both cytokine and surface marker). Of note from each of these studies was that they were conducted with antibodies to the lectins they were targeting because, in most of the cases, the physiological ligand for the receptors is unknown or because of the limited amount of purified glycan that is able to be obtained that would be specific for the receptor. Thus, the physiological response of the cells to ligation of the receptors with their natural ligand remains unknown and could therefore alter the understanding of the function of these receptors in the immune system. There are lectins, such as DC-SIGN, that have both known ligands and anti-bodies against them and an evaluation of receptor engagement of both could be performed but a direct comparison between them has not been shown in the literature. However, in the case of DC-SIGN, both have been extensively studied independently and through comparison it can be seen that a differential activation and response profile to ligand versus antibody occurs in DCs.[2,21,21,75,119,120,126,131–134]

The advantage of using anti-bodies as the triggering agent for these lectins is that no glycans or carbohydrate chemistries are needed to perform these assays. Thus, extremely limited amounts purified ligand is not the controlling factor in the above studies and cellular readouts such as cytokine profiles, cell surface marker expression, and effector cell proliferation were able to be obtained. These readouts are the most relevant when analyzing the affect a ligand has on the immune system prior to in vivo testing and thus the above studies are fairly complete in terms of cellular analysis. In fact several clinical therapies targeting lectins with anti-bodies are currently in phase I and phase II trials and are performing well due to the ease with which antibodies can be produced and manufactured.[100] However, due to the differential response of CLRs to antibodies versus glycan ligands antibody studies do not fully exploit the potential of

these receptors and more studies are needed to fully understand their capabilities in modulating immune responses.

3.2.1.3 Natural ligands for CLRS

A plethora of studies have shown DC interaction with natural ligands. These ligands are complex in nature and typically consist of glycans from sources such as yeast (mannans), bacterial or vial membrane glycoproteins, lipopolysaccharides, parasite surface glycans, or beta-glucans.[4,41,80,135,136] These complex sugar milieu have been used to identify molecular signaling pathways and general receptor specificity. However, even with these resources, in myeloid DCs, almost a third of all lectins currently identified do not have a molecular signaling pathway clarified and many more do not have the complete reaction cascade defined.[17,42,42,100] Generally, for the pathways that have been clarified, the CLRs can be divided into receptors that utilize TLR co-stimulation and those that signal independently from other receptor pathways.[75] The interaction of DC-SIGN with mannose-containing pathogens, such as Mycobacterium, HIV-1, measles virus, and Candida Albicans, affects TLR mediated immune responses from DCs.[137] It has been shown that the crosstalk between TLRs and DC-SIGN depends on the prior activation of NF-κB by TLR signaling from TLR3, TLR4, and/or TLR5[137]. DC-SIGN triggering activates the serine/ threonine protein kinase RAF1, which induces the phosphorylation of the NF-κB. This stimulation pathway has been shown to be involved in such downstream affecters as IL-8, IL-10, IL6, and IL12b production.[76] In contrast stimulation of DC-SIGN by antibody MR1, ligand Ara h1 (peanut allergen), or *Schistosoma mansoni* egg antigen as been implicated in activation of eRK. [138–140] The stimulation of eRK is linked to the activation of immunoreceptor tyrosine-based inhibitory motifs (ITIMs) which is conically thought to lead to the inhibition of pro-inflammatory cytokines. Thus, differential stimulation of this receptor independent of TLR activation may lead to inactivation of the DC. However, both of these pathways

have been discovered via interaction of DC-SIGN with mannosylated and fucosylated structures. The implications for fucose binding to modulate the DC-SIGN cascade has yet to be elucidated even though the binding of DC-SIGN to fucosylated glycans has been shown to be higher than that of mannose in vitro.[22] A further level of complexity for DC-SIGN exists in that it has also been shown to have competing roles in DC activation when binding to a single pathogen as demonstrated in HIV infection. Both Langerin and DC-SIGN recognize HIV-1 through the high-mannose motifs on its envelope glycoprotein gp120 yet they are expressed on distinct DC subsets and they have been shown to have opposite functions in handling HIV-1. Langerin targets HIV-1 for degradation while DC-SIGN binds HIV-1 and serves as a carrier molecule for HIV facilitating HIV transmission to T cells.[141]

Dendritic cell inhibitory immune receptor (DCIR) , MICL, and Siglecs 3-10 have been found to associate with ITIM intercellular motifs. Thus, when DCIR and MICL receptors are stimulated an inhibition of the TLR8 and TLR9, and TLR4 (respectively) activation in DCs has been shown.[142,143] The ITIM domains recruit the phosphatases sH2‐domain‐containing protein tyrosine phosphatase 1 (sHP1) or sHP2 following ligand engagement which leads to inhibition of the MyD88 pathway (via unknown intermediaries.)[144] However, similarly to DC‐SIGN, neither DCIR nor MICL have been proven to induce immune responses independently of TLRs but instead modulate the response of DCs if the TLRs are co-stimulated. If DCIR is bound by an antibody it causes internalization of the opsonized pathogen and trafficking of the complex to the endosomal compartments where TLR8 and TLR9 are present. It simultaneously begins the cascade described above to inhibit the affecter function of these TLRs. If MICL is bound activation of eRK is thought to occur and thus suppression of TLR‐induced IL‐12 expression has been shown.[142] Additionally, several studies have shown that siglecs can recruit the inhibitory tyrosine phosphatases SHP-1 and SHP-2.[145] However, relatively

little work has been done specifically on DCs and siglecs. So while these cells have been shown to express many of the Siglec family (See table 1) the exact effect of ligation of these receptors in DCs is largely unknown. However, they have generally been shown to contain the same adapter proteins as other immune cells containing these receptors and thus it is largely thought that they serve similar functions as they do in macrophages, monocytes, and B cells.[87,146] For most CD33-related siglecs (Siglec 3, 5-11, and 14) ligand engagement results in tyrosine phosphorylation of ITIM by the Src family tyrosine kinases with subsequent association with the Src homology 2 (SH2)- domain containing phosphatases such as SHP-1 and SHP-2, which control cellular activation by attenuating tyrosine phosphorylation.[147,148]

Finally, the lectins Dectin 1&2 have been shown to have a signaling cascade independent of other PRRs. Dectins activate gene expression through the recognition of β-1,3-glucan PAMPs expressed by a broad range of fungal pathogens, including C. albicans, Aspergillus fumigatus and Pneumocystis carinii, which then leads to the activation of NF-κB[40,72,149,42]. Dectin 1 stimulation leads to the activation of syK which has been shown to lead to NF-κB stimulation via a protein known as Card9[149–151]. This stimulation pathway has been determined previously for other receptors and thus is known as the canonical stimulation of NF-κB. But, in addition to the activation of NF-κB via the canonical activation pathway, Dectin 1 has also shown that through activation of the syK pathway an induction of the non-canonical NF-κB pathway can occur. Activation of this pathway has previously been described only for a few members of the TNF receptor superfamily, such as lymphotoxin-β receptor and CD40 neither of which signals through syK.[152,153] Stimulation via this pathway typically ends in TNF production and few other pro-inflammatory cytokines unlike stimulation via the canonical pathway. Thus, Dectin 1 is able to signal through several pathways ending in diverse cellular outcomes independently of any other PRRs via binding of β-glucans.

Dectin 1 and TLRs can cross-talk as well, as demonstrated for dectin-1 and TLR2. Co-expression of both molecules on the APC surface enables cooperative, synergistic signaling by TLR2 and dectin-1 in response to the common ligand zymosan.[154,155] Dectin 2, while not as well studied as Dectin 1, has also shown a diverse range of immunomodulatory effects. Dectin 2 is known to associate non-covalently with the ITAM-bearing signaling adaptor molecule FcRγ and activation of NF-κB. Typical downstream effects of FcRy activation and NF-κB stimulation are pro-inflammatory cytokine production and immune activation. That engagement of the dectin 2 receptor works through this canonical pathway is supported by data showing that dectin 2 recognition of fungi *C. albicans*, *Trichophyton rubrum* and *Microsporum audouinii* leads to production of the pro-inflammatory cytokines TNFα, IL-1ra, and IL-6, and stimulation of Th_{17} effector cell activation and proliferation.[42,156,157] Furthermore, dectin 2 recognition of house dust mite allergens generates allergic inflammation mediators known as cysteinyl leukotrienes in the lungs as activated by syk through FcRγ.[158]

The above studies only scratch the surface of natural ligand interactions with DCs and their subsequent immunological outcomes. Extensive reviews have been written highlighting these interactions and further detail will not be gone into here.[3,16,17,42,87,129,131,146,159–162] The understanding of natural ligands that can be bound by DCs and cause functional outcomes is important for clinical studies and for etiology of disease. It also has implications in ligand identification when the receptor has no known specificity and in molecular pathway elucidation. The advantages of using natural ligands for DCs is that, as long as the pathogen/parasite can be grown in vitro, large amounts of the ligand are able to be obtained. This leads to the ability to determine cellular readouts such as cytokine profiles, cell surface marker expression, and effector cell proliferation. Because the receptor is being engaged by its natural ligand the effects seen in these studies have direct physiological implications and a much greater

understanding of the range of responses possible for CLRs on DCs can be obtained. To this end, the above studies showed a range of DC responses and interactions spanning direct pro-inflammatory stimulation upon receptor ligation, to indirect tolerogenic phenotype inducement, and everything inbetween.[5,76,97,140,159,163] Thus, CLRs are a receptor class ripe with possibilities for clinical therapies

3.2.1.4 Synthetic ligands for CLRS

An underlying mechanism for the biological function of carbohydrates is multivalent recognition, which is being exploited in vaccine development by displaying multiple sugars on the backbone of a polymer to either promote or inhibit immunoreactivity.[164] However, these delivery systems are not as efficacious if they cannot mimic native tissue glycan presentation. Thus, strategies have been developed to promote immunoreactivity[165], such as combining antigens with naturally occurring glycan scaffolding (e.g. chitosan), and using adaptable supramolecular pseudopolyrotaxanes that multi-valently display mobile ligands that have rotational freedom about the polymer backbone.[165,166] These and similar polymer systems, when linked to an antigen, such as Diphtheria toxoid, have been shown to significantly increase antibody production over delivery of the antigen without polymer-glycan presentation. These systems have been shown to provide upwards of 47% antibody production increase upon rechallenge with the antigen, showing not only their effectiveness in initially creating adaptive immunity, but also in sustaining immune memory.[166,167] Similar glycan-polymer systems have also been used to inhibit infection and promote immune response by designing their carbohydrate moieties to mimic the glycan presentation seen in bacterial and viral surfaces.[164] These polymer-glycan systems act as "subunit" vaccines by helping stimulate the immune response against a specific bacteria or virus by synthetically inducing immune response against the outer surface components of the bacteria or virus without the actual infectant being present. Furthermore, vaccines are

targeted to DCs CLRs using glycans, particularly mannosylation of antigens[168,169] or of polymer carrier systems delivering the antigen[170–172] with significant enhancements in humoral immune responses and T cell stimulation, supported by DC maturation.

Conversely, multivalent carbohydrate presentation can also be used in immunosuppression by exploiting the tolerance pathways present in the immune system. In areas of high immunostimulation, such as the mucus lining in the lungs or gut, tolerance to foreign non-pathogenic antigens is common. The pathway for this tolerance is unclear; however, studies have begun to elucidate a complex relationship between CLRs and TLRs in tolerance to non-pathogenic antigens.[7] It has been postulated that if antigens do not present a known pathogenic moiety and do not stimulate other 'danger signals' from the surrounding tissue, then immunetolerance can occur.[7] Thus, polymer presentation of self-glycans in such a way as to mimic both density and composition of self-glycan could lead to tolerance. It has been shown that with an equivalent passivation system, tolerance to ovalbumin, a model antigen, can occur in vivo.[121,122] The immune evasion strategies of tumors[173] and viruses[174] based on glycan presentation appear to represent other immunosuppressive strategies. Such glycan-based immunosuppressive approaches could be applied to develop novel biomaterial surfaces to be used for tissue engineered and other implanted devices to induce immune-tolerance to the implanted device to enhance device integration and function. The research presented herein is aimed at discovering novel glycans with immunomodulatory effects for exploitation in a biomaterials context.

3.3 Overview of Glycan Nomenclature and Glycosylation of Proteins

Carbohydrates are referred to in literature under several headings: carbohydrates, sugars, saccharides, and/or glycans. Generally, they divided into four structural groupings: monosaccharides, disaccharides, oligosaccharides, and polysaccharides. These groupings indicate increasing structural complexity and thus also scale with

molecular weight of the carbohydrate. A typical carbohydrate consists of an aldehyde or ketone with many hydroxyl groups appended to it; generally a hydroxyl group is linked to each carbon atom that is not part of the aldehyde or ketone functional group of the carbohydrate. Examples of typical monosaccharides that follow this rule are glucose, fructose, and galactose. The hydroxyl rule is not a defining feature of carbohydrates as uronic acids and deoxy-sugars such as fucose are considered carbohydrates as well. At physiological temperatures carbohydrates exist in both a closed ring and open chain form. Mechanistically, the aldehyde carbonyl group carbon and hydroxyl group, from an open chain carbohydrate, reversibly react to form a hemiacetal (C-O-C) that closes the ring. This state is thermodynamically favored for most carbohydrates and thus most carbohydrates at physiological temperatures predominate in the closed ring form.[175] When the aldehyde/ketone reacts reversibly with the hydroxyl group a heterocyclic ring forms; these rings typically form to include five or six atoms and are called furanose and pyranose forms respectively.

While converting from the straight-chain form to the cyclic form, the anomeric carbon containing the carbonyl oxygen becomes a stereogenic center with two possible configurations either above or below the plane of the ring. The resulting possible pair of stereoisomers are called anomers. The α anomer contains the hydroxyl of the anomeric carbon on the trans side of the ring from the CH_2OH side branch. The β anomer contains the hydroxyl of the anomeric carbon on the cis side of the ring from the CH_2OH side branch. Because the ring and straight-chain forms readily interconvert, both anomers exist in equilibrium.[175]

Carbohydrates have very complex structures that are difficult to understand using IUPAC nomenclature. For instance lactose, a common disaccharide consisting of a glucose linked to a galactose is named β-D-galactopyranosyl-(1→4)-D-glucose under IUPAC standards. This naming strategy conveys much more information than would naming the carbohydrates by their atomic constituents ($C_{12}H_{22}O_{11}$) however, to convey

even moderately complex carbohydrate structures the names would take 100s of characters. Thus, a glycan nomenclature was developed by those in the field that used abbreviations for the glycan structures separated by their linkages. An example of this can be seen in Figure 1B and in the case of lactose would be Galβ1-4Glu. However, even this nomenclature can become untenable when trying to quickly assess the structure of complex carbohydrates such as those shown in Figure 1B and C. Thus, glycan symbol nomenclature was developed. The symbols and colors of carbohydrates can be seen in Figure 1A as well as an example of using these symbols to represent a glycan structure can be seen in Figure 1C. Using this nomenclature allows researchers to quickly and easily identify glycan components of complex polysaccharides and their linkage to each other.[176]

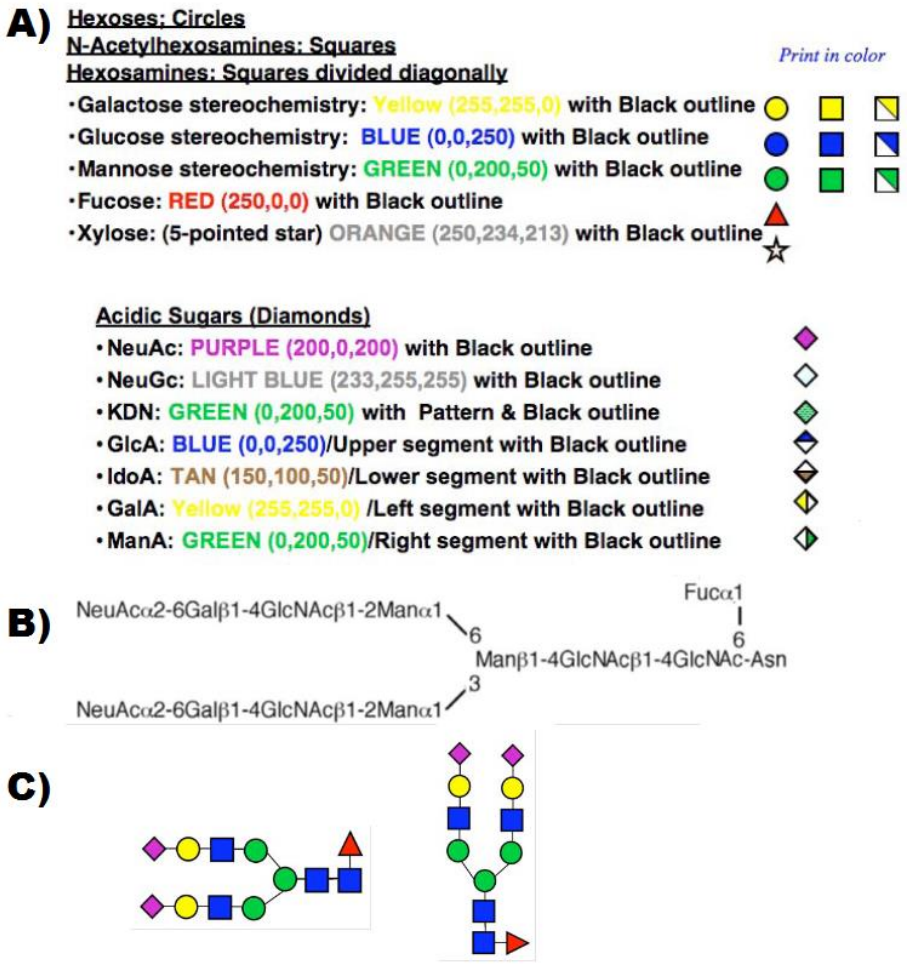

Figure 1: Carbohydrate symbol nomenclature.[176]

3.3.1 Glycosylation of Proteins

In Eukaryotes post translational modification of proteins predominantly occurs in the endoplasmic reticulum (ER) and Golgi apparatus. In both the ER and Golgi carbohydrates are added to proteins via enzymes known as glycosyltransferases. Additionally, many O-linked glycans are added to proteins in the cell cytoplasm.[176] Regardless of the location, most glycosylation reactions use activated forms of monosaccharides (most often nucleotide sugars) as precursors for reactions that are catalyzed by the glycosyltransferases. Functionally, post translation of a protein the protein is shuttled to the Golgi where specific glycosyltransferases attach saccharides to

the protein's polypeptide side chains. Two main classes of glycosylation occur Nitrogen-linked (N-linked) and oxygen linked (O-linked) and the glycosyltransferases for each of these classes are unique.

O-glycosyltransferases transfer *N*-acetylgalactosamine from UDP-GalNAc to serine or threonine residues, which is catalyzed by a polypeptide-N-acetyl-galactosaminyltransferase (ppGalNAcT).[176] There are at least 21 polypeptide-N-acetylgalactosaminetransferases (ppGalNAcT-1 to -21) that differ in their amino acid sequences and are encoded by different genes. [176] Post modification of the GalNAc residue occurs in the Golgi apparatus and appears to be a stochastic event in which the longer the residence time of the protein in the Golgi, the more modification of the protein occurs. This modification is performed by a plethora of glycosyltransferases and is heavily dependent on cell type, cell cycle status, extracellular signaling, etc.[176] However, in general each glycosidic linkage is the product of a single enzyme[176] (with a few exceptions not covered here). The human B blood group α1–3 galactosyltransferase provides an excellent example of such specificity.[176] This enzyme catalyzes a glycosylation reaction in which galactose is added in α linkage to the C-3 hydroxyl group of a galactose residue on the protein. However, the enzyme only acts on galactose containing fucose in α1–2 linkage. [176]

In contrast, N-linked glycans are initiated by the action of oligosaccharyltransferase, an enzyme that transfers the glycan Glc3Man9GlcNAc2 to the side chain of asparagine residues in the sequence motif Asn-X-Ser/Thr.[176] N-glycan modification begins on the ER membrane with the transfer of GlcNAc-P from UDP-GlcNAc to the lipid-like precursor dolichol phosphate (Dol-P) to generate dolichol pyrophosphate N-acetylglucosamine (Dol-P-P-GlcNAc).[176] Fourteen sugars are sequentially added to Dol-P before en bloc transfer of the entire glycan to an Asn-X-Ser/Thr sequence onto a protein.[176] The protein-bound N-glycan is subsequently remodeled in the ER and Golgi by a complex series of reactions catalyzed by membrane-

bound glycosidases and glycosyltransferases. Glycosidases are enzymes that remove monosaccharides to form intermediate sugar structures that are then able to be recognized by glycosyltransferases and have more sugars attached or removed from them. Most of these enzymes are sensitive to the physiological and biochemical state of the cell in which the glycoprotein is expressed.[176] Thus, the populations of sugars attached to each glycosylated asparagine in a mature glycoprotein will be completely dependent on the cell type in which the glycoprotein is expressed and on the physiological status of the cell, a status that may be regulated during development and differentiation and altered in diseases such as cancers and prion diseases.[176]

3.4 High Throughput Methodologies in Glycobiology and Immunology

A HTP approach is necessary to assess functional phenotypic effects of complex carbohydrates on DC phenotype for four key reasons. First, only limited amounts of oligosaccharides (typically at sub-µmol levels) can be isolated from natural sources when cleaved from proteins or lipids and they are highly heterogeneous in structure. [4,177–179] Second, the structural diversity of oligosaccharides leads to difficulties in their structural characterization; currently, there is a lack of an efficient means of automated assignment and the characterization is mainly reliant on expert interpretation by MS analyses.[180] Third, the biosynthesis of oligosaccharides is not template driven like DNA or protein synthesis, and thus the diverse repertoire of oligosaccharides that would be representative of the glycoform of a typical glycoprotein is extremely difficult to reproduce by chemical synthesis.[181–183] Fourth, most carbohydrate-protein interactions are of low affinity, and there is a requirement of multivalent presentation of carbohydrate ligands for detection of binding in microscale screening analysis.[104,105,184] To mitigate these concerns several approaches have been attempted by current laboratories. The most predominant approach is to create glycan microarrays using shotgun glycomics or solid state carbohydrate synthesis.

Currently, many high throughput screening technologies are being used to show relationships that they were not designed to elucidate and thus the results from these assays are said to only have "indications" for further study. The most common and well known is genomic and transcriptional HTP screening using DNA and RNA microarrays that are used to measure the change and/or quantity of transcription that occurs in cells in response to a challenge. While these assays are excellent to determine what is happening to a cell in terms of transcription, it has been confirmed many times and in multiple models that transcriptional activity does not necessarily directly relate to translational activity, which does not necessarily lead to functional protein expression/ secretion. Thus, because the assay does not directly show functional effects many more, non-HTP, techniques must be used in order to actually confirm what was implicated in the original HTP assay. This process, while significantly reducing the complexity of the original problem, is not ideal as the HTP assay tells very little about actual functionality and in order to add this level of analysis non-HTP techniques that are very time and resource intensive must be employed. Ideally, HTP screening utilizes only HTP strategies and directly assesses what the investigator is interested in. To address this need many novel HTP strategies are being developed, specifically in immunology, where assessment of relevant effector functions are critical for designing potent therapies. Immunology presents a unique level of complexity in that it involves an unusual dearth of interactions. The complete immune response requires an analysis of surface molecule expression, intra and intercellular interaction, secreted molecules, and temporality of these factors. Just a few of the functional outcomes of these processes is a recruitment of other immune cells to the site of infection, secretion of pro- or anti-inflammatory molecules, development of distinct cellular phenotypes, clonal expansion of cells, cell inactivation/death, antibody production, etc. These outcomes all rely on multiple factors occurring simultaneously or in a specific time frame and sequence in order for them to elicit the desired immune response.[64] Thus, designing a HTP strategy that can monitor multiple factors over a

relatively long time course (days) is necessary for the investigator to obtain an idea of the functional effect of their treatment. This has yet to be seen in the literature. The current state of the art for high throughput technology in immunology involves one of ten reporters:

1. Live dead assays to determine a ligand or biomaterial cytotoxicity[185]
2. Cellular proliferation[186]
3. Phagocytosis of functionalized micro/nano-particles[187–189]
4. Adherence/migration assays to determine if ligands affect cell binding and migration[187,190]
5. Transcriptional analysis of RNA or DNA regulated after stimulation[191–193]
6. Proteome analysis [194]
7. Colorimic or fluorescent production obtained from immune cell transduction/ tranfection[195,196]
8. Colorimic or fluorescent production obtained from non-immune cells transduced to produce immune receptors[197]
9. Assessment of phosphorylation of key intracellular intermediates[198,199]
10. Microarray analysis of recombinant proteins to determine if receptors found on leukocytes can bind to a variety of ligands[200–202]

Reporters one through three are binary assays in that they measure the extent that an outcome either occurs or does not occur. While if a cell lives, proliferates, or phagocytosis a particle in response to a challenge is useful information to know, the immune response is a much more complex and intricate process than the above factors. An analysis of functional intermediaries such as soluble factors and surface marker expression are not assessed in these methodologies and in order to understand the immune response these factors must be analyzed. In particular DCs are insensitive to reporters two and three because they are not typically considered proliferative cells[203] and thus their proliferation or lack thereof has little immunological consequence. Similarly,

phagocytosis can lead to a variety of phenotypes in DCs or no change in phenotype at all[45,204,205] and thus phagocytosis is also a poor reporter for DC function.

The fourth reporter, cellular adhesion/migration, is a poor indicator of DC phenotype as DCs up and down regulate many adhesion receptors throughout their maturation process.[206] The end result of this maturation process, whether its pro or anti-inflammatory, CD4 or CD8 stimulating, etc. is independent of adhesion and thus, adhesion is also not an ideal reporter for DC, and in general APC, activation.[207]

The next two factors are also not ideal candidates to assess DC phenotype because of their inability to be used across a large number of treatments in a cost effective manner. Proteomic microarrays are able to assess a large variety of secreted proteins simultaneously and if cells are lysed they are also able to assess the expression of many intracellular proteins. However, each array can only be used once and are extremely costly to purchase or develop. Thus, each treatment you perform on your DCs requires its own assay which, if you have a 100 treatment groups, means you must have 100 separate assays. This approach also doesn't account for temporality of expression which is also a factor in immunology and therefore more assays would be needed to determine the protein expression as a function of time. Therefore, while an extremely powerful method, proteomic analysis is too cost prohibitive in its approach to screen multiple treatment groups. A discussion of the other limitations of using transcriptional DNA/RNA microarrays have been discussed previously in this review and will not be further expounded upon here.

Reporters seven and eight, cell transfection/transduction assays, are limited in several respects. First, these assays utilize a reporter for a single protein such as NF-κB and then quantify how much of this factor is expressed in the cells over different treatments. Because the immune response involves multiple secreted and surface presented proteins an analysis of a single factor, even a very important factor such as NF-κB, is insufficient to determine the functional immune response. Secondly, DCs are very

difficult to stably transfect or transduce and are canonically thought to be completely insensitive to transduction.[203] While recent reports have shown that transfection of DCs is possible, the efficiency of transfection is still relatively low, the amount of plasmid used to achieve this transfection very high, and the transfection was only seen transiently.[196] Thus, transfecting DCs is still not a viable option for true high throughput screening because of its relative cost and time commitment as well as its limited timespan for use as a reporter. Successful transduction of DCs has also recently been reported, however the MOI to transduce the cells efficiently was very high[195] and thus this methodology is also not seen as a truly viable approach as it is cost prohibitive to transduce multiple donors at a quantity of cells that is high enough to be able to use in HTP screening.

Reporter nine, protein phosphorylation, has broad applicability for identifying signaling intermediates in a signaling cascade. It has been shown that the phosphorylation of key signaling proteins such as JAK and STAT can be measured in high throughput arrays with great specificity.[198,199] However, these proteins are not the functional effectors of the cells. Thus, what the actual phenotypic outcome of the phosphorylation of these proteins is remains unknown with these assays. Dendritic cells utilize the same signaling proteins across multiple receptors, (MyD88, TRIF, TRAF, etc.)[64] and thus the increased/decreased phosphorylation of any of these signaling intermediates is not able to identify specifically what proteins were stimulated and what the likely functional outcome will be.

3.5 Engineered Presentation of Glycans to Dendritic Cells

In order to harness and modulate DC phenotype in a controllable manner with CLRs a more mechanistic understanding of how specific glycan structures, presentation modalities, and molecular environments effect DC phenotype and systemic immunity must be had. Natural ligands are often complex and heterogeneous in nature and can provide confounding factors to mechanistic studies. In the majority of the studies

previously mentioned there were multiple opportunities for confounding ligand-receptor interactions, e.g., through protein epitopes, opsonization of the carrier, non-specific recognition by other CLRs, etc. While these studies were well done and had appropriate controls their models did not allow for a controlled mechanistic assessment of DC interaction. Thus, it makes elucidation of exact molecular motifs and environments necessary for modulation of DC behavior (whether that be pro-inflammatory, tolerogenic, or phagocytic) difficult. Several studies have attempted to do this and from them better understanding of exact molecular characteristics necessary for modulation of DC phenotype have been found.

3.5.1 Glycan Structure and Dendritic Cell Phenotype

In an elegant study by Wattendorf et al. human DCs were cultured with phagocytosable polystyrene microbeads functionalized with di-branched PLL-PEG that had a man, triman (α1-3 α1-6), or mannan attached to the end of the PEG branch.[107] The mannan and PLL were passively adsorbed onto the PS beads leaving the mannan and PEG functionalized glycan monomers free in solution instead of being found on the bead surface. This PEG branch coating had been found previously to remove non-specific protein adsorption and thus interactions with the bead were mediated solely by the intended glycan-lectin interactions. A comparison of phagocytosis between sugar structures was performed and it was found that the mannan coated particles had the highest uptake, followed by the mannose, with the lowest phagocytosis seen in the triman functionalized particle. In general, however, mannose-mediated phagocytosis was lower than other reports in the literature and was not statistically higher than RGD immobilized in an identical system. The paper accounts the absence of other mediators in the conjugate, such as lipid components in the lipisome used by other groups, as the reason for this lower uptake. Also, the study took the beads that showed the highest level of phagocytosis for the mannan, tri-man, and mannose and looked at DC surface marker

expression after incubation with these conjugates. No change was seen in CD80, CD86, and MHCII from iDCs for any of the conjugates, including the mannan. The negative outcome of the mannan conjugates goes against previous studies that showed that mannan was an immune agonist.[108,208,209] However, in these studies mannan was combined with particulates based on liposomes linked through membrane lipids, such as cholesterol[108] or palmitoyl-mannan.[208] Therefore, it could have been the synergistic effect of the lipids and the mannan that led to these activation reports. This implies that the Th1/Th2 cell proliferation that was seen in these studies, that were thought to be mediated through mannan, may not represent the result of the ligand alone but through the synergistic recognition of the conjugates by TLR4 and CLRs. Unfortunately, in the Meyer-Wentrop et al. study no analysis of cytokines was performed and thus the phenotype of the cells remains elusive as several reports have shown differential cytokine profiles without up-regulation of surface receptors in response to CLR stimulation.[49,81,126]

Several labs have shown the high specificity of lectins by taking recombinant forms of the receptors and incubating them with glycan structures of interest or with glycan microarrays. Feinberg et al. did one of the most thorough analysis of glycan binding specificity of DC-SIGN to carefully controlled glycan structures. In this paper it showed that di-mannose and tri-man structures have a higher affinity for DC-SIGN than did mannose alone and that either of two Man6 isomers bind with similar affinity which was 9–14-fold higher than mannose, whereas two isomers of Man9 bound approximately twice as strongly then the Man6 glycans. The full Man9GlcNAc2 glycan consistently showed 2–3-fold stronger binding than either of the Man9 isoforms. In general anything with an α1-α2 mannose linkage showed a drastically higher binding affinity than did those structures that did not and that branched structures bound with higher affinity than did linear structures. Another study by van Vliet et al. showed high specificity for MGL to terminal GalNAc structures when coupled to a variety of sugar backbones. While binding affinity wasn't directly assessed in this study amount of binding of glycan to an

array, a rough proxy for binding affinity, was assessed and it was found that terminal GalNAc structures showed a 12-20 times higher amount of binding than did non-GalNAc structures.[78] Similar results to the DC-SIGN study have been confirmed by other researchers across different systems and array based assessment of other several other lectins have been performed by multiple researchers and thus these results are seen as robust and applicable to in vitro receptor specificity.[101,210–213]

3.5.2 Molecular Factors of Glycoconjugates and DC Phenotype

In the study by Wattendorf et al. mentioned above not only was the glycan structure altered in a controllable fashion but also the density of the displayed ligand was varied. Carbohydrate density on the microspheres' surface was controlled through the adsorption of polymer mixtures with (ligand-free) PLL-PEG and mannoside functionalized PEG. Two linker lengths were also chosen to allow for adjusted glycan mobility for receptor binding. It was found that the efficiency of phagocytosis by DCs increased with increasing amounts of mannose exposed from microspheres' surface regardless of sugar structure used.[109] This was in agreement with the findings of other groups with different platforms for sugar presentation, such as mannosylated emulsions[214] or liposomes.[215] While the characterization of the DC phenotype in each of these studies was limited, generally it was found that regardless of sugar structure DC phenotype was not altered but phagocytosis was statistically increased as sugar density was increased. Also, in a study varying density of anti-bodies to Dec-205 on the surface of nanoparticles the amount of anti-inflammatory cytokines increased with increasing amounts of Abs immobilized on the bead surface.[99] Furthermore, the phagocytosis of the beads was also shown to increase. While, this study was not a ligand for the CLR it does show phenotypic modulation of DCs with increasing ligation of CLRs.

To date no direct studies have been performed that compare how charge of a glyco-conjugate alters DC phenotype. However, historically cationic vaccine conjugates

have been found to play an important role in increasing the immune response to any conjugate.[24–28] The addition of protamine (small, arginine-rich, nuclear proteins that are highly positive) is a common component in microparticle vaccines to enhance immunogenicity. Protamine has been shown to produce more potent anti-tumor vaccines,[216] non-viral transduction of cells, enhanced siRNA delivery,[217] enhanced allergy vaccine efficacy[218], etc. Another cationic polymer, poly L-lysine (PLL), has been shown to induce similar effects but in a more tunable fashion due to its ability to be engineered to desired lengths and levels of branching. [219–221] Furthermore, several cationic glycan carriers have shown increased phagocytosis higher than that of other reported glycoconjugates.[222] Due to these reports carrier charge appears to be a promising field where little direct research has been done in the glycoimmunology field.

Finally, the carrier and linker that a glycan is attached to could play a large role in how the glycan is recognized and in what way DC phenotype is affected. This has not been shown directly in immune cells. However, Andre et al. displayed glycans to cells expressing transduced forms of CLRs and compared cell adhesion to glycan presenting compounds across flexible and rigid scaffolds and also compared differing spatial arrangement of ligands presented on two rigid macrocyclic scaffolds.[223] They found that reduction of the inherent level of flexibility of the linker had a favorable impact on cell binding especially for cells displaying a high CLR density, and the structure of the carrier can modulate inhibitory potency when comparing different lectins. This not only shows that lectin affinity can be modulated via linker properties but it also shows that different lectins have a differential ideal molecular signature that is optimal for maximum glycan binding. In addition to conformational restraints it was shown that three-dimensional presentation of glycans drastically altered cellular adhesion.[223] While a fully reductive study has not been performed with DCs the important role that carrier and linker play in CLR recognition in DCs can also be indirectly observed by the differential phenotypes noted in the papers displaying mannan to DCs via differential linkers.[108,208] Cui et al.

utilized cholesterol as the linker and found enhanced CD80 and CD86 levels on the surface of DCs and increased peptide presentation by the MHC class-1 molecule.[108] While the paper by Jain et al. showed DC phenotype that had been pushed toward increasing the Th_2 responses due to increased IL2 and MHC class II presentation. The conclusion that carrier properties can modulate DC response was further supported by literature from van Stijn et al.[149] which showed that recognition of soluble glycolipid motifs were able to activate DCs but could not activate DCs with any single component of the carrier.

3.5.3 Modality of Glycan Display Altering DC Phenotype

Soluble and phagocytosable glycan presentation to APC has been studied but little direct comparative data between the two and no comparison to non-phagocytosable well surface displayed glycans has been seen.[20,21] Furthermore, due to the extremely limited supply of well-defined oligosaccharides capable of being obtained via synthetic or biological means surface interaction with recombinant CLRs or other lectins to glycan microarrays has been used as a proxy for direct cellular response for glycoconjugate creation and therapeutic approaches.[22,23] The experiments performed herein seek to address these issues by use of a novel cellular HTP methodology perfected in house.[224] This method allows for an order of magnitude less glycan to be used than previous functional assays, both pro- and anti-inflammatory immune responses to be monitored, and testing of multiple surface display modalities simultaneously. Additionally, the studies performed here challenge the conventional view that glycan structure and density of presentation alone determines phenotypic modulation of DCs.

Several studies have analyzed the cell response to glycans between soluble and particulate modalities but these studies used complex not well defined systems to identify differential activity that could be confounded by a variety of factors. For instance Qi et al.[225] looked at the differential effect of β-glucan in particulate (nanoparticle) and soluble

form on DC phenotype. They found that β-glucan particles, derived from yeast, activated DCs and macrophages via dectin-1 stimulation and that β-glucan delivered in its soluble form caused no increase in activation markers.[225] When used in an in vivo study the particulate delivered β-glucans showed potent anti-tumor effects: down-regulating T_{regs} and delaying tumor progression while the β-glucan in soluble form had no therapeutic effect but significantly augmented antitumor monoclonal antibodies.[225] However, the β-glucan particles were not characterized for molecular weight, size, glycan structural composition, and were known to have variability in protein composition. All of these factors could easily influence the affects seen and confound the results obtained. Another study comparing particulate and soluble presented carbohydrates was performed by Le Cabec et al.[112] who showed that when chinese hamster ovary (CHO) cells were transfected to express mannose receptor (MR) it mediated endocytosis of mannosylated glycoproteins in solution but did not support phagocytosis of three of its known particulate ligands: zymosan, Mycobacterium kansasii, and mannosylated latex beads. The cells were shown to possess phagocytic machinery when other receptors were expressed on them and thus it was concluded that MR alone was not sufficient to trigger phagocytosis and that there must be co-stimulatory receptors on macrophages and DCs that, in concert with MR, were able to cause phagocytosis. Furthermore, a differential response from DC receptor ligation when identical ligands were presented in different modalities was shown in this study. However, in this study CHO cells were transduced to express human MR and therefore strict conclusions between these cells and naturally occurring DCs/macrophages is difficult.

A variety of studies have shown that modulation of DC phenotype with phagocytosable nano- and micro-particles bearing carbohydrates is possible.[107,108,208,209,226] These studies have shown that increased ligand density as well as sugar structure play an important role in phenotype modulation. Thus, it is known that particulate delivered glycans are able to be seen and recognized by DCs but no comparisons have been

performed as to whether this response is consistent when ligands are displayed across different modalities.

Non-phagocytosable surface display of glycans has not been as intensively studied as soluble and particle delivery of glycoconjugates. However, van Vliet et al. showed that GalNAc (Tn antigen) when immobilized on a non-phagocytosable surface, drastically alters DC mobility as compared to other sugars.[20] The Tn antigen has also been shown to affects DC differentiation and maturation[227] whereas MUC1 purified from tumor cells, which is extremely high in GalNAc, induced differentiation of DCs, but prevented the development of an efficient Th_1-type response.[228] Napoletano et al. observed that a Tn- conjugated protein did not affect DC differentiation or their ability to produce IL-12p70 and that Tn-protein can specifically bind MGL expressed by iDCs and this binding resulted in the internalization of the glycopeptides and their delivery into HLA class I and II compartments.[229] Furthermore, several labs have shown the high specificity of lectins by taking recombinant forms of the receptors and incubating them with glycan structures of interest or with glycan microarrays. A study by van Vliet et al. showed high specificity for MGL to terminal GalNAc structures when coupled to a variety of sugar backbones.[78] While binding affinity wasn't directly assessed in this study amount of binding of glycan to an array, a rough proxy for binding affinity, was assessed and it was found that terminal GalNAc structures showed a 12-20 times higher amount of binding than did non-galNAc structures.[78] Similar results have been seen with DC-SIGN and have been confirmed by other researchers across different systems and have been performed by multiple researchers and thus these results are seen as robust and applicable to in vitro receptor specificity.[101,210–213] In conclusion, from these reports it is clear that modality of presentation of glycan to DCs drastically alters the outcome and that a direct comparison between display modalities using well defined ligands is needed.

3.6 Motivations for Research

From the literature review it is clear that DCs are powerful immunomodulators and that the lectins they express have the ability to tune the DC phenotype toward a pro-inflammatory or anti-inflammatory phenotype. Furthermore, glycan presentation to DCs has been shown to produce sensitive and specific immune responses from DCs. Thus, it is hypothesized that glycans could have significant impacts when designing the next generation of biomaterials and combination products. However, from Chapter 3.5 it is clear that current research has focused little attention to non-phagocytosable display of glycans to DCs. To date few studies have placed glycans on a non-phagocytosable surface and analyzed the DC response to the presented glycans. Thus, little information is known about optimal molecular factors for phenotype modulation of DCs toward a pro-inflammatory or anti-inflammatory state. If glycans are to be used in biomaterial coatings or combination products a more in-depth knowledge of the molecular factors important for DC stimulation must be had. Also, no evidence linking the DC response to glycans and glycoconjugates delivered across different presentation modalities has been seen in the literature. This is of importance to the field because with the growing popularity of glycan microarrays in glycomics it is critical that an association between lectin binding on these surfaces and functional cell responses in vitro and in vivo be obtained. Finally, due to the extremely limited supply of complex glycan structures that are capable of being obtained, in-depth, fully reductive cell response to glycans and glycoconjugates experiments are almost impossible to perform. Thus, it is thought that modeling can solve these problems by identifying molecular factors of importance for simple sugars and extrapolating them to more complex sugar structures. This has been performed previously with other materials and DCs[47,55] and thus it is expected that modeling can be used with glycans to predict DC phenotype in response to surface presented glycoconjugates.

CHAPTER 4 ELUCIDATION AND OPTIMIZATION OF PERTINENT MOLECULAR FACTORS FOR DENDRITIC CELL RESPONSE TO ADSORBED GLYCOCONJUGATES

4.1 Overview

Optimal molecular factors for glycans presented from non-phagocytosable surfaces to DCs for maximal phenotypic modulation has not been studied to date. Due to the pleiotropic effects of CLRs in DCs, the optimization of presentation of glycans to the immune system has implications in both vaccine design and implanted devices where a tolerogenic immune response is desired. This study began with an assessment of carrier appropriateness for glycan presentation to DCs using a novel, in house, high throughput assay. Then DC response to a range of carriers that had been engineered to vary in charge and density of glycan presentation was assessed. Next, the properties of the carrier were modeled using a multivariate regression and trends for ideal properties of non-phagocytosable display of glycan for maximal DC inflammatory response were identified. The DC response to the adsorbed conjugates was then assessed in the presence/absence of EDTA to determine the CLR dependence of the interaction with the conjugates. Next, conjugates were created with the optimized carrier charge and density found from the modeling but with six new complex carbohydrate structures. Finally, after assessing DC phenotype to these conjugates a model was created to assess the importance of various structural motifs found in the carbohydrate structures.

It was found that highly cationized (pI above 9.75) high density (more than 20 glycans/BSA) glycoconjugates were able to stimulate DC phenotype to the greatest extent. Furthermore, DC response to these conjugates was mediated by EDTA and therefore inferred to be CLR mediated. Finally, DC response to optimized conjugates presenting oligomannose glycans was found to be structure dependent and when modeled, unique epitopes were found to be predictive of DC phenotype.

The experiments in this chapter show that density of glycan display and charge of carrier are critical for significant alteration of a proinflammatory maturation factor used to assess DC phenotype. This response is mediated by lectins and is structure specific as several polymannose structures did not show DC maturation. Furthermore, the model from this chapter show that grouping glycan structure by terminal glycan motif significantly influences a proinflammatory maturation factor used to assess DC phenotype. The exact molecular mechanisms for why and how phenotype modulation is occurring were not uncovered in this report but future works are discussed to address this shortcoming.

4.2 Materials and Methods

4.2.1 Fluorescent Modification and Biotinylation of Glycans

Isolation, functionalization, and quantification of Man5-br was performed via an established method.[210] Briefly, ribonuclease B (RNase B) was denatured using a denaturing buffer (20%SDS, 2.5M Tris pH 6.8, 14.3mM beta-mercaptoethanol) at 100˚C for 10 minutes. The solution was then allowed to cool and the denatured protein was digested using pronase. After digestion the RNase B was diluted 1:5 with Nonidet-P40 and 1:5 of solution of 50 mM Sodium Phosphate and the N-linked glycans were removed by Peptide N-Glycolsidase F (PNGase F). The cleaved free reducing glycans were then isolated via carbograph and C18 cartridges (Pierce).

The glycans were then functionalized with a fluorescent linker to be used to further purify and isolate individual glycan structures. This functionalization was done using a 90mg/ml 2-Amino-N-(2-amino-ethyl)-benzamide (AEAB; A gift from Dr. Richard Cummings, Emory University) solution which was prepared in a DMSO/Acetic acid (7:3 v/v) solution. To this solution $NaCNBH_3$ was added to a concentration of 1M,

64mg/ml. To this solution free reducing glycans were quickly added at a molar ratio of 1:10 to the AEAB. The solution was vortexed heavily for 20 seconds and allowed to react for three hours at 65˚C. After which acetonitrile was added to the solution at a 10:1 volume ratio and vortexed. The solution was then cooled to -20°C and spun down at 10,000g for 5 minutes. The supernatant was aspirated and discarded and the glycan-AEAB/AEAB pellet was vacuum centrifuged for 2 hours or until the remaining pellet was completely dry. The pellet was then dissolved in 1ml of water and fractions were collected using reverse phase HPLC with an excitation of 330 nm and emission at 420 nm. The collected conjugates were then frozen and lyophilized.

Glycan-AEAB conjugates were thiolated via Traut's reagent using a known protocol.[230] Briefly, Glycan-AEAB conjugates were dissolved in 2 mM endotoxin free EDTA (Sigma). A 10 fold molar excess of Traut's reagent (Pierce) was then added to the protein solution and allowed to react for one hour at room temperature. After conjugation the glycoconjugates were purified using 10K Membrane Centrifugal Filter Unit (Milipore) using 9 rounds of 1:10 buffer exchanges against distilled, endotoxin free, water. The glycan solutions' sulfhydryl groups were then measured using Ellman's Reagent (Pierce) and compared to a standard thiol solution for molar concentration.

Glycan-biotin conjugates used in the carrier selection study were created using thiol-OEG2 functionalized glycans (Sussex Research) and maleimide-PEG_2-biotin (Pierce) using a standard protocol.[231] Briefly, thiol-OEG_2 functionalized glycans (Sussex Research) were reduced in TCEP reducing gel (Pierce) in sealed spin cups (Pierce) for one hour in degassed buffer 1 (0.1M EDTA, 0.15M NaCl, 0.1M NaH_2PO_4) at room temperature while shaking at 600RPM. Glycans were then spun down at 100 RCF and the resultant effluent was immediately added to 20mM maleimide-PEG_2-biotin to a concentration of 10 to 1 molar ratio of biotin to glycan. The maleimide-PEG_2-biotin was dissolved in moisture free DMSO prior to addition of the glycan solution. The solution was allowed to react overnight at 4°C

4.2.2 Carrier Functionalization and Purification

Thiol-OEG_2 functionalized glycans (Sussex Research) or OEG_3-SH (A kind gift from Dr. Daniel Ratner) were reduced in TCEP reducing gel (Pierce) in sealed spin cups (Pierce) for one hour in degassed buffer 1 (0.1M EDTA, 0.15M NaCl, 0.1M NaH_2PO_4) at room temperature while shaking at 600RPM. Glycans were then spun down at 100 RCF and the resultant effluent was immediately added to 1mg/ml Maleimide functionalized carrier protein, OVA or BSA (Pierce) in the indicated molar ratio as compared to the maleimide functionalized carrier (0:1, 1:1, 25:1 or 100:1 sugar: carrier ratio). The conjugates created for the initial carrier selection study were all reacted at 100:1 sugar to carrier molar ratios. The carriers were dissolved in degassed Buffer 1 and after combining the reduced glycan and the carrier, argon gas was passed over the solution and the tubes were sealed with paraffin and allowed to react for 16 hours at room temperature. After conjugation the glycoconjugates were purified using 10K Membrane Centrifugal Filter Unit (Millipore) using 9 rounds of 1:10 buffer exchanges against distilled, endotoxin free, water. The glycoconjugate solutions were then assessed for their protein concentration using a micro-bicinchoninic acid (BCA) assay and resuspended at 1mg/ml. Conjugates with permanently opened rings were created via periodate oxidation and sodium borohydride reduction via the standard protocol.[232]

An identical procedure was followed for the GlcNAc, Man3-Br, Man3-A2, Man4-A2, Man5-Br, and Man5-A conjugates except that only a molar ratio of 100:1 glycan:BSA was used. All glycan thiols were given by Dr. Daniel Ratner, University of Washington or produced as discussed in section 4.2.2 of this document and thiolated via Traut's reagent (Pierce).

4.2.3 Cationization of Carrier

Prior to beginning cationization, three solutions of ethylenediamine (EDA) (0.1, 0.3, or1.8M) were prepared and pH adjusted to pH 4.5 using 2M NaOH and ultrapure

endotoxin free water. Additionally, a 200mg/ml 1-Ethyl-3-[3-dimethylaminopropyl] carbodiimide hydrochloride (EDC or EDAC; Pierce) was prepared using ultrapure endotoxin free water. Using a stock 1mg/ml glycoprotein solution a 1:1 volume ratio of EDA was added to the glycoprotein making the final concentration of EDA 0.05, 0.15, or 0.9M. 0.9M EDA was used in all cases where excess EDA is specified. To these solutions EDC was added until EDC reached a 7.5mM concentration. The resultant glycoprotein, EDA, and EDC solution was then immediately vortexed for 30 seconds and allowed to react for two hours at room temperature while being shaken at 900RPM. Then, 0.5 volume percent of 4M acetate buffer, pH 4.75, was added to the glycoprotein solutions to quench the EDC reaction. After conjugation the glycoconjugates were purified using 10K Membrane Centrifugal Filter Unit (Millipore) using 9 rounds of 1:10 buffer exchanges against distilled, endotoxin free, water. Figure 2 shows an overview of the process of creating each of the conjugates and gives a list of all 40 conjugates created.

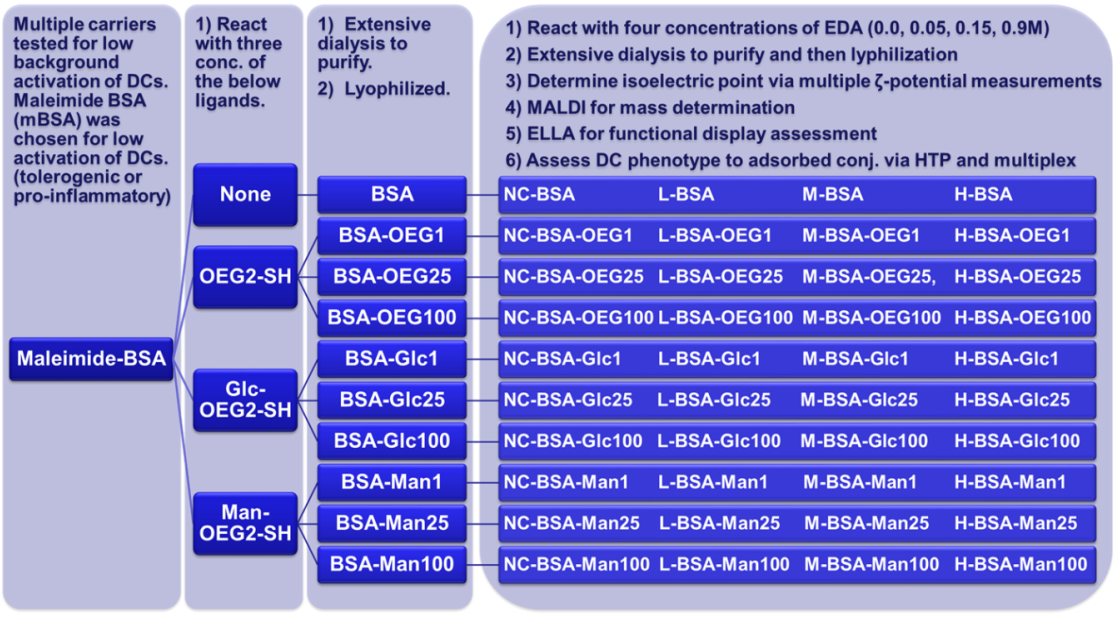

Figure 2: Process and characterization methodology that was used to create the 40 conjugates tested in Figure 9.

4.2.4 Streptavidin Preparation and Glycoconjugate Presentation

A 384 well tissue culture polystyrene (TCPS) plate was coated with 20µg/ml streptavidin or 20µg/ml of the BSA glycoconjugates overnight at room temperature. Next, for the streptavidin coated wells, the plates were washed 5 times with a wash solution 1 (1mM PBS, 0.5mg/ml HSA, and 0.01% TWEEN20) and then biotinylated glycans at 40µM were incubated in the plate for 2 hours at 37°C. Then, all the wells were washed with complete DC medium (RPMI-1640 (Invitrogen) supplemented with 10% heat inactivated fetal bovine serum Cellgro MediaTech) and 100 U/ml penicillin/streptomycin (Cellgro MediaTech)) and blocked for two hours at 37°C with 5mg/ml biotin free HSA in 0.1M $NaHCO_3$. After blocking the plates were then washed 5x with complete DC media and 40 µl of cells at 7.5x 10^5 cells/ml were added to each well.

4.2.5 Preparation and Assessment of ζ-Potential, Mass and Endotoxin Content of Glycoconjugates

Mass spectra of the cationized and non-cationized glycoconjugates were determined using Matrix Assisted Laser Desorption Ionization (MALDI) Mass Spectrometry. The glycoconjugates were first dissolved in ultrapure, endotoxin free water, and then were spotted in a 1:1 vol. ratio with diammonium hydrogen citrate (DHC) onto a MALDI plate. A linear positive detection method was used for the conjugates. Mass profiles were then exported, plotted and the mean of each mass peak was determined. After verification of functionalization and determination of number of glycans/BSA the glycoconjugates were then resuspended at 3.0 mg/ml in PBS, aliquoted and frozen for later use.

To determine the isoelectric point of all glycoconjugates conjugates were diluted to 500ng/ml in ultrapure endotoxin free water and then each conjugate was divided between five different cuvettes. The pH in each cuvette was then adjusted to 3.0, 5.0,

7.0, 9.0, or 11.0 using 1M sterile NaOH or 1M sterile HCl. Using a Malvern Nano-zetasizer the ζ-potential and hydrodynamic radius of each solution was then determined. The pH vs the ζ-potential was then plotted and the subsequent isoelectric point of each conjugate was then determined via interpolation of the least squares regression to which point the ζ-potential equaled 0. The solutions for each conjugate were then recombined, lyophilized, quantified via BCA assay, resuspended at 3000ug/ml in PBS, and aliquoted and frozen for later use.

The endotoxin contents of the glycoconjugates at a concentration of 100µg/ml (5x the coating concentration used) were measured using an endotoxin assessment kit (QCL-1000 LAL assay, Lonza). Briefly, 50µl of 100µg/ml of pre-warmed glycoconjugates in PBS were incubated at 37˚C with 50 µl of LAL Proenzyme for 10 minutes. Next, 100µl of chromogenic substrate was added and allowed to incubate for six minutes. Then 100 µl of 25% (v/v) Glacial acetic acid in distilled water was added to stop the reaction. The absorbance at 405 nm was taken for conjugates and standards and the endotoxin content of all glycoconjugates was determined to be less than 0.2 EU/mL, which is well below the FDA limit of 0.5 EU/mL. Furthermore, all mannose conjugates were below the detection limit of the assay for endotoxin content. All conjugates tested in this paper were from a single preparation and thus the parameters determined by the above procedure are applicable for all figures and tables seen in this report.

4.2.6 Enzyme Linked Lectin Assay for Adsorbed Glycoconjugates

A tissue culture polystyrene (TCPS) plate was coated with 20µg/ml streptavidin or 20µg/ml of the cationized BSA glycoconjugates overnight at RT. Next, for the streptavidin coated plates, the plates were washed 5 times with a wash solution 2 (1mM PBS, 0.5mg/ml BSA, and 0.01% TWEEN20) and then biotinylated glycans at 40µM were incubated in the plate for 2 hours at 37°C. Then, all the plates were washed and blocked for two hours at 37°C with 5mg/ml biotin free HSA in 0.1M NaHCO3 and 0.1%

TWEEN 20. After blocking the plates were washed 5x with the wash solution 2. Next, a lectin specific for the given sugar 15 µg/ml Narcissus pseudonarcissus-biotin (NPA-biotin) (EY Labs; specific for α-D-mannose) or 15 µg/ml Concanavalin A-biotin (ConA-biotin) (Sigma; specific for mannose or glucose) was incubated with the adsorbed conjugates for two hours at 37°C. The plates were then washed 5 times with the wash solution 2 and 50µl of a streptavidin-HRP (BD Pharmingen) solution diluted 100x with PBS from stock was added to each well and allowed to incubate in the well for 2hrs at RT. The plate was then washed 5x more with the wash solution 2 and a TMB (3,3',5,5'-tetramethylbenzidineperoxide) substrate (BD Pharminogen) was added and the plates allowed to develop for 10 minutes. Then, 1.0N sulfuric acid was added to stop the reaction and the absorbance at 450nm was determined. A preliminary study was performed and it was found that for all biotinylated sugar structures 4000 pmol of biotinylated glycan needed to be delivered per well, (40 µM) in order for binding sites to be maximized, data shown in Appendix Figure A 1. Figure 3 below shows the overall process used in this assay for either streptavidin presented glycans or BSA-adsorbed glycoconjugates.

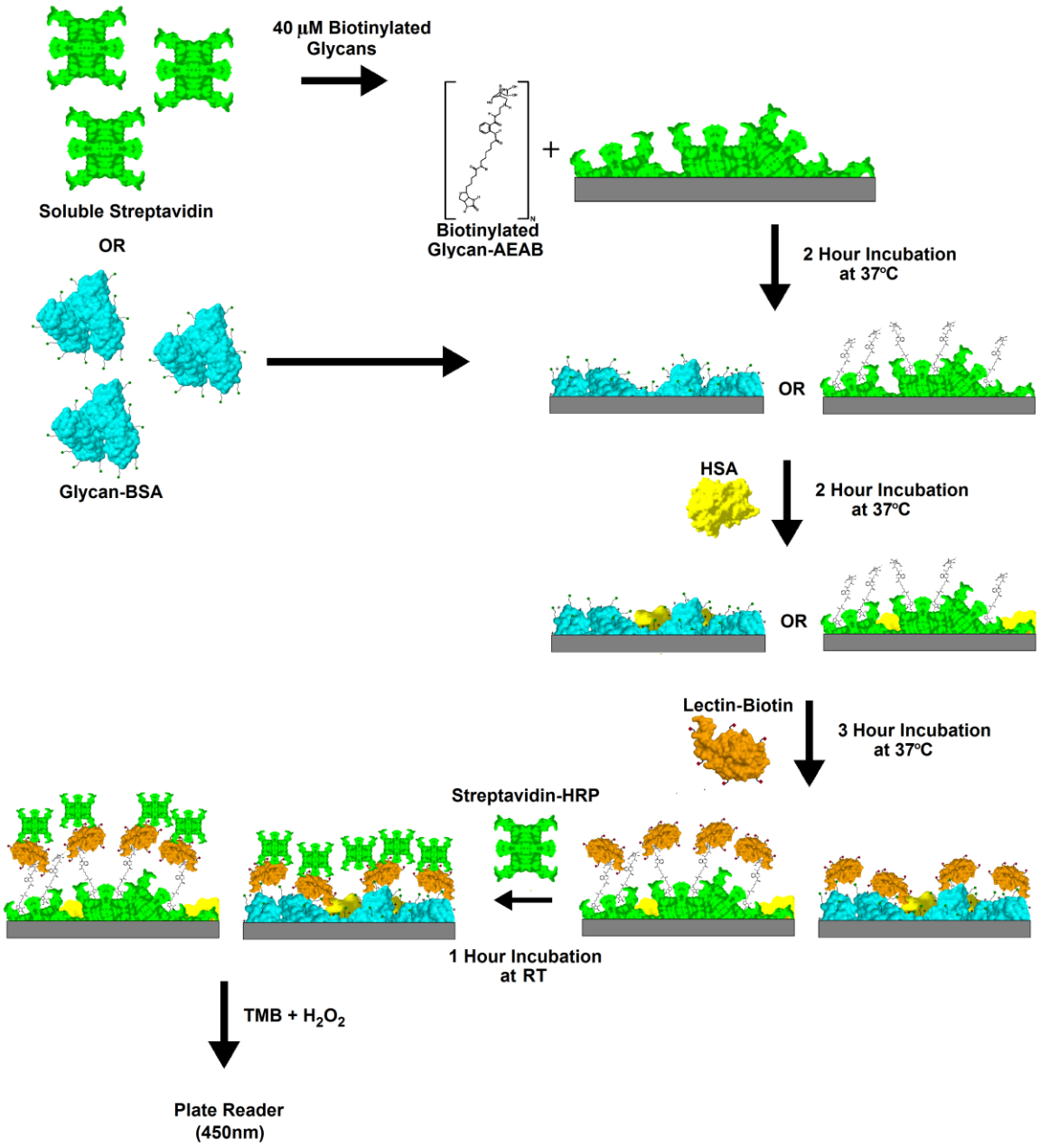

Figure 3: Procedure for ELLA used for adsorbed streptavidin or adsorbed BSA glycoconjugates.

4.2.7 Dendritic Cell Culture

Human blood was collected from healthy donors with informed consent and heparinized (333 U/ml blood) (Abraxis Pharmaceutical Products, Schaumburg, IL) at the Student Health Center Phlebotomy Laboratory, in accordance with protocol H10011 of the Institutional Review Board of Georgia Institute of Technology. Dendritic cells were

derived from human peripheral blood mononuclear cells (PBMCs) using a previously described method[233] with some modifications.[224] Briefly, the collected blood was diluted 1:1 in Mg^{2+} and Ca^{2+} free phosphate buffer saline (D-PBS; Invitrogen, Carlsbad, CA), and the PBMCs were isolated by differential centrifugation using lymphocyte separation medium (Cellgro MediaTech, Herndon, VA). After the lysis of residual erythrocytes with RBC lysis buffer (155 mM NH_4Cl, 10 mM $KHCO_3$, 0.1 mM EDTA), the PBMCs were washed with D-PBS. Ten milliliters of PBMCs were plated in a Primaria 10x20 mm^2 tissue-culture dish (Becton Dickinson, Franklin Lakes, NJ) at a concentration of $5x10^6$ cells/ml in DC media [RPMI- 1640 (Invitrogen), 10% heat inactivated FBS (Cellgro MediaTech) and 100 U/ml of penicillin/streptomycin (Cellgro MediaTech)]. After 2 hours of incubation at 95% relative humidity and 5% CO_2 at 37˚C for the selection of adherent monocytes, the dishes were washed three times with warm DC media to remove non-adherent cells. The remaining adherent monocytes were incubated with 10 ml/plate fresh warm DC media, supplemented with 1000 U/ml GM-CSF and 800 U/ml IL-4 (PeproTech, Rocky Hill, NJ), for 5 days to induce the differentiation of monocytes into iDCs

4.2.8 Exposure of DCs to glycoconjugate adsorbed wells

On day 4 after DC isolation glycan solutions were added to wells of a 384-well TCPS plate in quadruplicate. The solutions were allowed to incubate in the well in a humidity chamber at 37°C overnight. On day 5 of culture, loosely adherent and non-adherent cells containing iDCs were harvested and resuspended in DC media with 1000 U/ml GM-CSF and 800 U/ ml IL-4 at $7.5x10^5$ DCs/ml. These cells were plated in 40 µl of cell suspension ($3.0x10^4$ DCs) on glycoconjugate adsorbed wells in quadruplicate in the wells of the coated 384 well TCPS plate. The extent of DC maturation was compared to untreated DCs (iDCs) for the negative reference control and lipopolysaccharide (LPS) (1 mg/ml; E. coli 055:B5; Sigma)-treated DCs (mDCs), adsorbed zymosan A

(Saccharomyces cerevisiae; Sigma), or Mannan (Saccharomyces cerevisiae; Sigma) for the positive reference control for IMF. The positive control for the TMF (tDC) is human IL10 and human IFNα (R & D Systems) treatment of DCs for 24 hours at 3500 units/ml and 35000 units/ml respectively.

4.2.9 High Throughput Evaluation of Dendritic Cell Phenotype to Adsorbed Glycoconjugates

Differentially-treated and reference control DCs were harvested after 24 h for analysis using an HTP method previously described with modifications. [224] Briefly, DCs were placed in treatment wells on day 5 after isolation at $7.5x10^5$ cells/ml. After 24 hours all treated DCs and controls were transferred via multi-channel pipette to a black 384-well filter plate (Pall Life Sciences), and the supernatants were immediately collected into a 384-well plate through the filters by stacking the filter plate on top of the collection plate and centrifuging at 300 RCF for 4 min. While spinning down the filter plate, wells of the TCPS plate with glycoconjugates adsorbed to them were incubated with Non-Enzymatic Cell Disassociation Solution (CDS; Sigma). The CDS treated cells were then lightly pipetted up and down and transferred to the black filter plate after its first spin-down. The CDS was removed by stacking the filter plate on top of a new collection plate and centrifuging at 400 RCF for 4 min. To the retained cells 50 µl of 0.05% formaldehyde solution was added and the cells were allowed to fix for 40 minutes at room temperature while being shaken at 600 RPM. The formaldehyde solution was then removed via centrifugation at 400 RCF for 4 minutes. The cells retained in the wells were assessed for phenotype by immunostaining using antibodies anti-CD86-PE (Clone BU63; Ancell), anti- DC-SIGN-FITC (Clone 120507; R & D Systems), and anti-ILT3-AF647 (Clone ZM4.1, Biolegend). IgG_1-PE (clone MOPC31C; Ancell) and IgG_{2B}-FITC (clone 133303; R&D Systems) isotype-stained DCs were used for background fluorescence subtraction in separate treatment for control wells. CD86 is a costimulatory

molecule that is up-regulated upon pro-inflammatory DC maturation,[224] DC-SIGN is an endocytic receptor that is slightly down-regulated upon pro-inflammatory maturation,[224] and ILT3 is a member of the immunoglobulin superfamily which signals via the immunoreceptor tyrosine-based inhibitory motifs and is up-regulated upon anti-inflammatory DC maturation.[234] After 30 minutes of staining the cells were washed three times. For each well, at the emission/excitation wavelengths for each fluorophore 535/590 PE, 485/535 FITC, and 650/668 AF647. The geometric mean fluorescent intensities (gMFIs) were then calculated with a Tecan Infinite F500 microplate reader, and the ratio of respective gMFIs were determined as CD86/DC-SIGN, a cell number independent metric named "inflammatory maturation factor" (IMF), and ILT3/CD86, a cell number independent metric named "tolerogenic maturation factor" (TMF) was used to represent DC phenotypic outcomes. Figure 4 shows a schematic of the 384 well plate high-throughput methodology for assessment of DC phenotype to adsorbed glycoconjugates.

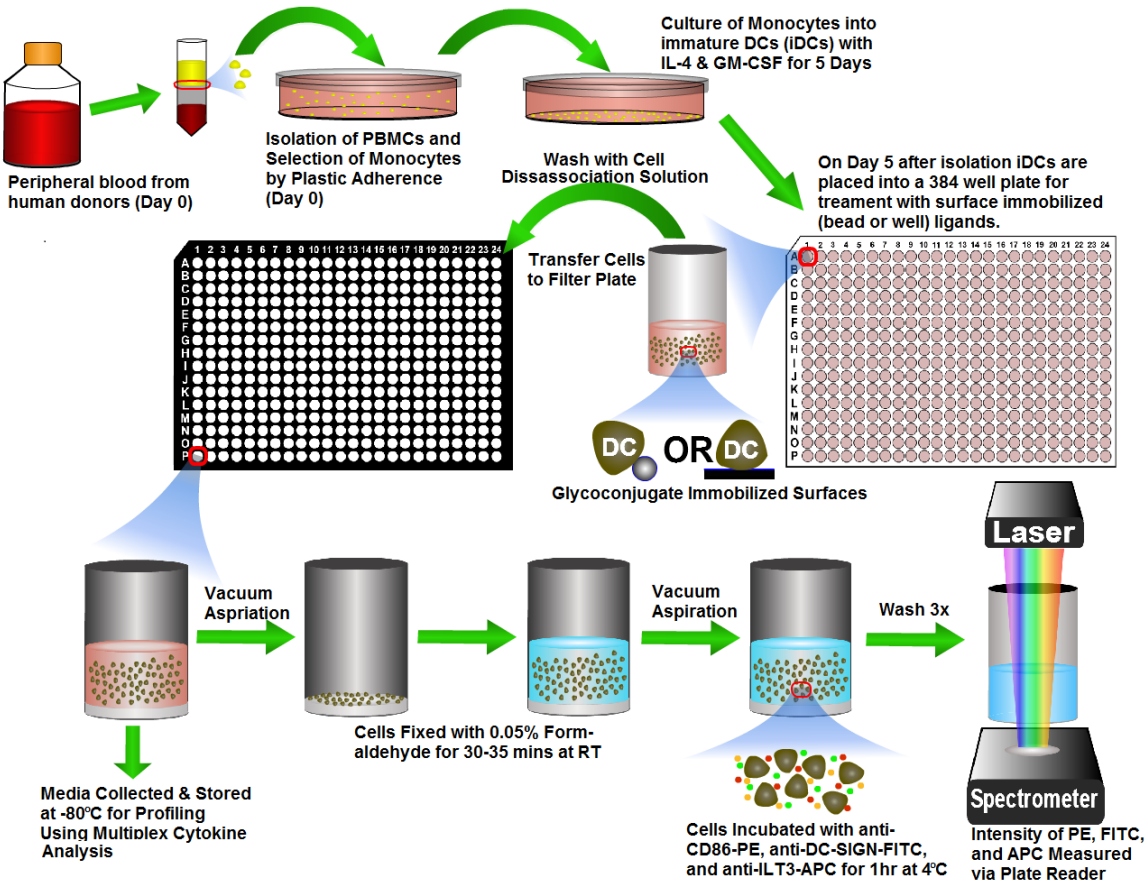

Figure 4: Diagram of the high throughput cellular assay to assess IMF and TMF of DCs when exposed to adsorbed glycoconjugates.

For the studies where EDTA was used to block CLR receptors, cells were treated with either 10mM or 5mM EDTA for one hour at 37°C before exposure to 1 µm bead adsorbed glycoconjugates. Cells were then transferred, with media still containing EDTA, to the wells with the adsorbed glycoconjugates and the subsequent phagocytosis of the 1 µm beads was assessed after 4hrs or DC phenotype assessed via the above HTP methodology after 24hrs. For assessment of phagocytosis cells were transferred to a filter plate, washed with PBS, fixed with 1% formaldehyde for 30 minutes, washed again with PBS, and incubated with 0.1% trypsin for 1 minute. Cells were then washed three times with PBS, and visualized via a Nikon Ti fluorescent microscope (Nikon, Tokyo).

4.2.10 Viability/Cytotoxicity of Glycoconjugates

Cytotoxicity associated with adsorbed glycoconjugate treatment was assessed via live/dead staining of the cells using a predefined method.[235] Briefly, cells were treated with adsorbed glycoconjugates as in the HTP methodology for 24 hours. Cells were transferred to a 384 well filter plate and supernatants removed as in the HTP methodology. The cells were then stained with calcein AM and ethidium homodimer-1 for 40 minutes. Cells were then washed 3x with PBS and the fluorescent intensity of the cells (excitation/emission 495/530 nm – live and 528/630nm – dead) was taken. Additionally, the amount of cell apoptosis was of interest due to possibility that cells were impermeable to Ethidium homodimer but still in the process of apoptosis. To assess apoptosis DCs were stained for Annexin V-FITC and the extent of binding to phosphatidylserine was measured via the HTP format. No treatments showed a significantly different viability from untreated cells and no treatment showed a statistical increase in Annexin V binding.

4.2.11 Statistical Analysis

To observe any significant differences between all sample groups in pairs, a pairwise two-way ANOVA followed by Tukey's posttest was performed using the SAS software (Cary, NC), and the p-value equal to or less than 0.05 was considered significant. Significance of general linear statistical model parameters discussed in section 4.2.12 of this report and seen in **Equation 1a-d** and **Equation 2** was determined by T value in reference to referent group discussed in section 4.2.12 of this report.

4.2.12 Statistical Modeling

Table **2** lists the quantitative parameters that were collected and separates them by variable classification: Continuous, categorical/nominal, and binomial. The characterization of the variables *Inflammatory Maturation Factor (IMF), Tolerogenic Maturation Factor (TMF), isoelectric point* of glycoconjugate, *ligand* attached to carrier,

donors, and *density* of sugars per glycoconjugate can be seen in Table 2A-C. Table 2A contains *IMF*, *TMF*, *isoelectric point*, and *density* continuous variables. Table 2B contains the variables*: Ligand, Isoelectric point, density and donor.* There were 13 total donors for this analysis.

Equation 1a-d shows general linear models that have IMF (a,b) or TMF (c,d) as outcome variables and are a function of the isoelectric point of the conjugates, the ligand conjugated to BSA, the number of ligands per BSA, and the donor. The models in **Equation 1a-d** sought to isolate and compare the isoelectric point, or ligand density to that of a reference group, denoted below. The null hypothesis was that charge or density did not play a role in IMF or TMF and thus that these variables, is continuous or categorical form, would not have a significant T value when compared to the referent group discussed below. **Equation 1a** and **Equation 1c** both use isoelectric point and density as continuous variables while **Equation 1b** and **Equation 1d** treat isoelectric point and density as categorical variables. This was done to first isolate the significance of these factors in their continuous form and then to quantitatively compare the effect of the categories to each other without bias of scale in the categorical models. The coding of these variables is shown to denote the reference group, always denoted by the coding value of 0. The reference ligand was none and thus its value for this variable is shown as 0 in Table **2**B. Three other ligands were analyzed in this model: *oligoethylene glycol linker (OEG), glucose (Glc), and mannose (Man).* Similarly, non-cationized conjugates with no ligands attached to them were counted as the reference groups for both isoelectric point and density. Finally, the variable *donor* was included in the analysis to account for the repeated measures of each donor across conjugates and to help limit the large inter-donor variability that is seen with primary donors. The reference donor was chosen at random and because all other factors control for donor in their calculation of beta no influence on the calculated coefficients or their significance was seen when changing between reference donors.

$IMF = \beta_1 + \beta_2 * Isoelectric + \beta_3 * ligand + \beta_4 * density + \beta_5 * donor$ **Equation 1a**

$IMF = \beta_1 + \beta_2 * Isoelectric\_cat + \beta_3 * ligand + \beta_4 * density\_cat + \beta_5 * donor$ **Equation 1b**

$TMF = \beta_1 + \beta_2 * Isoelectric + \beta_3 * ligand + \beta_4 * density + \beta_5 * donor$ **Equation 1c**

$TMF = \beta_1 + \beta_2 * Isoelectric\_cat + \beta_3 * ligand + \beta_4 * density\_cat + \beta_5 * donor$ **Equation 1d**

To better understand how the models utilizes these categorical variables Table 2C further divides several of the variables defined in Table 2A and B into binomial variables. In each case the variables have been divided such that the group that is being analyzed is singled out from the rest of the population. For instance the *ligand* is divided into three dummy variables *OEG, Glc, and Man* and the *no ligand* is still the global reference group and thus its value is always 0 so no dummy variable is needed to define this parameter. The variables *density* and *isoelectric point* were also divided into three dummy variables denoted as *low, medium,* and *high* respectively. Finally, the donor variable was redefined as a series of binomial variables each depicting a unique donor (not shown in Table 2C). Therefore, the reference group was any donor with a conjugate that had no cationization, no ligand, and thus no ligand density.

T**able 2: Analysis of Continuous Variables Measured for Regression Analyses**

	IMF	TMF	Isoelectric Point	Density
Number of Measures	520	520	520	520
Mean	0.952	0.109	8.102	8.905
Standard Dev.	0.433	0.133	2.097	9.418
Minimum	0.326	-0.491	3.47	0
Maximum	3.846	0.527	10.1	34
Skewness	1.481	0.033	-0.932	1.113
Kurtosis	1.040	2.030	-0.642	0.018

Table 2B: Analysis of Nominal Variables Measured and Coding Convention for Regression Analyses. Count refers to number of measures of IMF or TMF for that

class of variable that were measured. Percentage refers to the percent of total measures the individual class variable count accounts for.

Variable	Sub Category	Code	Count[*1]	Percentage[*2]
Ligand				
	None	0	52	10.0
	OEG	1	156	30.0
	Glc	2	156	30.0
	Man	3	156	30.0
Isoelectric Point				
	No Cationization (pI < 5.5)	0	117	22.5
	Low (5.5 ≤ pI < 7.75)	1	39	7.5
	Medium (7.75 ≤ pI < 9.5)	2	169	32.5
	High (pI ≥ 9.5)	3	195	37.5
Density (Sugars/BSA)				
	None (0)	0	52	10.0
	Low (den. < 5)	1	182	35.0
	Medium (5 ≤ den. < 20)	2	182	35.0
	High (den. ≥ 20)	3	104	20.0
Donor				
	1-13	1-13	40	100.0

*1 **Count refers to number of measures of IMF or TMF for that class of variable that were measured.**
***2 Percentage refers to the percent of total measures the individual class variable count accounts for.**

Table 2C: Analysis of Binomial Variables Measured and Coding Convention for Regression Analyses.

	Category	Coding	Count*1	Percentage*2
Ligand				
OEG	Not OEG	0	364	70.0
OEG	OEG	1	156	30.0
Glc	Not Glucose	0	364	70.0
Glc	Glucose	1	156	30.0
Man	Not Mannose	0	364	70.0
Man	Mannose	1	156	30.0
Isoelectric Point				
Low	Not Low	0	481	92.5
Low	Low	1	39	7.5
Medium	Not Medium	0	351	67.5
Medium	Medium	1	169	32.5
High	Not High	0	325	62.5
High	High	1	195	37.5
Density (Sugars/BSA)				
Low	Not Low	0	338	65.0
Low	Low	1	182	35.0
Medium	Not Medium	0	338	65.0
Medium	Medium	1	182	35.0
High	Not High	0	416	80.0
High	High	1	104	20.0

*1 **Count refers to number of measures of IMF or TMF for that class of variable that were measured.**
***2 Percentage refers to the percent of total measures the individual class variable count accounts for.**

Equation 2 shows a general linear model that has IMF as an outcome variable and is a function of the ligand conjugated to BSA (*ligand*), the number of ligands per BSA divided as indicated in Table 3B (*density_cat)*, and the donor (*donor*). The models in **Equation 2** sought to isolate and compare the structural motifs present in the ligands outlined in Table 3B controlling for ligand density and donor. The null hypothesis was that ligand structure did not play a role in IMF and thus that this variable would not have a significant T value when compared to the referent group discussed below. Table 3 lists the quantitative parameters that were collected and separates them by the variable classifications continuous and categorical/nominal. The variable breakdown and

nomenclature is identical to that of the first model for the second model in this paper but instead of four ligand structures in the second model there are seven. Also, because an optimized carrier was used no ranges in cationization were seen and the TMF was not assessed due to its insignificance from the first model. The seven structural motifs assessed in the second model are *None, OEG, N-acetylglucosamine (GlcNAc), Mannose (Man), Glucose (Glc), Terminal Branched Mannose (Branch),* and *α1-2 Terminal Mannose (Alpha).* The model from **Equation 2** utilizes an identical subdivision of categorical variables into binomial variables as model 1 (seen in Table 2C). However, an equivalent table was not created for this model because structurally it is an identical process as that of model 1. All categorical variables were sub-divided into binomial variables and the reference group remains the group that had a 0 value in Table 3B. Also, similarly to model 1, the donor variable is counted as a categorical variable to account for the repeated measures of each donor across conjugates and to help limit the large inter-donor variability that is seen with primary donors. The reference donor was chosen at random and because all other factors control for donor in their calculation of beta no influence on the calculated coefficients or their significance was seen when changing between reference donors. For either model the R^2 and correlation coefficients between variables were compared to determine how well the model fits the data. Furthermore, the IMF data has historically been shown to be approximately normal and the variance of the data remains constant across all samples thus the linear model used herein is further deemed as a valid analysis method.[224]

$$IMF = \beta_1 + \beta_2 * ligand + \beta_3 * density\_cat + \beta_4 * donor \qquad \textbf{Equation 2}$$

Table 3A: Analysis of Continuous Variables Measured for Regression Analyses

	IMF	Density
Number of Measures	131	131
Mean	0.951	9.535
Standard Dev.	0.613	8.35
Minimum	0.258	0
Maximum	3.184	26.2
Skewness	1.560	0.901
Kurtosis	2.262	-0.527

Table 3B: Analysis of Nominal Variables Measured and Coding Convention for Regression Analyses

Variable	Sub Category	Coding	Sample Size	Percentage
Ligand				
	None	0	17	13.0
	OEG	1	17	13.0
	GlcNac	2	10	7.6
	Glc	3	13	9.9
	Man	4	17	13.0
	Branched (Man3-Br and Man5-Br)	5	20	15.3
	Alpha (Man3-A2, Man4-A2, Man5-A2)	6	37	28.2
Density (Sugars/BSA)				
	None (0)	0	27	20.6
	Low (den. < 5)	1	20	15.3
	Medium (5 ≤ den. < 15)	2	54	41.2
	High (den. ≥ 15)	3	30	22.9
Donor				
	1-17	1-17	10	100.0

4.3 Results

4.3.1 Carrier Selection

This study began with an assessment of carrier appropriateness for glycan presentation to DCs. It was found that BSA cationized with an excess of EDA and functionalized with mannose had the largest change in DC IMF as compared to its unfunctionalized control and thus this platform would be used for further study. To determine this Ovalbumin (OVA), bovine serum albumin (BSA), and streptavidin (SA) and their highly cationized counterpart were chosen as three model carriers. Each of these six carriers was then adsorbed to the wells of a 384 well plate and the subsequent DC phenotype in response to these adsorbed conjugates was assessed after 24 hrs. It was found that all the carriers except cationized OVA did not show an increase in IMF or TMF over untreated cells (data not shown). Thus, five protein carriers were initially functionalized with glycans or linkers to determine a suitable glycan carrier that had no appreciable alteration in DC phenotype but that could serve as a platform for glycan presentation. Figure 5 shows the results of this study. Both cSA and cBSA were able to increase the IMF above that of untreated cells (iDCs) to a statistically significant degree. No change in TMF from untreated cells was shown for any conjugate (data not shown). Positive control, lipopolysaccharide (LPS) treated cells (mDCs) were also shown to

activate DCs to a statistically significant extent.

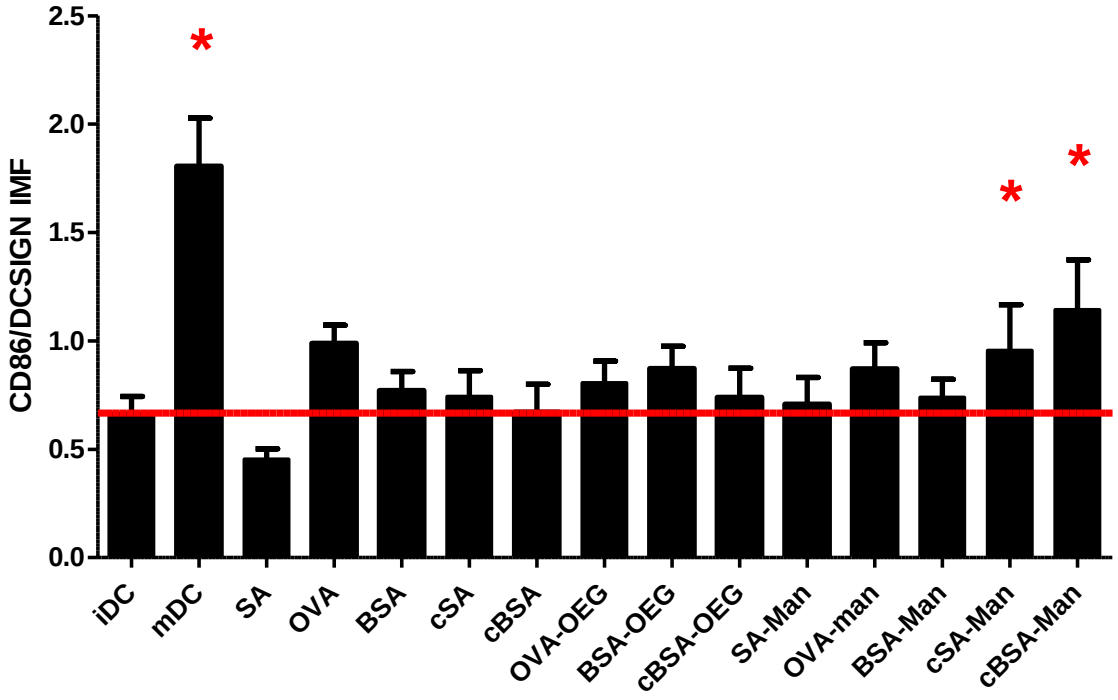

Figure 5: Selection of a carrier for use as a platform for assessment of DC response to adsorbed glycoconjugates. The DC response to adsorbed conjugates and subsequent measured IMF is shown. The IMF was shown to be statistically different than untreated cells (iDC) for both cationized streptavidin presenting biotinylated mannose and cationized BSA presenting mannose. No other conjugate showed a statistical increase in IMF as compared to untreated cells. The positive control for IMF, LPS treated DCs (mDC), also showed a statistical increase in IMF. N=7 donors. Error bars represent standard error, red line indicates mean iDC response, * indicates statistical difference from iDC.

4.3.2 Conjugate Creation and Validation

4.3.2.1 Glycoconjugates were engineered to scale in density and charge.

The conjugates from Figure 5 were cationized with an excess of EDA and 100:1 molar ratios of ligand to carrier and thus no idea of the level of cationization or glycan density necessary for DC phenotype modulation could be obtained from this study. Thus, 40 glycoconjugates were made that scaled both density and charge of BSA from its non-

cationized state, pI of approximately 4.6, to a pI of approximately 10 and from no ligand per BSA to approximately 26.

After formulation all conjugates' mass spectra ware taken via MALDI mass spectrometry and the subsequent average molecular weight was calculated. The change in mass between the conjugate and its unfunctionalized analog was calculated and the molecular weight of the ligand was divided into the change in mass for a calculation of the average number of ligands/BSA. Figure 6A shows the average number of ligands/BSA of the 36 conjugates. For glucose and mannose conjugates ligand density scaled well with increased molar ratios. At higher molar ratios more glycans per BSA were found. The OEG linker however showed no trend of increasing number of functionalizations per BSA regardless of molar ratio used. The average number of ligands per BSA also showed very little variance between conjugate cationization levels. Thus, in Figure 6A the average number of ligands per BSA can be seen as a function of molar conjugation ratio below the graph. Additionally, a preliminary study with a 500:1 glycan to protein carrier ratio was also performed and showed no increase in number of ligands/BSA over that of the 100:1 molar ratio (data not shown).

Figure 6B shows the calculated isoelectric point (pI) for each conjugate. For all conjugates the isoelectric point increased with increasing concentration of EDA. The mean isoelectric point of each conjugate showed very little variance between EDA concentrations. Thus, in Figure 6B the average pI for each level of cationization is shown in the table below the graph. Between each level of cationization there is a ~1 pI increase in the conjugates.

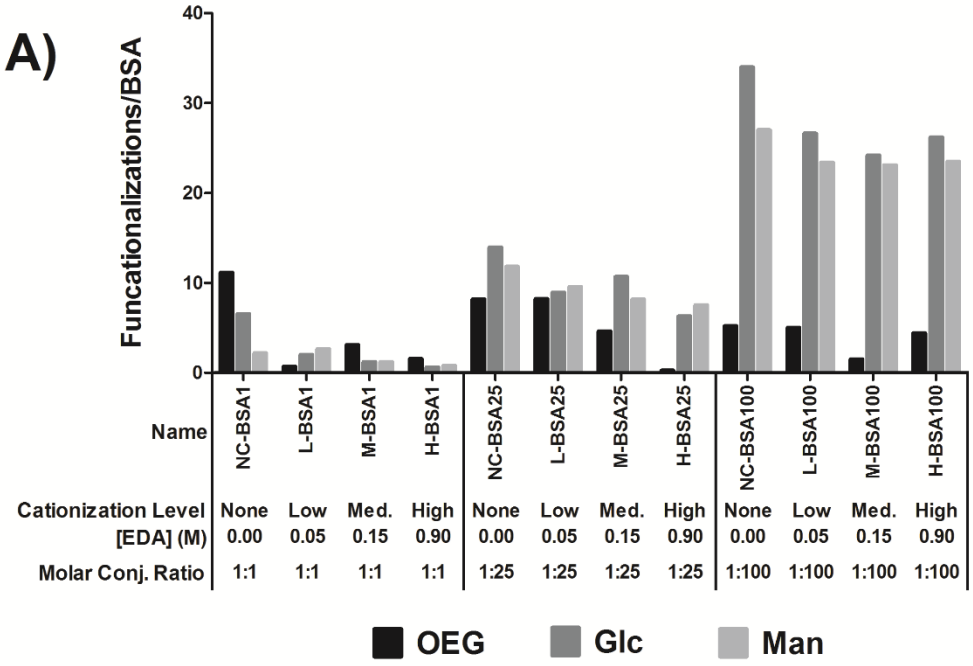

Name	X-BSA	X-BSA1	X-BSA25	X-BSA100
Glycan conjugation ratio	0:1	1:1	25:1	100:1
Mean Functionalization/BSA	0	~2.0	~9.6	~26.0

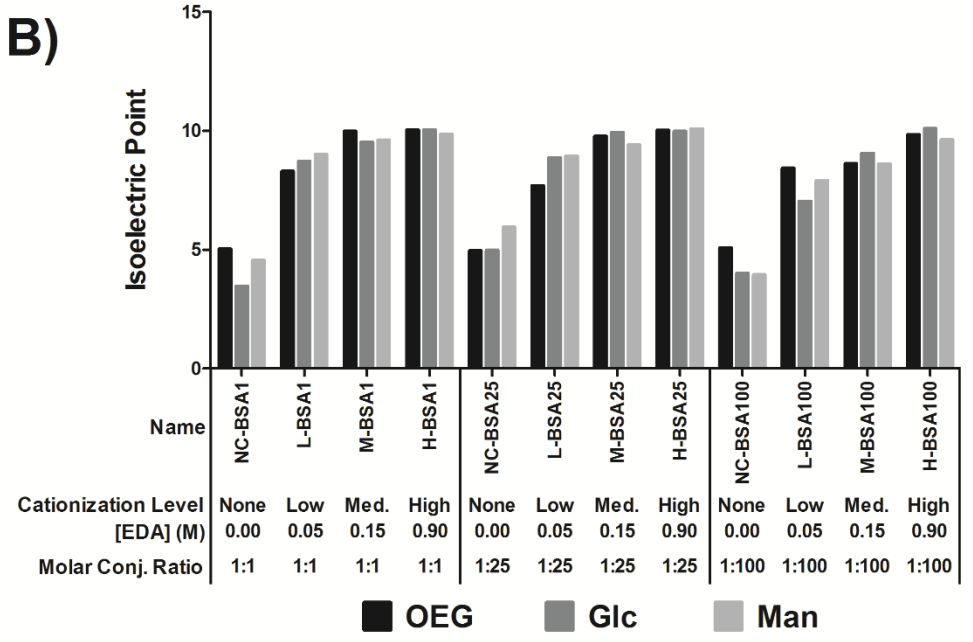

Name	NC-BSA	L-BSA	M-BSA	H-BSA
[EDA] (M)	0	0.05	0.15	0.9
Mean Isoelectric Point	4.67	8.32	9.06	9.96

Figure 6: Mass and isoelectric point of all conjugates. All from Figure 2. were characterized for their mass and average number of ligands per BSA (A) and for their mean isoelectric point (B). The average mass of each conjugate discussed in Figure 2 was determined via MALDI mass spectrometry. The arithmetic mean of the mass peak profile was calculated and plotted in (A). The table under (A) shows the average number of ligands per BSA across each level of cationization. The isoelectric point was calculated for each conjugate from the conjugate's ζ-potential versus pH plot and can be seen in (B). The average isoelectric point at each ligand density can also be seen in the table below (B).

4.3.2.2 Glycoconjugates contain bioavailable glycans that scale in density and are structurally distinct.

Finally, to confirm that the adsorbed conjugates still had biologically available glycans and that the adsorption of these conjugates produced relatively consistent presentations of glycans; ELLAs were performed with two different lectins on all conjugates adsorbed to the wells of TCPS plates. It was found that conjugates with increased glycan/BSA bound more lectin and that this presentation was structure specific as lectins that were specific for mannose did not bind glucose conjugates.

Figure 7 shows the results of the ELLAs performed with both ConA and NPA. Figure 7A-C shows the normalized absorbance of ConA ELLAs at 450nm when incubated with the adsorbed glycoconjugates. Conjugates with more glycans/BSA show increased functional binding of lectins as evidenced by increased absorbance in wells containing higher density conjugates. Also, as cationization level of conjugate increased so did the amount of lectin bound to the plate. Additionally, the signal from the non-cationized, low, and medium cationized glucose conjugates (Figure 7A,C) is significantly lower than that of the same conjugates when conjugated to mannose (Figure 7B). However, the trend between these conjugates is similar as can be seen from the subset of Figure 7A shown in Figure 7C. Figure 7D shows the results of uncharged and highly charged mannose and glucose conjugates with the lectin NPA which is specific for mannose conjugates. Figure 7D shows that the signal from NPA-HRP for the adsorbed

mannose conjugates is much higher than for that of the adsorbed glucose conjugates especially for any conjugate above 6 sugars/BSA. This is expected as NPA is a multivalent receptor and thus as glycan density increases so should the specific binding of the lectin.

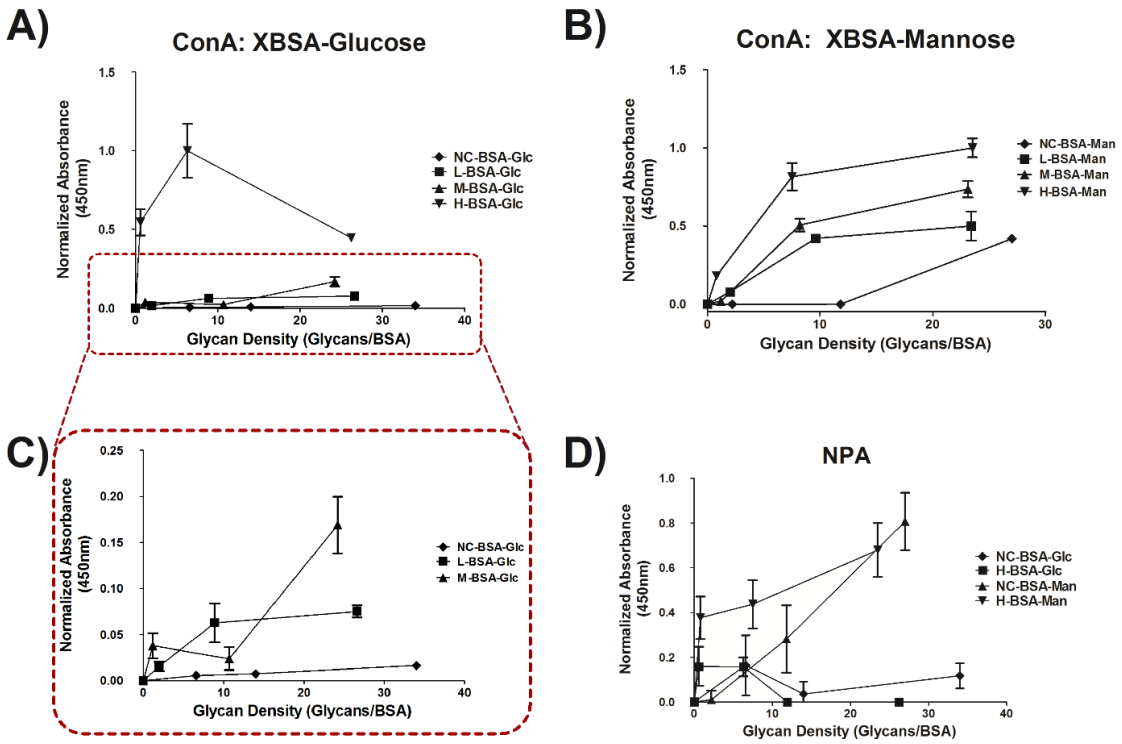

Figure 7: ELLA using plant lectins on adsorbed glycoconjugates from Figure 2 in a 384 well plate. Lectin affinity increases with increasing amounts of sugar on conjugates and lectin binding is higher for highly cationized glycoconjugates than for non-cationized conjugates. Binding of the lectin ConA to adsorbed glucose glycoconjugates (A) and to adsorbed mannose glycoconjugates (B) can be seen. The subset of (A) shows a consistent trend with what would be expected. Also, sugar linkage to carriers shows lectin binding specificity as shown by (C) which shows that NPA (mannose specific) binds to the mannose glycoconjugates with a much high affinity than it does to glucose glycoconjugates. N=3 for A and B, N=5 for C. Error bars represent SE. Conjugate absorbance normalized by treatment with highest absorbance to provide similar scales between ELLAs.

4.3.3 Cationized, High Density, Mannose Conjugates were Able to Activate Dendritic Cells.

After the conjugates had been characterized and validated for biological availability the DC response to each adsorbed conjugate was obtained via the HTP method shown in Figure 4. It was found that the IMF was statistically increased for all levels of high density mannose conjugates above that of iDCs and TMF was not significantly unregulated for any of the glycoconjugates. Figure 9 shows the results from these studies. Controls mDC (LPS treated DCs), adsorbed mannan, and adsorbed β-glucan all showed a statistical increase in IMF as compared to untreated cells (iDC). Also of interest from Figure 9A is that the level of IMF for the cationized glucose conjugates was raised. No known receptors on DCs can bind to single glucose and thus the glucose conjugates were thought to be a control.

While the glucose glycoconjugate treatments did not obtain statistical significance the trend is obvious and thus another control was tested to ensure that any glycan presented from the conjugates did not activate the DCs. The highly cationized mannose and glucose glycoconjugates were treated with periodate and sodium borohydride and thus their carbohydrate rings were permanently opened. These conjugates were then adsorbed to the wells of TCPS plates and the subsequent DC phenotype was assessed via the HTP methodology. No statistical increase in IMF or TMF was seen from these conjugates as seen in Figure 8.

Figure 9B shows the mean TMF of DCs for all treatments. No treatment other than the positive control, tDC, showed an increase in TMF as compared to untreated cells. Of note is an inverse trend of that which was seen in the IMF. Low density low cationized conjugates appeared to increase the level of TMF. The apparent shift in trends was analyzed with the statistical models discussed in Chapter 4.3.4 to determine their significance.

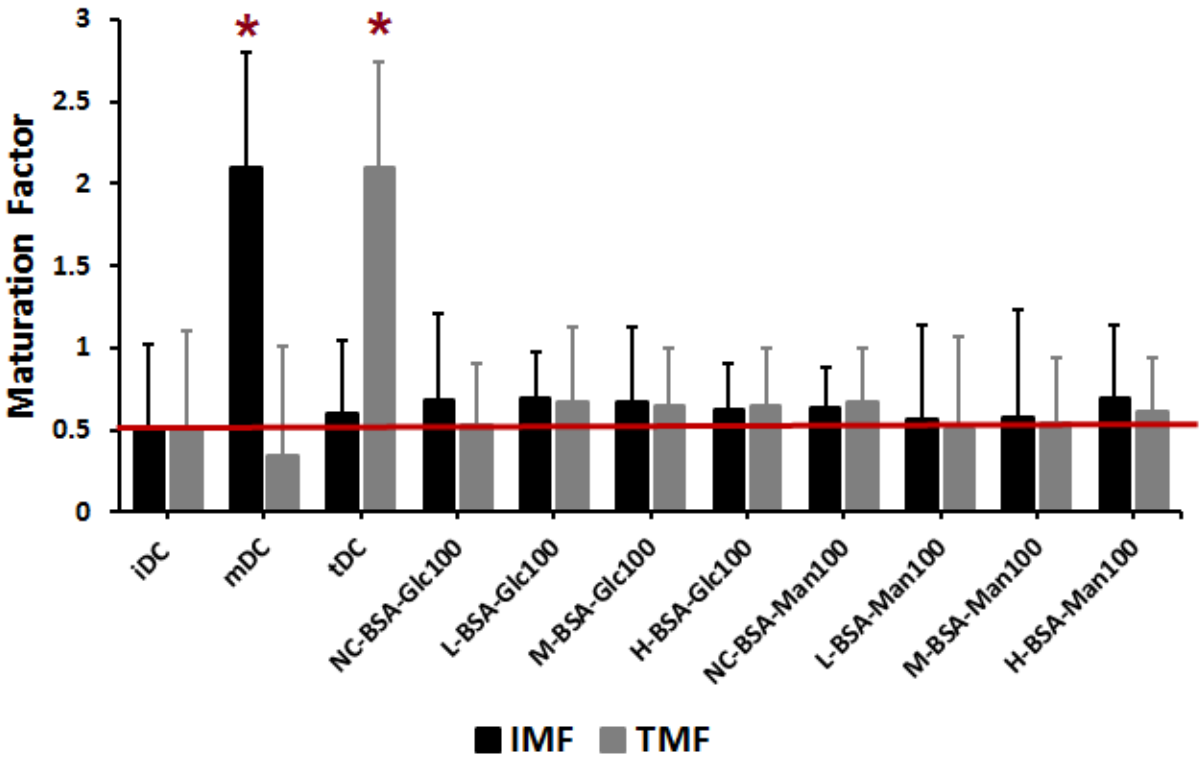

Figure 8: DC Response to open ringed glycoconjugates. No statistical increase in IMF or TMF can be seen for any conjugate at any cationization level if the carbohydrate ring has been opened. The positive control for IMF, mDCs, showed a statistical increase in IMF as did the positive control for TMF, tDCs. N=3 donors. Error bars represent standard error, red line indicates mean iDC response, * indicates statistical difference from iDC.

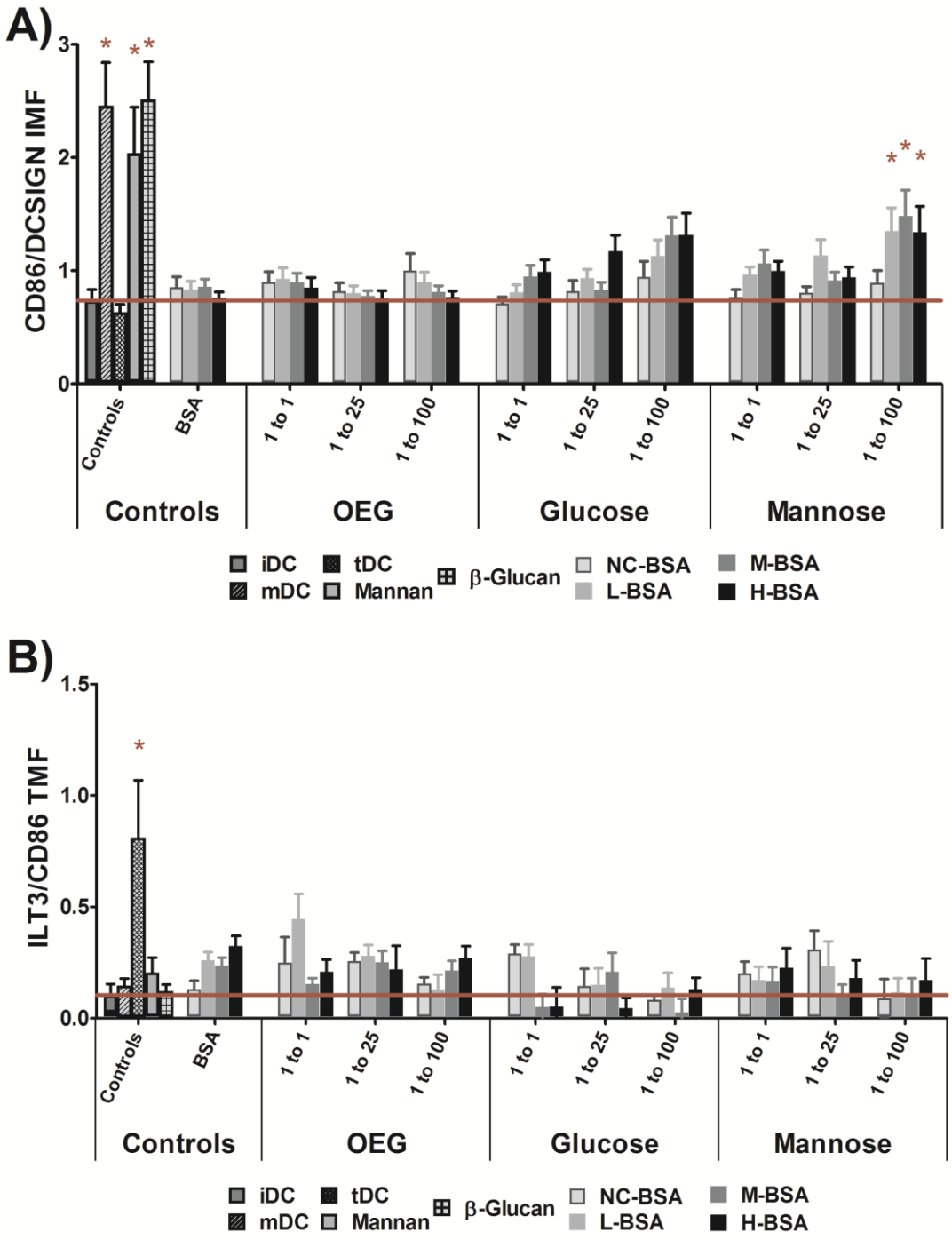

Figure 9: Dendritic cell IMF and TMF levels in response to all engineered well adsorbed conjugates from Figure 2. All positive controls were statistically different from iDC and L-, M-, and H-BSAMan100 conjugates showed a statistically increased fold change in IMF (A). No treatment showed a statistically increased TMF level as compared to iDCs (B). The positive control, tDC, did show an increased level of TMF as compared to iDC (B). Error Bars Represent ±SE, * = P<0.05 from iDC, n=13 donors, red line indicates mean iDC response.

4.3.4 Density and Carrier Charge Significantly Influence Dendritic Cell IMF but not TMF.

From Table 2 the mean IMF, TMF, isoelectric point and density were all found to have a skewness and kurtosis less than |3.0| which is associated with mild non-normality. From Table 3 the mean IMF and density were also found to have a skewness and kurtosis less than |2.0| which again is associated with mild non-normality. Additionally, while the TMF factor from Table 2A has a relatively large skewness and kurtosis upon analysis of residuals all factors fall close enough to a normal distribution that they can be assessed using analyses that assume normal distributions of data. Also, all four variables were plotted against normal percentiles and no outliers of the data were seen (data not shown). These measures further validate the assumptions of normalcy of variables used in general linear modeling and allowed for the analyses of the data using parametric analysis means.

An assessment of the statistical significance of each factor and its global ability to influence the DC phenotype controlling for all other factors was desired. A general linear model was created and can be seen in **Equation 1a**. From this model it can be seen that isoelectric point, density of conjugates, and donor all had significance in the model indicating that each of these factors significantly alters IMF in DCs and is important to phenotypic modulation of DCs. Furthermore, both *density* and *isoelectric* variables showed a positive increase in IMF (positive β coefficients), meaning that as they increased so too did the IMF, when controlling for all other variables measured. Also of note, is that each ligand did not significantly influence IMF and thus density and charge are dominant factors for presentation of glcyans to DCs. The significance of the ligand variables was seen when controlling for density, charge and donor used. The results from this model can be seen in Table **4**A. The model shown in **Equation 1a** was run treating both *ligand* and *donor* as categorical variables and the *isoelectric* and *density* variables as continuous variables. The reference for this model was any donor who was treated with a conjugate that had no cationization, no ligand immobilized and thus no density of ligand.

The model shown in **Equation 1a** treats both isoelectric point and density as continuous variables and shows them both to be significant. However, what specific levels or ranges were significant of each variable would be valuable information for those trying to design optimized glycoconjugates for activation of DCs. Thus, **Equation 1b** was created. This equation treats both isoelectric point and density as the categorical variables with the ranges shown in Table 2B and C**.** The results for this model, shown in Table 4B, indicate that high glycan density had the greatest impact on IMF while having a high cationization level was next as shown by the magnitude of their β coefficients. The variables medium isoelectric point, medium density, and any donor were all also significant variables in the model. Of note is that low isoelectric point conjugates, those with a pI below 7.5, had no significant impact on IMF. Also, it should be noted that low density conjugates were linearly related to the conjugates with no ligand and thus these conjugates had to be excluded from the model. Both low isoelectric point conjugates and OEG ligands had a negative effect on IMF. No ligand had a statistically significant impact on IMF when controlling for density and isoelectric point. The results of **Equation 1b** can be seen in Table 4B.

Finally, the R^2 of both models was calculated to determine the goodness of fit and the appropriateness of these models in assessing the data. **Equation 1a** had an adjusted R^2 of 0.621 and **Equation 1b** had an adjusted R^2 of 0.639. These indicate that approximately 60% of the variance seen in the data can be explained by the model used. These R^2 values were seen as fairly good for the relatively small sample size used (13 donors) and high variability of primary donors.

Table 4A: Parameter estimates for model 1 using continuous isoelectric point and density.

Variable	βs	β Parameter Estimate	Standard Error	t Value	Pr > |t|
Intercept	β_1	0.50603	0.05453	9.28	<.0001
Isoelectric Point	β_2	0.03965	0.00592	6.7	<.0001
Ligand OEG	β_3	-0.03324	0.04325	-0.77	0.4425
Ligand Glc	β_4	-0.0041	0.04718	-0.09	0.9308
Ligand Man	β_5	0.06817	0.04623	1.47	0.141
Density	β_6	0.01382	0.00152	9.07	<.0001
Donor*	$\beta_{7\text{-}18}$	-0.59434 - 0.66049	0.05966	-9.96 - 11.07	<.0001

*** All donor estimates, standard errors, t values, and probabilities can be seen in the Table A 1 in the appendix.**

Table 4B: Parameter estimates for model 1b using categorical isoelectric point and density.

Variable	βs	β Parameter Estimate	Standard Error	t Value	Pr > |t|
Intercept	β_1	0.92276	0.01557	59.57	<.0001
Isoelectric High	β_2	0.17195	0.03355	5.12	<.0001
Isoelectric Med.	β_3	0.15722	0.03243	4.85	<.0001
Isoelectric Low.	β_4	-0.00784	0.04854	-0.16	0.8718
Ligand OEG	β_5	-0.0042	0.04426	-0.09	0.9245
Ligand Glc	β_6	0.0145	0.04791	0.3	0.7622
Ligand Man	β_7	0.06549	0.04656	1.41	0.1602
Density High	β_8	0.38133	0.03736	10.21	<.0001
Density Med.	β_9	0.09719	0.03118	3.12	0.0019
Density Low*	β_{10}	0	.	.	.
Donor*	$\beta_{11\text{-}22}$	-0.59434 - 0.66049	0.05818	-10.21 - 11.35	<.0001

*** All donor estimates, standard errors, t values, and probabilities can be seen in the Table A 2 in the appendix.**
**** Low density conjugates varied linearly with the control due to no difference between cell response to low density and no ligand groups. Thus, this group had to be removed from the model.**

An identical model to those shown in **Equation 1a** and **b** was run for TMF and can be seen in **Equation 1c** and **d**. Similarly to the IMF models, the reference for the TMF model was any donor who was treated with a conjugate that had no cationization, no ligand immobilized and thus no density of ligand. Table A 3 in the appendix shows the results of the model shown in **Equation 1c**. From this model it can be seen that isoelectric point, density of conjugates, and donor all had significance in the model.

Interestingly, both *density* and *isoelectric* variables showed a negative trend in TMF (negative β coefficients), meaning that as they increased the TMF decreased, when controlling for all other variables measured.

The trends seen in the continuous model shown in **Equation 1**c were recapitulated in the categorical model depicted by **Equation 1**d. Table 5 shows the results of this model. Table 5 shows that the higher density and higher cationization levels caused significant decreases in TMF. Conjugates with an isoelectric point less than 7.5 showed a significant positive increase in TMF. Finally, the R^2 of both models was calculated to determine the goodness of fit and the appropriateness of these models in assessing the data. **Equation 1**c had an adjusted R^2 of 0.530 and **Equation 1**d had an adjusted R^2 of 0.539. These indicate that approximately 53% of the variance seen in the data can be explained by the model used. While these values were approximately 10% lower than those for the IMF these R^2 values were seen as fairly good for the relatively small sample size used (13 donors) and high variability of primary donors.

Table 5A: Parameter estimates for model 1d using categorical isoelectric point and density.

Variable	βs	β Parameter Estimate	Standard Error	t Value	Pr > |t|
Intercept	β_1	0.12018	0.00543	22.15	<.0001
Isoelectric High	β_2	-0.02412	0.01169	-2.06	0.0397
Isoelectric Med.	β_3	-0.00020723	0.0113	-0.02	0.9854
Isoelectric Low	β_4	0.03534	0.01692	2.09	0.0372
Ligand OEG	β_5	0.00662	0.01543	0.43	0.6681
Ligand Glc	β_6	-0.0291	0.0167	-1.74	0.0819
Ligand Man	β_7	-0.02491	0.01623	-1.54	0.1253
Density High	β_8	-0.06402	0.01302	-4.92	<.0001
Density Med.	β_9	-0.02769	0.01087	-2.55	0.0111
Density Low**	β_{10}	0	.	.	.
Donor*	$\beta_{11\text{-}22}$	-0.59434 - 0.66049	0.05818	-6.22 - 10.57	<.0001

*** All donor estimates, standard errors, t values, and probabilities can be seen in the Table A 5 in the appendix.**

**** Low density conjugates varied linearly with the control due to no difference between cell response to low density and no ligand groups. Thus, this group had to be removed from the model.**

4.3.5 Dendritic Cell IMF and Phagocytosis of Glyconjugate Coated Microbeads is Inhibited by EDTA

Finally, determining whether the interaction with the ligand coated wells was lectin mediated or whether it was through some other receptor was desired. A pan CLR inhibitor rather than a specific antibody was chosen as an inhibitor because of the numerous receptors capable of binding mannose conjugates on DCs.[236] Figure 10 shows the results of this test. Two different methods were used to assess CLR interaction with the adsorbed glycoconjugates. First conjugates were adsorbed to 1µm fluorescent polystyrene beads and then incubated with DCs for 4 hours. Fluorescent images were then taken of the cells and beads for a visual assessment of bead internalization or binding when incubated with cells in the presence of EDTA and not. Figure 10A-C shows the micrographs of DCs with H-BSA and H-BSA-Man100 coated beads and no EDTA. As is apparent in these micrographs, after 4 hours in wells not treated with EDTA, DCs had internalized many beads and many DCs had internalized >10 beads per cell. However, Figure 10C shows beads coated with H-BSA-Man100 in the presence of 5mM EDTA. As is apparent from this micrograph DCs had internalized few if any of the beads and no cells were seen that had internalized more than two beads per cell.

The second method chosen for these experiments was to look at the HTP readout of the cells in the presence and absence of 5mM and 10mM EDTA. Figure 10D shows the results of this experiment. Only DCs treated with adsorbed H-BSA-Man100 conjugates without EDTA treatment had a statistically significant up-regulation of IMF.

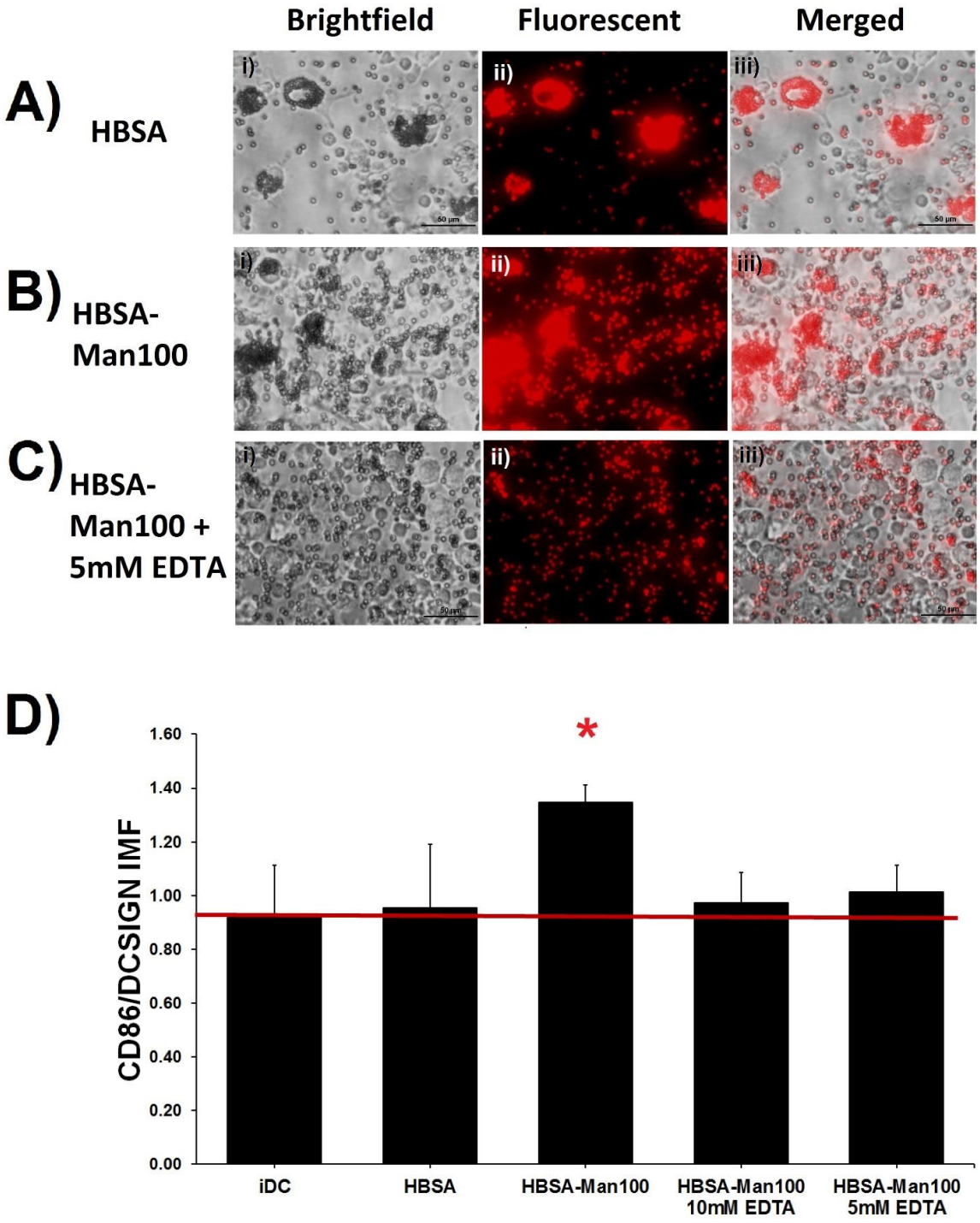

Figure 10: DC response to H-BSA-Man100 conjugates adsorbed onto 1.0µm fluorescent polystyrene beads and subsequent IMF in the presence of 10mM or 5mM EDTA. DCs phagocytized H-BSA and H-BSA-Man100 coated beads to a much greater extent than they did H-BSA-Man100 coated beads in the presence of 5mM EDTA (A-C). No fold change in IMF was seen between iDCs and the EDTA treated cells. The unblocked HBSA-Man100 conjugate showed a statistical increase

in IMF (D). N=4 donors. Error bars represent standard error, red line indicates mean iDC response, * indicates statistical difference from iDC.

4.3.6 Dendritic Cell IMF is Significantly Influenced by Terminal Glycan Structural Motif.

The models shown in **Equation 1a-d** all indicate that ligand was not a significant factor in either IMF or TMF. Thus, a study to determine if the optimized conjugates indicated from **Equation 1a-d** were able to distinguish between sugar structures was performed. Six different mannose structures were then conjugated to highly cationized BSA in a 100:1 molar ratio. These conjugates were then adsorbed to the wells of a TCPS plate and the DC phenotype was assessed via the HTP methodology after 24 hours. Figure 11 shows the results from this study. Figure 11A shows the glycan structures assessed in this study. An additional control sugar was added for these experiments to further validate that glycan presentation from the adsorbed highly cationized BSA did not activate DCs. The monosaccharide N-acetyl-glucosamine was chosen as a control sugar because it has no known receptor on DCs. Figure 11B shows that, as expected, the positive control, mDC, and the highly cationized BSA-Man conjugate showed a statistical increase in IMF over iDC. However, Figure 11B also shows that the H-BSA-Man5-A2 conjugate caused a significant increase in IMF as compared to iDC. Interestingly, an α1-3, α1-6 branched structural homolog for Man5-A2, Man5-Br, showed no activation of DCs. Furthermore, an α1-3, α1-6 branched trimannose (Man3-Br) also showed no activation of DCs.

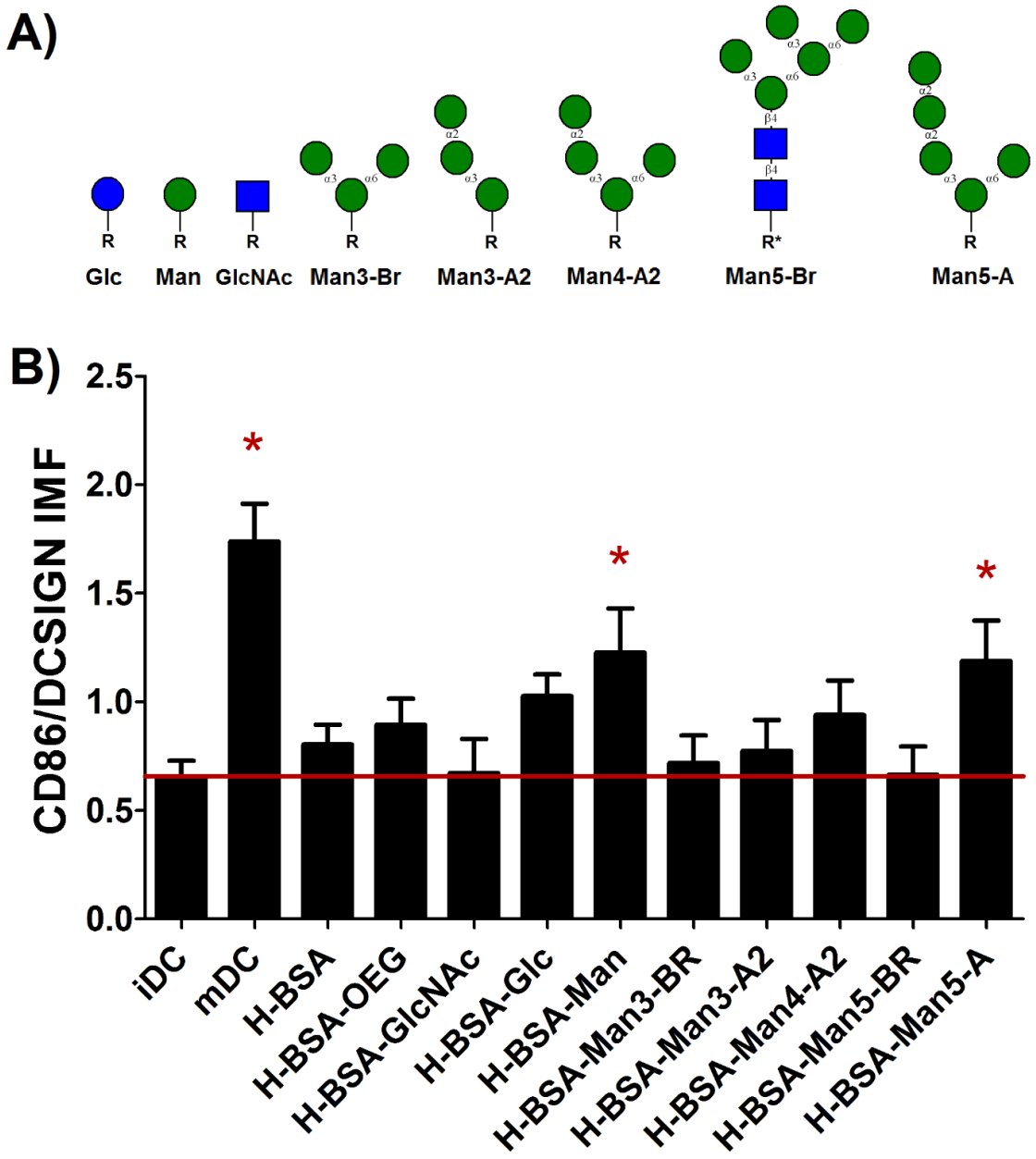

Figure 11: Assessment of DC phenotype in response to poly-mannose structures. The structures tested can be seen in (A). Here R and R* represent the linker used for the glycan. R= $(CH_2CH_2O)_3SH$ and R*= AEAB-$NH_2C(CH_2)_3SH$, The IMF was assessed for all adsorbed conjugates and H-BSA-Man and H-BSA-Man5-A had had a statistically increased expression over iDC (B). mDCs also showed a statistical increase in IMF. N=17 donors. Error bars represent standard error, red line indicates mean iDC response, * indicates statistical difference from iDC.

Due to the fact that two different mannose structures were shown to increase the IMF a model that could group or characterize these structures and use them to predict the

structural relevance of the glycans for DC maturation was desired. The model shown in **Equation 2** has the variables *density_cat*, *ligand* and *donor*. **Equation 2** shows density modeled as a categorical variable because it was first tested as a continuous variable, as in **Equation 1a**, and found to be significant. Isoelectric point was not included in this model because all conjugates were the highly cationized form of BSA and thus their isoelectric points only varied between 9.9 and 10.1. The *ligand* variable was divided into the subclasses seen in Table 3B. Glycan structural motifs α1-3, α1-6 terminal branched mannose and α1-2 terminal linked glycan structures were grouped together for this analysis. The results from the modeling of **Equation 2** can be seen in Table 6. In this model structural variables *glucose*, *mannose*, and *alpha* all had a statistically significant effect on DC phenotype. No density variable had a statistically significant influence on phenotype nor did any α1-3, α1-6 branched mannose structure or N-acetylglucosamine. Of note is that low and medium density had a negative impact on IMF and all ligand classes analyzed had a positive influence on DC phenotype. Because the results from Figure 9 clearly show that no mannose or glucose conjugate had a significant effect on TMF, only IMF results were assessed and for this study.

The R^2 of the model shown in **Equation 2** was calculated to determine the goodness of fit and the appropriateness of these models in assessing the data. **Equation 2** had an adjusted R^2 of 0.622. This indicate that approximately 62% of the variance seen in the data can be explained by the model used. These R^2 values were seen as fairly good for the relatively small sample size used (17 donors) and high variability of primary donors.

Table 6: Parameter estimates for model 2 using categorical isoelectric point and density.

Variable	βs	β Parameter Estimate	Std. Error	t Value	Pr > |t|
Intercept	β_1	1.01253	0.04706	21.52	<.0001
Density High	β_2	0.09053	0.12926	0.7	0.4852
Density Med	β_3	-0.05344	0.16854	-0.32	0.7518
Density Low	β_4	-0.17087	0.21251	-0.8	0.4232
OEG**	β_5	0	.	.	.
Glc	β_6	0.52008	0.14115	3.68	0.0004
GlcNac	β_7	0.135	0.2286	0.59	0.5561
Man	β_8	0.47628	0.2124	2.24	0.027
Alpha	β_9	0.43799	0.2124	2.06	0.0416
Branch	β_{10}	0.12871	0.15445	0.83	0.4065
Donors 1-16*	$\beta_{11\text{-}26}$	-0.45111 - 1.07452	0.22732	-1.98 - 4.23	0.0005

*** All donor estimates, standard errors, t values, and probabilities can be seen in the Table A 6 in the appendix.**

**** OEG conjugates varied linearly with the control due to no difference between cell response to OEG and no ligand groups. Thus, this group had to be removed from the model.**

4.4 Discussion

4.4.1 Carrier Selection

From the results shown in Figure 5 bovine serum albumin, and specifically cationized BSA, was chosen over cationized streptavidin due to its ability to be functionalized with upwards of 37 glycan ligands according to literature.[237] Also, Oyelaran et al.[238] showed that BSA was capable of scaling in density to a physiologically relevant density (>20 sugars/protein) to drastically enhance CLR binding. Additionally, many studies have shown that BSA is a non-activating background for which to deliver molecules to DCs.[239,240] Also of importance from Figure 5 is that the base cBSA protein tested with no ligand or with OEG linker attached caused no statistical increase in IMF from DCs and in the case of the highly cationized cBSA had a slightly lower (0.021) average IMF than did untreated cells.. Furthermore, display of glycans in a relatively physiological setting (conjugated to a protein backbone instead of synthetic polymer) was seen as advantageous as cells rarely encounter unbound complex glycan structures in nature. To date no direct studies have been performed that compare how charge of a glycolconjugate alters DC phenotype. However, historically cationic vaccine conjugates have been found to play an important role in increasing the immune response to any conjugate.[24–28] Thus, it was not seen as surprising that cationized BSA conjugates with high ligand densities activated DCs to the greatest extent.

4.4.2 Conjugate Creation and Validation

Mass spectra of the conjugates showed that glycan moieties scaled in density with increased molar ratios of glycan. The scaling agrees well with results shown by Oyelaran et al.[238] However, it was found that OEG conjugates did not appear to scale with increased molar ratios. This, was unexpected as OEG conjugates were created at the same time with identical conditions to those of the other glycoconjugates. It was

therefore concluded that the OEG linker mass was small enough that the number of functionalizations per BSA were lost in the noise generated by MALDI mass spectra. While no direct evidence of this has been shown in the literature, the average standard deviation of the mass profile for each of the OEG100 conjugates was 11774 ± 6180 Da. With an average standard deviation of over 10kD and a maximum weight of OEG ligands reaching approximately 3kDa it would be no surprise that the OEG linker weight could be lost in the noise of the mass profile. Figure 12 shows two typical sets of MALDI mass profiles for produced glycoconjugates.

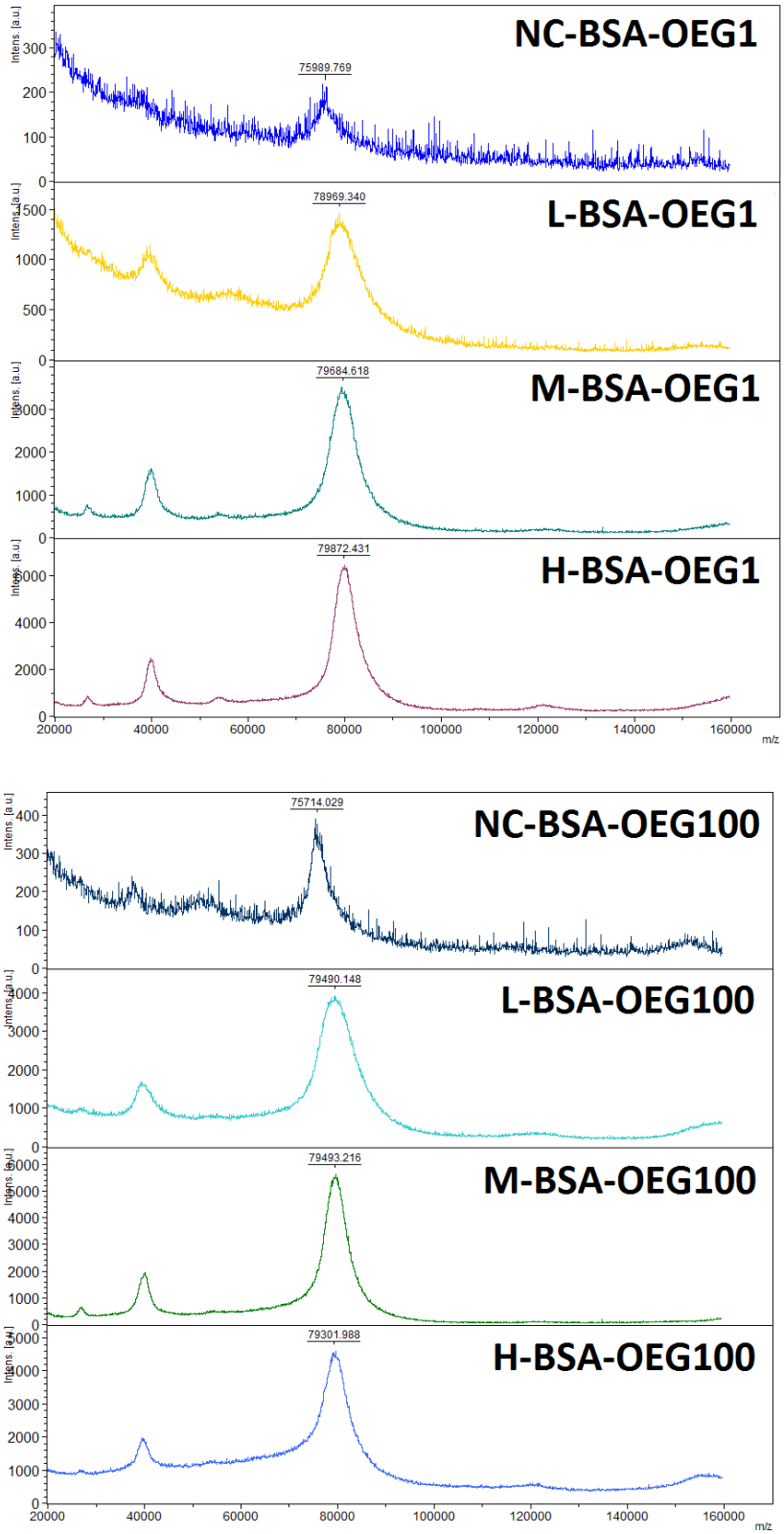

Figure 12: MALDI mass spectra of four levels of cationization of glucose and mannose glycoconjugates.

Figure 6D shows that the range of isoelectric points tested was fairly small (approximately two pI units) between low and highly cationized conjugates. However, the pI is the pH at which a particular molecule or surface carries no net electrical charge and thus a single unit increase in pI indicates a 10 fold increase in charged moieties per conjugate. Thus, while the difference between low and high is only approximately two units this represents 100 times the charge density per conjugate and thus is seen as an acceptable range especially when including the non-cationized conjugate as a reference which increases the range of pI's test from pI 4.5 to pI 10.1.

The ELLAs shown in Figure 7A-C show that the glycoconjugates, when adsorbed to TCPS plates, are able to present their ligands in a biologically available manner. This is indicated by the fact that lectins were able to bind to the conjugates when they were adsorbed to the wells of a TCPS plate and that the higher density conjugates showed an increase in signal. This was expected as ConA binding has been shown to scale with density of glycan presentation.[241] Also, because the lectins used are multivalent the increased binding trend is most consistent and reproducible with higher glycan density conjugates. This is indicated by clear differences in density being shown with glycoconjugates that have more than 6 glycans/BSA. Also noted in Figure 7A-C is the trend of increased signal with increased cationization of adsorbed glycoconjugate. This was unexpected but the natural isoelectric point of ConA is approximately 5.0 and thus its negative zeta potential at neutral pH could lead it to non-specifically bind more strongly to the cationized conjugates and thus allow for longer and more intimate association of the lectins with the glycans presented from these conjugates. This longer and stronger association has been hypothesized to lead to more multivalent interaction with the lectins and thus higher overall binding of the lectins to the cationized conjugates.[242] Also of interest when comparing Figure 7A to Figure 7B is that the signal from the less cationized glucose conjugates is much lower than that of the equivalent

mannose conjugate. This is expected as ConA has historically been shown to have a lower affinity for glucose as compared to mannose conjugates.[243]

Finally, Figure 7D indicates that the sugars presented from the glycoconjugates are structurally distinct and biologically identifiable. This is shown by the affinity of the NPA being significantly higher for the mannose glycoconjugates than for the glucose glycoconjugates. Because NPA has been shown in the literature to bind to mannose and not glucose glycoconjugates this confirms the specificity of the glycan presentation.[244] This was expected as CLRs have been shown to have high structural specificity in the literature and all glycans were closed ring structures that were recognizable by the NPA.

An inherent limitation of ELLAs is their inability to quantitatively state surface densities of ligand. The measures produced by ELLA are always relative to each other. However, a rough estimate of surface density of ligand would be useful for reference to future researchers designing novel combination products that include glycans. Thus, an order of magnitude calculation was performed by assuming that the hydrodynamic radius obtained when the ζ-potential of each conjugate was measured at pH 7.0 was performed. In this estimate the conjugates were spheres with the averaged measured hydrodynamic radius of 3.64×10^{-9}m and that the conjugates adsorbed to the surface without deforming outside of this radius. In other words, the conjugates had perfectly circular cross-sections on the surface. Using this assumption and maximum packing, the surface packing factor was calculated to be 0.9069. Glycans were assumed to be uniformly distributed across the surface of the conjugate and upon adsorption on average half of the glycans were covered by the protein structure adsorbing to the surface of the TCPS dish. Using these assumptions conjugates with 26 glycans/BSA had an average density of approximately 2.83×10^{5} glycans/μm^2. Using the densities found by Osborne et. al.[245] for BSA proteins adsorbed per unit area in a polystyrene tube, as measured by ^{125}I-labeled proteins, and an average molecular weight of BSA of 66,460 Da, it was found that 3.52E+05 sugars/μm^2 were present on the surface. This continues with the assumption that conjugates had 26

glycans/BSA and that half of these glycans would be covered by the adsorbed protein. The calculation of these densities can be seen in Figure A 2 in the appendix, of this report. These two numbers are seen as a low and high estimate for glycan density of the "high" density conjugates produced in this study.

4.4.3 Cell Response to Adsorbed Conjugates

The results from Figure 9A show that there is a necessity for cationization of the carrier in order for DCs to be able to recognize and respond to surface adsorbed glycoconjugates. Also, only the highest density of conjugates showed significant activation of DCs when the glycoconjugates were cationized so not only is a high (~>20glycan/protein) density of glycan needed but also there is a synergistic affect between charge and density of display. The BSA backbone appears to not be required for activation as identical carriers with different charges showed no change in DC activation at equivalent glycan densities and/or charges.

Another point of interest for Figure 9 is that the cationized forms of the glucose glycoconjugates showed an increase in IMF. The monosaccharide glucose was thought to be a negative control because no known receptor on DCs binds single β-D-glucose.[236] However, upon searching the literature it was found that Dectin-1, a CLR expressed on DCs, can bind to β-glucan which is an extremely high density, structurally heterogeneous, polymer of β-D-glucose.[154] Thus, it could be possible that the high density β-D-glucose conjugates have enough glucose to marginally engage Dectin-1, and thus a slight up-regulation of IMF can be seen for these conjugates. Most concerning from this result is that it leaves the possibility that any glycan could activate DCs when presented from the adsorbed H-BSA conjugate. However, concerns over non-specific glycan activation of conjugates were allayed by the results from the open ring conjugates shown in Figure 8. Figure 9B shows the TMF expression level by DCs. No differences between conjugates were seen for TMF. However, a trend was seen between low glycan

density and low cationization levels and increased TMF. The associations between charge and density and TMF were analyzed in the models of this data and discussed more in-depth below.

Due to the inherent variability of formulation of protein glycoconjugates results produced by different formulations of conjugates are frequently varied and thus direct associations and recapitulation of experimental results is challenging. Thus, there is an advantage to modeling the data so that direct comparisons between different formulations and experimental conditions can be made. To that end, the models shown in **Equation 1a-d** were produced. The validity of using these types of models has been discussed previously in this report. Furthermore, the data collected in this study has historically been shown to be approximately normal and the variance of the data remains constant across all samples.[224]

Table 4A and B show that both isoelectric point and glycan density are significant factors in the regulation of IMF. When comparing the coefficients seen in Table 4B *high density* and *high cationization* have the largest effect on IMF of any other conjugate characterization variable. Additionally, *High density* has twice the magnitude of impact than does having a *high isoelectric* value; indicating that density is the most important factor for consideration when designing glycoconjugates. Interestingly, the models shown in **Equation 1a-d** all indicate that ligand was not a significant factor in either IMF or TMF. This is surprising given that in the ANOVA analysis only the cationized mannose conjugates showed a significant increase in IMF over untreated cells. It was hypothesized that this was due to the fact that all conjugates were pooled together for these analyses and compared controlling for densities and cationization levels. Thus, two-way interaction variables between ligand, cationization level, and density were introduced to the model (equation not shown). However, due to the limited number of donors capable of being tested the model with these interaction variables could not converge and thus was not able to be used. Thus, the study shown in **Equation 2** was

performed to remove the variability of isoelectric point and compare glycan structures of similar density and charge to each other directly.

Also of note, is that an inverse correlation between variables was seen between IMF and TMF which would be expected as they are measuring inverse relationships between DCs (pro-inflammatory versus tolerogenic). Keeping this in mind, and comparing between the two models it can also be noted that the coefficients for all variables in the TMF model were lower in magnitude from those of the IMF model indicating that they play a smaller roll in modification of the TMF than they do in the IMF. This indicates that optimal factors for modification of TMF might not have been assessed in these studies and that more variables and ligands are necessary for a more thorough understanding of how to optimally modify DCs toward a tolerogenic phenotypic state.

To help ensure that activation of DCs was occurring through CLRs DCs were incubated with the adsorbed high density mannose and glucose conjugates in the presence and absence of EDTA. All CLRs are calcium mediated and thus it has been shown in literature that incubating DCs with a calcium chelater, in this case EDTA, can drastically impair the function and signaling of a variety of CLRs.[176] EDTA is a broad spectrum inhibitor and was chosen due to the plethora of CLRs that can bind mannose on DCs.[236] Several of these receptors have no known blocking antibody and others have not had the molecular signaling pathway that they signal through elucidated yet. [236] Thus, treating DCs with EDTA was seen as the best approach for confirmation of CLR interaction with the conjugates. Figure 10A-C shows internalization of coated 1um fluorescent beads in the presence or absence of EDTA. Phagocytosis was chosen as a readout because the CLRs DC-SIGN and mannose receptor (MR), two of the most studied and understood of the mannose binding lectins on DCs, are known phagocytic receptors. Thus, an inhibition of phagocytosis of the beads would indicate that these two receptors were inhibited. Figure 10A-C clearly shows this inhibition. Furthermore, the DC phenotype

was assessed in the presence and absence of 10mM and 5mM EDTA and the adsorbed conjugates and the IMF was found to not be statistically increased in conjugates when in the presence of EDTA. These two concentrations of EDTA were chosen as common concentrations known to inhibit CLR binding in DCs without activating DCs.[204,246]

4.4.4 Dendritic Cell Response to Diverse Mannose structures

One of the glycan structures used had a base GlcNAcβ1-β4GlcNAc motif that was modified with AEAB and a thiol. This structure is distinct from the other glycans which are homogenous for mannose and have no fluorescent linker (AEAB) attached to them. This seemingly random sugar was chosen because this glycan structure is a common motif found in humans from which many other glycan motifs are added.[176] The other glycans are not commonly found in healthy humans and are instead found Entamoeba.[247] The change in linking chemistry was chosen because the sugar was isolated from a protein, RNase B, and not made via synthetic carbohydrate chemistry and thus had to be identified in HPLC for purification and isolation. Carbohydrates modified in this way have been used frequently in glycan arrays made by the Consortium for Functional Glycomics, one of the largest providers of carbohydrate resources to the glycan community, and thus it is seen as unlikely to of caused the difference in cell response between it and its structural homolog Man-5-A2. In support of this conclusion Feinberg et. al.[248] found that any glycan structure with a terminal α1-α2 man-man linkage showed a drastically higher binding affinity for DC-SIGN than did those structures that did not. Also, Wattendorf et al.[107] showed that for Man3-Br conjugates presented from a non-fouling PEG backbone produced no change in CD80, CD86, and MHCII from iDCs which also agrees with the results herein. Not only does this confirm the results shown here but it also has implication for the Man5-Br structure tested in Figure 11 because this structure is two Man3-Br conjugates linked via an α1-α6 linkage. Thus, the fact that glycan structure had a significant impact on IMF was not surprising. The results from the

model shown in **Equation 2** that indicate that terminal branched structures were not able to significantly change DC IMF while man α1- α2man terminal linked conjugates were is supported by the literature but has never been shown to be applicable across sugar structures before this report.

A discussion of why the donor variables were kept in all models is necessary as these variables were always statistically significant. First, donors' response to a multitude of ligands for each study was performed and thus the repeated measures of the donor needed to be controlled for in the analysis. If we did not do this then underlying associations between variables for a given donor would not be accounted for in the analysis and thus the beta values calculated would be skewed. Secondly, models without donors included had R^2 values below 20% due to the high variability of primary donors. Because of the small amount of glycan structures available small sample sizes were required when testing all conjugates. Donors that vary in their response to carbohydrate ligands frequently vary by an order of magnitude, though underlying trends remain constant. Thus, without being able to sample a large population inter-donor variability must be controlled for in order to see other significant trends. All tested models showed identical trends to those discussed for each model regardless of inclusion of the *donor* variable but the overall fit of the model was poor and thus the *donor* variable was retained in the models.

The model seen in **Equation 2** was the result of an unbiased analysis of structure groupings. All combinations of glycan motifs were tested and models run for each combination. Grouping glycans via terminal linkage of glycan, via α1-3, α1-6 branched or α1-2 mannose, showed the highest statistical significance for ligands and also produced the greatest R^2 value for the model. Furthermore, the resultant glycan groups used in **Equation 2** yielded the most significant grouping of structures. Algorithmically generated grouping was seen as a strength of the model as the data was used to determine the underlying trends and no bias was introduced by the researchers. The grouping that

were determined as significant were then assessed for their physiological implications and two instances of the truncated mannose structures were found. First, the α1-2 terminal linked mannose structures have been shown to be expressed on the surface of Entamoeba.[247] Second, the α1-2 mannose terminal mannose structures can be seen in class E Thy-1 negative mutant lymphomas.[249,250] The Thy-1 negative mutants show an inability to produce dolichol-P-mannose and thus cannot effectively modify the block transferred N-glycan core structure.[250,251] Thus, it is hypothesized that since these structures are never found in healthy tissue and only in a pathogen, Entamoeba, or on lymphomas, that CLRs have evolved to recognize these structures as DAMPs or PAMPs and become activated by them. Futhermore, that CLRs could recognize these structures was not surprising considering the affinity studies that were completed by Feinberg et.al., Ratner et.al. and the Consortium for Functional Glycomics open database.[211,248,252] In these studies a complex lectin specificity for glycans is consistently shown and high structural specificity is common among lectins. For example, the Consortium has shown that DC-SIGN is able to distinguish between two isoforms of Man3, one branched α1-3, α1-6, the other linear α1-3, α1-2, with high prejudice since version 2.1 of its Mammalian Printed Array.

To our knowledge, modeling ligands based on terminal sugar epitopes and density of glycan to predict cellular outputs has not been seen before in the literature. The significance of the structural factors and of density indicates a trend that could be used in future studies that attempt to model DC interaction with complex carbohydrate structures. Combining inferences made from the models in both **Equation 1a-d** and **Equation 2** it could be theorized that permutating a limited number of terminal glycan structural motifs across densities could account for the largest impact on DC phenotype. However, this conclusion is seemingly confounded in **Table 6** because in this model density is not a significant factor. However, this can be explained by the fact that all conjugates used in this study were conjugated at the 100:1 molar ratio. Thus, the variance that was seen

between number of ligands per BSA was much smaller than that of the previous study. This lack of variance leads to the density variable being a relatively uninformative variable in this model. However, it was retained in the model so that future researchers are able to compare their glycoconjugates to ours regardless of density or formulation used.

CHAPTER 5 ELUCIDATION OF HOW PRESENTATION MODALITY OF GLYCOCONJUGATES ALTERS DENDRITIC CELL PHENOTYPE

5.1 Overview

Currently the field of glycobiology is focused on assessing the immunomodulatory ability of different glycan structures, densities, and molecular contexts of presentation. However, the experiments performed herein test the hypothesis that it is also modality of glycan display that can shape DC phenotype. The study began by using the optimized glycoconjugates from Chapter 4 and assessing these conjugates' ability to be bound by recombinant human CLRs. After confirming that recombinant human CLRs could bind to the conjugates the DC response to these conjugates presented in three modalities (a range of soluble concentrations, adsorbed to 1 μm polystyrene beads, and adsorbed to the wells of a 384 well plate) was performed. The DC response to different modalities of presentation were found to be have differential DC responses across each of the conjugates tested. Thus, a confrimation of whether this difference was due to DC apoptosis and/or necrosis was measured in response to each of the conjugate modalities to ensure that cell viability was not the cause of the differential response. It was found that cell viability was not altered for any of the modalities from that of untreated cells, however, cell apoptosis was increased for high amounts of β-glucan. Once confirmed that cell response to the conjugates presented in different modalities was not due to cell viability, a general linear model was created to determine if differences in cell response to different modalities of display were statistically significant. In this model β-glucan and mannan were removed to avoid the confounding viability results. The

model showed a difference in DC IMF between modalities and thus confirmation of what receptors DCs were using to interact with these conjugates was performed. Dendritic Cell CLRs were blocked with antibodies specific for two likely candidates for glycoconjugate interaction and compared to DCs that were isotype control Ab treated or treated with non-specific CLR inhibitor EDTA. These studies showed that DC IMF, in response to adsorbed mannose conjugates, was inhibited by antibody blocking and EDTA treatment. Finally, with the knowledge that DCs were using CLRs to interact with the adsorbed mannose conjugates an assessment of whether internalization of the adsorbed conjugates was occurring was determined. It was found that fluorescently modified adsorbed conjugates were internalized by DCs, though to a lesser extent than soluble conjugates. Thus, it was concluded that removal of glycoconjugates from adsorbed surfaces was occuring but that internalization of conjugates was not sufficient to cause cell activation.

The experiments in this chapter show that modality of display of glycoconjugate is significant in determining DC phenotype in response to the conjugates. The response to the mannose conjugates is mediated at least in part by lectins and it is not internalization of the conjugates that is causing DC phenotype to change. The exact molecular mechanisms for why and how phenotype modulation is occurring were not uncovered in this report but future works are discussed to address this shortcoming.

5.2 Methods

5.2.1 Glycoconjugate Presentation to Dendritic Cells in Three Modalities

For all experiments where glycan conjugates were adsorbed to flat wells a 384 well tissue culture polystyrene (TCPS) plate was coated with 20µg/ml of the BSA

glycoconjugates dissolved in PBS overnight at room temperature. Then, all the wells were washed with complete DC medium five times and blocked for two hours at 37°C with 5mg/ml biotin free HSA in 0.1M $NaHCO_3$. After blocking the plates were then washed 5x with complete DC media and 40 µl of cells at 7.5x 10^5 cells/ml were added to each well and allowed to incubate for 24 hours. DC phenotype was then assessed using the HTP methodology discussed in Chapter 4.2.9.

For all soluble conjugate deliveries wells of a 384-well plate were pre-coated with complete DC medium overnight and then washed and blocked as per the method used above for glycan conjugates adsorbed to flat wells. Glycoconjugates were dissolved in complete DC medium at concentrations starting at 100 µg/ml with 1:10 dilutions and used to resuspend DCs which were then immediately added to the pre-blocked wells of the 384-well plate for 24hours of incubation. DC phenotype was then assessed using the HTP methodology discussed in Chapter 4.2.9.

For all experiments where DCs were treated with glycoconjugates adsorbed to 1 µm beads treatment, wells of the 384-well plate were treated as per the method used above for glycan conjugates adsorbed to flat wells. Polystyrene beads (1 µm; Fisher Scientific, Waltham, MA) polystyrene beads were coated with 20µg/ml of the BSA glycoconjugates dissolved in PBS overnight at room temperature. Beads were then centrifuged at 10K RCF for 3 minutes, supernatants removed, and beads resuspended in complete DC medium with vortexing for dispersion of beads. This process was repeated twice more to wash beads. Beads were then resuspended to their original volume in complete DC medium and added to DCs in the blocked wells of the 384 well plate at bead numbers corresponding to 0.2x, 1.0x, 5.0x and 25.0x the surface area of a well and

incubated for 24 horus. DC phenotype was then assessed using the HTP methodology discussed in Chapter 4.2.9.

5.2.2 Assessment of DC Uptake of Fluorescent Glycoconjugates

To assess uptake of glycoconjugates from flat-well surfaces to which they had been pre-adsorbed as described above or as soluble glycoconjugates, the conjugates were fluorescently modified with Alexa-fluor-488-TFP Ester (AF488, Invitrogen according to manufacturer's directions). Briefly, cationized glycan functionalized glycoconjugates were incubated with AF488, 5mg/ml in sterile PBS, at a 10:1 AF488 to protein molar ratio (1 hour, room temperature). After conjugation the glycoconjugates were purified using 10KDa molecular weight cut-off Membrane Centrifugal Filter Unit (Millipore) using 9 rounds of 1:10 buffer exchanges against distilled, endotoxin free, water and stored in the dark. When delivered to cells in a soluble form all wells were precoated with complete DC medium overnight prior to addition of cells or soluble conjugates. To determine internalization of conjugates, cells were harvested onto a filter plate and analyzed for fluorescence uptake. Thus, after 24 hours of incubation with fluorescent conjugates cell suspensions were pipetted up and down vigorously 3 times and then transferred to a 384 well filter plate (Pall). Cells were then spun down at 400 RCF for 5 minutes and the resultant supernatant was removed. While this was occurring adherent cells remaining in wells were incubated with non-enzymatic cell dissociation solution (CDS; Sigma Aldrich) for 2 minutes and then transferred to the spun down filter plate. Cells were then spun down at 400 RCF for 5 minutes and the resultant supernatant was removed. In the 384 filter plate, cells were then washed with wash buffer (1.0 wt.% BSA, 0.1 wt.% TWEEN 20, 1x PBS) one time, fixed with 1% formaldehyde for 30 minutes,

washed with PBS, and incubated with 0.1% trypsin (Sigma Aldrich) for 1 minute. Cells were then washed three times with wash buffer, resuspended in wash buffer and quantification of fluorescent-glycoconjugate internalization was performed via plate reader with fluorescence Excitation/Emission of 488/520.

5.2.3 Assessment of DC Uptake of Glycoconjugate Coated Fluorescent Microbeads in the Presence of Blocking Agents

All studies where ethylenediaminetetraacetic acid (EDTA) or blocking anti-bodies were used to block CLR receptors, cells were treated with either 10mM EDTA, 10 µg/ml of mouse anti-human Dentin-1 (clone 259931, R&D Systems), 10 µg/ml of mouse anti-human DC-SIGN (clone 120507, R&D Systems) or 10 µg/ml of mouse anti-human IgG2B (Clone 20116, R&D Systems) for 30 minutes at 37°C before exposure to adsorbed glycoconjugates. Similarly, for the negative control cells were incubated at 4°C for 30 minutes prior to exposure to the glycoconjugates and then maintained at 4°C for four hours in the presence of the coated fluorescent microbeads (1 µm Purple high intensity, Exc./Emm. 590 nm/ 630 nm, Sphereotech). The 4°C treatment is a common non-specific inhibitor of DC phagocytosis and thus was seen as a negative control and non-specific inhibitor for DC phagocytosis. EDTA is a common inhibitor of CLR activity in DCs because it chelates calcium and prevents these calcium dependent receptors from forming a functional binding pocket. However, EDTA also has broad effects on DC behavior.[246] Thus, two blocking antibodies specific for common, well characterized CLRs, Dectin 1 and DC-SIGN, were chosen to show specific inhibitory ability of DC interaction with conjugates. Cells were then transferred, with media still containing EDTA or antibody (where applicable) to the wells with the fluorescent bead adsorbed glycoconjugates in a

1:10 cell to bead ratio and the subsequent phagocytosis was assessed after 4hrs. For assessment of phagocytosis cell suspensions were pipetted up and down vigorously 3 times and then transferred to 1.5ml eppendorf tubes. Cells were then spun down at 300 RCF for 10 minutes and the resultant supernatant was removed. Cells were then washed with PBS, fixed with 1% formaldehyde for 30 minutes, washed again with PBS, and incubated with 0.1% trypsin for 1 minute. Cells were then washed three times with PBS, and quantification of phagocytosis was performed via flow cytometry (BD LSR II Flow Cytometer, BD Biosciences).

5.2.4 Preparation and Assessment of ζ-Potential, Mass and Endotoxin Content of Glycoconjugates

All mass spectra and ζ-potential measurements were performed in an identical manner to that of Chapter 4. The endotoxin contents of the glycoconjugates was assessed in an identical manner to that of Chapter 4. The endotoxin content of all glycoconjugates was determined to be less than 0.2 EU/mL, which is well below the FDA limit of 0.5 EU/mL. Furthermore, all mannose conjugates were below the detection limit of the assay for endotoxin content.

5.2.5 Binding Assay of Recombinant Human C-Type Lectin Receptors to Adsorbed Glycoconjugates

A 384 well tissue culture polystyrene (TCPS) plate was coated with 20μg/ml of the glycoconjugates overnight at room temperature. During this incubation, rhDectin-1 or rhDC-SIGN-Fc Chimera (R&D Systems) were biotinylated according to manufacturer's direction from Solulink's ChromaLink™ Biotin Protein Labeling Kit. Briefly, biotin-PEG_3-bis(arylhydrazine)succinimidyl ester dissolved in

dimethylformamide at 5 mg/ml was added to rhDectin-1 or rhDC-SIGN-Fc in a 10:1 biotin to protein molar ratio and allowed to react for 2hrs at room temperature mixing at 900 RPM. Next, proteins were purified via provided Zeba spin columns (Pierce) and then diluted to 15 µg/ml with lectin buffer (0.1 mM $MgCl_2$, 0.1mM $CaCl_2$, and 1x PBS) (Sigma). Extent of biotinylation was then confirmed via included standards and UV fluorescence at 354nm.

After the completion of the overnight incubation all wells with glycoconjugates were washed and blocked for two hours at 37°C with block solution (1x PBS, 5 mg/ml biotin free BSA, 1mM $MnCl_2$, 1mM $CaCl_2$ and 0.1wt% TWEEN20). After blocking the plates were then washed 5 times with the wash solution 3 (0.5mg/ml BSA in 0.1x PBS, 0.1mM $MnCl_2$, 0.1mM $CaCl_2$, and 0.01wt% TWEEN 20). Next, a 15 µg/ml rhDectin1-biotin or 15 µg/ml rhDC-SIGN-FC-biotin (diluted in lectin buffer: 1x PBS, 1mM $MnCl_2$, and 1mM $CaCl_2$) was incubated with the adsorbed conjugates for three hours at 37°C or overnight at 4°C. The plates were then washed 5 times with wash solution 3 and 40µl of a streptavidin-HRP (BD Pharmingen) solution diluted 100x with lectin buffer from stock was added to each well and allowed to incubate in the well for 1 hour at room temperature. The plate was then washed 5x more with the wash solution 3 and a TMB (3,3',5,5'-tetramethylbenzidine-peroxide) substrate (BD Pharminogen) was added and the plates were allowed to develop for 10 minutes. 1.0N sulfuric acid was then added to stop the reaction and the absorbance at 450nm was determined.

5.2.6 Culture and Phenotype Assessment of DCs.

Culture and HTP assessment of DC phenotype upon treatment with glycoconjugates presented on various modalities of display was identical to that of Chapter 4. The extent of DC maturation was compared to untreated DCs (iDCs) for the negative reference control and lipopolysaccharide (LPS) (1 mg/ml; E. coli 055:B5; Sigma)-treated DCs (mDCs) for the IMF control, and IL10 and IFNα (R&D Systems) at 3500 units/ml and 35000 units/ml respectively for the TMF control.

5.2.7 Viability/Cytotoxicity and Apoptosis Assessment of Glycoconjugates

Cytotoxicity associated with glycoconjugate treatment was assessed via live/dead staining in an identical manner to that of Chapter 4. The amount of cell apoptosis was of interest due to possibility that cells were impermeable to Ethidium homodimer but still in the process of apoptosis. To assess apoptosis DCs were stained for Annexin V-FITC (BD Biosciences) and the extent of binding to phosphatidylserine was measured. No treatments showed a significantly different viability from untreated cells and no treatment showed a statistical increase in Annexin V binding except for 100 μg/ml β-glucan which showed a statistically significant increase in Annexin V from untreated cells (Data shown in Figure 16) Dead controls were freeze-thawed two times prior to placement into wells.

5.2.8 Statistical Analysis

To observe any significant differences between all sample groups in pairs, a pairwise repeated measures two-way ANOVA followed by Tukey's posttest was performed using the SAS software (Cary, NC), and the p-value equal to or less than 0.05 was considered significant. Significance of general linear statistical model parameters discussed in section 5.2.9 of this report and seen in **Model 3a** and **b** and **Model 4** was

determined by T value in reference to referent group discussed in section 5.2.9 of this report.

5.2.9 Statistical Modeling

Table 7 lists the quantitative parameters that were collected and separates them by variable classification: Continuous, categorical/nominal, and binomial. The characterization of the variables *Inflammatory Maturation Factor (IMF), Tolerogenic Maturation Factor (TMF), ligand* attached to carrier, *modality* of display, and *donors* can be seen in Table 7A and B. Table 7A contains *IMF* and *TMF* continuous variables. Table 7B contains the variables*: Ligand, modality*, and *donor*. There were 20 total donors for this analysis.

Model 3a and **b** show the general linear models that have IMF (a) or TMF (b) as outcome variables and are a function of the ligand conjugated to BSA, modality of display, and the donor. The models in **Model 3a** and **b** sought to isolate and compare the effect of presentation modality when controlling for ligand and donor variations. The null hypothesis was that modality of presentation did not play a role in IMF or TMF and thus that this variable would not have a significant T value when compared to the referent group discussed below. The coding of these variables is shown to denote the reference group, always denoted by the coding value of 0. The reference ligand was none and thus its value for this variable is shown as 0 in Table 7B. Three other classes of ligand were analyzed in this model: *oligoethylene glycol linker (OEG),* monosaccharide *glucose (Glc),* and monosaccharide *mannose (Man).* Similarly, adsorbed glycoconjugates were the reference group for the modalities of display and 1μm beads at a surface area ratio of 1x to that of well adsorbed and 1.0 μg/ml soluble modalities were the other modalities compared in the model. Finally, the variable *donor* was included in the analysis to account for the repeated measures of each donor across conjugates and to help limit the large inter-donor variability that is seen with primary donors.

$IMF = \beta_1 + \beta_2 * donor + \beta_3 * ligand + \beta_4 * modality$ **Model 3a**

$TMF = \beta_1 + \beta_2 * donor + \beta_3 * ligand + \beta_4 * modality$ **Model 3b**

The reference donor was chosen at random and because all other factors control for donor in their calculation of beta no influence on the calculated coefficients or their significance was seen when changing between reference donors. Thus, the reference group was any donor with a conjugate that had no ligand and was adsorbed to the well of a plate.

Table 7A: List of continuous variables and their statistics

	IMF	TMF
Number of Measures*	96	93
Mean	0.9705	0.1081
Standard Dev.	0.5833	0.1414
Minimum	0.273	-0.107
Maximum	3.309	0.735
Skewness	1.552	1.952
Kurtosis	2.656	5.821

*Three donors fell below the detection limit of the assay for TMF and were not included in the dataset.

Table 7B: List of categorical variables, their coding in the model, and the frequency of occurrence.

Variable	Sub Category	Code	Count
Ligand			
	None	0	24
	OEG	1	24
	Glc	2	24
	Man	3	24
Modality			
	Adsorbed	0	48
	1 um Bead	1	24
	Soluble (1ug/ml)	2	24
Donor			
	1-20	0-19	96

For the comparative model used the R^2 was calculated to determine how well the model fits the data. The R^2 value of model was 0.874 and thus the model was seen as a reasonably good model for the data. Furthermore, the IMF data has historically been shown to be approximately normal and the variance of the data remains constant across all samples thus the linear model used herein is further deemed as a valid analysis method.[224]

Model 4 shows a general linear model that has IMF as outcome variables and is a function of donor used (*donor*), ligand linked to BSA (*ligand*), modality of presentation (*modality*), and the interaction between modality and ligand (*ligand*modality*). **Model 4** sought to isolate and compare the pairwise comparisons between all pairs of ligand on BSA and modality of display of that ligand. The null hypothesis was that no ligand-modality combination would be different from each other. To make this comparison, after the ANOVA was performed, all ligand-modality combinations were compared using

Tukey's Post-test. In this model the reference group was any donor tested with a BSA conjugate with no ligand, presented from a well adsorbed modality. Finally, the variable *donor* was included in the analysis to account for the repeated measures of each donor across conjugates and to help limit the large inter-donor variability that is seen with primary donors. The reference donor was chosen at random and because all other factors control for donor in their calculation of beta no influence on the calculated coefficients or their significance was seen when changing between reference donors.

$$IMF = \beta_1 + \beta_2 * donor + \beta_3 * ligand + \beta_4 * modality + \beta_5 * ligand * modality \qquad \textbf{Model 4}$$

5.3 Results

5.3.1 Overall Experimental Approach

In house produced glycoconjugates were produced as per the methodology used in Chapter 4 for the highly cationized high density BSA conjugates. These conjugates were chosen based on the results from that section and because of the historical precedence of importance of cationization and high density of glycan for response from DCs. The bioavailability of sugars from adsorbed conjugates was confirmed via a binding assay of recombinant human CLRs, Dectin-1 and an Fc-DC-SIGN chimeric protein, to adsorbed glycoconjugates. The primary focus of this study was to assess how DC phenotype of presented glycoconjugates was affected by the modality of display: adsorbed to a flat well surface, soluble, or adsorbed to a 1 μm PS beads. The overall experimental approach is shown in Figure 13 including glycan modification of the maleimide functionalized BSA, cationization of the BSA with an excess of EDA, the subsequent adsorption of the glycoconjugates onto plates or microbeads, and finally assessment of DC phenotype to either soluble, bead adsorbed, or flat well surface adsorbed conjugates. Analysis of issues of DC interactions with glycoconjugates

included examining phenotype for DCs pretreated with blocking antibodies for the CLRs, DC-SIGN and Dectin-1, and uptake of fluorescently labeled glycans during DC treatment with these reagents.

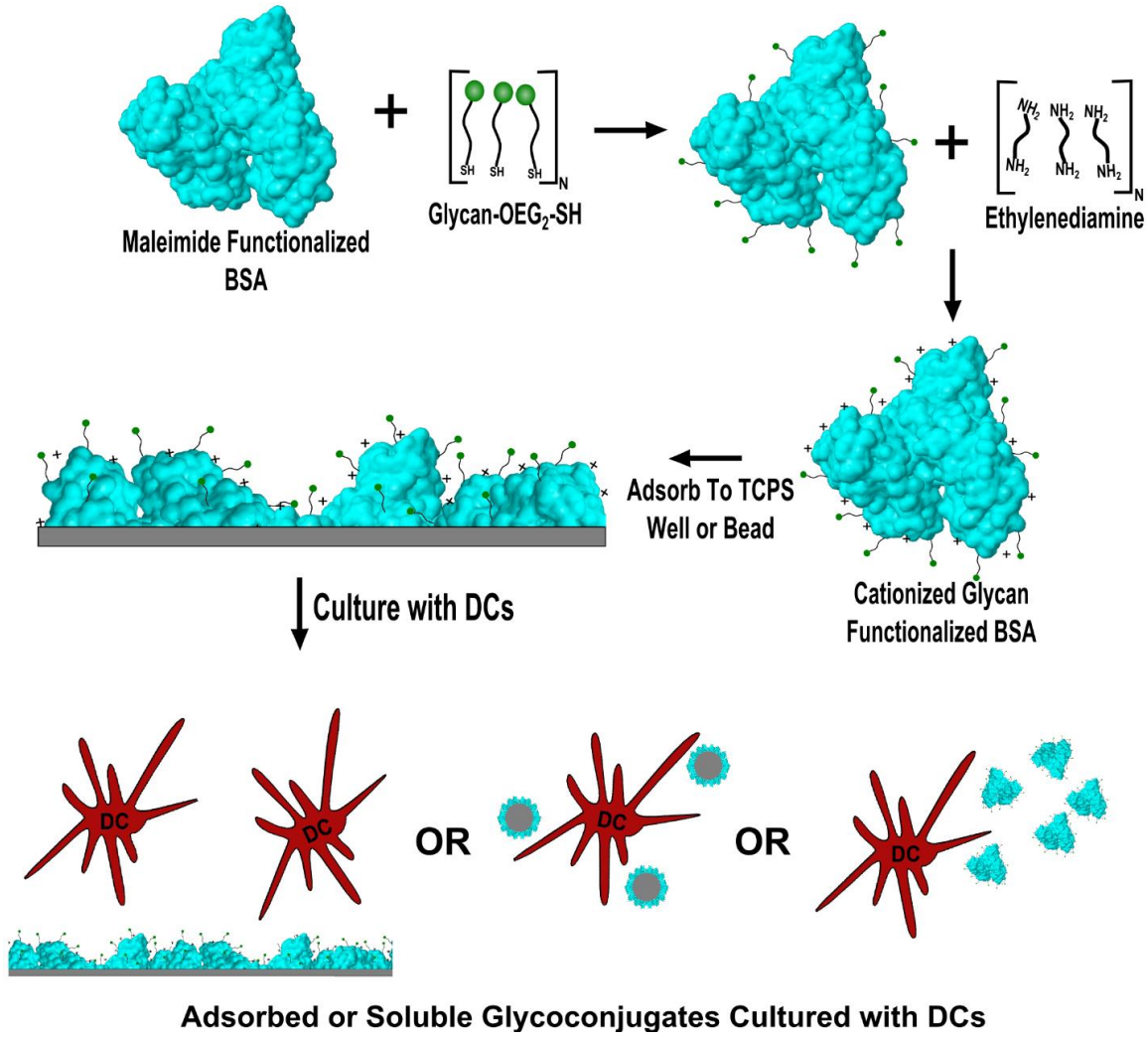

Figure 13: Diagram of the modification of BSA, adsorption onto well or microbead, then culture with DCs as either adsorbed to flat well surface, adsorbed to microbead, or soluble modalities.

5.3.2 Characterization of Glycoconjugates

The same set of glycans prepared for, characterized and used in the study described in Chapter 4 were used again for these studies. More specifically, Table 8 also

shows the calculated isoelectric point (pI), and hydrodynamic radius for each conjugate. The mean isoelectric point of each conjugate was approximately equal for all conjugates and was close to a pI of 10. While obtaining the ζ-potential of each conjugate the hydrodynamic radius was also measured and can also be seen in Table 8. Of interest is that each of the ligand reacted conjugates was smaller than that of the H-BSA alone.

Table 8: Molecular properties of the BSA conjugates used in this study.

Name	Ligand	Sugars/BSA	Isoelectric Point	Hydrodynamic Radius (nm)
H-BSA	**None**	0	10.08	5.12
H-BSA-OEG100	**OEG**	4.41	9.85	2.97
H-BSA-Glc100	**Glc**	26.2	10.1	3.62
H-BSA-Man100	**Man**	23.5	9.63	2.99

5.3.3 Recombinant Human Lectins Are Able to Bind to Flat Well Adsorbed Glycoconjugates.

To confirm that the adsorbed conjugates had biologically available glycans that were able to interact with CLRs on DCs and that the adsorption of these conjugates produced relatively consistent presentations of glycans; a binding assay with recombinant CLRs was performed on all conjugates adsorbed to the wells of 384 well TCPS plates. Unexpectedly, the mean absorbance for the H-BSA-Man100 conjugates with DC-SIGN, was higher than was observed for mannan, the positive control. Figure 14 shows the results of this study. Figure 14A shows the binding of rhDC-SIGN and Figure 14B shows the binding of rhDectin-1. Figure 14B shows little binding of Dectin-1 to any of the conjugates other than the positive control. This Positive controls Mannan for DC-SIGN and β-glucan for the Dectin-1 both showed high binding of DC-SIGN and Dectin-1 respectively. No signal above the detection limit of the assay was seen for H-BSA-Glc100, H-BSA-Man100, or mannan.

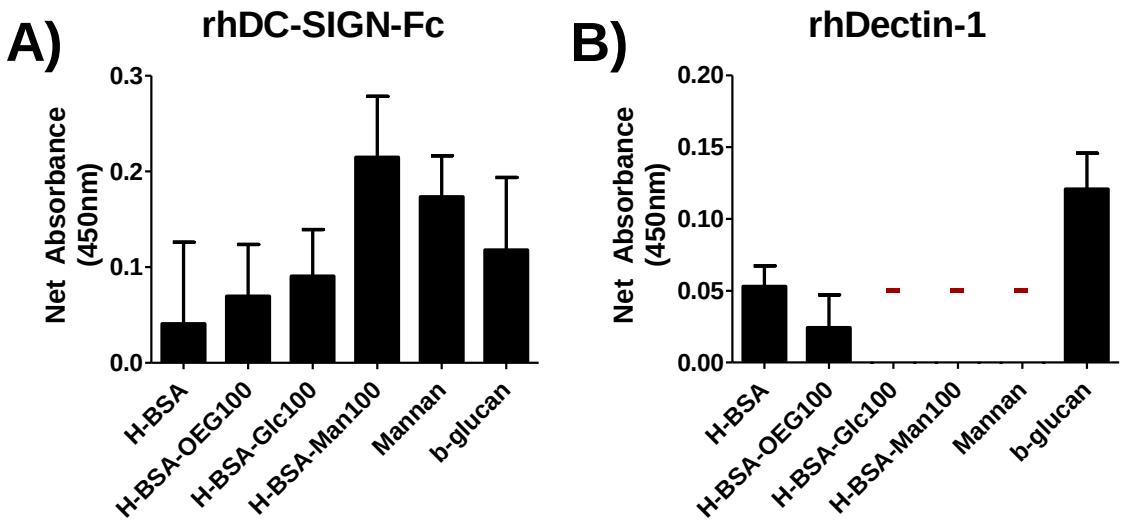

Figure 14: Binding assay for glycan recognition by recombinant human CLRs, rhDC-SIGN-Fc and rhDectin-1, showed CLR specificity for the conjugates. (A) Biotinylated rhDC-SIGN-Fc was incubated with adsorbed conjugates and the subsequent mean absorbance for each conjugate was measured. (B) Shows biotinylated rhDectin-1 incubated with adsorbed conjugates. All signals are background subtracted from untreated wells. N=4 Trials, 3 wells/trial. "-" indicates below detection limit of the assay.

5.3.4 Dendritic Cell Response to Glycoconjugates was Different Between the Three Display Modalities for Both DC IMF and TMF

Assessment of DC resposnes to glycoconjguates presented in three different modalities shows that glycans adsorbed to flat well surfaces support the highest level of IMF response (Figure 15E) while presentation of glycoconjugates in the soluble form (Figure 15A) resulted in the smallest effect on IMF, both compared to iDCs. Presentation of glycoconjugates adsorbed to 1 µm PS beads resulted in an intermediate level of induced IMF expression (Figure 15C) . Figure 15A and B show the DC response to glycoconjugates when adsorbed to 1 µm polystyrene (PS) beads at four different bead surface area ratios. Each ratio represents a multiplicative of the surface area of a well. The surface area of a well was chosen as a standard rather than bead number or ratio of

beads to cells because it was desired that the results from these studies be directly compared to those of the well adsorbed studies shown in Figure 15E and F. Figure 15A shows that when control ligands LPS, mannan, and β-glucan were adsorbed to 1μm beads all caused a statistically significant increase in IMF. LPS showed the highest level of activation, with significant increases in IMF at all surface area ratios while mannan and β-glucan showed a significant increase in IMF at 25x, and 5x ratios respectively. No other treatments were different from iDC except the positive control (mDC). However, of note is the increased trend in IMF for 5x and 25x surface area ratios for both H-BSA-Glc100 conjugates and H-BSA-Man100 conjugates. The trend of increasing IMF with increasing surface area ratio was then analyzed using a GLM in which donor and treatment were controlled for and surface area ratios were compared. Using Tukey's Post-test all pairwise comparisons between surface area ratios were performed and Table 9 shows the results. Both 5x and 25x surface area ratios were significantly different from 0.2x and 1.0x. However, 0.2x and 1.0x were not statstically different from eachother, nor were 5x and 25x ratios. Thus, the trend of increasing IMF with surface area ratio was further substantiated using this model. No significant increase in TMF for any conjugate adsorbed to 1 μm polystyrene beads was seen except for the TMF positive control, tDC. When TMF was modeled in a GLM with surface area, ligand, and donor as categorical predictor variables no surface area ratios reached significance.

Table 9: Pairwise comparisons between all surface area ratios for DC IMF.

Surface Area Ratio	0.2x	1.0x	5.0x	25.0x
0.2x		0.8146	0.0002	0.0006
1.0x	0.8146		0.004	0.0092
5.0x	0.0002	0.004		0.9928
25.0x	0.0006	0.0092	0.9928	

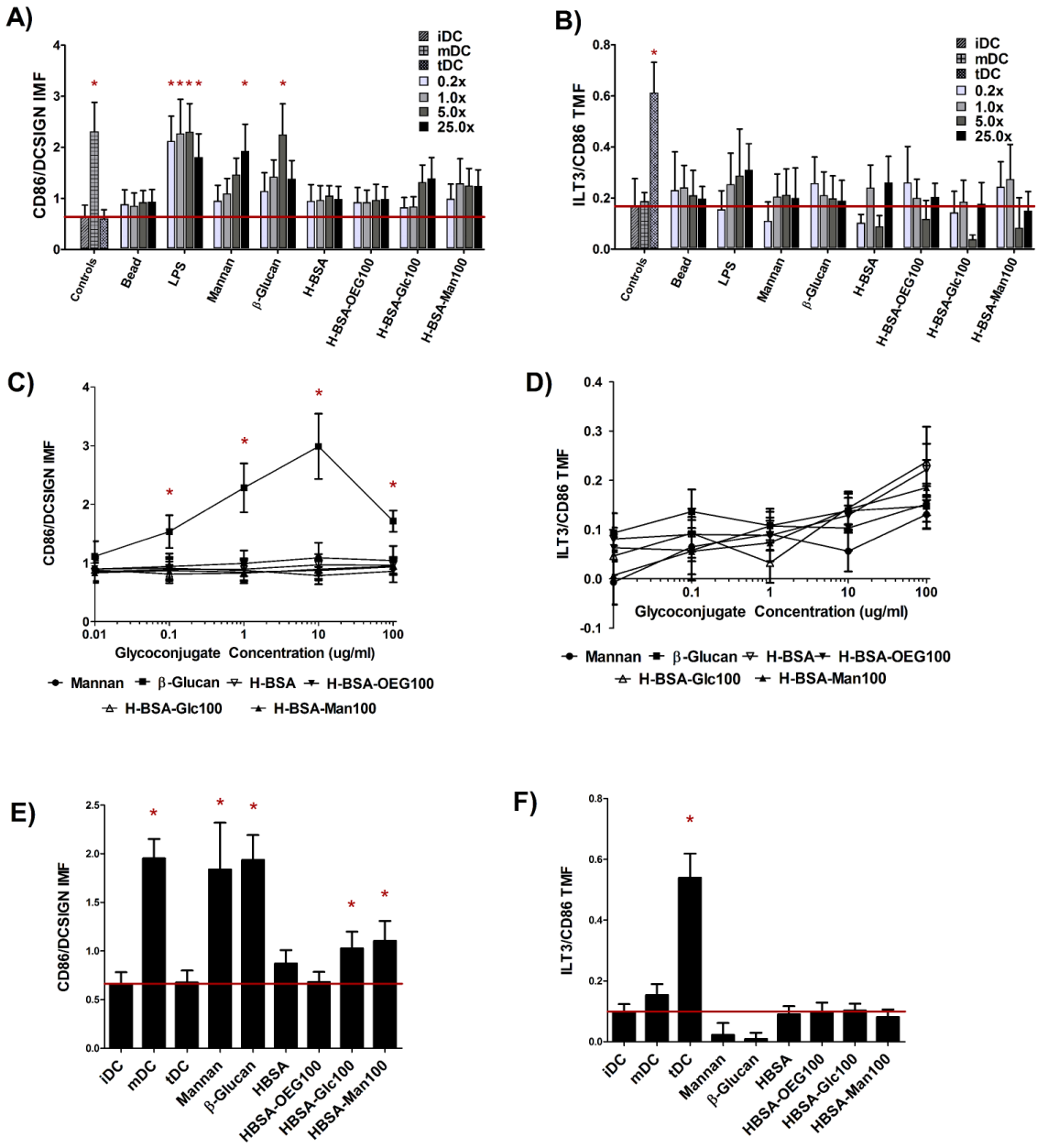

Figure 15: DC Response to glycoconjugates presented in three modalities of display. (A), (C), and (E) show the IMF response of DCs to the conjugates and (B), (D), and (F) show the TMF response from DCs. (A) and (B) show the DC response to glycoconjugates when adsorbed to 1 µm PS beads at 0.2x, 1.0x, 5.0x and 25.0x the surface area of a well. Bead surface area was scaled by increasing bead number until the desired ratio was reached. (C) and (D) indicate DC response to soluble conjugates across five orders of magnitude of concentration. (E) and (F) show DC response to well adsorbed conjugates. For A-D N=6 donors, E and F N=12 donors. Error bars represent standard error, red line indicates mean iDC response, * indicates statistical difference from iDC.

Figure 15C and D show the DC response to glycoconjugates when delivered in five different soluble concentrations. The concentration of conjugate was varied over 5 orders of magnitude, from 10 ng/ml to 100 µg/ml. Figure 15C shows that when control ligand β-glucan is delivered to DCs at any concentration between 100 ng/ml to 100 µg/ml IMF increases significantly over that of untreated cells. Interestingly, the 100 µg/ml treatment did not cause the highest level of IMF. This was due to statstically significant increases in apoptosis of DCs at this β-glucan concentration as measured by Annexin V-FITC. Results of the apoptosis test can be seen in Figure 16. No other treatments, including soluble mannan, at any concentration, were statistically different from untreated cells. No significant increase in TMF for any concentration of soluble conjugate was seen. However, for BSA glycoconjugates as soluble concentration increased an increasing trend in TMF is seem. This trend, when modeled using a general linear model, was not found to be statistically significant. However, β coefficients were found to be consistent with visual trends showing that β coefficients for concentration were positive when predicting TMF as a function of concentration, BSA conjugate, and donor (data not shown because βs did not reach 0.05 significance.).

Figure 15E and F show the DC response to glycoconjugates when adsorbed to the wells of a 384 well TCPS plate. Figure 15E shows that when control ligands Mannan or β-glucan were adsorbed to wells and displayed to DCs, IMF increases significantly over that of untreated cells. The positive IMF control, mDC, was also shown to be statistically different from untreated cells. Interestingly, both adsorbed H-BSA-Glc100 and H-BSA-Man100 were also significantly increased over untreated cells. Figure 15F shows that no

significant increase in TMF for any adsorbed conjugate was seen except for that of positive control tDC.

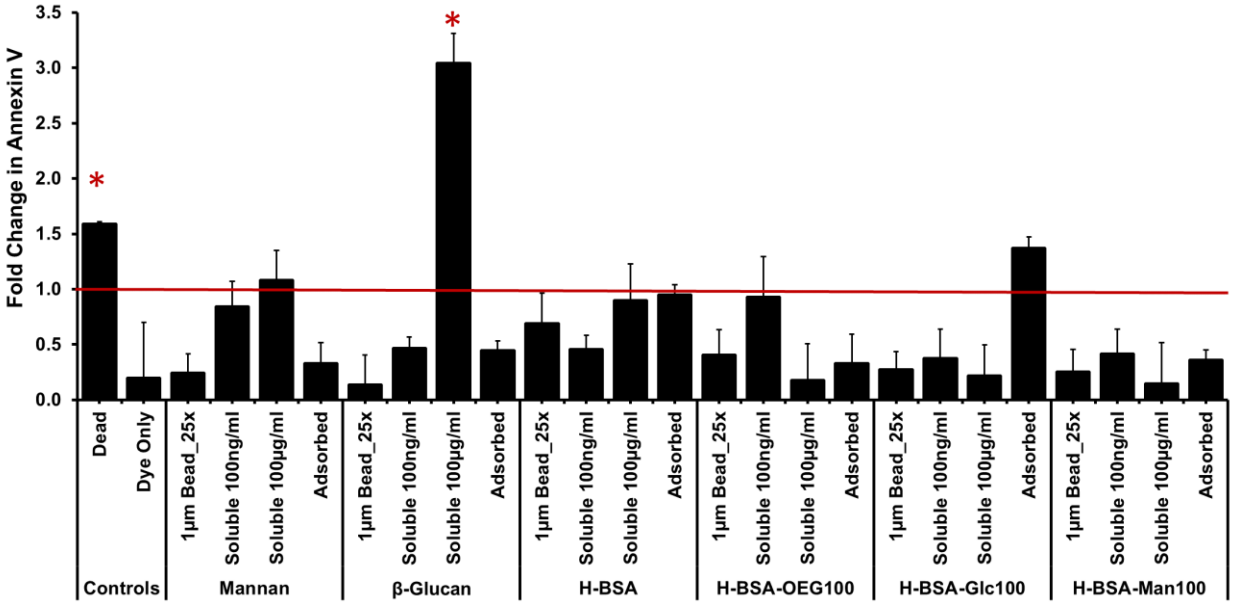

Figure 16: DC apoptosis as measured by Annexin V-FITC Binding. The average fold change over untreated cells is shown. Positive control (dead) and 100 µg/ml β-glucan showed a statistical increase in fold change of Annexin V binding. N=3 donors. Error bars represent standard error, red line indicates mean iDC response, * indicates statistical difference from iDC.

5.3.5 Display Modalities are Significantly Different for DC IMF when Statistically Modeled.

A measure of whether DCs showed an altered phenotype when exposed to conjugates displayed in different modalities, when controlling for ligand used and donor, was desired. Thus, two sets of statistical models were created. The first set of models assessed whether DC response to modality of display was different controlling for ligand of glycoconjugate and donor and can be seen in **Model 3a** and **b**. The second model

assessed which specific conjugates and display modality combinations were statistically different for IMF. This models can be seen in **Equation 1**.

The results of **Model 3a** show that for IMF all modalities are statistically different from each other controlling for ligand and donor with all probabilities being lower than $P<0.0042$. The results of **Model 3b** showed that for TMF no modalities are statistically different from each and that adsorbed and bead adsorbed modalities are co-linear and thus can either be combined or one must be excluded from the model for it to converge. In both **Model 3a** and **b** all variables were treated as categorical variable as seen in Table 7B and when modeled were divided into their binomial substituents as indicated in the methods of this dissertation. A table of the comparison between all modalities and their P values can be seen in Table A 7 of the appendix.

Based off of the results from **Model 3a** and **b** a model assessing the interaction between ligand and modality was desired to determine which ligand/modality combinations were significantly different from each other. **Model 4** showed that Adsorbed H-BSA-Man100 was statistically different from soluble delivery of H-BSA-Man100 and soluble H-BSA-Glc100. To do compare these ligand/modality pairs **Model 4** creates an interaction variable to determine which specific pairwise comparisons between the modality/ligand combinations are different. No other differences between modalities of display were noted from this analysis. A TMF model using an interaction variable was not performed due to the instability of **Model 3b.**

5.3.6 Cell Interaction with Glycoconjugates

5.3.6.1 DC phagocytosis of mannose glycoconjugate coated microbeads is inhibited by anti-CLR antibodies

After identifying that display modalities altered DC phenotype an attempt to determine which receptors DCs were using to respond to these glycoconjugates was performed. An assessment of DC phagocytosis of conjugate coated 1 μm fluorescent polystyrene beads was performed. Dendritic cell phagocytosis of the mannose glycoconjugate coated beads was significantly inhibited when blocked with antibodies specific for lectins DC-SIGN or Dectin-1, 10mM EDTA, or treatment at 4°C as can be seen in Figure 17D. No anti-body or EDTA significance was found for any of the other conjugates other than the mannan control (shown in Appendix Figure A 3). Figure 17 shows the results from this study. In Figure 17A-C only the negative control, 4°C treated DCs, were statistically different from the isotype control treated cells. From Figure 17D it is clear that EDTA and 4°C treatment of DCs has a larger impact on phagocytosis as compared to the antibody treated cells, however no statistical differences can be seen between these groups. Figure 17D thus indicates that for beads coated with H-BSA-Man100 phagocytosis is mediated through lectin interaction and specifically can be inhibited partially by blocking DC-SIGN or Dectin-1. Phagocytosis of other conjugate coated beads is not mediated by lectins as indicated by lack of statistical inhibition via EDTA. The controls uncoated bead, mannan coated beads, and β-glucan coated beads can be seen in the Appendix of this report in Figure A 3. The uncoated bead showed similar results to that of H-BSA while mannan was significantly inhibited by the EDTA and 4°C.

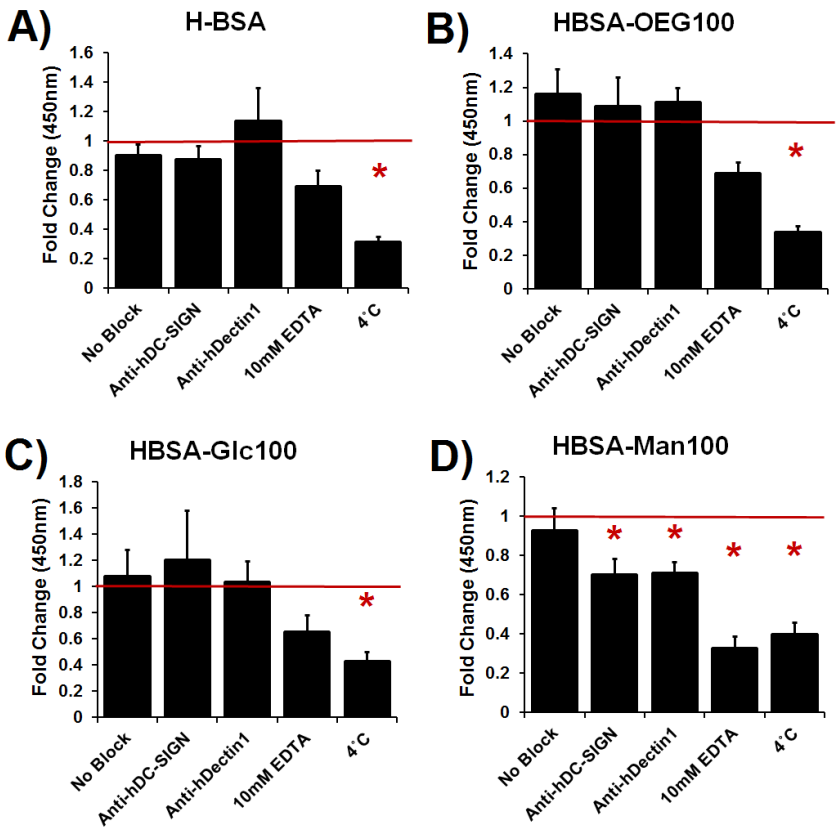

Figure 17: Antibody blocking to confirm receptor specificity. Blocking antibodies reduce phagocytosis of beads. Data is fold change over isotype treated DCs. N=4 donors. Error bars represent standard error, red line indicates mean isotype Ab treated cells' internalization of beads fluorescence, * indicates statistical difference from isotype Ab treated cells.

5.3.6.2 DCs are internalizing adsorbed conjugates but to a lesser extent than soluble conjugates

Finally, whether DCs were internalizing conjugates from adsorbed surfaces was quantified to determine if cells were capable of removing adsorbed conjugates from the surface. DCs internalized both adsorbed and soluble conjugates as indicated by all treatments in Figure 18 having a net positive fluorescence when cultured with fluorescently modified BSA conjugates. From Figure 18 it can be seen that for the adsorbed conjugates, as compared to the H-BSA coated wells, more glycoconjugate was taken into cells for both the H-BSA-Glc100 and H-BSA-Man100. The results from

Figure 18 were produced from conjugates that were fluorescently modified and adsorbed to well surfaces or delivered in a soluble form to DCs for 24 hours. Two concentrations of soluble ligand were chosen to test the hypotheses that 1) DCs were capable of internalizing these conjugates and 2) that at a concentration on the same order of magnitude as that of adsorbed glycoconjugates a greater fluorescence was seen for soluble conjugates than for adsorbed conjugates. All conjugates delivered at 10 µg/ml had a fluorescence above the detection limit of the plate reader when set at a gain which allowed for resolution of DC/conjugate fluorescence at 1.0 µg/ml and when conjugates were adsorbed to wells. Also of note was that adsorbed H-BSA-Man100 conjugates had a higher mean net fluorescence than did H-BSA-Glc100, though not to a statistically significant amount. Also, the soluble 1 µg/ml conjugates showed a higher mean net fluorescence regardless of ligand used than that of the adsorbed conjugates. Finally, adsorbed H-BSA-OEG100 conjugates had a lower mean net fluorescence than did any other group.

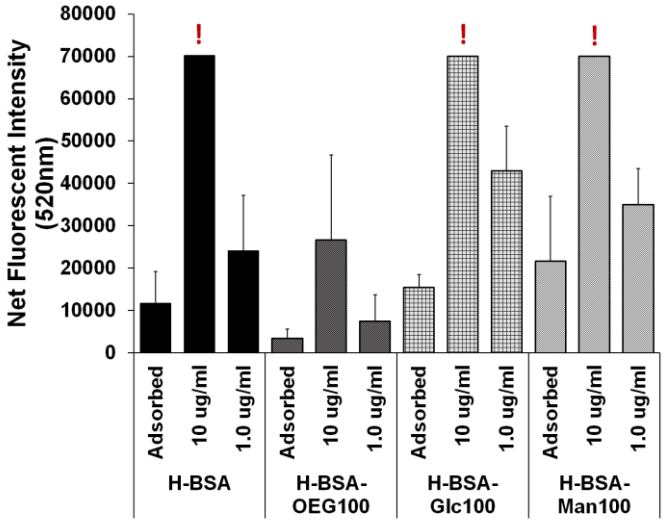

Figure 18: Quantification of internalized fluorescent adsorbed conjugates. The relative amount of fluorescent glycoconjugates adsorbed to wells or in soluble form internalization by DCs after 24 hour incubation. Net fluorescence measured by subtracting signal from DCs treated with non-fluorescent equivalent conjugate. N=2 donors. Error bars represent one half range. ! indicates above the maximum detection limit for the plate reader.

5.4 Discussion

In the studies herein we test only two types of sugars, mannose and glucose conjugates. Glucose was chosen because no known CLR on DCs can bind to the monosaccharide glucose. Mannose was chosen because mannose CLRs on DCs are some of the most heavily studied and well characterized CLRs. Additionally, DCs constantly encounter mannose glycans in different modalities: soluble glycoproteins (plasma glycoproteins)[253], particulate bound glycoproteins (bacterial and viral surfaces)[254,255], and non-phagocytosable glycoproteins (endothelium and parasites).[119,256] The outcome from stimulation by each of these modalities ranges from tolerogenic to pro-inflammatory. Thus, we hypothesized that DCs will react to each modality in a different fashion even if identical glycans are presented. Finally, the studies from Chapter 4 show that DC IMF was increased to an equal amount using the monosaccharide mannose as it was with more complex mannose structures. Thus, single mannose was used in these assays because of its availability, relatively inexpensive cost, and for its ability to provide no confounding structural indications in the modality comparison.

Cellular adhesion or migration were not used in this report as an indicator of DC phenotype because these outputs have been shown to be poor indicators of DC phenotype.[206] Also, the end result of the DC maturation process, whether its pro or anti-inflammatory, CD4 or CD8 stimulating, etc. is independent of adhesion and thus, adhesion was not seen as an ideal reporter for DC, and in general APC, activation.[207]

5.4.1 Characterization of Glycoconjugates

The ELLAs in Figure 14 showed that not only were the H-BSA-Man100 conjugates capable of being bound by rhDC-SIGN-Fc but also that the Glc conjugates were not recognized by rhDC-SIGN-Fc or rhDectin-1. The magnitude of rhDC-SIGN binding to the H-BSA-Man100 conjugates was seen to be greater in magnitude than that of mannan, the positive control; however, this difference was not statistically different

and thus was seen as a confirmation that ligand density was high enough for these conjugates to cause functional binding of rhDC-SIGN-Fc. Additionally, the higher mean fluorescence of the H-BSA-Man100 conjugates from that of wells treated with HBSA, HBSA-OEG100, and H-BSA-Glc100 indicate that rhDC-SIGN-Fc was able to bind to the glycoconjugates with relatively high specificity. Therefore, from this the results of the rhDC-SIGN-Fc bidnign assay in Figure 14A it was inferred that H-BSA-Man100 conjugates could be bound by CLRs found on DCs. The Glc conjugates did not show a higher binding affinity for the recombinant Dectin-1 receptor as no signal was above the detection limit of the assay. Because the positive control worked for this ELLA the conclusion that the activation seen in Figure 15 was not mediated by Dectin-1 and therefore unlikely to of occurred through any lectin mediated process on DCs was made. A discussion of what possible receptors could be playing a role is further discussed below.

5.4.2 Cell Response to Glycoconjugates Across Three Modalities

From Figure 15 it is clear that DC response to identical glycoconjugates displayed in different modalities is disparate. Adsorbed mannan, H-BSA-Man100 and H-BSA-Glc100 conjugates were all able to increase DC IMF to a statistically relevant amount as compared to untreated controls. However, whe these same glycoconjugates were delivered in a soluble form no change in IMF for any of these conjugates was seen. Also, when H-BSA-Glc100 and H-BSA-Man100 were adsorbed onto 1 μm beads and cultured with cells a statistical increase in IMF was not seen even for treatments containing enough beads for 25 times the surface area of that of well adsorbed conjugates. From Figure 17 and Figure 18 it is clear that DCs are able to recognize and internalize these

conjugates when adsorbed to 1 μm beads or delivered at low soluble concentrations. Thus, we hypothesize that a different molecular signaling mechanism is involved between each of the modalities. From the raw IMF averages compared between modalities for both mannose and glucose conjugates DC activation is highest for well adsorbed glycoconjugates and lowest for soluble conjugates even delivered at the relatively high concentration of 100μg/ml. DC activation when exposed to 1 μm beads is between these two but a significant trend was seen between surface area and increased IMF and thus it is possible that high ligand concentration is needed to activate DCs in this modality. This has been postulated by other researchers and this report further supports the assertions made by Dam et al.[257]

Of note is that DCs did not respond to soluble mannan at any of the concentrations tested. The negative outcome of the mannan conjugates goes against previous studies that showed that mannan was an immune agonist.[108,208,209] However, in these studies mannan was combined with particulates based on liposomes linked through membrane lipids, such as cholesterol[108] or palmitoyl-mannan.[208] Therefore, it could have been the synergistic effect of the lipids and the mannan that led to these activation reports. This implies that the Th_1/Th_2 cell proliferation that was seen in these studies, that were thought to be mediated through mannan, may not represent the result of the ligand alone but through the synergistic recognition of the conjugates by TLR4 and CLRs. Indeed, in an elegant study by Wattendorf et al.[107] human DCs were cultured with phagocytosable polystyrene microbeads functionalized with di-branched PLL-PEG that had a man, Man3-Br (α1-3 α1-6), or mannan attached to the end of the PEG branch. The mannan and PLL were passively adsorbed onto the PS beads leaving the mannan and

PEG functionalized glycan monomers free in solution instead of being found on the bead surface and no DC maturation was found. This finding further supports our hypothesis not only by confirming the findings herein but also by showing the mannan did not activate cells when in solution and not "bound" to the bead surface.

The fact that the DC response to different modalities appears to be different from Figure 15 was then confirmed using a general linear model, **Model 3a. Model 3a** shows that cell response is statistically different between all modalities of display even when controlling for ligand and donor variances. Furthermore, all pairwise comparisons between modalities of display for **Model 3a** and **b** were done using a Bonferroni correction for multiple comparisons. A Bonferroni correction was used for these models so as to be more conservative in estimation of significance. However, the argument could be made that the glycan display density on well adsorbed surfaces is much higher than that of the soluble or phagocytosable modalities. Because CLRs are multivalent receptors this increased density could be causing the increased activation of the DCs. Determining quantitative estimates of glycan surface density presented to cells is extremely technically challenging when looking at microbead presentation and virtually impossible in solution. Thus, large ranges in concentration and bead number were tested to try to mitigate this concern. Additionally, the same material is used between the well adsorbed and 1 μm bead adsorbed modalities. Thus, the surface density between these two should theoretically be identical as steric hindrance of protein adsorbtion on such relatively large beads (1 μm versus a maximum hydrodynamic radius of 5.2 nm) has been shown to not affect protein adsorbtion.[258,259]

Equation 1a used the interaction variable between ligand and modality to assess differences between modality/ligand combinations. The results of the modeling yielded that Adsorbed H-BSA-Man100 was statistically different from soluble delivery of H-BSA-Man100 and soluble H-BSA-Glc100. In this model, and in **Model 3a** and **b**, mannan and β-glucan were not included. This was done so as not to skew the data toward showing different modalities as significantly different when using poorly defined ligands that clearly showed differences in cell response between modalities. While the result that adsorbed H-BSA-Man100 was different than soluble glycoconjugates was anticipated from a cursory comparison of the statistics shown in Figure 15. Confirmation that DCs' IMF was statistically different between the mannose conjugate modalities further confirms the hypothesis of this report: that modality of glycan display alters DC phenotype; especially when combined with the anti-body blocking data seen in Figure 17.

Finally, no significance for any ligand or modality, other than the positive control, was seen in any of the TMF studies or models. This was not unexpected as mannose conjugates are frequently used as agonists for vaccines and to increase DC recognition and uptake of particles.[107,260,261] Similarly, no known effect of the monosaccharide glucose has been shown on DCs. Thus, that no treatments or modality claims were significant for the tolerogenic reporter was expected. These data were left in the manuscript as validation that such an assessment is possible for DCs using this HTP methodology. This is valuable because CLRs on DCs are also known to be instrumental in promoting tolerance and maintaining immune cell homeostasis.[2,40,63,262] The assessment of tolerogenic phenotypes is especially important for DCs when CLRs are ligated because it has been shown that identical CLR stimulation can promote tolerance

or pro-inflammatory responses from DC depending on if the bound.[1,263,264] Thus, any methodology that assesses activation and pro-inflammatory responses from DCs using CLRs must also evaluate tolerogenic responses from DCs.

5.4.3 Cell Interaction with Glycoconjugates

When combining the cell response data from Figure 15E and the antibody blocking data of Figure 17 it is clear that at least some of the DC response is due to lectin interaction with the H-BSA-Man100 conjugates. However, from Figure 17 it is clear that the lectins tested do not mediate H-BSA-Glc100 activation of DCs shown in Figure 15E. This indicates that the DC response to the H-BSA-Glc100 glycans is independent of lectin activation due to the fact that no other lectin known on DCs, other than Dectin-1, can bind glucose.[42] Thus, another mechanism for DC response to the H-BSA-Glc100 conjugates must be used for activation of the DCs. Other groups have shown that Complement receptor-3 (CR3), lactosylceramides, and scavenger receptors [265] can all bind β-D-glucose and thus it is hypothesized that it is these receptors that are mediating the increase in IMF for adsorbed H-BSA-Glc100 conjugates.

Phagocytosis of beads was chosen as a way to assess DC interaction with any form of glycoconjugate for two reasons. 1) Mannose CLRs on DCs are known to be phagocytic receptors thus this was a functional reporter. 2) Using the HTP reporter of IMF or TMF could not be performed after 24hrs due to activation of cells occurring with prolonged incubation of relatively high concentrations of Abs. All Ab treatments of DCs with 10 μg/ml of Ab, including isotype, were found to activate DCs significantly at 24hrs. A 2 μg/ml concentration of Ab was attempted but showed no functional blocking of the receptors in terms of phagocytosis at 4hrs and no influence of IMF or TMF at 24

hours (Data not shown). IMF and TMF were checked at 4 hours with 10 μg/ml and no up-regulation of either was seen for any conjugate. However, this does not mean that DCs were not being activated by these high concentrations of Ab, just that up-regulation of surface receptors had not occurred yet. Thus, isotype antibody control treated DCs were chosen as the referent group in these studies to overcome concerns over non-specific activation and thus phenotype modulation of DCs due to Ab treatment. Finally, mannan was not inhibited by either of the lectin blocking antibodies, however this was not surprising given that many other CLRs on DCs are capable of binding and recognizing mannan, as indicated in Table 1.

From Figure 18 it can be seen that for the adsorbed conjugates, as compared to the H-BSA coated wells, more glycoconjugate was taken into cells for both the H-BSA-Glc100 and H-BSA-Man100. This further provides evidence indicating that internalization is receptor mediated, especially for H-BSA-Man100 when combined with the Ab blocking data shown in Figure 17. Receptor meditated internalization is further supported by the fact that the adsorbed H-BSA-Man100 conjugates had a higher mean net fluorescence than did other conjugates, though not to a statistically significant amount. Also of interest from Figure 18 is that adsorbed H-BSA-OEG100 conjugates had a lower mean fluorescence than did any other group. This was expected as PEG coated ligands have frequently been reported to in inhibit phagocytosis in the literature.[266,267] Additionally, when looking at any conjugate's soluble delivery it is clear that DCs are internalizing the soluble conjugates. Thus, the internalization of conjugates from the adsorbed wells must not be the sole process necessary for the increase in DC IMF seen in Figure 15.

Finally, the soluble 1 µg/ml conjugates showed a higher mean net fluorescence than adsorbed conjugates regardless of ligand used. This is significant because an approximately equal amount of soluble BSA was delivered as was present on the surface of the adsorbed wells. This calculation came from using the surface density of BSA found by Osborne et. al.[245] for BSA proteins adsorbed per unit area in a polystyrene tube, as measured by ^{125}I-labeled proteins. Using this calculation, 0.0168 µgs of protein are adsorbed to each well surface and thus an equivalent amount of BSA in 40µl of media would be needed. This amounts to 0.438 µg/ml of conjugate being delivered per well. Assumptions for this calculation were that BSA had an average molecular weight of 66,460 Da and that the surface area of the 384 well TCPS plate was 5.6 mm^2. The 1 µg/ml concentration was chosen over delivering 0.438 µg/ml because a direct comparison between the DC internalization of fluorescent conjugates to that of the soluble delivery in Figure 15C and D was desired.

CHAPTER 6 CONCLUSIONS AND FUTURE DIRECTIONS

6.1 Conclusions

This study uncovered a novel mechanism for the alteration of DC phenotype with adsorbed glycoconjugates that had not been reported in the literature before. Furthermore, this report showed quantitatively for the first time that density had the largest impact on DC IMF response and that charge also was a significant factor in DC response to adsorbed glycoconjugates. Additionally, this report showed that factors for promotion of IMF were inversely correlated to factors that promoted TMF. While this claim seems to be common sense, to the knowledge of the authors, this is the first time this has been shown to be statistically true. Finally, this report showed that DC response to oligomannose structures presented from adsorbed conjugates was different between glycan structures. When these structures were grouped in a model by terminal glycan motif it was found that terminal structural motifs played a significant role in the prediction of DC IMF. To date this is the first time that terminal glycan structural motifs have been found to correlate to DC phenotype in response to adsorbed glycoconjugates across a variety of glycan structures. Finally, this study showed that general linear modeling of DC interaction with adsorbed glycoconjugates produced models that had relatively high predictive capabilities, $R^2 \approx 0.6$ for all models, for a study using primary human donors with relatively small sample sizes ($N<20$). It is expected that based off of these results other labs will incorporate this type of modeling into their analyses of DC response to glycoconjugates.

This report also quantitatively shows for the first time that glycoconjugate presentation modality alters DC phenotype. This is of importance for the glycobiology field because it challenges the precepts that glycan structure, density, and context are the only factors of importance for recognition and response from DCs. This paper also helps to resolve conflicts in reports from multiple labs showing differential DC profiles in

response to similar if not identical ligands delivered in different modalities. Additionally, this study beings to bridge the gap between microarray binding data and functional cell responses by highlighting the different phenotypes induced from adsorbed conjugates as compared to those in solution or adsorbed onto microparticles. However, this study leaves many questions unanswered that must be investigated in the future. First, given that different modalities of display are capable of producing differential DC phenotypes, what molecular signaling mechanism is involved in the differential response? Possible explanations include mechanical interaction, length of time of interaction with CLRs on the surface, ability of CLRs to co-localize in a single area for extended periods of time on the cell surface, and/or generation of a "frustrated phagocytosis" state in which DCs release ROS and MMPs that leads to activation of surrounding DCs. A more in-depth discussion of these can be found in the future directions of this chapter.

Second, for the H-BSA-Glc100 conjugates we hypothesized that the activation seen in Figure 15F was not caused by lectin interaction. However, this was not directly proved and anti-body blocking produced inconclusive results. Thus, cell knockout studies should be performed with these adsorbed conjugates to determine if dectin-1 is necessary for DC activation by the H-BSA-Glc100 conjugates and if not which receptors are necessary for activation (see Albeituni et al. for probably receptor classes.)[265] Finally, the results from Figure 18 show that adsorbed conjugates are being internalized by DCs. Whether this internalization is necessary for DC activation and to what extent the internalization of conjugates plays in the phenotype modulation of DCs is an important and unanswered question. A more in-depth discussion of these issues can be found in the future directions of this chapter.

Overall, the experiments proposed above and discussed in detail in the future directions of this chapter are not trivial and will require large amount of glycans and reagents. However, with the use of statistical modeling it was shown in this report that important and here-to-fore unknown associations between glycan structure and DC

phenotype are capable of being uncovering using statistical modeling with relatively small amounts of glycan used (mg quantities). This report showed the power of modeling and from this modeling strong indicators for future carbohydrate presentation approaches were uncovered. Not only was it found that density and charge are both significant factors in adsorbed glycoconjugate alteration of DC phenotype but that grouping carbohydrate structures by terminal motifs one can create a model that has significant structural variables for the modification of DC phenotype. Therefore, it is expected that this report will provide a guide for future glycobiologists to analyze their data so that different glycan formulations can be compared more easily and so that underlying trends in the data can be uncovered. Also, with the relative robustness of the models presented herein, as judged by R^2 values, it is considered rational that other studies will use multivariate linear modeling of their data to determine the relative significance of other molecular factors not considered here (linker charge, length, or flexibility or different polymeric carriers, etc.) that are relevant to phenotype modulation of DCs via CLRs.

In addition to the modeling significance of this work, this dissertation uncovers the importance of non-phagocytosable display of glycans to DCs. This area has generally received little attention in the field of glycobiology and it is expected that this report will increase its exploration and attention. Use of glycans for implant coatings or as adjuvants for combination products for any other purpose than to increase phagocytosis or targeting of APCs is still relatively unexplored. This dissertation shows that not only are glycans able to perform the functions typically associated with glycans but that they can serve as immunomodulators in their own right especially when delivered in a modality that DCs are able to recognize. It is expected that with further optimization of molecular factors glycoconjugates could be engineered to tune the immune response to any desired outcome. Furthermore, the work shown here begins to demonstrate what molecular

factors are of importance for DC recognition of non-phagocytosable glycans which could eventually lead to more efficacious clinical therapies.

6.2 Future Directions

While the studies conducted herein took large steps toward the elucidation and analysis of pertinent molecular factors and modalities of glycan display for optimal DC phenotypic modulation; they do not bridge the gap between basic science and clinical therapy. The field of glycoimmunology, specifically at the cellular and systemic level, is still in its infancy. Many steps are needed to cross the divide between the fundamental cellular responses and potent clinical therapies. This project was seen as building part of the foundation necessary to create these therapies and the future directions listed below are seen as the next steps that would be necessary to begin to fully understand, optimize, and engineer a relevant diagnostic/therapy based on glycoimmunology in the future. The field is still rife with challenges including amount of complex glycan structures able to be produced, scale of assays conducted, relevant and accurate controls, and highly efficacious and specific blocking agents. These are fundamental building blocks that must be created prior to the field being able to quickly, easily, and accurately assess cell responses and are seen as more broad areas of exploration for the field that do not necessarily stem from this project but that are important to its continued advancement.

The immediate future directions of this project can be seen to work in two parallel tracks. Track one is the elucidation and assessment of underlying molecular mechanisms for the response discovered in this dissertation. Track two is the development of a synthetic polymeric carrier that recapitulates the results seen in this study for the adsorbed conjugates but that has more fine control over density of carbohydrate display, charge of carrier, and sugar linker length and motility. Also, varying simple sugars

(disaccharides or less) with the polymer across a range of charges, densities, linker lengths, and linker motilities would be advantageous for this track.

After these two tracks are completed tracks three, four, five and six can be performed in concert. Track three, which was found to be desirable as a result of this dissertation, would be to further scale down the HTP assay to a 1536 well plate and print glycan arrays within the wells of these plates. Ideally, the polymers developed in track 2 would be used here and thus development of a delivery/coating system that delivered the polymer from track 2 with reproducible coating densities and glycan presentations would be needed for the successful completion of this track. Additionally, the fundamental reporting mechanism of this assay would need to be different than the current HTP assay as filter plates are not available in this size and signal to noise ratios of staining antibodies at the volumes necessary for 1536 well plate assays are too low. Track four would be to assess the DC response to a diverse set of well-defined sugar structures using the polymer developed in track 2. Here, well defined sugar structures in each class of sugar known to bind to CLRs on DCs would be iterated to determine the exact structural motifs needed to stimulate DC IMF or TMF. Essentially, taking the basic sugar structures possible in each class of glycan and iterating them over the optimized polymer seen from track 2 and modeling these interactions for prediction of DC response to more complex structures. The sensitivity and specificity of predictive models could be determined by using the motifs as the training and validation set and then then more complex structures as the "test" set. The fifth track would be a clinical study that would isolate and functionalize glycans from the glycoproteins of cancer patients, which are known to show aberrant glycosylation, and display these carbohydrates to DCs for use in

identification of novel targets for therapeutics and novel detection or screening methodologies. Finally, track six would be to isolate, functionalize, and identify glycans from serum glycoproteins that mediate the immune response to implanted materials and utilize these glycans in vaccine or combination products.

6.2.1 Molecular Mechanisms of Dendritic Cell Response to Adsorbed Glycoconjugates.

This dissertation uncovered a previously unknown response of DCs to an adsorbed glycoconjugate. It was shown also shown that cationized conjugates produced a much greater response than did non-cationized carriers. The question then must be asked: why is the response to the cationized adsorbed conjugates by DCs so much higher than that of the non-cationized conjugates? The cationization of carriers and its effect on immune response has been studied a great deal and an in-depth discussion has been performed for other cell types[242,268–270] Perhaps the most obvious explanation for these data is the fact that cationized proteins tend to adhere better to the slightly anionic cell membrane[271] However, this has not been shown on DCs and thus a study similar to that of the Schalkwilk et. al. could be performed with labeled cationized BSA glycoconjugates and DCs to determine if cationized conjugates adhere better to DC surfaces. The possibility also exists that cBSA may be recognized more efficiently by DCs because of its altered structure. This is more difficult to assess but a study could be performed in which a Acrylic acid N-hydroxysuccinimide ester (Sigma) was used to cap all the amine groups of the cationized glycoconjugate and look at the subsequent DC response. However, this is seen as a less definitive experiment because by altering the

charge of the protein the structure of the protein is altered and thus confounding structural changes are introduced.

While this dissertation uncovered a novel ligand capable of inducing DC maturation, how this ligand was able to do so was not uncovered. What signaling and specific receptors are mediating this response? Aim 2 implicates both DC-SIGN and Dectin-1 are important to the DC interaction with the conjugates however, it does not conclusively show that these receptors are necessary for DC IMF up-regulation due to the activation caused by the high concentration of Ab necessary for blocking of these receptors. Thus, DCs from DC-SIGN and Dectin-1 knockout mice could be obtained and treated with the conjugates to determine the receptors necessary for activation. DC-SIGN KO mice are available through the Consortium for Functional Glycomics and Dectin-1 KO mice can be generated as per Taylor et al.[272] The response to surface adsorbed and the conjugates in different modalities should be assessed as DC response was found to vary drastically between modalities of display as well.

Also, given that different modalities of display are capable of producing differential DC phenotypes, what molecular signaling mechanism is involved in the differential response? Possible explanations include mechanical interaction, length of time of interaction with CLRs on the surface, ability of CLRs to co-localize in a single area for extended periods of time on the cell surface, and/or generation of a "frustrated phagocytosis" state in which DCs release ROS and MMPs that leads to activation of surrounding. Mechanical testing could be performed by displaying covalently bound carbohydrates to DCs from polymers with different rigidities and exploring the subsequent DC response. Substrate rigidity has recently been found to influence T cell

activation and proliferation[273] and thus it is expected that DC response would also scale with these factors and could be assessed in a similar fashion to the O'Connor study. Transducing DCs to express fluorescently tagged DC-SIGN and Decint-1 and then measuring the length of time of interaction with fluorescently labeled glycoconjugates via confocal microscopy could be used to determine the length of time of interaction between adsorbed and soluble conjugates. These same transduced DCs could then be used to look at CLR co-localization in response to different modalities of glycoconjugate presentation. Finally, measuring ROS and MMPs in solution after exposure of DCs to adsorbed conjugates could be performed to determine whether DCs were entering into a "frustrated" phagocytic state.

Of additional interest from these studies is how the cells treated with the adsorbed conjugates affect the systemic immune system, i.e. Th_1 or Th_2 proliferation, cytokine and chemokine production, MHC and other costimulatory molecule expression, and presentation of co-delivered antigen. The supernatants from the studies performed in this dissertation were saved at -80°C and can be assayed at any time for cytokine and chemokine content. However, due to the large number of groups that could be tested and the relatively large variability that has been shown to exist for the profiles in the assays[224] the benefit to performing these assays versus the cost of them was seen as low. However, a smaller study could be done in which the highly cationized conjugates were compared across display modalities for a limited number of donors and the subsequent cytokine and chemokine profiles assessed. Additionally, in this reduced study DCs could be stained with a variety of anti-bodies for a range of costimulatory molecules and analyzed via flow cytometry.

For a more functional immune response assessment co-delivery of a model antigen, OVA, with the H-BSA-Man100 conjugates could be performed and the subsequent proliferation of OTI and OTII T cells could be measured. This would identify whether the high IMF seen in the DCs led to a high Th_1 or Th_2 response. Also, the DCs could be assessed for epitopes presented on the MHCI and MHCII of these molecules via antibodies known to bind to OVA or BSA for an assessment of how well the DCs were presenting the co-delivered antigen.

Also, Aim 2 showed that DCs were being activated by the adsorbed H-BSA-Glc100 conjugates. However, in the dectin-1 blocking studies and the ELLAs performed in this Aim, no interaction with Dection-1 was shown for these conjugates. It is known that CR3, lactosylceramide and scavenger receptors all can bind glucose and thus a fully reductive study blocking each of these receptors and assessing the DC phenotype to the adsorbed H-BSA-Glc100 conjugates could be performed.[265]

Finally, the results from Aim 2 showed that adsorbed conjugates were being internalized by DCs but whether this internalization was necessary for DC activation and to what extent the internalization of conjugates plays in the phenotype modulation of DCs was not uncovered. Thus, a study where DCs are treated with the adsorbed conjugates at 4°C and the subsequent DC phenotype assessed after 24 hours could be performed. In all Ab blocking experiments performed in Aim 2 internalization of coated beads was the lowest for DC treated at 4°C thus, internalization and subsequent maturation of well adsorbed conjugates should be performed at 4°C to determine extent of maturation of DCs when minimal internalization of conjugates is occurring.

6.2.2 Development of a Tunable Synthetic Polymeric Carrier for Non-Phagocytosible Display of Glycans to Dendritic Cells.

Track two is the assessment of mannose and sialic acid in mono and disaccharide form from a polymeric structure. Functionally, this track will be very similar to that of Aim 1 in this dissertation. However, instead of development of the BSA carrier the researcher would develop a polymeric carrier for glycans. This polymer would need to be able to be able to scale in charge, glycan density, glycan linker length, and motility/lability of linker. Several types of polymers are possible but Dr. Ravin Narain of the University of Alberta has already developed a library of cationic glycopolymers of pre-determined molar masses and narrow polydispersities ranging from 3 to 30 kDa that were synthesized using RAFT polymerization techniquess. Furthermore, using RAFT polymerization it is easy to scale the level of cationization to that of virtually any desired level using different block copolymers. This chemistry is standard and well characterized.[274] Thus, in collaboration with Dr. Narain a library of conjugates scaling in glycan density, level of cationization, and in linker length could be produced.

In this track only two sets of sugars are proposed to be tested: Mannose and sialic acid. Mannose was chosen because the mannose binding CLRs are the most studied and well understood DC CLRs. Additionally, mannose was shown in this dissertation to produce a pro-inflammatory response from DCs. Thus, the results from this dissertation could be compared to the results of the RAFT polymers produced in this Track. Sialic acid, was chosen as the other sugar of interest because this sugar is known to be bound by Siglecs which have ITIM motifs.[87,100] Ligation of Siglecs has been shown to induce tolerance and apoptosis in DCs[275] and thus it is expected that using sialic acid will increase the TMF in DCs. Though no literature has shown that Siglec ligation leads to

increased ILT3, Siglecs are sialic-acid-binding immunoglobulin-like lectins and thus are in the same receptor super family as ILT-3 and it is therefore seen as likely that these two are linked.

Thus, a polymeric carrier can be optimized for both a pro-inflammatory and anti-inflammatory DC phenotype using these two glycans. Optimization for TMF was a shortcoming of this dissertation as no combination of properties were found to significantly up-regulate TMF; though trends of low density and cationization being favorable for TMF was shown in the models. Furthermore, the properties of the polymer can be optimized for each glycan and then applied to other sugar classes in later studies. Mono- and disaccharides are recommended for use in this section so as to increase lectin affinity for the glycan moieties and to better permutate possible structural motifs found in nature.

6.2.3 High Throughput Development of a Functional Cellular Output in 1536 Well Plates for Use with Printed Glycan Arrays.

This track of experiments has two main development components that can be developed simultaneously. The first is the printing and validation of glycoconjugates in the wells of a 1536 well plate. For this Track the RAFT polymer developed in Track 2 would be immobilized in the wells of a 1536 well plate. Ideally, from Track 2, several polymer formulations would be necessary to exploit the range of DC phenotypes desired across different sugar structures (from tolerogenic to pro-inflammatory) and thus the subsequent characterization of the spotted glycopolymers will need to be performed. A liquid handling system will need to be purchased and ideally the glycopolymers would be formed and spotted simultaneously. The heterogeneity of the spotted conjugates could then be assessed via standard MS and SPR methodologies. This process would be similar to the process used by Langer et. al. and Bradley et. al.[276,277] except using glycopolymers

instead of strictly polymeric or hydrogel substituents. Also, instead of being performed on non-welled slides the procedure would have to be optimized for a 1536 well plate.

The second is a 1536 well HTP approach that uses DCs and T cells to produce a functional output. HTP approach is necessary to assess functional phenotypic effects of glycans for four key reasons. First, only limited amounts of oligosaccharides (at sub-μmol levels) can typically be isolated from natural sources when cleaved from proteins or lipids and they are highly heterogeneous in structure. [4,177–179] Second, the structural diversity of oligosaccharides leads to difficulties in their structural characterization; currently, there is a lack of an efficient means of automated assignment and the characterization is mainly reliant on expert interpretation by MS analyses.[180] Third, the biosynthesis of oligosaccharides is not template driven as it is for DNA and proteins, and thus the diverse repertoire of oligosaccharides that would be representative of the glycoform of a typical glycoprotein is extremely difficult to reproduce by chemical synthesis.[181–183] Fourth, most carbohydrate-protein interactions are of low affinity, and there is a requirement of multivalent presentation of carbohydrate ligands for detection of binding in microscale screening analysis.[104,105,184] All of these challenges are addressed and mitigated by using a carbohydrate microarray as indicated herein.

While the HTP assay developed in this dissertation is a significant improvement over other HTP screening strategies in terms of functional assessment of DC phenotype the assay does have several limitations. First, the assay only assesses three surface markers on the DCs. Many more surface markers show differential expression on DCs in response to various challenges and thus the full repertoire of effector functions these DCs are capable of producing is not assessed in this assay. Second, in order to determine the cytokine profile a relatively expensive bioplex assay is needed. While many cytokines profiles can be determined using this methodology the expense of performing this assay on every well of a HTP assay is prohibitive. Thirdly, no time course of expression is seen in this assay. This assay uses a static time point analysis and no information about

temporality of expression/secretion can be gleaned from it. Finally, this assay only provides a read out for the non-adherent fraction of DCs that have responded to an agonist. The adherent fraction could be substantial if a surface is modified with an adhesive ligand. As many CLRs on DCs are known to be adhesion receptors[79,278] the loss of this population could result in a biased cell assessment. Thus, designing a new HTP methodology that addresses these shortcomings would have large implications for DC response to glycan arrays.

The new assay must still rely on wells for DC treatment because DCs are loosely adherent and thus can migrate to other treatment spots in un-welled arrays. Additionally, DCs also produce large amounts of soluble cytokines and therefore cross-contamination of soluble factors between treatment groups is a concern in an un-welled array format. This is especially valid if longer time courses of response than a few hours are of interest. The smallest welled plate currently commercially available is a 1536 well plate. The advantage of utilizing this format over the 384 well assay is the reduction in reagent use. The 384 well screen uses nanomoles of glycan per assay and the 1536 well plate reduces the amount of glycan needed into the picomolar range. Furthermore, the scale down to the 1536 well plates has the potential to increase the number of ligands tested in a single test by a factor of 4.

Unfortunately, the scale down to a 1536 well plate changes the nature of the assay because 1536 well filter plates are not produced. However, the removal of the filter plate is not necessarily a negative aspect of a new assay. The use of filter plates increases the complexity of the assay in that more washes and incubation steps are needed and because the cell culture is performed in a separate, non-filter plate, well only the non-adherent fraction of DCs is assessed in the current protocol. Thus, elimination of the filter plate potentially reduces the complexity of the assay and allows for the assessment of the adherent DC population. A new reporter would be needed for a read out in these plates as Ab staining, which is the current reporter mechanism, is not able to be used without a

filter plate. A mixed lymphocyte reaction (MLR) was chosen as the reporter mechanism for this assay because T cells can become highly proliferate when exposed to activated DCs. The basic principle of the MLR is that when allogeneic T cells are added to a culture of APCs, in this case DCs, the TCR recognizes the MHC, either MHC I or MHC II depending on T cell phenotype, of the APC as being foreign and the T cell becomes primed to clonally expand. However, clonal expansion requires more than just recognition of a foreign MHC, the T cell must also have its costimulatory molecules activated in order to clonally expand. This can only occur if the APC has been activated. Thus, in an MLR clonal expansion of the T cell occurs only when the APC has been activated and when the T cell recognizes the MHC presented from the APC as being foreign. Therefore, if one can quantify the amount of T cell expansion as compared to an unstimulated control one could assess the activation state of the APC. When using DCs in a MLR there is the added advantage of being able to stimulate $CD4^+$, $CD8^+$, and T regulatory (T_{reg}) cells in an antigen independent manner as DCs have a high expression of MHC I & II as well as the ability to stimulate T_{regs}.[279–290] Thus, this new reporter has the advantage of directly assessing a complete DC phenotype across multiple activation profiles. T cell expansion is itself an effector function of DCs and thus is an extremely applicable reporter. The new methodology addresses the shortcomings of the previous assay in that the surface marker and cytokine profile is indirectly assessed. The proliferation of T cells requires the appropriate regulation of many surface markers and the secretion of many cytokines not to mention accurate temporal expression of these molecules. Therefore, if a T cell population expands it could be inferred that the DC has become activated and has up and down regulated the expression of the correct surface molecules and cytokines. In summary, the new methodology is able to directly assess an effector function of DCs in its reporter unlike any HTP methodology before it, it assess the effector function of the entire DC population as it does not require a transfer of cells to a filter plate, it can assess 4x as many ligands as the current HTP protocol, it requires

5x less reagent to perform, and is cheaper to perform as it does not require expensive antibody or bioplex assays for its reporter.

Two protocols to quantify the amount of T cell proliferation have been considered for further development and are outlined below. Each protocol has its own strengths and weaknesses that will be discussed.

6.2.3.1 *T Cell Hybridoma High Throughput Assay*

The first protocol involves the use of an antigen specific T cell hybridoma that has been transduced to express a fluorophore. T cell hybridoma are a combination of a healthy antigen specific T cell and a lymphoblast. Due to the nature of these cells they do not proliferate as traditional T cells do and are considered immortal. Of note is that while T cell hybridoma are lymphomas they express relatively normal signaling and surface markers, as compared to T cells lines, for DCs to recognize, signal, and/or activate.[291–295] For this assay the hybridoma could be cultured with primary DCs in the presence of the antigen that the T cell is specific for. The hypothesis is that if the DC is activated then the hybridoma will clonally expand more quickly than if the DC is not activated. Expansion of the T cell would be measured by fluorescent intensity as compared to the intensity of unstimulated wells. Through careful analysis of literature five T cell lines have been identified that have correct surface marker expression of T cell signaling molecules and do not autologously proliferate excessively, doubling time $\geq$ 48 hours. These cell lines are: Jurkat, Molt-3, Molt-16, CCRF-HSB2, and TALL-104. Thus, while these cell lines are lymphomas they express relatively normal signaling and surface markers for DCs to recognize, signal, and/or activate and are seen as good candidates for creation of T cell hybridoma.

There are many advantages to using T cell hybridoma. First, these cells are capable of being stably transduced with a fluorescent marker that is constitutively expressed. This fluorescent tagging can be used as a reporter for cell number as the cells proliferate. Therefore, if a DC stimulates the T cell it will begin to clonally expand and, if this occurs in a well, the GMFI of that well will increase as compared to the mean fluorescence of an unstimulated well. A second advantage of this method of analysis is that it also allows for a time course study to be possible as the fluorescent intensity of the well can be taken at multiple time points to determine how fast and to what magnitude the cells are proliferating. A third advantage of using T cell hybridoma is that they expedite the high through put nature of the assay. The cells need only be cultured, transduced, and then selected out for their GFP production. After this process the cells can be frozen and then thawed several days before use. This provides for easy access to an almost infinite amount of GFP expressing T cells that are ready without any real culture time, reagent expenditure, or in-depth preparation. The final advantage of using hybridoma is that they allow for a similar reaction to be assessed for each culture condition and each DC donor. T cell hybridoma are clones of cells and thus their response is very homogeneous and so variability of two donors, one for DCs and one for T cells, does not have to be accounted for when performing this assay.

The use of T cell hybridoma vs. primary cells has its caveats in that the T cells are lymphomas and therefore not a completely accurate representation of healthy T cell proliferation. This reduces the ability of the assay to determine actual effector function of the DC stimulation which is one of the main strengths of the assay. However, stimulation of T cell proliferation still requires the up and down regulation of many surface receptors, intercellular interaction, and secretion of a dearth of cytokines[296], regardless of if it is a hybridoma or primary cell, and thus is still a much more relevant output versus current HTP strategies.

6.2.3.2 *Primary Allogeneic T cell High Throughput Assay*

The second protocol involves the use of primary allogeneic T cells. This protocol more closely follows the MLR protocol previously established in this lab. T cells are co-cultured with DCs from a different donor to determine if the DCs are activated. This protocol involves only measuring an end point replication. This end point is total quantification of DNA present in the well as measured by the fluorescent intensity of the DNA of all of the cells in a well stained by Pico-green. The cell proliferation would be assessed by staining with pico-green 5 days after the DCs and T cells have been seeded together in the wells. This reporter is chosen because of the previously mentioned resistance of primary cells to be stably transduced with a reporter and because even if this stable transduction occurs it is in very low prevalence.

This assay has the advantage of using primary T cells that are healthy and fully functional. However, it has several weaknesses that make this a non-ideal assay in a high throughput evaluation. First, the quantification is an endpoint and thus no time course of replication can be easily determined. Second, the quantification is non-specific. What cells have proliferated and to what extent they have proliferated is unknown, only the total DNA concentration per well can be determined. Thirdly, T cells must be taken from a second donor for every experiment. This not only entails significantly more time and work for every donor tested but also introduces another level of variability in the data. It is thought that it is this added variability that has caused confounding results in the 96 well plate MLR that has been performed in the Babensee lab.

6.2.3.3 *High Throughput Assay Conclusions*

With either methodology before the final analysis the supernatant of the DC – T cell co-culture can be taken and applied to a different well of activated clonally expanding GFP expressing T cells. This assay will be performed to determine if the co-culture of the cells has created an anti-inflammatory, immunosuppressive microenvironment. This is valuable because two types of tolerance are possible. One type of tolerance is active tolerance in which T_{regs} are stimulated and clonally expand to actively inhibit the inflammatory response. However, another type of tolerance can be seen in the literature that shows the release of anti-inflammatory cytokines that inhibit the further activation and maturation of immune cells without causing T cell expansion. This second kind of tolerance is much more common but also difficult to detect with a typical MLR. An additional analysis of the soluble factors must be done in order to determine if this is the case. At the volumes possible in a 1536 well plate soluble factors cannot be analyzed. Thus, this further culture with activated T cells will allow for the determination of this second type of tolerance. There are technical concerns for this methodology because of the small volume of liquid in each well of a 1536 well plate, $\leq$10µl. These are valid concerns and cell count assays should be done initially on the supernatants to determine if it is possible to remove them without significant simultaneous cellular uptake. After validation a liquid handling robot would be needed to perform this expiration of supernatants and so it is expected that after optimization this will significantly reduce the variability of the removal.

6.2.4 Assessment and Modeling of the DC response to a Diverse Set of Incremental, Well-Defined, Sugar Structures.

In this dissertation it was shown that glycan structure and specifically terminal structural motif of glucan is a significant predictor of DC phenotype. Additionally, microarray studies have repeatedly shown drastically altered affinity for different glycan structures from the same lectin.[211] However, the analysis conducted in Aim 1 of the dissertation was not a thorough and mechanistic study of glycan structure versus cell function. Additionally, not enough glycan structures were able to be tested to create a validation and test set for the models created. Thus, a future proposal for this Track would be to assess DC phenotype to a diverse set of incremental, well defined, sugar structures presented from the polymer surface optimized in Track 2. From the study conducted in Aim 1 it was found that α1-α2 linked terminal glycan structures were associated with IMF and α1-α3, α1-α6 branched mannose structures were not. However, this grouping left out single α1-α3 mannose linkages as well as combinations of the above motifs. Therefore, a complete understanding of which components of the glycan structures affect DC phenotype is unknown. Figure 19 shows the oligomannose structures that could be tested to quantitatively prove which structural motifs were necessary for DC activation.

With the glycan structures proposed in Figure 19 a predictive model could be created using the general linear model technique used in Aims 1 and 2 of this report. The model would be similar to that shown in **Equation 2** of Aim 1 of this dissertation, just with more structural ligands. The hypotheses would be the same for this model as for the model shown in **Equation 2**.

The difference between the proposed model and the model shown in **Equation 2** would be that the proposed model has a fully reductive set of terminal glycan motifs and that the purpose of these experiments would be to validate the model against more complex glycan structures and against another donor "test" pool. With this setup one set

of donors could be used to create the proposed model, the output for which would be DC IMF and be obtained from the HTP assay developed in this dissertation. In this model DC IMF would be modeled as a function of glycan terminal motif. Iterative models could be created including each level of mannose from below Man2-X, Man3-X, etc. and its predictive ability could be measured against that of a second "test" set of donors. Additionally, these models could then be used to predict the DC phenotype to the more complex sugar structures shown in Figure 19. This could originally be performed with the same set of donors to determine which motifs are predictive of DC phenotype and then applied to the DC response of a "test" set of donors to these high mannose structures. The predicted values would be compared to the actual values via least squares regression and the models compared based upon their relative R^2 values. Glycans from Figure 19 could be produced in house or purchased from LuCella Biosciences. However, it is recommended that the glycan be produced in house via the solid state glycan synthesis perfected by Ratner et. al.[297] due to the prohibitive cost of producing a large array of glycan structures.

In addition to the scientific value of the modeling and DC response above the DC response to complex mannose structures and an understanding of which structures modulate DC phenotype to the greatest extent could be applied to vaccine adjuvants, combination product formulation, and for coating for implants. Additionally, several of the structures from Figure 19 are known glycan structures of pathogens such as Entamoeba[247] and could be used to develop a vaccine for these parasites.

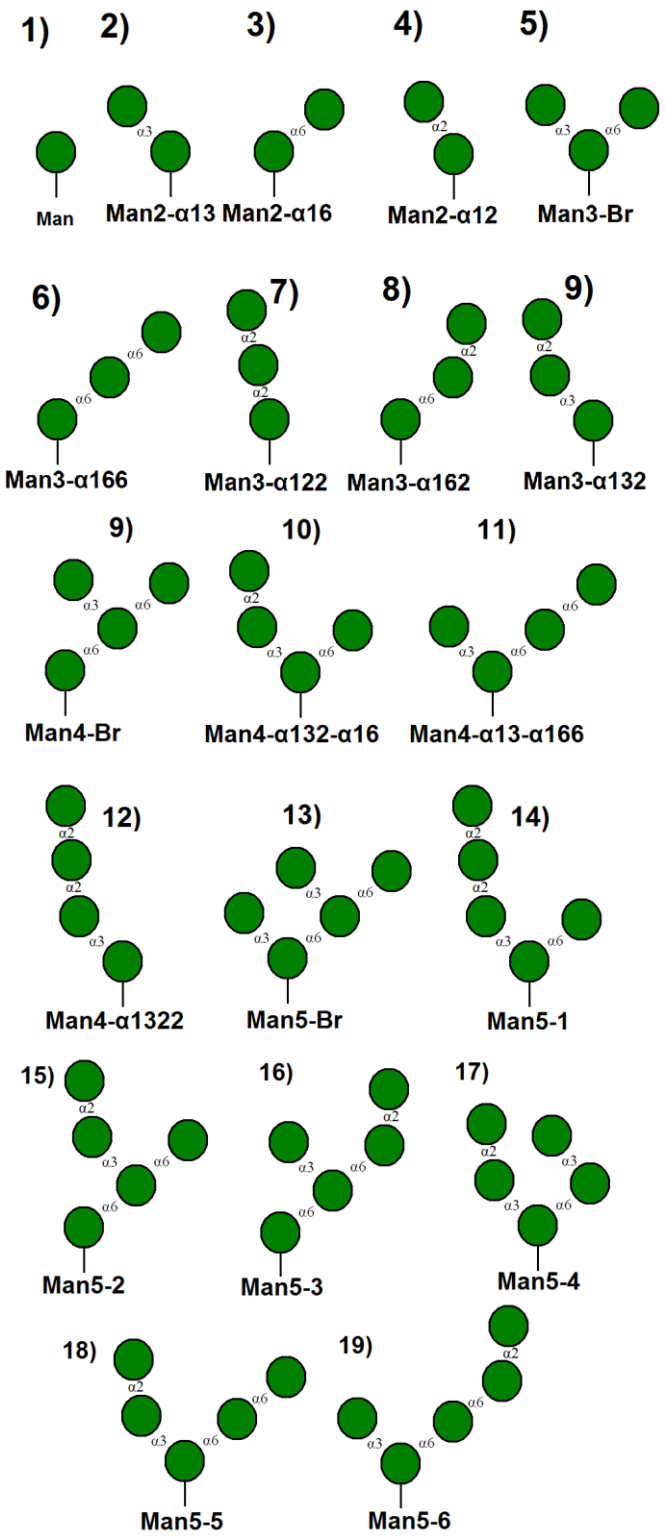

Figure 19: Mannose glycan structures for training, validation, and test set analysis.

After proving that this methodology is valid for the test set and for prediction of phenotype of DCs in response to more complex structures this methodology could then be applied to another set of sugars. Glycan classes of possible interest include the Lewis glycan structures and human Blood antigens, (lacto-N-tetraose) LNT based strucutres, sialyl derivitized structures known to bind Siglecs, and Core 1-4 structures. A fully reductive study could be done for each of these sets of sugars in an identical fashion to that of the polymannose described in detail herein. Each of these classes is of interest for different reasons: knowledge of the blood antigens and Lewis structures could provide novel mechanisms for adjuvants for vaccines or combination products or for immune avoidance for implanted materials/scaffolds. The LN based structures are commonly found in breast milk[298] and as antibody targets for Schistosoma mansoni infection.[299] Sialyl derivatized structures are targets for siglecs which have broad immune regulatory ability from cell adhesion to inhibiting immune cell activation via ITIMs.[87] Finally, Core 1-4 structures are found on a variety of mucins and mammalian glycoproteins and have been shown to have broad antigenic capabilities.[176]

Finally, the cost of producing the sugars suggested for further research would be prohibitive for a fully reductive study on each sugar class. However, the Consortium for Functional Glycomics has a large library of glycans that are readily available in quantities that would be well suited to the HTP polymeric assessment of DC phenotype. Currently, the Consortium makes 85 sugar structures available in 1 or 5 mg quantities which would be enough to produce the optimized sugar/polymer conjugates. These sugars span the Lewis and blood antigens, LN based structures, and contain many sialyl functionalized structures. Table 10 shows the list of all available structures from the consortium. With the structures provided by the Consortium it would be possible to easily model the Lewis, blood, and TN antigens in fully reductive structural models.

Table 10: List of sugars available from the Consortium for Functional Glycomics.

No.	Consortium Compound #	Saccharide Structure and Type of Spacer	Common Name	Quantities Available
1	M5	GlcNAcb-Sp	GN	1 or 5 mg
2	D11	Galb1-3GalNAca-Thr	TF	1 mg
3	D8	Galb1-3GlcNAcb-Sp	Lec	1 or 5 mg
4	D9	Galb1-4Glcb-Sp	Lac, L	1 mg
5	D10	Galb1-4GlcNAcb-Sp	LacNAc, LN	1 mg
6	D14	Neu5Aca2-6GalNAca-Thr	STn	1 mg
7	Tr116	Fuca1-2Galb1-3GlcNAcb-Sp	H-type1	1 or 5 mg
8	Tr120	Fuca1-2Galb1-4Glcb-Sp	2'FL	1 or 5 mg
9	Tr117	Fuca1-2Galb1-4GlcNAcb-Sp	H-type2	1 or 5 mg
10	Tr260	Gala1-3Galb1-3GlcNAcb-Sp	Gala3-type1	1 mg
11	Tr59	Gala1-3Galb1-4Glcb-Sp	Galili-tri	1 or 5 mg
12	Tr60	Gala1-3Galb1-4GlcNAcb-Sp	B2-tri	1 mg
13	Tr61	Gala1-4Galb1-4Glcb-Sp	Pk	1 or 5 mg
14	Tr62	Gala1-4Galb1-4GlcNAcb-Sp	P1 tri	1 or 5 mg
15	Tr57	Galb1-3[Fuca1-4]GlcNAcb-Sp	LeA	1 or 5 mg
16	Tr38	Galb1-3[Neu5Aca2-6]GalNAca-Thr	6'STF	1 or 5 mg
17	Tr58	Galb1-4[Fuca1-3]GlcNAcb-Sp	Lex	1 or 5 mg
18	Tr307	GlcNAcb1-3Galb1-3GlcNAcb-Sp	3'GN type1	1 mg
19	Tr55	GlcNAcb1-3Galb1-4GlcNAcb-Sp	GNLN	1 or 5 mg
20	Tr54	GlcNAcb1-3Galb1-4Glcb-Sp	LNT-2	1 or 5 mg
21	Tr48	KDNa2-3Galb1-3GlcNAcb-Sp	3'-KDNLec	1 or 5 mg
22	Tr47	KDNa2-3Galb1-4GlcNAcb-Sp	3'KDNLN	1 or 5 mg
23	Tr34	Neu5Aca2-3Galb1-3GlcNAcb-Sp	3'SLec	1 or 5 mg
24	Tr113	Neu5Aca2-3Galb1-4Glc	GM3 (no spacer)	1 or 5 mg
25	Tr32	Neu5Aca2-3Galb1-4Glcb-Sp	GM3	1 or 5 mg
26	Tr33	Neu5Aca2-3Galb1-4GlcNAcb-Sp	3'SLN	1 or 5 mg
27	Tr35	Neu5Aca2-6Galb1-4Glcb-Sp	6'SL	1 or 5 mg
28	Tr36	Neu5Aca2-6Galb1-4GlcNAcb-Sp	6'SLN	1 mg
29	Tr269	Neu5Aca2-6GalNAcb1-4GlcNAcb-Sp	6'SLDN	1 or 5 mg
30	Tr323	Neu5Ac(9Ac)a2-3Galb1-3GlcNAcb-Sp	9OAc3'Slec	1 mg
31	Tr322	Neu5Ac(9Ac)a2-3Galb1-4GlcNAcb-Sp	9OAc3'SLN	1 mg
32	Tr41	Neu5Gca2-3Galb1-3GlcNAcb-Sp	3'SLec (Gc)	1 mg
33	Tr39	Neu5Gca2-3Galb1-4Glcb-Sp	3'SL (Gc)	1 mg
34	Tr40	Neu5Gca2-3Galb1-4GlcNAcb-Sp	3'SLN (Gc)	1 mg
35	Tr43	Neu5Gca2-6Galb1-4GlcNAcb-Sp	6'SLN (Gc)	1 mg

Table 10 Continued

36	Te134	Fuca1-2(Galb1-4GlcNAcb1-3)2b-Sp	H2	1 or 5 mg
37	Te118	Fuca1-2Galb1-4[Fuca1-3]GlcNAcb-Sp	Ley	1 or 5 mg
38	Te212	Fuca1-2Galb1-4[Fuca1-3]GlcNAcb1-3Galb1-4[Fuca1-3]GlcNAcb-Sp	Ley -Lex	1 or 5 mg
39	Te267	Fuca1-2Galb1-4[Fuca1-3]GlcNAcb1-3(Galb1-4[Fuca1-3]GlcNAcb1-3)2b-Sp	Ley-Di-Lex	1 mg
40	Te135	Fuca1-2(Galb1-4GlcNAcb1-3)3b -Sp	H3	1 mg
41	Te258	Gala1-3[Fuca1-2]Galb1-3GlcNAcb-Sp	B tetra type 1	1 mg
42	Te262	Gala1-3[Fuca1-2]Galb1-4[Fuca1-3]GlcNAcb-Sp	2'F-B type 2	1 mg
43	Te225	Gala1-3[Fuca1-2]Galb1-4Glcb-Sp	B tetra L	1 mg
44	Te223	Gala1-3[Fuca1-2]Galb1-4GlcNAcb-Sp	B tetra type 2	1 mg
45	Te221	Gala1-3Galb1-4[Fuca1-3]GlcNAcb-Sp	Gala3Lex	1 mg
46	Te327	Gala1-4Galb1-4GlcNAcb1-3Galb1-4Glcb-Sp	P1 penta	1 mg
47	Te287	Galb1-3[Fuca1-4]GlcNAcb1-3Galb1-4[Fuca1-3]GlcNAcb-Sp	LeALex	1 mg
48	Te318	Galb1-3[Fuca1-4]GlcNAcb1-3Galb1-3[Fuca1-4]GlcNAcb-Sp	Di-LeA	1 mg
49	Te286	Galb1-3GlcNacb1-3Galb1-4[Fuca1-3]GlcNac-bSp	Lec-LeX	1 mg
50	Te302	Galb1-3GalNAcb1-3Gala1-4Galb1-4GlcNAcb-Sp	P1 penta	1 mg
51	Te271	Galb1-3GlcNAcb1-3Galb1-4GlcNAcb-Sp	LNT	1 mg
52	Te316	Galb1-3GlcNAcb1-3Galb1-3GlcNAcb-Sp	Di-Lec	1 mg
53	Te101	(Galb1-4[Fuca1-3]GlcNAcb1-3)2b-Sp	Di-Lex	1 mg
54	Te102	(Galb1-4[Fuca1-3]GlcNAcb1-3)3b-Sp	Tri-Lex	1 mg
55	Te319	Galb1-4[Fuca1-3]GlcNAcb1-3Galb1-3[Fuca1-4]GlcNAcb-Sp	Lex-LeA	1 mg
56	Te98	(Galb1-4GlcNAcb1-3)2b-Sp	Di-LN	1 or 5 mg
57	Te100	(Galb1-4GlcNAcb1-3)3b-Sp	Tri-LN	1 or 5 mg
58	Te72	Galb1-4GlcNAcb1-3Galb1-4Glcb-Sp	LNnT	1 or 5 mg

Table 10 Continued

59	Te259	GalNAca1-3[Fuca1-2]Galb1-3GlcNAcb-Sp	A tetra type 1	1 mg
60	Te261	GalNAca1-3[Fuca1-2]Galb1-4[Fuca1-3]GlcNAcb-Sp	2'F-A type 2	1 mg
61	Te224	GalNAca1-3[Fuca1-2]Galb1-4Glcb-Sp	A tetra L	1 or 5 mg
62	Te222	GalNAca1-3[Fuca1-2]Galb1-4GlcNAcb-Sp	A tetra type 2	1 mg
63	Te289	GalNAcb1-3Gala1-4Galb1-4GlcNAcb-Sp	P1 tetra	1 mg
64	Te99	GlcNAcb1-3(Galb1-4GlcNAcb1-3)2b-Sp	3'GN-Di-LN	1 mg
65	Te325	Neu5Aca2-3(Galb1-3[Fuca1-4]GlcNAcb1-3)2b-Sp	3'S-Di-LeA	1 mg
66	Te304	Neu5Aca2-3Galb1-3[Fuca1-4]GlcNAcb1-3Galb1-4[Fuca1-3]GlcNAcb-Sp	3'SLeA-LeX	1 mg
67	Te291	Neu5Aca2-3Galb1-3GalNAcb1-3Gala1-4Galb1-4Glcb-Sp	SSEA-4	1 mg
68	Te321	Neu5Aca2-3Galb1-3GlcNAcb1-3Galb1-3GlcNAcb-Sp	3'S-Di-Lec	1 mg
69	Te288	Neu5Aca2-3Galb1-3GlcNAcb1-3Galb1-4GlcNAcb-Sp	3'SLecLN	1 mg
70	Te75	Neu5Aca2-3[Galb1-3GalNAcb1-4]Galb1-4Glcb-Sp	GM1	1 mg
71	Te64	Neu5Aca2-3Galb1-4[Fuca1-3]GlcNAcb-Sp	3'SLex	1 or 5 mg
72	Te140	Neu5Aca2-3(Galb1-4[Fuca1-3]GlcNAcb1-3)2b-Sp	3'S-Di-Lex	1 mg
73	Te175	Neu5Aca2-3[Galb1-4GlcNAcb1-3)2b-Sp	3'S-Di-LN	1 or 5 mg
74	Te192	Neu5Aca2-3[Galb1-4GlcNAcb1-3)3b-Sp	3'STri-LN	1 mg
75	Te320	Neu5Aca2-3Galb1-4GlcNAcb1-3Galb1-3GlcNAcb-Sp	3'SLN-Lec	1 mg
76	Te74	Neu5Aca2-3[GalNAcb1-4]Galb1-4Glcb-Sp	GM2	1 mg
77	Te201	Neu5Aca2-3[GalNAcb1-4]Galb1-4GlcNAcb-Sp	CT/Sda	1 mg
78	Te303	Neu5Aca2-3[Neu5Aca2-3Galb1-3GalNAcb1-4]Galb1-4Glcb-Sp	GD1a	1 mg
79	Te176	Neu5Aca2-6[Galb1-4GlcNAcb1-3)2b-Sp	6'S-Di-LN	1 or 5 mg
80	Te324	Neu5Aca2-6Galb1-4GlcNAcb1-3Galb1-3GlcNAcb-Sp	6SLN-Lec	1 mg

Table 10 Continued

81	Te78	Neu5Aca2-8Neu5Aca2-3[GalNAcb1-4]Galb1-4Glcb-Sp	GD2	1 mg
82	Te79	Neu5Aca2-8Neu5Aca2-3Galb1-4Glcb-Sp	GD3	1 or 5 mg
83	Te97	Neu5Aca2-8Neu5Aca2-8Neu5Aca2-3Galb1-4Glcb-Sp	GT3	1 mg
84	Te119	Neu5Aca2-8Neu5Aca2-8Neu5Aca2-3[GalNAcb1-4]Galb1-4Glcb-Sp	GT2	1 mg
85	Te306	Neu5Aca2-8Neu5Aca2-8Neu5Aca2-8Neu5Aca2-3[GalNAcb1-4]Galb1-4Glcb-Sp	GQ2	1 mg

6.2.5 Isolation, Functionalization, and Identification of Serum and Pathologic Glycan Motifs from Cancer Patients for Use in Identification of Novel Targets for Therapeutics and/or Detection/Screening Methodologies.

Track five and six can be performed while the models and testing of the consortium glycans is being performed. These tracks will be discussed in concert due to their similarity and structure and ultimate goals. For these tracks endogenous glycans from the plasma of healthy human donors and that of cancer patients, here pancreatic cancer patients, could be tested. It is important to note that many cancers have shown aberrant glycosylation and that pancreatic cancer was chosen as a model here due to its low survival rates and clinical ties with Dr. John Kauh from Emory University of my Committee. More in-depth discussion of pancreatic cancer and other cancer's glycosylation is discussed below.

The first hypothesis is that glycans from the plasma of healthy donors will differentially modulate DC phenotype. This hypothesis stems from the idea that glycoprotein adsorption to a biomaterial can modulate DC phenotype via the glycan moieties of the glycoproteins found in plasma. Also implicit to this step is the hypothesis that glycans presented in a non-physiological milieu will be able to modulate DC phenotype. After this assessment is completed the DC response to glycans from the

plasma of patients with pancreatic cancer should be determined and compared to that of healthy patients. The inherent hypothesis here is that the principle constituents of plasma glycans from pancreatic cancer patients can modulate DC phenotype differentially as compared to plasma glycans from healthy donors. After obtaining DC response to both healthy donor and pancreatic cancer patient glycans the structure of glycans that show promising results would be determined for use in vaccine development and biomarker identification.

6.2.6 Endogenous Glycans

6.2.6.1.1 Isolate the glycans from plasma proteins of healthy donors and sort them by molecular weight.

Plasma glycans from a pool of healthy donors (Approximately 30 donors) would be isolated and sorted by molecular weight. A discussion of the sample size will be performed later in this discussion. The outcome of these experiments would be an array of glycan fractions, that each contains a milieu of glycans of similar molecular weight. In order to easily separate and quantify glycans that have been cleaved from glycoproteins a fluorescent linker is necessary.[210] Cummings et. al. have developed a simple chemistry that will non-specifically functionalize free reducing glycans with a fluorescent linker that can be easily functionalized with N-hydroxy succinimide (NHS) chemistry.

There is precedent in the literature to isolate differentially-glycosylated proteins from the milieu of plasma proteins of cancer patients via their carbohydrate motifs.[300–302] Also, glycans isolated from plasma glycoproteins have been successfully obtained, isolated, and characterized before.[300,302] Thus, this track is seen as a novel combination of these two techniques. In order to obtain glycans from plasma the plasma proteins must first be digested, and N- and O-linked glycans separated from the proteins. This step is necessary as separation of the glycan from their protein carriers is necessary to isolate the effects of the differential glycosylation from the effects of the protein carrier. A simple

size exclusion separation of the glycans was chosen based on its speed and simplicity. Further chromagraphic separation techniques should be used in later steps to isolate and purify glycans more thoroughly if they show a functional DC response when cultured for 24hrs with DCs.

6.2.6.1.2 Identify glycan fractions of interest from donors that show a functional phenotypic effect from the immobilize glycans using a HTP format.

The objective is to identify glycan fractions that cause mature pro-inflammatory DC phenotype or an immunosuppressive/tolerogenic DC phenotype upon contact with surface-immobilized glycans. The initial size exclusion sorting of glycans will yield a heterogeneous mix of glycans at each molecular weight separation, but as glycans are almost never seen in an isolated form in nature and are always presented from the heterogeneous glycocalyx around cells it is thought that separation in this fashion will still be able to elicit responses from DCs. This novel approach was chosen because it allows for a significantly reduced amount of processing of the glycans and because unlike contemporary HTP methods presented in the literature this will allow for assessment of functional immunological outcomes prior to structural identification and characterization of glycans of interest.

Many oligosaccharides have different structures but identical molecular weights due to the chemical composition of each carbohydrate being identical/similar. For instance, mannose, glucose, galactose, and altrose all have identical molecular weights but are bound by drastically different lectins. All of these structures also have alpha and beta confirmers that have identical molecular weights but that differ in binding specificity. This functionally means that at any given size range for the glycan fractions isolated by size, many different glycan structures could be present. Thus, if a well is shown to modulate DC phenotype many different sugar structures would be present in the well. Therefore, several rounds of separation and isolation should be performed in order

to reduce the number of glycans in each fraction down to almost single structures after the initial DC response assay. Initially, the size sorted glycans can be assessed using the polymeric carriers from Track 2 and the HTP method used in this dissertation or from Track three of the future work. Wells showing a DC response using these methodologies can then be further sorted using reverse phase and normal phase high pressure liquid chromatography. The constituents will then be immobilized in a well again and DC phenotype assessed.

6.2.7 Aberrant Endogenous Glycans

Differential activation of the DCs between the two patient groups is expected due to reports in literature that glycans from onco-glycoproteins have shown immunomodulatory effects on DCs.[18,301,303] Current methods for relevant glycan identification center around the hypothesis that in order to be a therapeutically relevant glycan it must be relatively high in abundance AND that in order to be in high abundance this structure must therefore be on highly prevalent proteins. This has been shown numerous times in the literature by the analysis of the elevated proteins in a given cancer and then the subsequent analysis of the glycoform of the protein. However, unlike proteins and DNA which are template driven processes glycosylation is regulated by a set of glycosyltransferases and in general time spent in the Endoplasmic Reticulum and Golgi apparatus (also for select O-glycans time spent in the cytoplasm). This time is not as rigidly regulated as transcription or translation and thus a diverse glycoform is often seen on a single protein originating from a single cell. The other key facet of this processes is that a single set of post translational proteins, the glycosyltransferases, are responsible for glycosylation of all proteins and lipids[304]. Therefore, if a glycosyltransferase activity is altered or has an altered expression due to abnormal oncogene regulation not just one protein or type of protein is altered but all proteins that would undergo post translational modification by that glycosyltransferase are altered in a

similar fashion. Thus, a glycan structure could in theory, be highly prevalent and have a high biological significance and only be present on low prevalence proteins. This is possible because while the low prevalence proteins may individually be rare their aggregate occurrence accounts for a significant portion of the protein found in blood. Therefore, a protein independent analysis of glycan structures is needed in order to determine which structures are prevalent and which have biological significance regardless of protein carrier.

Based on the plasma protein content, blood would be collected from healthy human donors or from patients with pancreatic cancer (in collaboration with Dr. John Kauh, Winship Cancer Center, Emory University); objective is 30 donors per group. Plasma is composed of ~75mg/ml of protein and if one were to obtain 600 ml of plasma from a pool of 30 random donors approximately 45 grams of protein would be isolated. Approximately half of this protein is human serum albumin (HSA) which is a non-glycosylated protein in healthy patients.[305] Thus, from 600 ml of plasma one would obtain approximately 22.5 grams of glycoprotein. A general estimate for glycan weight of glycoproteins is that ~10% of the molecular weight is carbohydrates and thus we should obtain about 2.25 grams of carbohydrates. Currently it is thought that plasma is composed of approximately 3020 proteins.[306] Knowing that the lowest concentration of the 60 most abundant proteins in plasma is 50mg/L[307] and assuming that all the glycoproteins that have a relative abundance of at least 1000 times lower than this concentration are desirable because they are abundant enough to contribute significantly to the glycan pool (50ug/L or a 1:1,500,000 molecular weight prevalence) it can be calculated that approximately 20.0 nmol of the least abundant sugar from 600 ml of plasma would be collected. As one would need a minimum of 10nmol of glycan to perform our study 600 ml of blood is seen as a sufficient quantity of blood to isolate the glycans of interest that are at the lowest relevant concentration while allowing for decreases in glycan pool due to conjugation efficiencies and incomplete reactions.

The isolation, separation, cell response, and identification process would be identical to that discussed for endogenous glycan study. To conserve time and resources the healthy donors in this study would be the patients from the endogenous glycan work and would be chosen to be age, gender, and race matched to the pancreatic cancer patients. The key difference between the endogenous and aberrant endogenous glycan study is that for the aberrant glycan study a differential activation profile from that seen in the endogenous glycan work would be the output. Thus, instead of looking for any activation of the DCs (as in the endogenous glycan work) only wells containing fractions of identical mass range showing activation of DCs that show no response in the healthy donors would be analyzed in in the exogenous glycan work. This comparison is possible because wells would be sorted in both healthy and pancreatic cancer patients using the same size exclusion column methodology. Care should be taken to sort identical mass ranges into identical wells for comparison. While it will not be known if the exact glycans are identical in between the two wells it will confirm that all glycans at X size range for each sample are represented and thus if there is a difference in DC response between the two it is due to some difference in either glycan constituents or concentration between the two sets of donors. In either case this would be interesting and identifiable with further analysis.

6.2.8 Experimental Design

6.2.8.1 Endogenous Glycans

The blood can be obtained from primary donors, treated with 10 mmol/dL[308] of Disodium Ethylenediaminetetraacetic acid, EDTA, spun down at 1000g for 10 minutes and the plasma supernatant collected and collectively pooled from 30 donors. While these donors are being obtained the plasma would be stored at -80°C. Once all patients' plasma has been obtained the plasma would be lyophilized. The resulting lyophilized

protein powder would then be dissolved in denaturing buffer, at a concentration of 20mg/ml and heat to a boil for 10 minutes. Lyophilize this denatured solution.

For N glycan isolation dissolve the lyophilized plasma in a 0.1% (w/v) RapiGest solution (Waters Inc.) add Pronase (Sigma) in sufficient quantity to digest all protein overnight at 37°C. After an overnight incubation freeze and lyophilize the solution again. Dissolve in fresh RapiGest solution and add an equal amount of pronase to that which was added previously. After another overnight run an SDS-PAGE gel to determine if all digestion has occurred. If not, repeat the above steps until all protein has been completely digested. After this digestion has occurred and the resulting solution lyophilized take the resulting powder and dissolve and then add PNGase F (Sigma). Initially add 1500 units of PNGase F per ml of solution and incubate for 48 hours. Repeat this process for 8 days. Boil the solution for 5 minutes to inactivate the PNGase F and pass the slurry through a 2g C18 Sep-Pak cartridge. Collect the flow through. Wash the column with methanol to collect the protein trapped in the cartridge. Collect this methanol flow through as well and dry this solution under vacuum. Take the initial flow through and apply to a carbograph coloumn. Elute the glycan off of the column. This fraction should contain all N-linked glycans from the plasma.

To isolate the remaining O-linked glycans use the methanol flow through that was previously obtained from the Sep-Pak cartridge. Resuspend the vacuum dried volume in water and then freeze and lyophilize. Make a 28vol% ammonium hydroxide solution saturated with ammonium carbonate (28AHAC). Add glycoprotein to the 28AHAC to a concentration of 1mg/ml. Add additional ammonium carbonate to the solution, ~10mg/ml and heat the solution at 60ºC for 96hrs. Remove the ammonium hydroxide and ammonium carbonate by repeated evaporation of water using vacuum centrifugation. Add 0.5M boric acid to powder and heat the solution to 37ºC for 90mins. Remove boric acid by adding methanol and passing nitrogen over solution until dry. Add a 50% boric acid solution and spin the resultant suspension down at 10000g. Collect the supernatant

and dry under vacuum centrifugation and then resuspend in H_2O. Finally, purify the glycans collected using the cerograph column method expounded upon above. The above protocols were developed by Song et al.[210].

The above N-linked and O-linked glycans are not to be combined as identification of the glycans later becomes much simpler if the linkage of the glycan is known. The above procedure would be performed for a pool of 30 healthy donors. After isolation the two glycan solutions would be non-specifically functionalize with a fluorescent linker as shown by Song et al.[210] Briefly, the fluorescent linker 2-amino-N-(2-amino-ethyl)-benzamide (AEAB) is added in a 10:1 molar excess of glycan. Dimethyl sulfoxide (DMSO) and sodium cyanoborohydride is added and this solution is allowed to incubate at 65ºC for 4 hours. After the reaction with AEAB the glycans would be separated non-specifically using a size exclusion column (SEC) and HPLC. The polyacrylamide P4 SEC columns provided by Bio-Rad are known to separate oligosaccharides differing by only one sugar, a pentasaccharide vs. a hexasaccharide, and thus these columns would be used for the separation of the above sugar solutions. Forty-six fractions would be collected for each set of glycans. Thus, 46 fractions of N-linked glycans and 46 fractions of O-linked glycans, for a total of 92 glycan fractions, would be collected. 92 fractions were chosen so that fractions could be spotted in quadruplicate wells of a 384 well plate using the HTP methodology used in this dissertation while still allowing for control wells to be used in the same plate.

The glycans would then be immobilized in a 384 well or 1536 well plate (whichever HTP methodology has been developed) via the optimized synthetic carrier developed in Track 2. The resultant DC response to the glycans can be assessed via the HTP method used in this dissertation or via the HTP methodology seen in Track 3 if it has been developed. The glycans from the wells showing a DC response, either pro or anti-inflammatory, will then be further separated.

The immobilization strategy for the 384-well plate would be to add ten microliters of each of the 92 N- or O-linked glycan fractions in triplicate into the Disuccinimidyl tartrate (DST) functionalized wells at a concentration of 100uM. The glycans would be allowed to conjugate to the NHS functionalized surface overnight. A fourth well will also be functionalized with each glycan fraction for use as an isotype control well to ensure that the glycan that is immobilized in the well does not randomly increase binding of the labeling antibodies that would be used later. In the 1536-well assay 1.5 microliter of each of the 92 N- or O-linked glycans fractions would be added to the plate in duplicate. Two additional wells would be functionalized for the later addition of DCs with no transduced T cells to ensure that any increase in signal found in the wells later is due only to the proliferative ability of the T cells.

After the first round of separation and cell response the wells showing positive response from the DCs will undergo reverse phase and normal phase HPLC separation. After the glycans have been separated using 3D-HPLC they will then be immobilized again in a 384 well microtiter plate and DC response to the isolated glycans would be assessed. Glycans that show an immunomodulatory effect will then be identified via matrix assisted laser desorption/ionization mass spectrometry (MALDI) and exoglycosidase array digestion. The information from these analysis techniques, mass and glycan constituents respectively, along with whether the glycans are N-linked or O-linked provides glycobiologists with enough information to accurately determine what the structure of the sugar is.[210] This information can then be used by synthetic chemists to replicate relevant and interesting glycans for further study and also by physicians and screening facilities to help identify cancer markers for pancreatic cancer.

6.2.8.2 Aberrant Endogenous Glycans from Pancreatic Cancer Patients

The exact experimental design seen in the endogenous glycan work would be used again for this section. Blood from patients who have a stage I or II pancreatic tumor

that is still resectable and is static would be collected. This group offers the dual benefit of being able to identify glycans that are of immunological interest and that can be used as early tumor biomarkers to identify pancreatic cancer in its early stages. Thus, by isolating the glycans/glycoproteins earlier in tumor development they will necessarily be at a lower concentration and thus if they are still able to elicit an immunomodulatory effect on the DCs at this lower concentration they are more likely to be an efficacious target for therapy. This fact coupled with the fact that the glycans could have a dual use as a novel biomarker outweighs the potential therapeutic benefit of obtaining blood from late stage patients.

One of five outcomes is anticipated when comparing the two carbohydrate activation profiles:

1) A differential profile is seen on a feasible number of wells for further study but the onco-glycan group causes less stimulation of DCs than does the healthy glycan group
2) A differential profile is seen on a feasible amount of wells for further study but the healthy glycan group causes less stimulation of DCs than does the onco-glycan group
3) No DC response difference between the two groups but an activation profile is seen in a feasible number of wells
4) Too many wells show activation of DCs to make further isolation and purification feasible.
5) No wells show activation of DCs to any significant level.

The term feasible is relative but here refers to any amount of wells over 10 positive "hits" as judged by the fold change parameter over iDC. Ten hits was chosen as

the threshold for feasibility as this is ~10% of the total glycans tested and any number higher than this begins to defeat the advantage of using a HTP methodology. Outcome one or two provides an interesting result as these wells can be further separated and characterized to better determine the cell response to smaller sets of glycans and to determine these glycan's structures. Outcome three could also be interesting as DC phenotype modulation to glycans immobilized in an array format has not been shown before and thus the information from this outcome could be used to further direct cancer vaccine and biomaterial research in the future. Outcome four could be mitigated by altering our initial criterion of a hit to be more selective, such as above two standard deviations of the inactivated signal or not statistically different from DCs treated with LPS. Finally, outcome five could also prove interesting as there are many reports in literature of glycans produced by tumors having immunomodulatory effects on DCs [18,301,303] and thus the fact that they do not modulate DC phenotype when immobilized on a surface could be used to further direct cancer therapy development in the future.

Outcomes four and five are seen as unlikely because DC activation in many wells would indicate that the glycans across a wide range of molecular weights obtained from plasma are capable of activating myeloid derived DCs or that glycans immobilized on a surface are unable to modulate DC phenotype. The former seems unlikely as DCs encounter these glycans in tissue and blood constantly and thus to avoid autoimmunity would need to have a high level of tolerance to the majority of them regardless of presentation strategy. The latter seems unlikely because DC phenotype has been shown to be modulated by glycans in the literature previously. [18,301,303]

The aberrant endogenous study is meant to test the hypothesis that a differential DC phenotypic profile is capable of being produced from the glycoform of pancreatic cancer patients as compared to that of the profile produced by healthy donors. This track is not meant to be an in-depth analysis of the immune response to tumor glycans. As such additional controls and more in-depth analysis of glycans from these patients is not

proposed. However, for future studies, tissue samples of the tumor and healthy pancreatic tissue would be collected from the patients who undergo resection. Also, blood before tumor resection and 6-8 weeks after tumor removal could be collected as blood after tumor resection could serve as an excellent control for the patients. In addition, common controls for pancreatic cancer patients in studies similar to these include pancreatitis patients and diabetic patients as people with pancreatic cancer often share these comorbidities and thus the differential response seen between healthy donors and pancreatic cancer patients could be due to these comorbidities and not the pancreatic cancer itself.[309–311]

APPENDIX

A.1. Supplemental to Elucidation and Optimization of Pertinent Molecular Factors for Dendritic Cell Response to Adsorbed Glycocoonjugates.

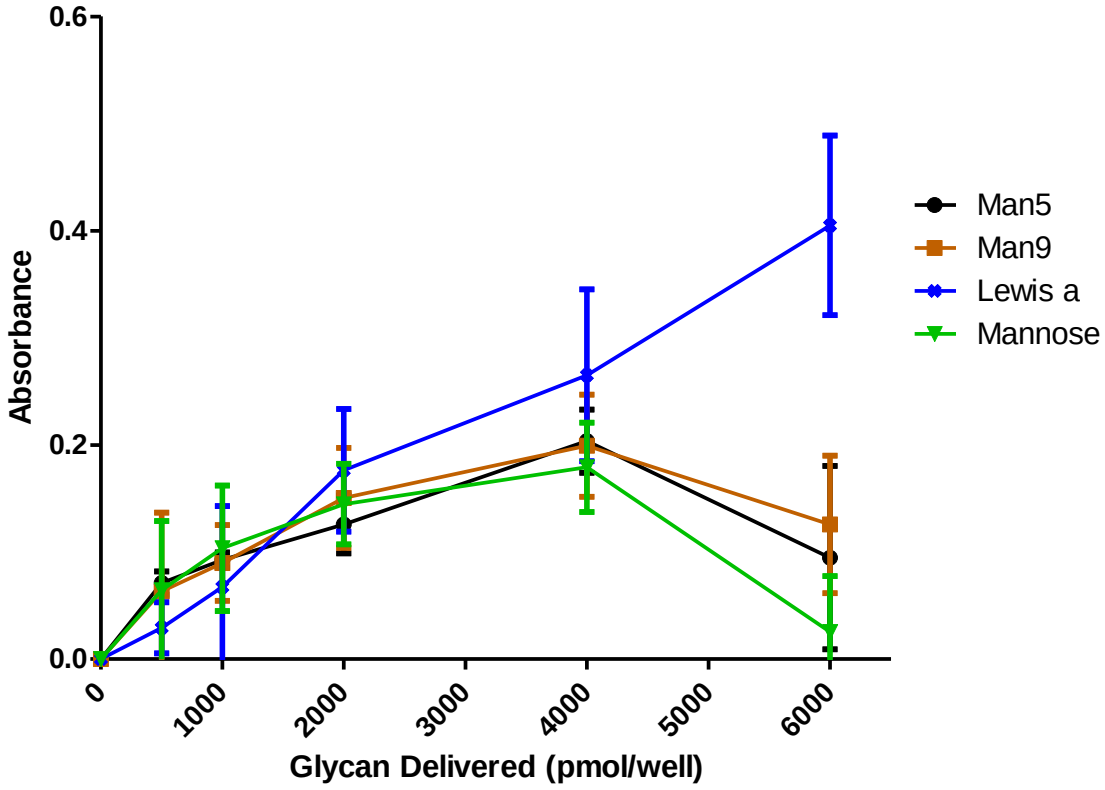

Figure A 1: Enzyme linked lectin assay detection of biotinylated glycans with a range of sizes [mono-saccharide (mannose) to an 11 sugar oligo-saccharide (Man9) immobilized on a SA-coated TCPS 96-well plate to determine the concentration of glycan that needed to be delivered per well to saturate the SA binding sites. Generally, 4000 pmol of biotinylated glycan needed to be delivered per well in order for binding sites to be maximized. Data presented as mean±S.D.; n=6 independent determinations

Table A 1: Full model of from Table 4A with all donor coefficients.

Variable	βs	β Parameter Estimate	Standard Error	t Value	Pr > |t|
Intercept	β_1	0.50603	0.05453	9.28	<.0001
Isoelectric Point	β_2	0.03965	0.00592	6.7	<.0001
Ligand OEG	β_3	-0.03324	0.04325	-0.77	0.4425
Ligand Glc	β_4	-0.0041	0.04718	-0.09	0.9308
Ligand Man	β_5	0.06817	0.04623	1.47	0.141
Density	β_6	0.01382	0.00152	9.07	<.0001
Donor	β_7	-0.59434	0.05966	-9.96	<.0001
Donor	β_8	-0.11864	0.05966	-1.99	0.0473
Donor	B_9	0.01207	0.05966	0.2	0.8398
Donor	β_{10}	-0.33773	0.05966	-5.66	<.0001
Donor	β_{11}	-0.57418	0.05966	-9.62	<.0001
Donor	β_{12}	-0.24482	0.05966	-4.1	<.0001
Donor	β_{13}	-0.14216	0.05966	-2.38	0.0176
Donor	β_{14}	-0.24173	0.05966	-4.05	<.0001
Donor	β_{15}	-0.42702	0.05966	-7.16	<.0001
Donor	β_{16}	0.66049	0.05966	11.07	<.0001
Donor	β_{17}	-0.35118	0.05966	-5.89	<.0001
Donor	β_{18}	-0.38287	0.05966	-6.42	<.0001

Table A 2: Full model of from Table 4B with all donor coefficients.

Variable	βs	β Parameter Estimate	Standard Error	t Value	Pr > |t|
Intercept	β_1	0.92276	0.01557	59.27	<.0001
Isoelectric High	β_2	0.17195	0.03355	5.12	<.0001
Isoelectric Med.	β_3	0.15722	0.03243	4.85	<.0001
Isoelectric Low	β_4	-0.00784	0.04854	-0.16	0.8718
Ligand OEG	β_5	-0.0042	0.04426	-0.09	0.9245
Ligand Glc	β_6	0.0145	0.04791	0.3	0.7622
Ligand Man	β_7	0.06549	0.04656	1.41	0.1602
Density	β_8	0.38133	0.03736	10.21	<.0001
Density	B_9	0.09719	0.03118	3.12	0.0019
Density	β_{10}	0	.	.	.
Donor	β_{11}	-0.59434	0.05818	-10.21	<.0001
Donor	β_{12}	-0.11864	0.05818	-2.04	0.042
Donor	β_{13}	0.01207	0.05818	0.21	0.8358
Donor	β_{14}	-0.33773	0.05818	-5.8	<.0001
Donor	β_{15}	-0.57418	0.05818	-9.87	<.0001
Donor	β_{16}	-0.24482	0.05818	-4.21	<.0001
Donor	β_{17}	-0.14216	0.05818	-2.44	0.0149

Table A 2 Continued

Donor	β_{18}	-0.24173	0.05818	-4.15	<.0001
Donor	β_{19}	-0.42702	0.05818	-7.34	<.0001
Donor	B_{20}	0.66049	0.05818	11.35	<.0001
Donor	B_{21}	-0.35118	0.05818	-6.04	<.0001
Donor	B_{22}	-0.38287	0.05818	-6.58	<.0001

Table A 3: Parameter estimates for model 1c using continuous isoelectric point and density.

Variable	βs	β Parameter Estimate	Standard Error	t Value	Pr > |t|
Intercept	β_1	0.16929	0.01871	9.05	<.0001
Isoelectric Point	β_2	-0.00474	0.00203	-2.34	0.0199
Ligand OEG	β_3	0.00301	0.01484	0.2	0.8395
Ligand Glc	β_4	-0.03615	0.01618	-2.23	0.0259
Ligand Man	β_5	-0.03053	0.01586	-1.92	0.0548
Density	β_6	-0.00209	0.000522	-4.01	<.0001
Donor*	$\beta_{7\text{-}18}$	-0.12619 - 0.21436	0.02036	-6.17 - 10.47	<.0001

*** All donor estimates, standard errors, t values, and probabilities can be seen in the Table A 4 in the appendix.**

Table A 4: Full model of from Table 5A with all donor coefficients.

Variable	βs	β Parameter Estimate	Standard Error	t Value	Pr > |t|
Intercept	β_1	0.16929	0.01871	9.05	<.0001
Isoelectric Point	β_2	-0.00474	0.00203	-2.34	0.0199
Ligand OEG	β_3	0.00301	0.01484	0.2	0.8395
Ligand Glc	β_4	-0.03615	0.01618	-2.23	0.0259
Ligand Man	β_5	-0.03053	0.01586	-1.92	0.0548
Density	β_6	-0.00209	0.00052	-4.01	<.0001
Donor	β_7	0.10193	0.02047	4.98	<.0001
Donor	β_8	0.20634	0.02047	10.08	<.0001
Donor	B_9	0.21436	0.02047	10.47	<.0001
Donor	β_{10}	-0.12619	0.02047	-6.17	<.0001
Donor	β_{11}	-0.01768	0.02047	-0.86	0.388
Donor	β_{12}	-0.02878	0.02047	-1.41	0.1603
Donor	β_{13}	0.07103	0.02047	3.47	0.0006
Donor	β_{14}	-0.03678	0.02047	-1.8	0.0729
Donor	β_{15}	0.03078	0.02047	1.5	0.1332
Donor	β_{16}	-0.02929	0.02047	-1.43	0.1531
Donor	β_{17}	-0.01219	0.02047	-0.6	0.5517
Donor	β_{18}	0.05221	0.02047	2.55	0.011

Table A 5: Full model of from Table 5B with all donor coefficients.

Variable	βs	β Parameter Estimate	Standard Error	t Value	Pr > |t|
Intercept	β_1	0.12018	0.00543	22.15	<.0001
Isoelectric High	β_2	-0.02412	0.01169	-2.06	0.0397
Isoelectric Med.	β_3	-0.0002072	0.0113	-0.02	0.9854
Isoelectric Low	β_4	0.03534	0.01692	2.09	0.0372
Ligand OEG	β_5	0.00662	0.01543	0.43	0.6681
Ligand Glc	β_6	-0.0291	0.0167	-1.74	0.0819
Ligand Man	β_7	-0.02491	0.01623	-1.54	0.1253
Density	β_8	-0.06402	0.01302	-4.92	<.0001
Density	B_9	-0.02769	0.01087	-2.55	0.0111
Density	β_{10}	0	.	.	.
Donor	β_{11}	0.10193	0.02028	5.03	<.0001
Donor	β_{12}	0.20634	0.02028	10.18	<.0001
Donor	β_{13}	0.21436	0.02028	10.57	<.0001
Donor	β_{14}	-0.12619	0.02028	-6.22	<.0001
Donor	β_{15}	-0.01768	0.02028	-0.87	0.3836
Donor	β_{16}	-0.02878	0.02028	-1.42	0.1564
Donor	β_{17}	0.07103	0.02028	3.5	0.0005
Donor	β_{18}	-0.03678	0.02028	-1.81	0.0703
Donor	β_{19}	0.03078	0.02028	1.52	0.1297
Donor	B_{20}	-0.02929	0.02028	-1.44	0.1493
Donor	B_{21}	-0.01219	0.02028	-0.6	0.548
Donor	B_{22}	0.05221	0.02028	2.57	0.0103

Table A 6: Full model of from Table 6 with all donor coefficients.

Variable	DF	Parameter Estimate	Standard Error	t Value	Pr > |t|
Intercept	β_1	**1.01253**	**0.04706**	**21.52**	**<.0001**
Density High	β_2	**0.09053**	**0.12926**	**0.7**	**0.4852**
Density Med.	β_3	**-0.0534**	**0.16854**	**-0.32**	**0.7518**
Density Low	β_4	**-0.1709**	**0.21251**	**-0.8**	**0.4232**
OEG	β_5	0	.	.	.
Ligand Glc	β_5	**0.52008**	**0.14115**	**3.68**	**0.0004**
Ligand Man	β_6	**0.47628**	**0.2124**	**2.24**	**0.027**
Ligand GlcNAc	β_7	**0.135**	**0.2286**	**0.59**	**0.5561**
Ligand Alpha	β_8	**0.43799**	**0.2124**	**2.06**	**0.0416**
Ligand Branch	β_9	**0.12871**	**0.15445**	**0.83**	**0.4065**
Donor	β_{10}	**-0.4511**	**0.22732**	**-1.98**	**0.0498**
Donor	β_{11}	**-0.3717**	**0.22732**	**-1.63**	**0.105**
Donor	β_{12}	**-0.2281**	**0.22732**	**-1**	**0.3179**
Donor	β_{13}	**-0.3564**	**0.22732**	**-1.57**	**0.1199**
Donor	β_{14}	**-0.4134**	**0.22732**	**-1.82**	**0.0718**
Donor	β_{15}	**-0.3026**	**0.22732**	**-1.33**	**0.186**
Donor	β_{16}	**-0.0399**	**0.22732**	**-0.18**	**0.8609**
Donor	β_{17}	**0.81132**	**0.22732**	**3.57**	**0.0005**
Donor	β_{18}	**-0.2714**	**0.22732**	**-1.19**	**0.2351**
Donor	β_{19}	**0.4375**	**0.22732**	**1.92**	**0.057**
Donor	β_{20}	**1.07452**	**0.25388**	**4.23**	**<.0001**
Donor	β_{21}	**-0.1844**	**0.25388**	**-0.73**	**0.4693**
Donor	β_{22}	**0.20063**	**0.25388**	**0.79**	**0.4312**
Donor	β_{23}	**0.98387**	**0.26648**	**3.69**	**0.0004**
Donor	β_{24}	**0.17857**	**0.26648**	**0.67**	**0.5042**
Donor	β_{25}	**0.55334**	**0.26648**	**2.08**	**0.0403**

Method 1:

R_1 = mean hydrodynamic radius of all conjugates = $3.64*10^{-9}$ m

P_F = Optimal Packing factor for a circle = 0.9069

S_U = Unit Surface area= 1 μm^2 = $1.0*10^{-12}$ m^2

L_M = Mean Glycans/BSA = 26

L_{M2} = Mean Displayed Glycans = $L_M/2$ = 13

Surface area footprint of a circle = $\pi * (R_1)^2$

Ligands Displayed Per Unit Surface Area =

$$P_F * \frac{L_{M2}(\pi*(R)^2)}{S_U} = 2.83 * 10^5$$

Method 2:

W1 = Weight of BSA/Weight of Polystyrene: (0.0171 g BSA)/(gram of PS)

D = Density of Polystyrene= 1.05 g/cm^3 = 1050000 g/m^3

R_2 = Radius of Polystyrene Bead = 5.0*10^{-7} m

W_{BSA} = 66463 g/mol

S_U= Unit Surface area= 1 μm^2 = 1.0*10^{-12}

S_U = Unit Surface area= 1 μm^2 = 1.0*10^{-12} m^2

N_A = Avagadro's Number = 6.02214*10^{23}

Surface Area of a Sphere = $4 * \pi * r^2$

Volume of a Sphere = $\frac{4}{3} * \pi * r^3$

Carbohydrates/um^2 =

$$S_U\left(\frac{4}{3} * \pi * R_2^3 * D * \frac{W_1}{W_{BSA}}\right) * \frac{N_A}{4*\pi*R_2^2} * L_{M2} =$$

$$\frac{S_U D W_1 R_2 N_A L_{M2}}{3 W_{BSA}} = 3.52 * 10^5$$

Figure A 2: Estimation of glycan density. Estimates calculated from the average measured hydrodynamic radius of the conjugates (Method 1). Estimates calculated from the average number of BSA proteins per unit area of polystyrene as measured by Osborne et. al.[245] (Method 2).

A.2. Supplemental to the Elucidation of How Presentation Modality of Glycoconjugates Alters Dendritic Cell Phenotype

Table A 7: ANOVA table comparing all modalities of display. Significance of comparison was determined using a Bonferroni correction to allow for a more conservative estimate of error. Thus, an $\alpha < 0.0167$ was used as the determinant of the level of statistical significance.

	1 µg/ml Soluble	1 µm Bead	Well Adsorbed
1 µg/ml Soluble		<0.0001	0.0042
1 µm Bead	<0.0001		<0.0001
Well Adsorbed	0.0042	<0.0001	

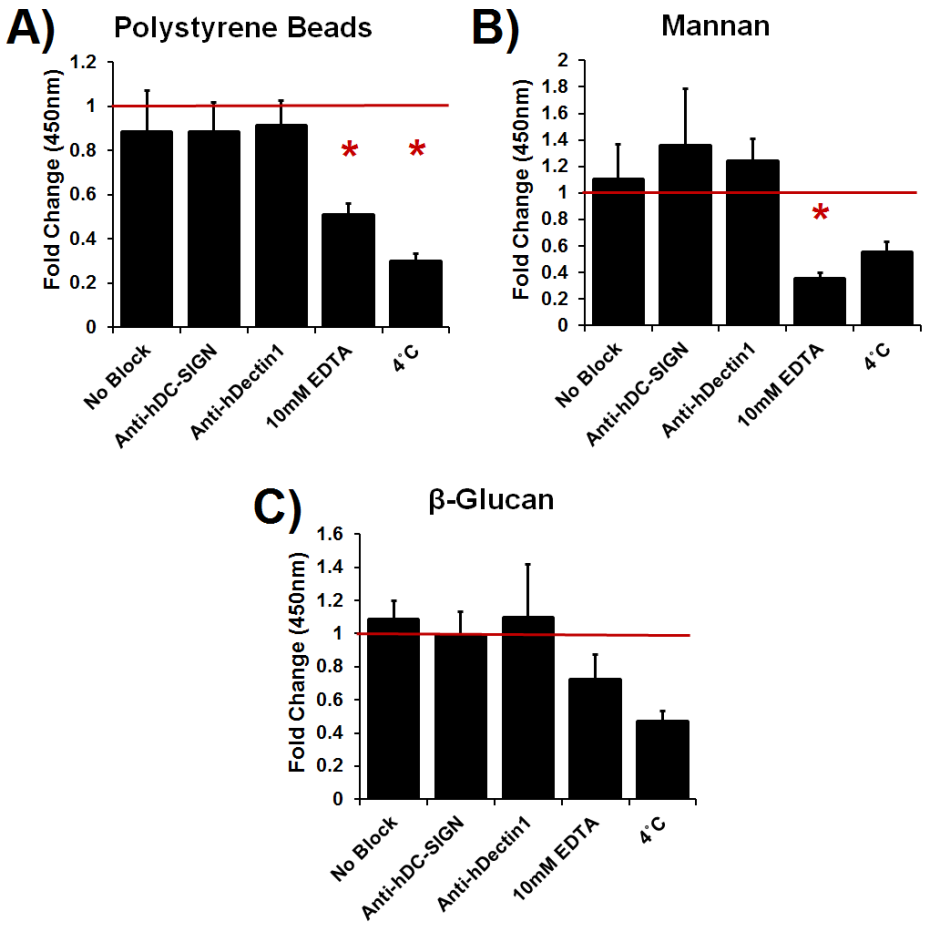

Figure A 3: Phagocytosis of 1 µm PS, mannan, or β-glucan coated fluorescent beads by DCs when exposed to blocking antibodies, EDTA, or 4°C.

A.3. Modification of High Throughput Assay for Assessment of Tolerogenic DC Phenotype

A.3.1. Overview

A HTP approach is necessary to assess functional phenotypic effects of complex carbohydrates obtained from natural sources on DC phenotype for four key reasons. First, glycan structures from natural sources are typically only available in sub-µmol levels and they are highly heterogeneous in structure.[4,177–179] Second, there is a lack of an efficient means of automated assignment and structural characterization of glycans from these sources.[180] Third, the biosynthesis of oligosaccharides is inherently heterogenous even between cells from the same cell line and thus developing a repertoire of oligosaccharides that would be representative of the glycoform of a typical glycoprotein is extremely difficult to reproduce by chemical synthesis.[181–183] Fourth, most carbohydrate-protein interactions are multivalent; thus, dense carbohydrate displays are necessary for detection of cellular interaction in screening analyses.[104,105,184] The combination of dense coating and low prevalence yields testing apparatuses that must have small presentation surfaces for cell interaction. Furthermore, when assessing the DC phenotype in response to glycoconjugates it is necessary to determine both pro-inflammatory and tolerogenic DC phenotypes as ligation of CLRs has been shown to have both pro- and anti- inflammatory phenotypic modulation, as can be seen in Table 1. Thus, a surface marker associated with a tolerogenic DC phenotype was desired. After reviewing the literature it was found that ILT3 was an excellent indicator of tolerogenic DC phenotype.[312–314] However, the current HTP assay does not assess tolerogenic phenotype in any way other than via analysis of cytokines. Due to its screening reporter (CD86/DC-SIGN fold change) being biased toward pro-inflammatory DC responses it is possible that treatments that induce a tolerogenic DC phenotype could not be assessed for cytokine profile and thus, missed as important modulators of DC phenotype.

To mitigate these concerns the HTP DC phenotype assessment assay originally developed by the Babensee lab was scaled down to a 384 well plate from a 96 well plate. To accomplish this the assay was first validated in a similar way to that of the original HTP assay. The 96 well HTP assay was originally validated using clinically relevant biomaterials PLGA and agarose. Of these materials only PLGA showed a statistically significant increase in CD86/DC-SIGN fold change over that of iDC. Additionally, the magnitude of the DC response to PLGA was at an intermediate level between that of iDCs and mDCs. Thus, for the HTP assay iDCs, mDCs, and PLGA treated DCs were tested for their CD86/DC-SIGN fold change in both 96 well plates and 384 well plates. Next, the addition of a tolerogenic reporter, ILT3/CD86 (TMF) was developed and validated via flow cytometry. Finally, the addition of cell disassociation solution (CDS) and effect of seeded cell number was assessed to determine if these factors needed to be varied to obtain more consistent results from the IMF and TMF assays in 384 wells.

It was found that 96 and 384 well assays produced results that were not statistically different from each other and showed identical trends in DC response to PLGA and LPS. Then TMF was found to be an excellent reporter for tolerogenic DC phenotype and that the HTP assay produced equivalent results to that of flow cytometry. Finally, it was found that for treatments where DCs were found to adsorb to plates more readily, LPS, use of CDS produced higher signals with lower variance than did the conventional HTP methodology. Additionally, it was found that seeding cells at $7.5x10^5$ cells/ml produced higher signals, particularly for the TMF, as compared to the conventional culture method.

The addition of a tolerogenic reporter to the HTP assay was seen as a significant improvement of the assay, increasing its ability to effectively screen ligands that induce both pro-inflammatory and tolerogenic phenotypes is an important step in functional assessment of DCs. Additionally, the scale down to 384 wells was seen as significant for reagents where quantities of ligand are precious. For glycans, and in particular complex

glycan structures, this is unilaterally the case and thus the scale down to 384 wells made this dissertation possible. On average, the scale down to 384 wells reduced the quantity of reagents needed by 5x while maintaining the number cells used for four times the number of treatments.

A.3.2. Methods

A.3.2.1. Original 96 well High Throughput Dendritic Cell Phenotype Methodology

Differentially-treated and reference control DCs were harvested after 24 h for analysis using an HTP method previously described.[224] Briefly, all treated DCs and controls were transferred via multi-channel pipette to a black 96-well filter plate (Pall Life Sciences), and the supernatants were immediately collected into a 96-well plate through the filters by stacking the filter plate on top of the collection plate and centrifuging at 300 RCF for 4 min. To the retained cells 150 µl of 0.05% formaldehyde solution was added and the cells were allowed to fix for 40 minutes at room temperature while being shaken at 600 RPM. The formaldehyde solution was then removed via centrifugation at 400 RCF for 4 minutes. The cells retained in the wells were assessed for phenotype by immunostaining using antibodies anti-CD86-PE (Clone BU63; Ancell) and anti- DC-SIGN-FITC (Clone 120507; R & D Systems). IgG_1-PE (clone MOPC31C; Ancell) and IgG_{2B}-FITC (clone 133303; R&D Systems) isotype-stained DCs were used for background fluorescence subtraction in separate treatment for control wells. CD86 is a costimulatory molecule that is up-regulated upon pro-inflammatory DC maturation,[224] DC-SIGN is an endocytic receptor that is slightly down-regulated upon pro-inflammatory maturation.[224] After 40 minutes of staining the cells were washed three times. The fluorescent intensity for each well was measured at the emission/excitation wavelengths for each fluorophore 535/590 PE and 485/535 FITC. The geometric mean fluorescent intensities (gMFIs) were then calculated with a Tecan Infinite F500 microplate reader,

and the ratio of respective gMFIs were determined as CD86/DC-SIGN, a cell number independent metric.

A.3.2.2. Initial 384 well High Throughput Dendritic Cell Phenotype Methodology

Prior to the addition of the ILT3 reporter and CDS solution DCs were assessed for their phenotype with an identical methodology to that of the 96 well plate described above but in a 384-well TCPS plate and 384-well filter plate. All volumes used in this assay were ¼ those used in the 96 well plate assay.

A.3.2.3. Comparison of 96 well high throughput to 384-well high throughput Methodologies

Primary human DCs were cultured as per 4.2.7. On day 5 after isolation DCs for experiments where the 96 well and 384 well methodologies were compared DCs were transferred to wells that had a PLGA film already in them and allowed to incubate in the presence of the PLGA film for 24 hours. LPS was also added to mDC wells at each plate as outlined in Chapter 4. The resultant DC phenotype was assessed via the methodologies described in A.3.2.1 and A.3.2.2.

A.3.2.4. Preparation of PLGA films

PLGA (molar ratio = 75:25, inherent viscosity = 0.70 dl/g in trichloromethane, MW = 100,000 Da; Birmingham Polymers, Birmingham, AL) films were prepared by solvent casting without a porogen as previously reported.[224] Briefly, PLGA was dissolved 20% w/v in dichloromethane overnight at room temperature and poured into a 50 mm Teflon dish (Cole-Parmer, Vernon Hills, IL) in a chemical fume hood. After evaporation of the solvent and drying to form films (48–72 h), the PLGA films were punched to fit into the wells of a 384- or 96-well plate, followed by three washing steps using endotoxin-free water (Cambrex, East Rutherford, NJ) and UV sterilization for 30 min on each side in the tissue culture hood before iDCs were plated on them.

A.3.2.5. Addition of CDS and optimization of cell count.

An identical assessment and culture methodology to that described in Chapter 4.2.9 was performed for these studies except that DCs were resuspended at $5.0x10^5$, $7.5x10^5$, or $1.5x10^6$ cells/ml and then placed in wells. For wells where IL10 was added 3500 units/ml of human IL10 was added.

A.3.2.6. Flow cytometric analysis and validation of ILT3 expression for tolerogenic DCs.

To show that the 384 well HTP methodology produced similar results to the of flow cytometry DCs were placed in treatment wells with 8 replicates for flow cytometry and four replicates for the HTP methodology. After 24 hours of treatments the levels of surface marker expression were monitored by flow cytometry per the methods described previously[224] and compared to the controls. Briefly, the cells were collected by centrifugation at 1100 rpm for 10 min, resuspended in 0.1% BSA and 2 mM EDTA in PBS, pH 7.2 (cell-staining buffer), and stained with fluorescently labeled antibodies discussed earlier. The cells were stained for 1 h at 4°C and analyzed using a BD LSR flow cytometer (Beckton Dickinson, San Jose, CA). Data analysis was performed using FlowJo (Tree Star, Ashland, OR) based on the differential shift of histograms compared to the controls unless otherwise indicated. The IMF and TMF values were determined by dividing the geometric mean fluorescence intensities (gMFIs) of anti-CD86-PE by that of anti-DC-SIGN-FITC or anti-ILT3-AF647 by that of anti-CD86-PE. ILT3/CD86 was chosen as the tolerance reporter due to the fact that LPS, and all other activating ligands tested in this dissertation, also showed a large increase in ILT3 expression. This is typical of healthy DCs as they have been shown to up regulate immune dampening receptors when highly activated so that sepsis does not occur. However, these activated cells also dramatically up-regulated CD86 and CD80 and tDCs and those cells treated by IL10 showed no increase in expression of these receptors. Thus, for tolerogenic DCs

CD86 became the normalizing agent of cell number per well and provided a stronger signal to noise ratio than ILT3 expression alone or that of ILT3 divided by DC-SIGN due to CD86 expression being strongly correlated to inflammatory activation and anti-correlated to tolerance of DCs.

A.3.3. Results

A.3.3.1. Validation of a 384-Well HTP Methodology Against that of the 96-Well HTP Methodology

Using the scaled down 384 well high throughput methodology discussed in Chapter 4.2.9 it was found that no difference between the 96 well and 384 well plate assays were found. Figure A 4 shows the results of this study. It was shown that both LPS treatment (mDC) and PLGA treatement of DCs caused a statistical increase in fold change of CD86/DCSIGN in either the 96-well or the 384-well assay. Furthermore, an ANOVA was run comparing all groups and it was found that no differences were significant between treatments run in 96 well plate versus the identical treatment in a 384 well plate.

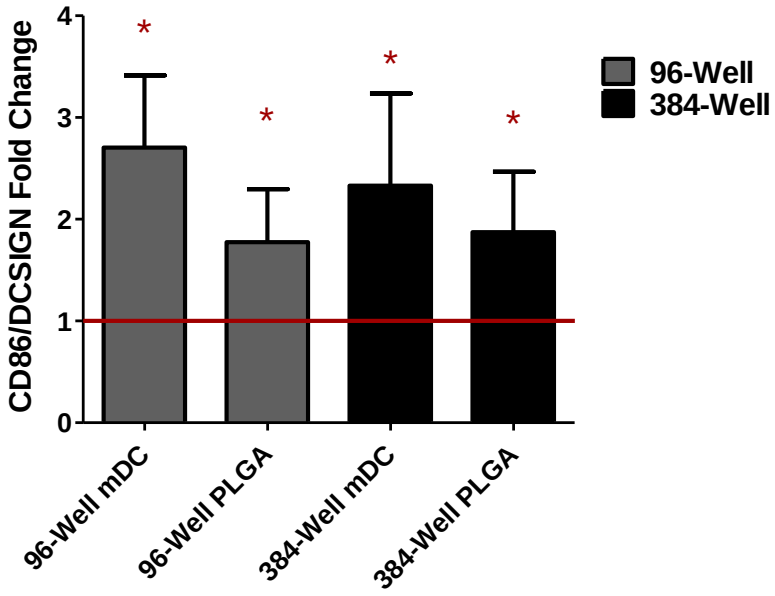

Figure A 4: The fold change in CD86/DCSIGN in a 384 well and 96 well plate was measured in response to LPS (mDC) and PLGA plate simultaneous. Mean of iDC normalized data shown. Error bars indicate standard error, N=8 independent donors, * represents statistical significance from iDC $\alpha<0.05$.

A.3.3.2. Development of a Tolerogenic Reporter

A.3.3.2.1. Cell Number and Cell Disassociation Solution Optimization

Dendritic cell IMF and TMF expression can be seen at three cell concentrations and with or without CDS washing for all controls in Figure A 5. Identical profiles for IMF can be seen at the classic cell concentration (5.0E5 cells/ml) as with 7.5E5 cells/ml. Additionally, while not statistically significant CDS treated wells generally had higher mean IMFs than did cells not rinsed with CDS. Additionally, the variance of IMF was seen to be lower for CDS washed cells. While IMF trends remained similar for all treatments at 5.0E5 and 7.5E5 cell/ml concentrations, a higher and more consistent TMF signal was shown for cells seeded at 7.5E5 cells/ml. Also of note was that cells treated with IL10 only were expected to have a lower TMF than tDC but a higher TMF than iDC. Using 7.5E5 cells/ml clearly showed this trend and thus 7.5E5 cells/ml with

washing with CDS were chosen as the ideal culture and processing steps for the 384-well HTP assay.

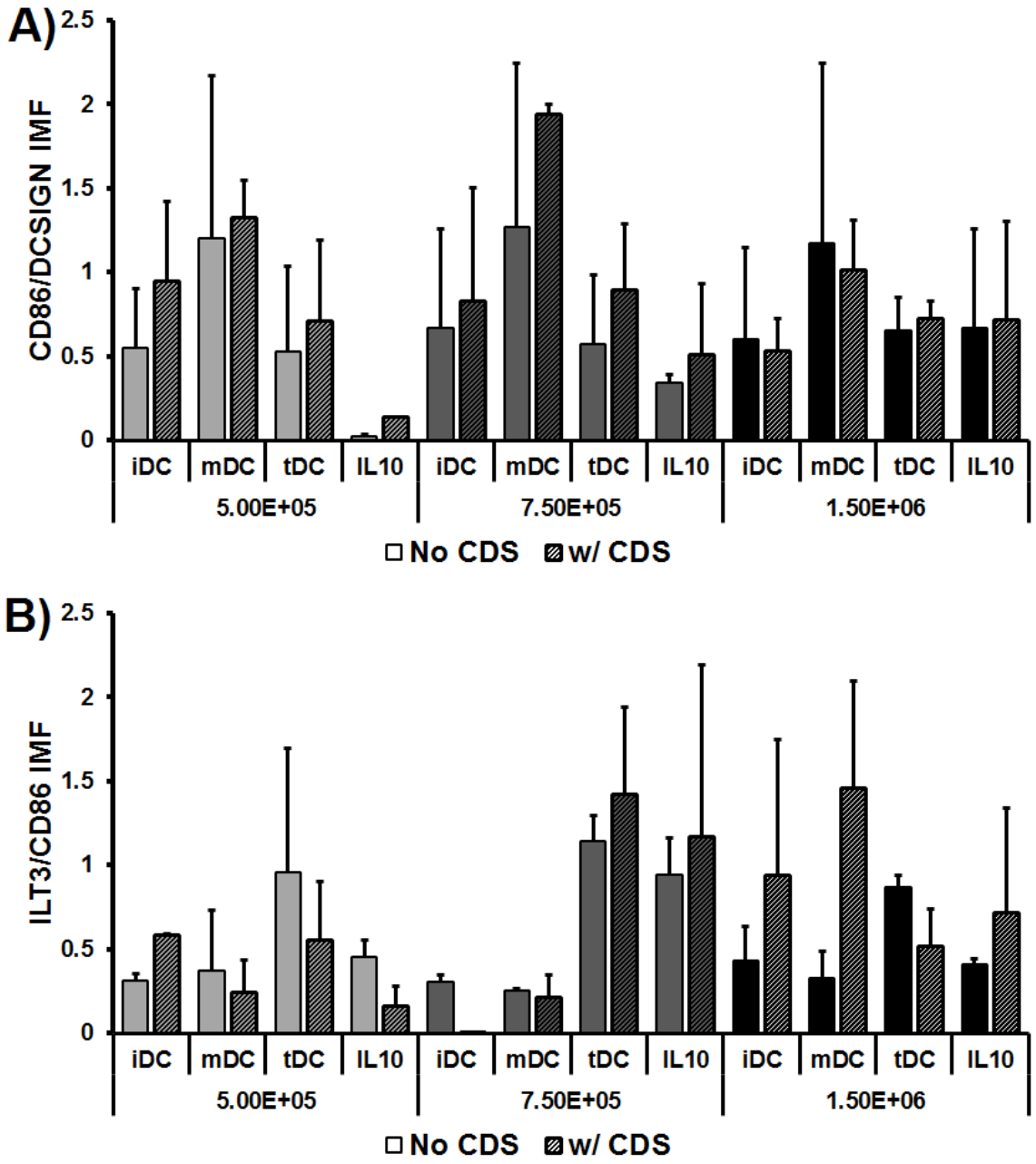

Figure A 5: Dendritic cell response to controls at three different cell seeding concentrations and when rinsed with CDS. Mean of two independent donors is shown. Error bars represent half range.

A.3.3.2.2. Validation of Tolerogenic Reporter

Once optimized, the tolerogenic reporter needed to be validated against flow cytometry to ensure consistency with an industry standard. Identical trends between flow cytometry and the HTP assay were seen. Figure A 6 shows the results from this study. In all graphs significance of positive controls were identical between assay types. Additionally, it was found that for TMF, the assay was able to measure an increase in TMF for IL10 treated cells that was smaller than that of tDC but greater than that of carriers and iDCs. Additionally, concerns of spectral overlap between reporting fluorophores were allayed by the fact that signal intensity and ratios of expression were similar in magnitude to that which was historically measured using the HTP technique without the tolerogenic reporter.

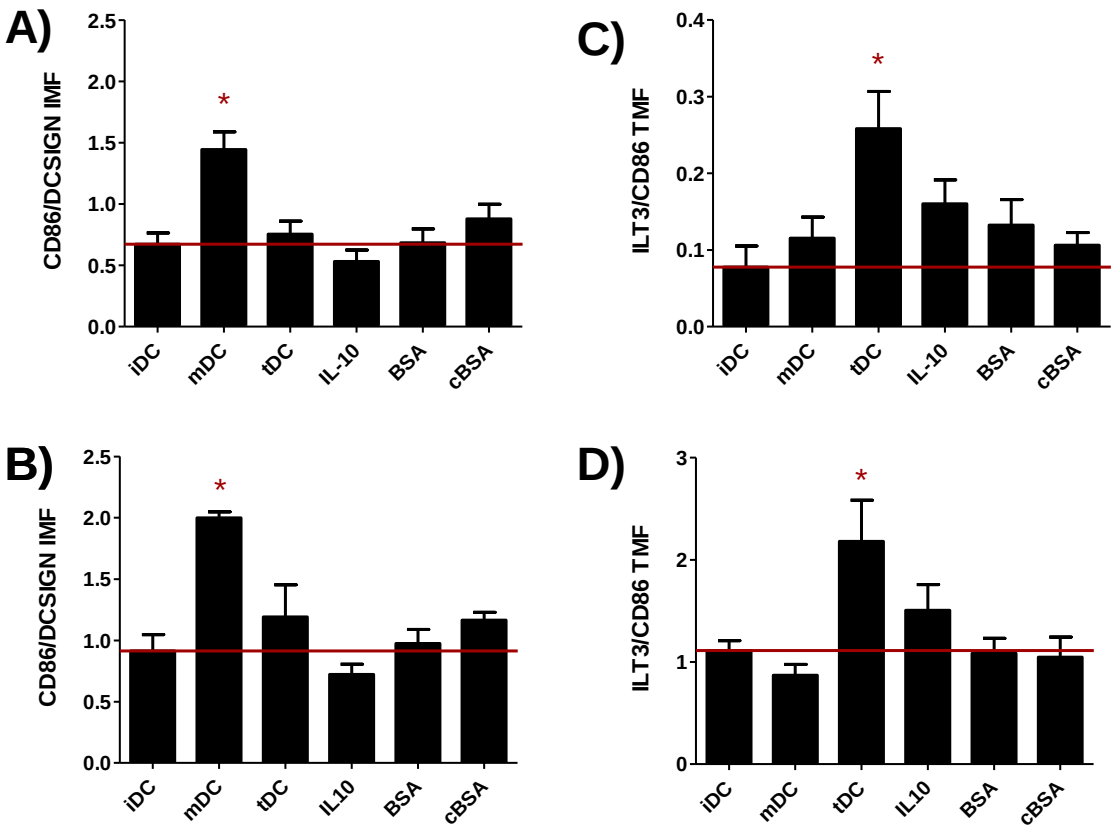

Figure A 6: Validation of HTP assay using ILT3 as a reporter for tolerogenic DCs. (A,B) Measure IMF via plate reader (A) and flow cytometry (B). (B,D) Measure

TMF via plate reader (C) and flow cytometry (D). IMF was measured simultaneously to TMF to ensure no confounding of the original reporters occurred. Data is mean expression ratio not normalized by iDC. Error bars indicate standard error, N=7 independent donors for (A,C) and N=3 independent donros for (B,D), * represents statistical significance from iDC $\alpha<0.05$.

A.3.4. Discussion and Conclusions

A.3.4.1. Validation of a 384-Well HTP Methodology Against that of the 96-Well HTP Methodology

To validate the HTP methology two requirements were set, 1) that the sensitivity of the assay was not diminished. 2) That the DC response to treatments that have been shown to historically activate cells in the 96-well HTP assay be statistically similar in the 384-well assay. An ANOVA showing identical statistical significance between mDC and PLGA treatments as compared to iDCs for both the 96-well and 384 well plates proved the first claim. However, a more rigorous ANOVA was performed in which all data from both 384 and 96 well plates was combined and compared. This comparison showed that there was no difference between identical treatments between assay types. Thus, with the information from these ANOVAs it was concluded that there was no significant difference between the assays.

A.3.4.2. Development of a Tolerogenic Reporter

A tolerogenic reporter was seen as critical for assessment of DC phenotype to glycans due to the plethora of CLRs on DCs that have been shown to induce a tolerogenic phenotype, as seen in Table 1. Thus, an antibody staining for ILT3, a tolerogenic cell surface marker on DCs, was added to the assay. However, it was found that ILT3 was not expressed to as great of an extent on DC cell membranes as that of CD86 or DCSIGN as indicated by the relatively high gain of the plate reader when measuring stained cells (data not shown). Thus, the number of cells per well was increased to try to increase the

signal produced by the stained cells. As expected , cells seeded at 7.5E5 cells/ml showed a dramatic increase in TMF signal intensity and a decrease in variability as compared to the 5.0E5 cells/ml treatments. Cells seeded at 1.5E6 cells/ml were found to clog fliter plates and provide inconsistent signals as indicated by the large error bars in many of their treatments in Figure A 5.

Additionally, because many CLRs on DCs are adhesion receptors ensuring that adherent DCs were being measured in the HTP assay was seen as important. Thus, a washing step was added to the classic HTP procedure in which DCs were treated with CDS and then transferred to the filter plate and spun down. Figure A 5 shows that cells washed with CDS appeared to provide a higher signal to noise ratio with lower variance in signal than their unwashed analogs. Additionally, wells were visualized before and after washing with CDS and it was visually confirmed that virtually all cells were being removed form wells after washing with CDS while many cells remained prior to CDS wash. Finally, it was desired that no difference in the profile between that of the old lower cell concentration and the new higher cell concentration be seen. Thus IMF and TMF trends between the concentrations were visually compared and found to be qualtitatively similar.

A more rigorous comparison of IMF and TMF activation between assays was desired than the qualitative comparison performed in Figure A 5. Thus, cell response in the optimized 384-well HTP protocol were compared to the industry standard flow cytometry. It wsa found that identical IMF and TMF trends were seen between that of flow cytometry and the 384-well HTP assay. Additionally, the magnitude of the response between these two was similar and response trends were identical between

methodologies. Flow cytometry showed a higher sensitivity to ILT3 staining than did the plate reader as indicated by the magnitude of the signal shown in Figure A 6C and D. However, the fold change of TMF over that of iDC was not statistically different between the two assays and thus the differences were not seen as significant.

In conclusion these studies show that the new HTP assay performs similarly to the previous assay while adding a tolerogenic reporter, allowing for assessment of adherent DCs, using 5x less reagent for surface modification, and assessing 4x as many treatment with the same volume of cells as the old assay. Assessment of tolerogenic DC phenotype is critical for future glycan work as CLRs have been shown to induce tolerogenic DC phenotypes repeatedly in literature.[18,84,264,315] Thus, the development of this assay is seen as pivital to continuing glycan research in the DC field. In addition to the studies performed here all studies performed in this dissertation were completed with the 384-well HTP assay; further verifying its applicability to glycan systems and its ability to assess DC phenotype across display modalities which has not been shown in the literature to date.

A.4. Development of Zero Length Fluorescent Linker for Carbohydrate Immobilization on Well and Bead Surfaces

A.4.1. Overview

Currently, isolating glycans from natural sources involves cleaving the glycan from the protein, functionalizing it with a fluorescent linker and then separating different glycan structures via HPLC. This method was shown in detail in the first Aim of this dissertation for the Man5-Br conjugate. Other chemistries have been used by other labs but the process essentially remains consistent.[316,317] This fluorescent modification serves

two purposes, first it makes glycan identification and isolation simple from an often complex milieu of glycans. The other is for quantifying the amount of glycan immobilized on a surface after functionalization to validate the glycan has been immobilized. The value of this was highlighted in 4.4.2 of this dissertation. Briefly, it is almost impossible to determine the density of glycan presentation from a surface quantitatively without that glycan being fluorescent or radio labeled to allow for quantification. However, the chemical moiety which the carbohydrate is attached drastically alters the binding affinity of carbohydrate binding proteins.[223] Briefly, it has been shown that reduction of the inherent level of flexibility of the linker had a favorable impact on cell binding especially for cells displaying a high CLR density, and the structure of the carrier can modulate inhibitory potency when comparing different lectins.[223] This not only shows that lectin affinity can be modulated via linker properties but it also shows that different lectins have a differential ideal molecular signature that is optimal for maximum glycan binding. Thus, the smaller and more labile a glycan linker can be made so that the carrier it is linked to can exhibit the optimal properties necessary for glycan display the better. A more detailed discussion of the influence of linker chemistry can be seen in section 3.5.2 of this report.

With this in mind the purpose of this project was to create a small linker whose attachment could still be quantified. Instead of linking a large fluorophore to the glycan, a smaller, less intrusive linker will be attached to the glycan; this linker will be used to attach the glycan to a surface. The surface that it links to would be fluorescently modified and ideally, the linker would substitute for the fluorophore, leaving a covalent link between the glycan and the surface and the fluorescent linker in solution to be

washed away. To accomplish this we chose a substitution reaction in which a fluorescent moiety (dansyl chloride (DsCl)) was substituted for an azidomethyl modified glycan. To accomplish this optimization of a DsCl coating was first performed on 1.5 and 45 μm silica beads. Then an azide modified fluorophore was used to substitute off the DsCl moiety and the effect of concentration of the fluorophore was measured. After that azidoethyl modified lactose was used as a model glycan to show that substitution of the DsCl group could occur with Glycan. Finally, stability of the structure in PBS was tested over a 48 hour period to ensure that the substitution was permanent in buffers commonly used by cells. It was found that both 1.5 and 45 μm amine modified silica beads could be modified with DsCl at a 5000:1 DsCl to Amine ratio and that fluorescence from these beads scaled linearly with bead number. Then it was found that the substitution reaction between azide modified Alexa Fluor 594 (AF594), and the DsCl beads occurred and could be easily quantified in a plate reader. Next, a concentration dependent reduction in fluorescence was shown between azide-glycans and DsCl beads. Finally, it was show that beads modified with the AF594 did not show a statistical decrease in fluorescence over the course of 48 hours in PBS but that background fluorescence from DsCl was almost completely abrogated. From these graphs we conclude that the chemical mechanism proposed by Suenaga et.al.[318] can be used for glycan substitution and that modification with glycan is capable of reducing fluorescence in such a way so as to be quantifiable. Future work to be done includes, ELLAs with the glycan modified beads and co-culture of beads with DCs to determine if DCs can recognize and respond to glycans reacted with this chemistry.

A.4.2. Methods

A.4.2.1. Conjugation of Lactic Acid to Amine Coated Silica Microbeads

First, amine coated silica microbeads (1.5 µm or 45 µm; Microspheres-Nanospheres) were aliquoted into a 15 ml polypropylene centrifuge tube and spun down at 2000 RCF for 5 minutes. The supernatant was removed and beads were resuspended in dichloromethane (DCM). Beads were then added to a 100 mM stock of lactic acid (Sigma) dissolved in DCM, in an equal volume ratio. Next, the bead/lactic acid solution was mixed with an equal volume of 2 mg/ml 1-Ethyl-3-(3-dimethylaminopropyl)carbodiimide (EDC) dissolved in water. The solution was allowed to react for 2 hours at room temperature. Finally, beads were spun down at 2000 RCF for 5 minutes, supernatants removed, and washed with DCM three times.

A.4.2.2. Dansylation of Lactic Acid Functionalized Microbeads

Lactic acid functionalized microbeads suspended in DCM were then functionalized with 5-(dimethylamino)naphthaline-1-sulfonyl chloride (Dansyl chloride, DsCl). Beads were added in a 1:1 volume ratio to 130mM DsCl dissolved in DCM. For experiments where optimization of DsCl concentration was performed beads were dissolved in a 1:1 volume ratio with twice the indicated concentration of DsCl. Tubes were then sealed with aluminum plate sealers (VWR) and covered from light. The reaction was allowed to run for 72 hours at room temperature while shaking at 600 RPM. Finally, beads were spun down at 2000 RCF for 5 minutes, supernatants removed, and washed with DCM three times.

For studies where bead number was varied and fluorescence of DsCl beads was measured, DsCl modified and unmodified beads were aliquoted into wells of a silica coated polypropylene Plate^{+} 384 well plate (SUN-SRi) and fluorescence was measured at excitation/emission 340 nm/535 nm using a Tecan Plate Reader (Tecan, Switzerland).

All measures in each well were performed twice with 1 second of shaking at 1000 RPM between each measurement and then averaged for the mean fluorescent intensity of each well.

A.4.2.3. Azide Substitution of Dansylated Microbeads

Dansyl chloride functionalized microbeads suspended in DCM were then functionalized with azide linked moieties. First, beads were spun down at 2000 RCF for 5 minutes, supernatants removed, and washed with dimethylformamide (DMF) three times. Beads were added in a 1:1 volume ratio to 20mM sodium azide dissolved in DMF. For experiments where Alexa Fluor 594 (AF) substitution was used beads were added to a 600 µM stock solution dissolved in DMF in a 1:1 volume ratio. For experiments where optimization of lactose-azide (Lac-N_3) concentration was performed beads were dissolved in a 1:1 volume ratio with twice the indicated concentration of Lac-N_3. Tubes were then sealed with aluminum plate sealers (VWR) and covered from light. The tube was then heated to 70°C in a water bath and allowed to react for 1 hour. Finally, beads were spun down at 2000 RCF for 5 minutes, supernatants removed, and washed with DCM three times. Figure A 7 shows a schematic of this overall process.

For studies where bead fluorescence of was measured, modified beads were aliquoted into wells of a Plate+ 384 well plate and fluorescence was measured at excitation/emission 340 nm/535 nm and 590 nm/ 635 nm by the Tecan Plate Reader. All measures in each well were performed twice with 1 second of shaking at 1000 RPM between each measurement and then averaged for the mean fluorescent intensity of each well.

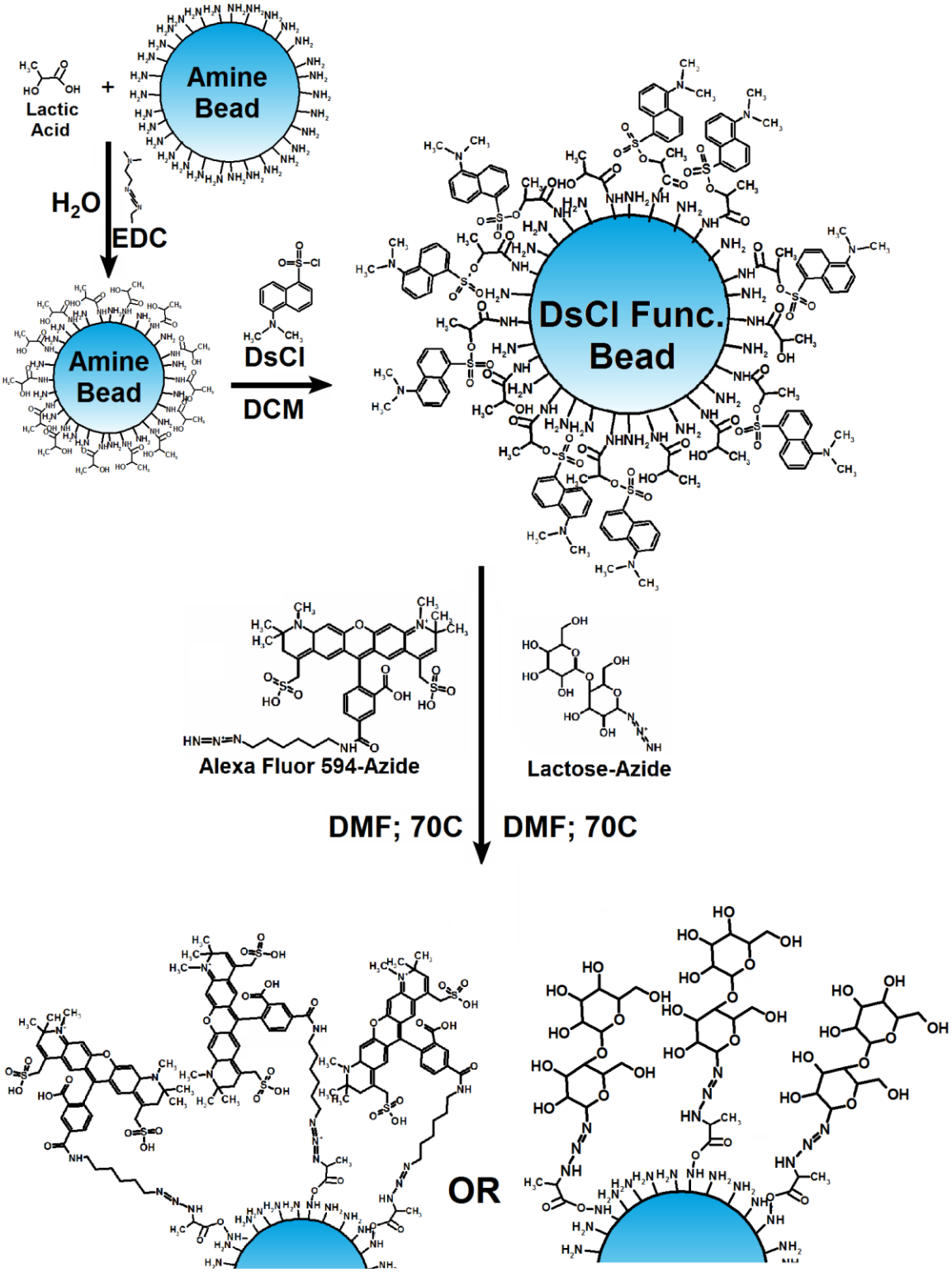

Figure A 7: Overview of chemistry for functionalization of amine beads via AF594 or Lac-N_3.

A.4.2.4. Stability of Azide-Linked Moiety on DsCl Modified Microbeads

Fluorescence from unmodified, DsCl functionalized, and AF functionalized beads was measured by placing beads into wells of a Plate+ 384 well plate and fluorescence was measured at excitation/emission 340 nm/535 nm and 590 nm/ 635 nm by the Tecan Plate Reader. To measure fluorescence of beads in different buffers beads were spun down at 2000 RCF for 5 minutes, supernatants removed, and washed with one of three buffers: DCM, PBS, or media (RPMI-1640 (Invitrogen) supplemented with 10% heat inactivated fetal bovine serum (Cellgro MediaTech) and 100 U/ml penicillin/streptomycin (Cellgro MediaTech)), three times. Then fluorescence was measured at excitation/emission 340 nm/535 nm and 590 nm/ 635 nm for each well at 0, 12, 24, or 48 hours after final buffer exchange. All wells were sealed with an aluminum plate sealer between measures to ensure no loss of buffer. All measures in each well were performed twice with 1 second of shaking at 1000 RPM between each measurement and then averaged for the mean fluorescent intensity of each well.

A.4.3. Results

A.4.3.1. Dansyl Chloride Saturates Binding Sites on Microbeads at a 65mM Concentration.

The desired amount of DsCl necessary to saturate binding sites on the amine functionalized microbeads was determined. It was found that DsCl at a concentration of 65mM saturated binding sites of beads as indicated by fluorescence of beads in wells not increasing significantly above this concentration. Figure A 8 shows the results of this experiment. Interestingly 1.5 µm beads appeared to saturate binding sites at a lower concentration that that of the 45 µm beads.

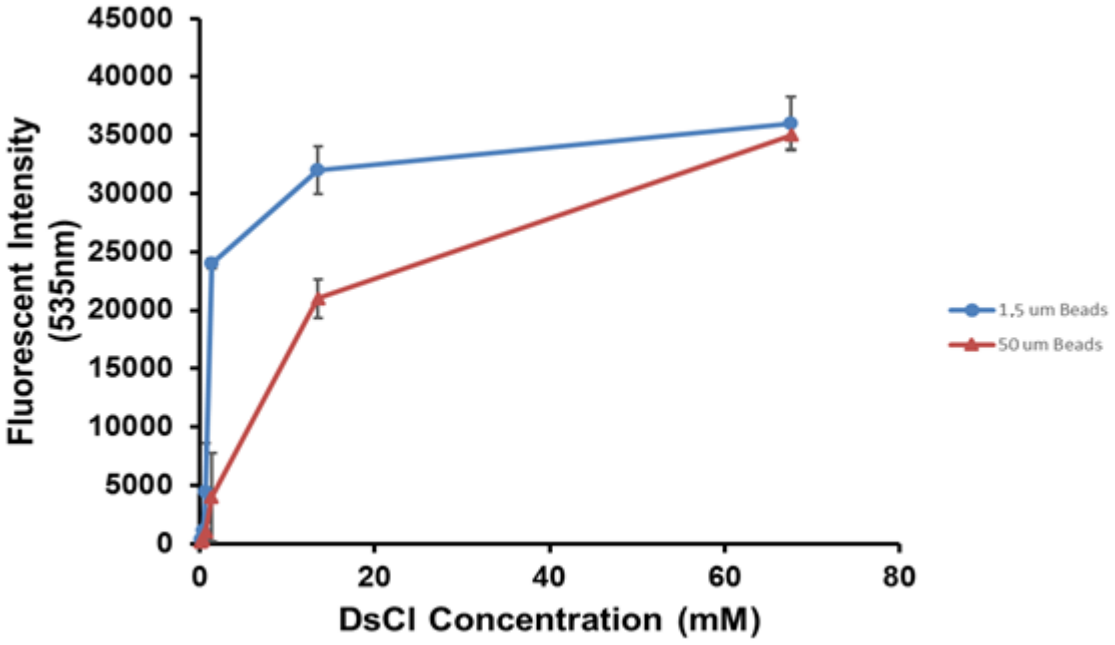

Figure A 8: Fluorescent intensity of 45 µm and 1.5 µm amine coated silica beads as a function of DsCl concentration. All data is background subtracted from unmodified beads. Error bars represent standard deviation of three wells.

Whether the fluorescence of the beads after functionalization with DsCl scaled linearly with bead number was tested next. This was of concern because beads were not optically clear and thus at high bead centrations occlusion of fluorescence could occur

from beads. It was found that for both 45 µm and 1.5 µm beads fluorescence scaled linearly over the range of bead concentrations tested (100 to 15 $x10^3$ and $5x10^3$ to $9x10^8$ respectively. Figure A 9 shows the fluorescence versus number of beads. Linear trend lines using least squares regression were added to each graph and the subsequent R^2 of the fit from the data was calculated. The R^2 for the 45 µm beads was found to be 0.9795 and The R^2 for the1.5µm beads was found to be 0.9876. Both of these R^2 values were above the 95% threshold considered as relevant to consider each trend linear in correlation.

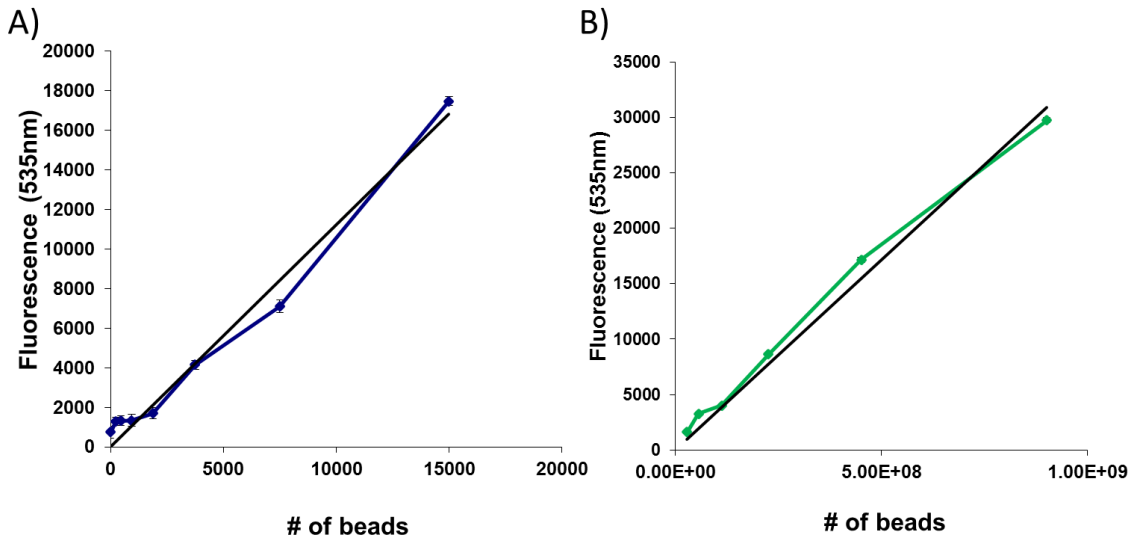

Figure A 9: Fluorescence of beads versus number of beads functionalized. (A) 45 µm bead fluorescence and (B) 1 µm bead fluorescence as a function of bead number. Linear trend lines are added to each graph in black.

A.4.3.2. Dansyl Chloride Fluorescence on Amine Modified Beads Scales Linearly with Bead Number

Finally, whether the DsCl group could be replaced by sodium azide as reported in Suenaga et.al. was confirmed via plate reader. It was found that in the presence of 10mM sodium azide fluorescence from DsCl beads returned to that of background. Figure A 10 shows the results from this study for 1.5 µm beads. Identical results were found for 45 µm beads (data not shown).

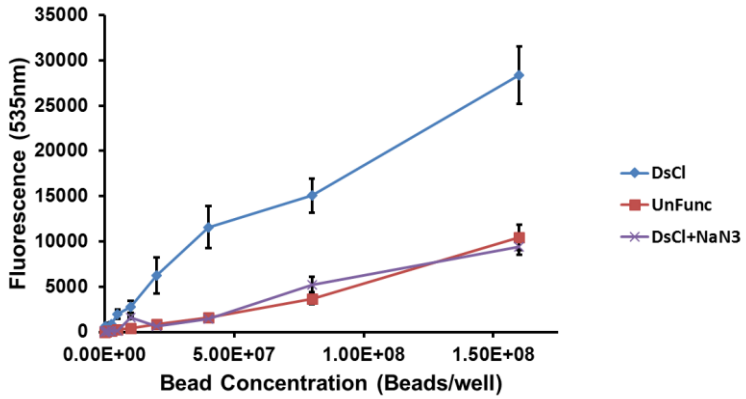

Figure A 10: Fluorescence at 535nm for unfunctionalized, DsCl modified, and DsCl modified with 10mM sodium azide beads. All data was background subtracted from unmodified beads. Error bars represent standard deviation, N=3 wells.

A.4.3.3. Azide Functionalized Fluorophores substitute Dansyl Chloride Groups From Beads

While Suenaga et.al. showed that DsCl fluorescence on microbeads decreased dramatically with the addition of sodium azide no other proof of functionalization was made. Thus, it was desired to show quantitatively that the fluorescence decrease in the DsCl functionalized beads was occurring via a substitution reaction with the azide. It was found that Alexa Fluor F594-azide (AF) reacted DsCl functionalized beads dramatically reduced their fluorescence, below that of background unfunctionalized beads, at the DsCl emission wavelength (535 nm). Additionally, AF reacted beads were found to dramatically increase their fluorescence at the AF emission wavelength (635 nm) over that of unfunctionalized beads. To determine this AF was incubated with DsCl functionalized beads and the resultant fluorescence at 535 nm (DsCl) and 635 nm (AF594) was measured as a function of time in a plate reader. Figure A 11 shows the results of three independent formulations of 1.5 µm beads. Similar results were found for 45 µm beads (data not shown). All plotted fluorescences were background subtracted from unfunctionalized beads.

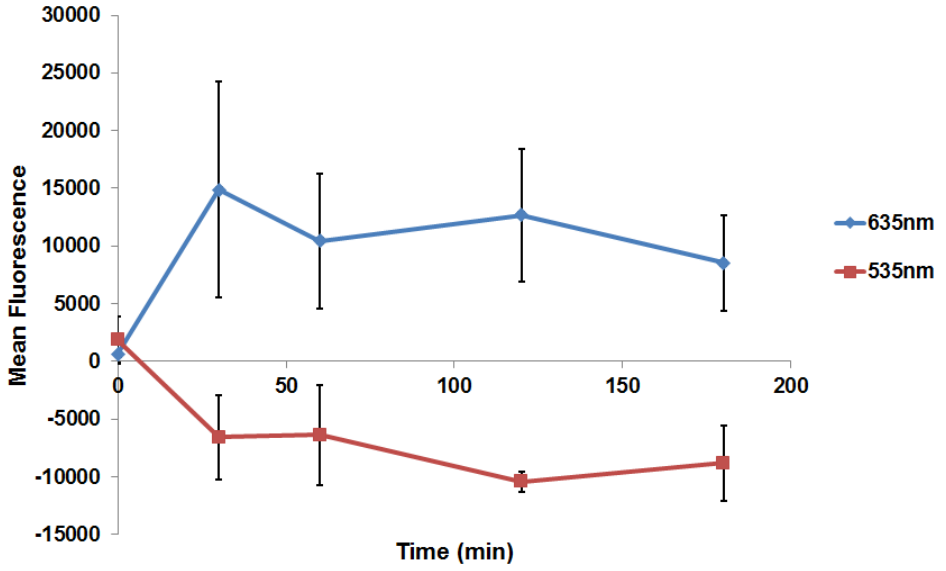

Figure A 11: Mean fluorescence of AF594 reacted DsCl modified beads as a function of time. The average fluorescence at the emission of AF594 (635nm) and DsCl (535nm) was plotted as a function of time. Error bars represent standard error of three independent formulations of beads.

Fluorescent images of AF reacted beads were taken at both 535 nm and 635 nm to qualitatively show that fluorescence decreased for AF reacted beads. It is clear from the pictures shown in Figure A 12 that AF reacted beads had a significant decrease in DsCl fluorescence and a significant increase in AF fluorescence. Figure A 12A and B were unfunctionalized beads that showed a very low fluorescence at both wavelengths. Figure A 12C and D were DsCl modified beads and had an expectedly high fluorescence at 535 and almost no fluorescence above background at 635. Figure A 12E and F were DsCl beads that had been reacted with AF. These beads showed a relatively low fluorescence at 535 but a very high fluorescence at 635. Interestingly, some fluorescence remained in the AF reacted beads as seen in Figure A 12E.

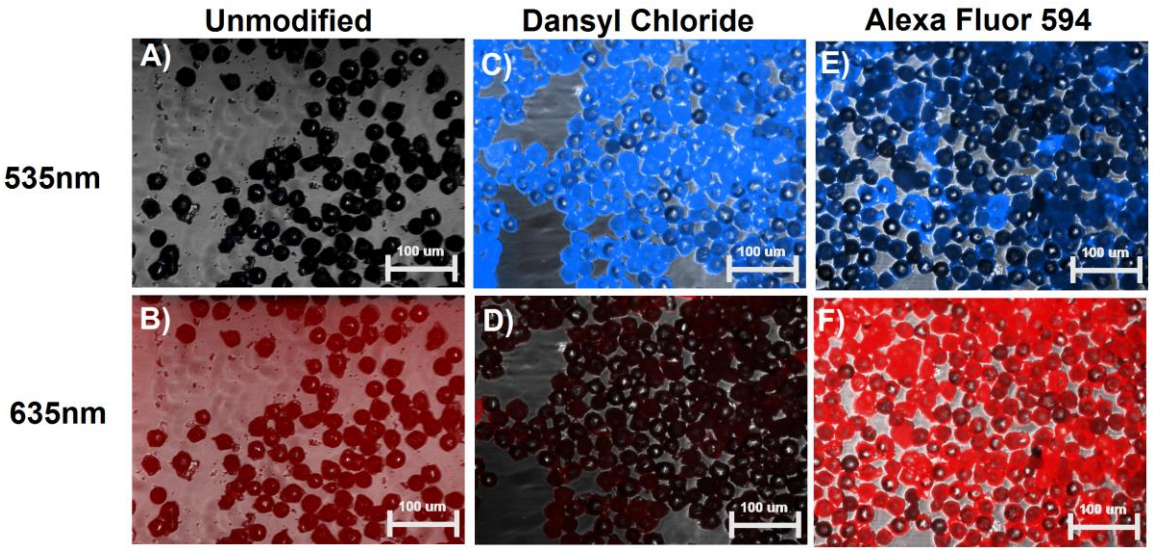

Figure A 12: Fluorescent micrograph of functionalized beads. Fluorescence of (A,B) unmodified beads, (C,D) DsCl modified beads, and (E,F) AF reacted DsCl beads was viewed at 535nm and 635nm.

A.4.3.4. Azide Functionalized Glycans Reduce Dansyl Chloride Fluorescence in a Concentration Dependent Manner

Now that the fluorescence studies had shown that beads were being modified with azide linked ligands the concentration of glycan necessary to abrogate DsCl fluorescence was determined. It was found that at 45 mM Lac-N_3 was able to attenuate DsCl fluorescence to that of background. Additionally, it was seen that as Lac-N3 concentration increased the mean fluorescence at each bead concentration decreased. Figure A 13 shows the results from the 1.5 µm bead study. Similar results were seen for 45 µm beads (data not shown).

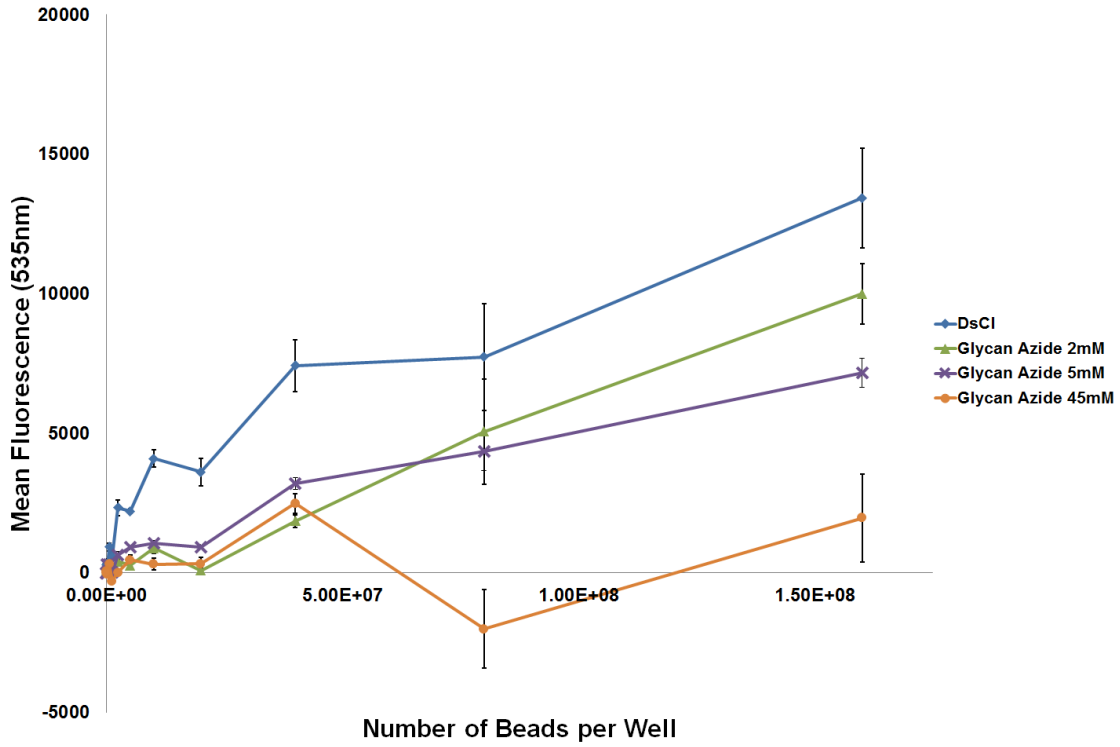

Figure A 13: Fluorescence of beads at multiple Lac-N_3 concentrations was plotted against bead number for 1.5 µm beads. Fluorescence was background subtracted from sodium azide treated DsCl beads. Error bars represent standard error of 3 independent formulations for 1.0 µm beads.

A.4.3.5. Functionalized Microbeads are Stable in Physiological Solutions

Finally, whether the azide substituted ligand was covalently bound and could stay attached in physiological media or was only adsorbed to the surface was determined. It was found that beads reacted with AF and suspended in PBS showed almost no attenuation of signal as compared to AF reacted beads in DCM that had been sealed for the 48 hours. Furthermore, fluorescence at 535 nm from AF reacted DsCl Beads in PBS decreased to background levels after only 12 hours. Figure A 14 shows the results from this study. Figure A 14A shows the fluorescent intensity of DsCl and AF reacted DsCl beads at 635 nm when beads were suspended in DCM, PBS, or media. Figure A 14B shows the fluorescent intensity of DsCl and AF reacted DsCl beads at 535 nm when

beads were suspended in DCM, PBS, or media. Interestingly, AF reacted beads in media showed a very high background fluorescence and thus when background subtracted results appear to not be consistent with the PBS data.

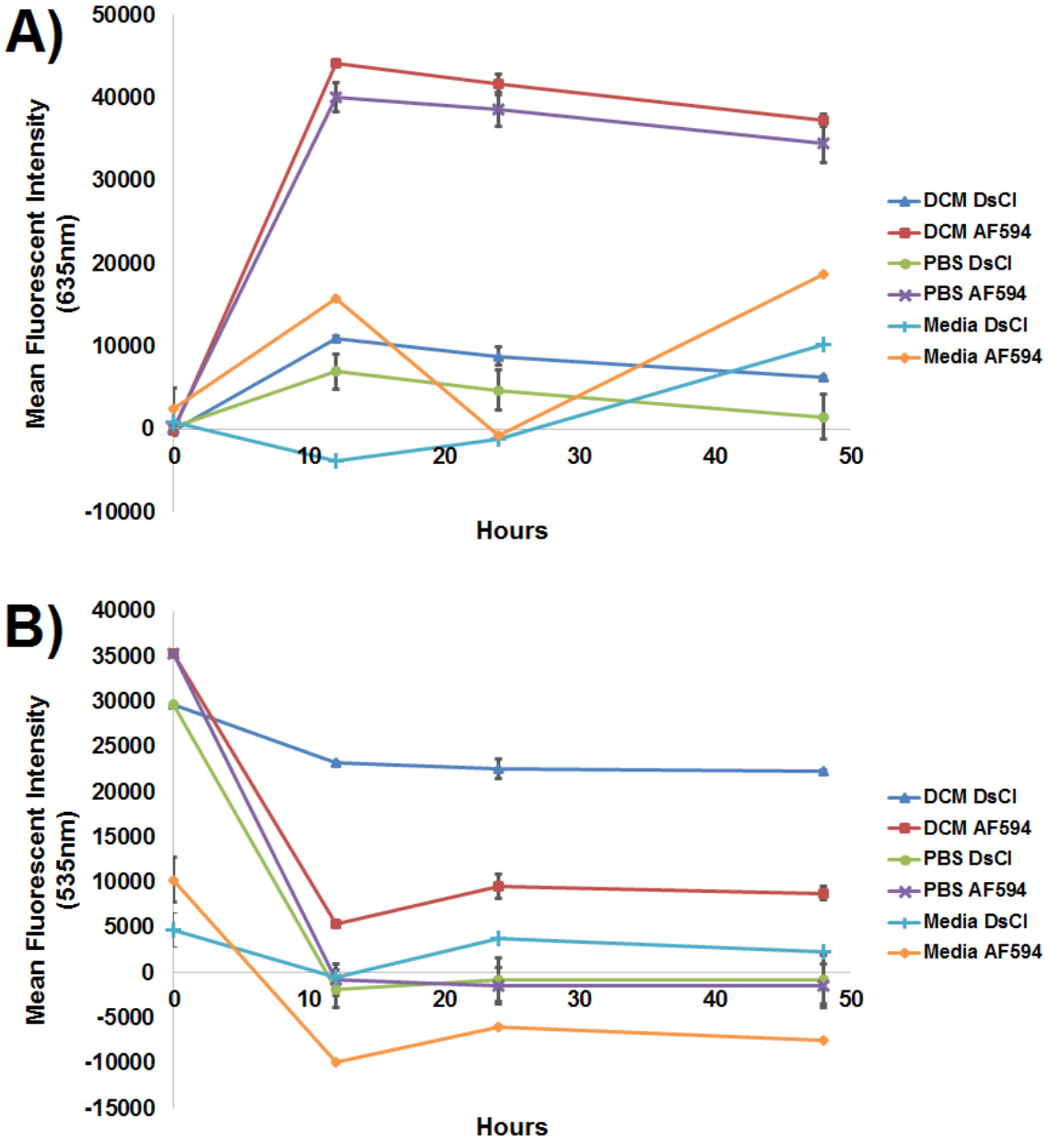

Figure A 14: Mean fluorescence of DsCl and AF modified DsCl 1.5 µm beads was determined when beads were suspended in DCM, PBS or media at 635 nm (A) and 535 nm (B). Mean of three wells is plotted; error bars represent standard deviation.

A.4.4. Discussion and Conclusions

A glycan presentation chemistry that could quantify the amount of glycan immobilized on a surface without having to have a large fluorescent moiety attached to the linker was desired due to the known influence that linkers play in CLR recognition of glycans.[223] Thus, a subtractive methodology was developed in which a fluorescent surface was functionalized with an azide modified ligand. This functionalization removed the fluorescent moiety from the surface, thereby allowing for the assessment of functionalization via a decrease is surface fluorescence. An azide was chosen because the library of glycans available from the Consortium for Functional Glycomics have azido linkers attached to them and thus a seamless integration with this library was desired.

In the experiments below large 45 μm beads and phagocytosable beads were both functionalized and tested. The reason for this was twofold: 1) this dissertation has highlighted the importance of modality of display in how DCs respond to glycans and thus a display chemistry that can quantify glycan immobilization on two modalities was seen as important and significant. 2) The chemistries used herein are not conducive to well plates as both DCM and DMF dissolve polystyrene and if left to incubate in polypropylene will eventually degrade the polypropylene. Thus, functionalization of TCPS wells or other cheap, readily available, cell culture surfaces cannot be performed with this chemistry and therefore cell response to flat well presented glycans cannot be easily obtained using this chemistry. Because this dissertation highlights the importance of this display modality an alternative display methodology was desired. Therefore, developing a chemistry that was able to be functionalize a large bead in a reaction vessel that would not be dissolved by DMF or DCM was developed. A large bead was chosen because we hypothesize that DCs would "see" and respond to glycans presented from a large non-phagocytosable bead in the same way as that of a flat well surface. Indeed preliminary work with DCs showed that 50 μm bead display of adsorbed glycans showed

an identical trend in DC phenotype. The results of this study can be seen in Figure A 15 below.

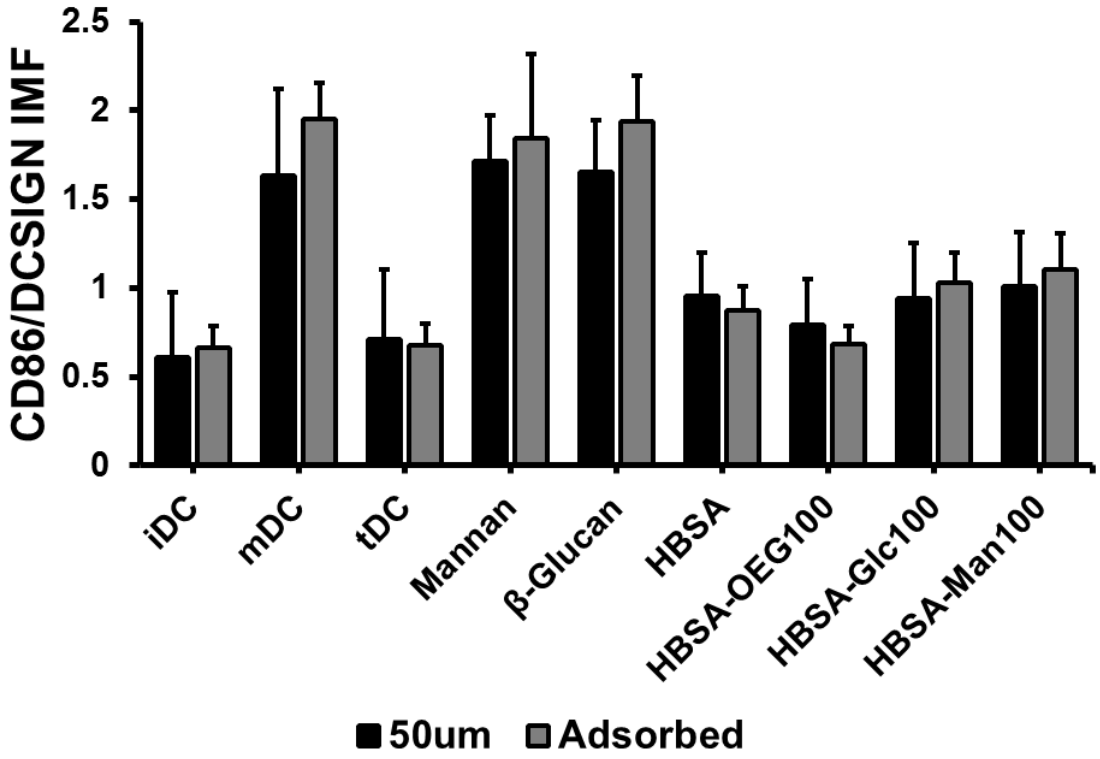

Figure A 15: DC response to conjugates adsorbed to flat wells or adsorbed to 50 µm PS beads. Error bars represent standard error. N=12 for adsorbed conjugates and N= 8 for 50 µm bead studies.

To accomplish this goal, the first step was to develop a fluorescent coating chemistry that could be substituted by an azide and optimize that reaction to obtain maximum fluorescence. A mechanism proposed by Suenaga et.al.[318] was found but this paper did not test the chemistry quantitatively or when azide what linked to other moieties such as glycans. Thus, we recapitulated the study performed by Suenaga et.al.[318] using quantitative fluorescence assessment and optimized the reaction elucidated by them for our purposes. It was found that 65mM DsCl saturated fluorescence on the DsCl beads for both 1.5 µm and 45 µm beads. The 1.5 µm beads saturated at a lower concentration of DsCl than did the 50 µm beads. This was hypothesized to be due to

poor mixing of the larger beads in the reaction vessel due to their increased size and thus increased settling time at the bottom of the wells. The 1.5 μm beads stayed in suspension for a long period of time and thus their functionalized could more readily occur.

Next, a validation of bead number versus fluorescence was needed to ensure that functionalized beads were not optically clear and thus at high bead concentrations occlusion of fluorescence could occur from other beads in solution. Additionally, auto-fluorescence measures could be of concern in a plate reader due to neighboring bead stimulation. It was found that this was not occurring and that fluorescence was linearly related to bead number for both 1.5 μm beads and 45 μm beads.

Following the validation of bead fluorescence reduction of DsCl fluorescence on bead surfaces by sodium azide was determined. The mechanism and work proposed by Suenaga et.al.[318] showed that this would occur however, a quantitative fluorescence measure was desired as none was given in their report. It was found that 30mM sodium azide abrogated all fluorescence as reported.

Next, proof of substitution of azide groups when connected to another ligand for that of DsCl groups was desired. For the reaction performed in Figure A 11 as AF fluorescence increased DsCl fluorescence decreased as expected. This trend was seen as consistent as three separate independently functionalized bead lots were measured and shown in Figure A 11. Further confirmation of this substitution was provided visually with images taken of the beads with a fluorescent microscope. Interestingly, while the plate reader shows a lower than background fluorescence for beads functionalized with AF fluorescent microscopy pictures show that some DsCl fluorescence remained. It is thought that this discrepancy was due to the relative insensitivity of the plate reader as compared to fluorescent microscope and thus this difference was not seen as significant.

After confirmation that azide substitution of DsCl groups could occur with a ligand attached to the azide an azide modified carbohydrate, lac-N3, was tested for concentration dependence of DsCl fluorescence. A relatively high concentration of

glycan, 45mM, was needed to abrogate DsCL fluorescence to that of background at all bead concentrations. Ideally, micro- to nano-molar concentrations of glycan would be needed to functionalize surfaces as these are the quantities able to be obtained from natural ligand sources. Thus, in future work for this aim it is proposed that more work be done to optimize this reaction for more efficient substitution of glycan azide. Factors such as temperature and incubation time can be varied, (temperature increased and incubation time increased) to get higher ligand substitutions at lower concentrations.

Finally, stability of azide reacted beads in physiological solutions was measured to ensure that reacted beads would be able to display glycans to cells. Stability of linked fluorophores over the course of two days was measured as 48 hours is twice as long as is typically measured in the HTP assays used in this dissertation. It was found that beads retained their fluorescence in PBS and that background fluorescence from DsCL decreased in incubations with PBS. The loss of DsCl fluorescence was expected as the DsCl can be reacted with water via a hydration reaction and removed from the surface. The stability of the AF indicates that reacted moieties were covalently bound to the beads and that they were not hydrolyzed form the surface significantly over the course of 48 hours. However, beads incubated in media were found to have a high background that overshadowed bead fluorescence. This was hypothesized to be due to the fact that bead fluorescence was measured in the presence of media and thus it is thought that if beads were removed and washed and then measured for fluorescence that results would be identical to that shown in the PBS. This experiment is also proposed for future work of this aim.

In conclusion, the work shown here constitutes a promising avenue for quantification of glycan immobilization on surfaces without using large and/or inflexible linkers. This immobilization strategy still has several key experiments before it can be seen as ready for use with the HTP assay. First, optimizing reaction temperatures and times with glycan azides to decrease the concentration of glycan-azide necessary to

saturate binding sites available is necessary for functional use with available glycan sources. Second, an actual quantification of glycan immobilized on the surface versus the fluorescence loss by DsCl must be performed. This could be easily done using a standard curve of amine modified DsCl and radiolabeled glycans. Third, proving that glycans are still on bead surfaces after incubation in PBS or media must be confirmed by performing ELLAs on immobilized surfaces. Fourth, confirmation that azide ligands are stable in media needs to be confirmed. Fifth, DC response to azide modified glycans immobilized on these surfaces must be performed in order to confirm that the chemistry creates a presentation context that is recognizable by DCs.

REFERENCES

1. Rabinovich, G. A. & Ilarregui, J. M. Conveying glycan information into T-cell homeostatic programs: a challenging role for galectin-1 in inflammatory and tumor microenvironments. *Immunological Reviews* **230,** 144–159 (2009).
2. Van Kooyk, Y. C-type lectins on dendritic cells: key modulators for the induction of immune responses. *Biochem. Soc. Trans* **36,** 1478–1481 (2008).
3. Mascanfroni, I. D. *et al.* Endogenous lectins shape the function of dendritic cells and tailor adaptive immunity: Mechanisms and biomedical applications. *International Immunopharmacology* **11,** 833–841 (2011).
4. Van Die, I. & Cummings, R. D. Glycan Gimmickry by Parasitic Helminths: A Strategy for Modulating the Host Immune Response? *Glycobiology* (2009). doi:10.1093/glycob/cwp140
5. Unger, W. W. & van Kooyk, Y. 'Dressed for success' C-type lectin receptors for the delivery of glyco-vaccines to dendritic cells. *Current Opinion in Immunology* **23,** 131–137 (2011).
6. Aarnoudse, C. A., Vallejo, J. J. G., Saeland, E. & van Kooyk, Y. Recognition of tumor glycans by antigen-presenting cells. *Current Opinion in Immunology* **18,** 105–111 (2006).
7. Geijtenbeek, T. B. H., van Vliet, S. J., Engering, A., 't Hart, B. A. & van Kooyk, Y. Self- and nonself-recognition by C-type lectins on dendritic cells. *Annu. Rev. Immunol* **22,** 33–54 (2004).
8. Varki, A. Letter to the Glyco-Forum: Since There Are PAMPs and DAMPs, There Must Be SAMPs? Glycan 'self-Associated Molecular Patterns' Dampen Innate Immunity, but Pathogens Can Mimic Them. *Glycobiology* **21,** 1121–1124 (2011).
9. Gorbet, M. B. & Sefton, M. V. Biomaterial-associated thrombosis: roles of coagulation factors, complement, platelets and leukocytes. *Biomaterials* **25,** 5681–5703 (2004).
10. Wu, P. & Grainger, D. W. Drug/device combinations for local drug therapies and infection prophylaxis. *Biomaterials* **27,** 2450–2467 (2006).
11. Polikov, V. S., Tresco, P. A. & Reichert, W. M. Response of brain tissue to chronically implanted neural electrodes. *J. Neurosci. Methods* **148,** 1–18 (2005).
12. Bauer, T. W. & Schils, J. The pathology of total joint arthroplasty. *Skeletal Radiology* **28,** 483–497 (1999).
13. Keselowsky, B. G. *et al.* Role of plasma fibronectin in the foreign body response to biomaterials. *Biomaterials* **28,** 3626–3631 (2007).
14. Duyck, J. & Naert, I. Failure of oral implants: aetiology, symptoms and influencing factors. *Clinical Oral Investigations* **2,** 102–114 (1998).
15. Bono, J. V., Scott, R. D., Ranawat, C. S. & Turner, R. H. *Revision Total Knee Arthroplasty*. (Springer, 2005).
16. Steinman, R. M. & Banchereau, J. Taking dendritic cells into medicine. *Nature* **449,** 419–426 (2007).
17. Steinman, R. M., Hawiger, D. & Nussenzweig, M. C. Tolerogenic dendritic cells. *Annual Review of Immunology* **21,** 685–711 (2003).

18. Ilarregui, J. M. & Rabinovich, G. A. Tolerogenic dendritic cells in the control of autoimmune neuroinflammation: an emerging role of protein-glycan interactions. *Neuroimmunomodulation* **17,** 157–160 (2010).
19. Unger, W. W. J. *et al.* Glycan-modified liposomes boost CD4+ and CD8+ T-cell responses by targeting DC-SIGN on dendritic cells. *Journal of Controlled Release* doi:10.1016/j.jconrel.2012.02.007
20. Van Vliet, S. J., Paessens, L. C., Broks-van den Berg, V. C. M., Geijtenbeek, T. B. H. & van Kooyk, Y. The C-type lectin macrophage galactose-type lectin impedes migration of immature APCs. *J. Immunol* **181,** 3148–3155 (2008).
21. Gaudart, N., Ekpo, P., Pattanapanyasat, K., van Kooyk, Y. & Engering, A. Leptospira interrogans is recognized through DC-SIGN and induces maturation and cytokine production by human dendritic cells. *FEMS Immunol. Med. Microbiol* **53,** 359–367 (2008).
22. Van Liempt, E. *et al.* Specificity of DC-SIGN for mannose- and fucose-containing glycans. *FEBS Letters* **580,** 6123–6131 (2006).
23. Nimrichter, L. *et al.* Intact cell adhesion to glycan microarrays. *Glycobiology* **14,** 197 –203 (2004).
24. Sayin, B. *et al.* Mono-N-carboxymethyl chitosan (MCC) and N-trimethyl chitosan (TMC) nanoparticles for non-invasive vaccine delivery. *Int J Pharm* **363,** 139–148 (2008).
25. Chen, H. *et al.* The promotion of type 1 T helper cell responses to cationic polymers in vivo via toll-like receptor-4 mediated IL-12 secretion. *Biomaterials* **31,** 8172–8180 (2010).
26. Martínez Gómez, J. M. *et al.* Surface coating of PLGA microparticles with protamine enhances their immunological performance through facilitated phagocytosis. *Journal of Controlled Release* **130,** 161–167 (2008).
27. Thiele, L. *et al.* Evaluation of particle uptake in human blood monocyte-derived cells in vitro. Does phagocytosis activity of dendritic cells measure up with macrophages? *Journal of Controlled Release* **76,** 59–71 (2001).
28. Wischke, C., Borchert, H.-H., Zimmermann, J., Siebenbrodt, I. & Lorenzen, D. R. Stable cationic microparticles for enhanced model antigen delivery to dendritic cells. *Journal of Controlled Release* **114,** 359–368 (2006).
29. Steinman, R. M. & Cohn, Z. A. Identification of a novel cell type in peripheral lymphoid organs of mice. I. Morphology, quantitation, tissue distribution. *J. Exp. Med.* **137,** 1142–1162 (1973).
30. Steinman, R. M. & Banchereau, J. Taking dendritic cells into medicine. *Nature* **449,** 419–426 (2007).
31. Banchereau, J. & Steinman, R. M. Dendritic cells and the control of immunity. *Nature* **392,** 245–252 (1998).
32. Shortman, K. & Naik, S. H. Steady-state and inflammatory dendritic-cell development. *Nat. Rev. Immunol.* **7,** 19–30 (2007).
33. Shortman, K. & Liu, Y.-J. Mouse and human dendritic cell subtypes. *Nat. Rev. Immunol.* **2,** 151–161 (2002).
34. Ouaaz, F., Arron, J., Zheng, Y., Choi, Y. & Beg, A. A. Dendritic cell development and survival require distinct NF-kappaB subunits. *Immunity* **16,** 257–270 (2002).

35. Romani, N. *et al.* Generation of mature dendritic cells from human blood. An improved method with special regard to clinical applicability. *J. Immunol. Methods* **196,** 137–151 (1996).
36. Zhou, L. J. & Tedder, T. F. CD14+ blood monocytes can differentiate into functionally mature CD83+ dendritic cells. *Proc. Natl. Acad. Sci. U.S.A.* **93,** 2588–2592 (1996).
37. Huber, R. *et al.* Regulation of monocyte differentiation by specific signaling modules and associated transcription factor networks. *Cell. Mol. Life Sci.* (2013). doi:10.1007/s00018-013-1322-4
38. Chomarat, P., Banchereau, J., Davoust, J. & Palucka, A. K. IL-6 switches the differentiation of monocytes from dendritic cells to macrophages. *Nat. Immunol.* **1,** 510–514 (2000).
39. Jia, L. *et al.* Expansion of Foxp3-expressing regulatory T cells in vitro by dendritic cells modified with polymeric particles carrying a plasmid encoding interleukin-10. *Biomaterials* **29,** 1250–1261 (2008).
40. Graham, L. M. & Brown, G. D. The Dectin-2 family of C-type lectins in immunity and homeostasis. *Cytokine* (2009). doi:10.1016/j.cyto.2009.07.010
41. Leibundgut-Landmann, S., Osorio, F., Brown, G. D. & Reis e Sousa, C. Stimulation of dendritic cells via the dectin-1/Syk pathway allows priming of cytotoxic T-cell responses. *Blood* **112,** 4971–4980 (2008).
42. Geijtenbeek, T. B. H. & Gringhuis, S. I. Signalling through C-type lectin receptors: shaping immune responses. *Nat. Rev. Immunol* **9,** 465–479 (2009).
43. Van Kooyk, Y. & Geijtenbeek, T. B. H. DC-SIGN: escape mechanism for pathogens. *Nat. Rev. Immunol* **3,** 697–709 (2003).
44. Bozzacco, L. *et al.* DEC-205 receptor on dendritic cells mediates presentation of HIV gag protein to CD8+ T cells in a spectrum of human MHC I haplotypes. *Proceedings of the National Academy of Sciences* **104,** 1289 –1294 (2007).
45. Yoshida, M. & Babensee, J. E. Differential effects of agarose and poly(lactic-<I>co</I>-glycolic acid) on dendritic cell maturation. *Journal of Biomedical Materials Research Part A* **79A,** 393–408 (2006).
46. Kou, P. M., Schwartz, Z., Boyan, B. D. & Babensee, J. E. Dendritic cell responses to surface properties of clinical titanium surfaces. *Acta Biomaterialia* **7,** 1354–1363 (2011).
47. Kou, P. M. *et al.* Predicting biomaterial property-dendritic cell phenotype relationships from the multivariate analysis of responses to polymethacrylates. *Biomaterials* **33,** 1699–1713 (2012).
48. Yoshida, M. & Babensee, J. E. Poly(lactic-co-glycolic acid) enhances maturation of human monocyte-derived dendritic cells. *J Biomed Mater Res A* **71,** 45–54 (2004).
49. Yoshida, M., Mata, J. & Babensee, J. E. Effect of poly(lactic-<I>co</I>-glycolic acid) contact on maturation of murine bone marrow-derived dendritic cells. *Journal of Biomedical Materials Research Part A* **80A,** 7–12 (2007).
50. Matzelle, M. M. & Babensee, J. E. Humoral immune responses to model antigen co-delivered with biomaterials used in tissue engineering. *Biomaterials* **25,** 295–304 (2004).

51. Norton, L. W., Park, J. & Babensee, J. E. Biomaterial adjuvant effect is attenuated by anti-inflammatory drug delivery or material selection. *Journal of Controlled Release* **146,** 341–348 (2010).
52. Bennewitz, N. L. & Babensee, J. E. The effect of the physical form of poly(lactic-co-glycolic acid) carriers on the humoral immune response to co-delivered antigen. *Biomaterials* **26,** 2991–2999 (2005).
53. Babensee, J. E. Interaction of dendritic cells with biomaterials. *Seminars in Immunology* **20,** 101–108 (2008).
54. Babensee, J. E. & Paranjpe, A. Differential levels of dendritic cell maturation on different biomaterials used in combination products. *J Biomed Mater Res A* **74,** 503–510 (2005).
55. Shankar, S. P., Petrie, T. A., García, A. J. & Babensee, J. E. Dendritic cell responses to self-assembled monolayers of defined chemistries. *J Biomed Mater Res A* **92,** 1487–1499 (2010).
56. Reddy, S. T., Swartz, M. A. & Hubbell, J. A. Targeting dendritic cells with biomaterials: developing the next generation of vaccines. *Trends Immunol.* **27,** 573–579 (2006).
57. Shokouhi, B. *et al.* The role of multiple toll-like receptor signalling cascades on interactions between biomedical polymers and dendritic cells. *Biomaterials* **31,** 5759–5771 (2010).
58. Rogers, T. H. & Babensee, J. E. The role of integrins in the recognition and response of dendritic cells to biomaterials. *Biomaterials* **32,** 1270–1279 (2011).
59. Acharya, A. P., Dolgova, N. V., Clare-Salzler, M. J. & Keselowsky, B. G. Adhesive substrate-modulation of adaptive immune responses. *Biomaterials* **29,** 4736–4750 (2008).
60. Kawai, T. & Akira, S. TLR signaling. *Cell Death Differ* **13,** 816–825 (2006).
61. Chun, K.-H. & Seong, S.-Y. CD14 but not MD2 transmit signals from DAMP. *International Immunopharmacology* **10,** 98–106 (2010).
62. Gill, R., Tsung, A. & Billiar, T. Linking oxidative stress to inflammation: Toll-like receptors. *Free Radical Biology and Medicine* **48,** 1121–1132 (2010).
63. Van Vliet, S. J., den Dunnen, J., Gringhuis, S. I., Geijtenbeek, T. B. & van Kooyk, Y. Innate signaling and regulation of Dendritic cell immunity. *Curr. Opin. Immunol* **19,** 435–440 (2007).
64. Kenneth Murphy, Paul Travers & Walport, M. *Janeway's Immunobiology*. (Garland Science, 2009). at <http://www.garlandscience.com/textbooks/0815341237.asp>
65. Pasare, C. & Medzhitov, R. Toll-like receptors and acquired immunity. *Semin. Immunol* **16,** 23–26 (2004).
66. Shen, H., Tesar, B. M., Walker, W. E. & Goldstein, D. R. Dual signaling of MyD88 and TRIF is critical for maximal TLR4-induced dendritic cell maturation. *J. Immunol* **181,** 1849–1858 (2008).
67. Thomas, P. G. *et al.* Maturation of dendritic cell 2 phenotype by a helminth glycan uses a Toll-like receptor 4-dependent mechanism. *J. Immunol* **171,** 5837–5841 (2003).
68. Kleinman, M. E. *et al.* Sequence- and target-independent angiogenesis suppression by siRNA via TLR3. *Nature* **452,** 591–597 (2008).

69. Kaisho, T. & Akira, S. Toll-like receptors and their signaling mechanism in innate immunity. *Acta Odontol. Scand* **59,** 124–130 (2001).
70. Kriehuber, E. *et al.* Balance between NF-{kappa}B and JNK/AP-1 activity controls dendritic cell life and death. *Blood* **106,** 175–183 (2005).
71. Ip, W. K. E., Takahashi, K., Ezekowitz, R. A. & Stuart, L. M. Mannose-binding lectin and innate immunity. *Immunol. Rev* **230,** 9–21 (2009).
72. Brown, G. D. Dectin-1: a signalling non-TLR pattern-recognition receptor. *Nat. Rev. Immunol* **6,** 33–43 (2006).
73. Cambi, A. & Figdor, C. Necrosis: C-Type Lectins Sense Cell Death. *Current Biology* **19,** R375–R378 (2009).
74. Hollmig, S. T., Ariizumi, K. & Cruz, P. D. Recognition of non-self-polysaccharides by C-type lectin receptors dectin-1 and dectin-2. *Glycobiology* **19,** 568–575 (2009).
75. Van Stijn, C. M. W. *et al.* Schistosoma mansoni worm glycolipids induce an inflammatory phenotype in human dendritic cells by cooperation of TLR4 and DC-SIGN. *Molecular Immunology* **47,** 1544–1552 (2010).
76. Gringhuis, S. I. *et al.* Dectin-1 directs T helper cell differentiation by controlling noncanonical NF-[kappa]B activation through Raf-1 and Syk. *Nat Immunol* **10,** 203–213 (2009).
77. Nonaka, M. *et al.* Glycosylation-dependent interactions of C-type lectin DC-SIGN with colorectal tumor-associated Lewis glycans impair the function and differentiation of monocyte-derived dendritic cells. *J. Immunol* **180,** 3347–3356 (2008).
78. Van Vliet, S. J. *et al.* Carbohydrate profiling reveals a distinctive role for the C-type lectin MGL in the recognition of helminth parasites and tumor antigens by dendritic cells. *Int. Immunol.* **17,** 661–669 (2005).
79. Figdor, C. G., van Kooyk, Y. & Adema, G. J. C-type lectin receptors on dendritic cells and Langerhans cells. *Nat. Rev. Immunol* **2,** 77–84 (2002).
80. Gabius, H.-J. Cell Surface Glycans: The Why and How of Their Functionality as Biochemical Signals in Lectin-Mediated Information Transfer. *Critical Reviews in Immunology* **6,** 43–80 (2006).
81. Van Vliet, S. J., García-Vallejo, J. J. & van Kooyk, Y. Dendritic cells and C-type lectin receptors: coupling innate to adaptive immune responses. *Immunol. Cell Biol* **86,** 580–587 (2008).
82. Sancho, D. & Reis e Sousa, C. Signaling by Myeloid C-Type Lectin Receptors in Immunity and Homeostasis. *Annual Review of Immunology* **30,** 491–529 (2012).
83. Stamenkovic, I., Sgroi, D., Aruffo, A., Sy, M. S. & Anderson, T. The B lymphocyte adhesion molecule CD22 interacts with leukocyte common antigen CD45RO on T cells and alpha 2-6 sialyltransferase, CD75, on B cells. *Cell* **66,** 1133–1144 (1991).
84. Pillai, S., Netravali, I. A., Cariappa, A. & Mattoo, H. Siglecs and Immune Regulation. *Annual Review of Immunology* **30,** 357–392 (2012).
85. Doody, G. M. *et al.* A role in B cell activation for CD22 and the protein tyrosine phosphatase SHP. *Science* **269,** 242–244 (1995).
86. Taylor, V. C. *et al.* The myeloid-specific sialic acid-binding receptor, CD33, associates with the protein-tyrosine phosphatases, SHP-1 and SHP-2. *J. Biol. Chem.* **274,** 11505–11512 (1999).

87. Crocker, P. R., Paulson, J. C. & Varki, A. Siglecs and their roles in the immune system. *Nat Rev Immunol* **7,** 255–266 (2007).
88. Cao, H. *et al.* SIGLEC16 encodes a DAP12-associated receptor expressed in macrophages that evolved from its inhibitory counterpart SIGLEC11 and has functional and non-functional alleles in humans. *Eur. J. Immunol.* **38,** 2303–2315 (2008).
89. Angata, T., Tabuchi, Y., Nakamura, K. & Nakamura, M. Siglec-15: an immune system Siglec conserved throughout vertebrate evolution. *Glycobiology* **17,** 838–846 (2007).
90. Angata, T., Hayakawa, T., Yamanaka, M., Varki, A. & Nakamura, M. Discovery of Siglec-14, a novel sialic acid receptor undergoing concerted evolution with Siglec-5 in primates. *FASEB J.* **20,** 1964–1973 (2006).
91. Cao, H. & Crocker, P. R. Evolution of CD33-related siglecs: regulating host immune functions and escaping pathogen exploitation? *Immunology* **132,** 18–26 (2011).
92. Pinheiro da Silva, F., Aloulou, M., Benhamou, M. & Monteiro, R. C. Inhibitory ITAMs: a matter of life and death. *Trends Immunol.* **29,** 366–373 (2008).
93. Blank, U., Launay, P., Benhamou, M. & Monteiro, R. C. Inhibitory ITAMs as novel regulators of immunity. *Immunol. Rev.* **232,** 59–71 (2009).
94. Cambi, A., Koopman, M. & Figdor, C. G. How C-type lectins detect pathogens. *Cell. Microbiol* **7,** 481–488 (2005).
95. Meyer-Wentrup, F. *et al.* DCIR is endocytosed into human dendritic cells and inhibits TLR8-mediated cytokine production. *Journal of Leukocyte Biology* **85,** 518 – 525 (2009).
96. Petzold, C., Riewaldt, J., Koenig, T., Schallenberg, S. & Kretschmer, K. Dendritic Cell-Targeted Pancreatic β-Cell Antigen Leads to Conversion of Self-Reactive CD4+ T Cells Into Regulatory T Cells and Promotes Immunotolerance in NOD Mice. *Rev Diabet Stud* **7,** 47–61 (2010).
97. Chen, C.-H. *et al.* Dendritic-cell-associated C-type lectin 2 (DCAL-2) alters dendritic-cell maturation and cytokine production. *Blood* **107,** 1459 –1467 (2006).
98. Carter, R. W., Thompson, C., Reid, D. M., Wong, S. Y. C. & Tough, D. F. Preferential Induction of CD4+ T Cell Responses through In Vivo Targeting of Antigen to Dendritic Cell-Associated C-Type Lectin-1. *The Journal of Immunology* **177,** 2276 –2284 (2006).
99. Bandyopadhyay, A., Fine, R. L., Demento, S., Bockenstedt, L. K. & Fahmy, T. M. The impact of nanoparticle ligand density on dendritic-cell targeted vaccines. *Biomaterials* **32,** 3094–3105 (2011).
100. O'Reilly, M. K. & Paulson, J. C. Siglecs as targets for therapy in immune-cell-mediated disease. *Trends in Pharmacological Sciences* **30,** 240–248 (2009).
101. Disney, M. D. & Seeberger, P. H. The Use of Carbohydrate Microarrays to Study Carbohydrate-Cell Interactions and to Detect Pathogens. *Chemistry & Biology* **11,** 1701–1707 (2004).
102. Zhang, Y., Li, Q., Rodriguez, L. G. & Gildersleeve, J. C. An Array-Based Method to Identify Multivalent Inhibitors. *J Am Chem Soc* **132,** 9653–9662 (2010).
103. Busch, J., McBride, R. & Head, S. R. Production and application of glycan microarrays. *Methods Mol. Biol* **632,** 269–282 (2010).

104. Taylor, M. E. & Drickamer, K. Structural insights into what glycan arrays tell us about how glycan-binding proteins interact with their ligands. *Glycobiology* **19,** 1155–1162 (2009).
105. Katrlík, J., Svitel, J., Gemeiner, P., Kozár, T. & Tkac, J. Glycan and lectin microarrays for glycomics and medicinal applications. *Med Res Rev* **30,** 394–418 (2010).
106. Liang, C.-H. & Wu, C.-Y. Glycan array: a powerful tool for glycomics studies. *Expert Rev Proteomics* **6,** 631–645 (2009).
107. Wattendorf, U., Coullerez, G., Vörös, J., Textor, M. & Merkle, H. P. Mannose-Based Molecular Patterns on Stealth Microspheres for Receptor-Specific Targeting of Human Antigen-Presenting Cells. *Langmuir* **24,** 11790–11802 (2008).
108. Cui, Z., Han, S.-J. & Huang, L. Coating of Mannan on LPD Particles Containing HPV E7 Peptide Significantly Enhances Immunity Against HPV-Positive Tumor. *Pharmaceutical Research* **21,** 1018–1025 (2004).
109. Faraasen, S. *et al.* Ligand-specific targeting of microspheres to phagocytes by surface modification with poly(L-lysine)-grafted poly(ethylene glycol) conjugate. *Pharm. Res.* **20,** 237–246 (2003).
110. Saeland, E. *et al.* The C-type lectin MGL expressed by dendritic cells detects glycan changes on MUC1 in colon carcinoma. *Cancer Immunology, Immunotherapy* **56,** 1225–1236 (2006).
111. Kamphorst, A. O., Guermonprez, P., Dudziak, D. & Nussenzweig, M. C. Route of Antigen Uptake Differentially Impacts Presentation by Dendritic Cells and Activated Monocytes. *The Journal of Immunology* **185,** 3426 –3435 (2010).
112. Le Cabec, V., Emorine, L. J., Toesca, I., Cougoule, C. & Maridonneau-Parini, I. The human macrophage mannose receptor is not a professional phagocytic receptor. *Journal of Leukocyte Biology* **77,** 934 –943 (2005).
113. Geijtenbeek, T. B. . *et al.* Identification of DC-SIGN, a Novel Dendritic Cell–Specific ICAM-3 Receptor that Supports Primary Immune Responses. *Cell* **100,** 575–585 (2000).
114. Cambi, A. *et al.* Dendritic cell interaction with Candida albicans critically depends on N-linked mannan. *J. Biol. Chem* **283,** 20590–20599 (2008).
115. Kiessling, L. L. & Pohl, N. L. Strength in numbers: non-natural polyvalent carbohydrate derivatives. *Chemistry & Biology* **3,** 71–77 (1996).
116. Dutta, T. & Jain, N. K. Targeting potential and anti-HIV activity of lamivudine loaded mannosylated poly (propyleneimine) dendrimer. *Biochimica et Biophysica Acta (BBA) - General Subjects* **1770,** 681–686 (2007).
117. Agrawal, P., Gupta, U. & Jain, N. K. Glycoconjugated peptide dendrimers-based nanoparticulate system for the delivery of chloroquine phosphate. *Biomaterials* **28,** 3349–3359 (2007).
118. Hsu, D. K. *et al.* Endogenous galectin-3 is localized in membrane lipid rafts and regulates migration of dendritic cells. *J. Invest. Dermatol* **129,** 573–583 (2009).
119. García-Vallejo, J. J. *et al.* DC-SIGN mediates adhesion and rolling of dendritic cells on primary human umbilical vein endothelial cells through LewisY antigen expressed on ICAM-2. *Mol. Immunol* **45,** 2359–2369 (2008).

120. Engering, A. *et al.* The Dendritic Cell-Specific Adhesion Receptor DC-SIGN Internalizes Antigen for Presentation to T Cells. *The Journal of Immunology* **168,** 2118 –2126 (2002).
121. Hawiger, D. *et al.* Dendritic Cells Induce Peripheral T Cell Unresponsiveness under Steady State Conditions in Vivo. *The Journal of Experimental Medicine* **194,** 769 –780 (2001).
122. Bonifaz, L. *et al.* Efficient Targeting of Protein Antigen to the Dendritic Cell Receptor DEC-205 in the Steady State Leads to Antigen Presentation on Major Histocompatibility Complex Class I Products and Peripheral CD8+ T Cell Tolerance. *The Journal of Experimental Medicine* **196,** 1627 –1638 (2002).
123. Bonifaz, L. C. *et al.* In Vivo Targeting of Antigens to Maturing Dendritic Cells via the DEC-205 Receptor Improves T Cell Vaccination. *The Journal of Experimental Medicine* **199,** 815 –824 (2004).
124. Chieppa, M. *et al.* Cross-Linking of the Mannose Receptor on Monocyte-Derived Dendritic Cells Activates an Anti-Inflammatory Immunosuppressive Program. *The Journal of Immunology* **171,** 4552 –4560 (2003).
125. Demangel, C. *et al.* Single chain antibody fragments for the selective targeting of antigens to dendritic cells. *Molecular Immunology* **42,** 979–985 (2005).
126. Tacken, P. J. *et al.* Effective induction of naive and recall T-cell responses by targeting antigen to human dendritic cells via a humanized anti–DC-SIGN antibody. *Blood* **106,** 1278 –1285 (2005).
127. Ryan, E. J., Magaletti, D., Draves, K. E. & Clark, E. A. Ligation of dendritic cell–associated lectin–1 induces partial maturation of human monocyte derived dendritic cells. *Human Immunology* **70,** 1–5 (2009).
128. Caminschi, I. *et al.* The dendritic cell subtype-restricted C-type lectin Clec9A is a target for vaccine enhancement. *Blood* **112,** 3264 –3273 (2008).
129. Sancho, D. *et al.* Identification of a dendritic cell receptor that couples sensing of necrosis to immunity. *Nature* **458,** 899–903 (2009).
130. Richard, M., Thibault, N., Veilleux, P., Gareau-Pagé, G. & Beaulieu, A. D. Granulocyte macrophage-colony stimulating factor reduces the affinity of SHP-2 for the ITIM of CLECSF6 in neutrophils: A new mechanism of action for SHP-2. *Molecular Immunology* **43,** 1716–1721 (2006).
131. Svajger, U., Anderluh, M., Jeras, M. & Obermajer, N. C-type lectin DC-SIGN: An adhesion, signalling and antigen-uptake molecule that guides dendritic cells in immunity. *Cellular Signalling* **22,** 1397–1405 (2010).
132. Gringhuis, S. I. & Geijtenbeek, T. B. H. in *Glycobiology* **Volume 480,** 151–164 (Academic Press, 2010).
133. Singh, S. K. *et al.* Targeting glycan modified OVA to murine DC-SIGN transgenic dendritic cells enhances MHC class I and II presentation. *Molecular Immunology* **47,** 164–174 (2009).
134. De Jong, M. A. W. P., de Witte, L., Bolmstedt, A., van Kooyk, Y. & Geijtenbeek, T. B. H. Dendritic cells mediate herpes simplex virus infection and transmission through the C-type lectin DC-SIGN. *J. Gen. Virol* **89,** 2398–2409 (2008).
135. Vu-Quang, H. *et al.* Targeted delivery of mannan-coated superparamagnetic iron oxide nanoparticles to antigen-presenting cells for magnetic resonance-based

diagnosis of metastatic lymph nodes in vivo. *Acta Biomaterialia* **7,** 3935–3945 (2011).
136. Lucas, A. H., Apicella, M. A. & Taylor, C. E. Carbohydrate Moieties as Vaccine Candidates. *Clinical Infectious Diseases* **41,** 705 –712 (2005).
137. Gringhuis, S. I. *et al.* C-type lectin DC-SIGN modulates Toll-like receptor signaling via Raf-1 kinase-dependent acetylation of transcription factor NF-kappaB. *Immunity* **26,** 605–616 (2007).
138. Agrawal, S. *et al.* Cutting Edge: Different Toll-Like Receptor Agonists Instruct Dendritic Cells to Induce Distinct Th Responses via Differential Modulation of Extracellular Signal-Regulated Kinase-Mitogen-Activated Protein Kinase and c-Fos. *J Immunol* **171,** 4984–4989 (2003).
139. Shreffler, W. G. *et al.* The Major Glycoprotein Allergen from Arachis hypogaea, Ara h 1, Is a Ligand of Dendritic Cell-Specific ICAM-Grabbing Nonintegrin and Acts as a Th2 Adjuvant In Vitro. *J Immunol* **177,** 3677–3685 (2006).
140. Caparrós, E. *et al.* DC-SIGN ligation on dendritic cells results in ERK and PI3K activation and modulates cytokine production. *Blood* **107,** 3950–3958 (2006).
141. Arrighi, J.-F. *et al.* Lentivirus-Mediated RNA Interference of DC-SIGN Expression Inhibits Human Immunodeficiency Virus Transmission from Dendritic Cells to T Cells. *J Virol* **78,** 10848–10855 (2004).
142. Richard, M., Thibault, N., Veilleux, P., Gareau-Pagé, G. & Beaulieu, A. D. Granulocyte macrophage-colony stimulating factor reduces the affinity of SHP-2 for the ITIM of CLECSF6 in neutrophils: A new mechanism of action for SHP-2. *Molecular Immunology* **43,** 1716–1721 (2006).
143. Marshall, A. S. J. *et al.* Identification and Characterization of a Novel Human Myeloid Inhibitory C-type Lectin-like Receptor (MICL) That Is Predominantly Expressed on Granulocytes and Monocytes. *Journal of Biological Chemistry* **279,** 14792–14802 (2004).
144. Bates, E. E. M. *et al.* APCs Express DCIR, a Novel C-Type Lectin Surface Receptor Containing an Immunoreceptor Tyrosine-Based Inhibitory Motif. *J Immunol* **163,** 1973–1983 (1999).
145. Paul R, C. Siglecs: sialic-acid-binding immunoglobulin-like lectins in cell–cell interactions and signalling. *Current Opinion in Structural Biology* **12,** 609–615 (2002).
146. Hajishengallis, G. & Lambris, J. D. Microbial manipulation of receptor crosstalk in innate immunity. *Nat Rev Immunol* **11,** 187–200 (2011).
147. Ikehara, Y., Ikehara, S. K. & Paulson, J. C. Negative Regulation of T Cell Receptor Signaling by Siglec-7 (p70/AIRM) and Siglec-9. *Journal of Biological Chemistry* **279,** 43117 –43125 (2004).
148. Paul, S. P., Taylor, L. S., Stansbury, E. K. & McVicar, D. W. Myeloid specific human CD33 is an inhibitory receptor with differential ITIM function in recruiting the phosphatases SHP-1 and SHP-2. *Blood* **96,** 483 –490 (2000).
149. Rogers, N. C. *et al.* Syk-dependent cytokine induction by Dectin-1 reveals a novel pattern recognition pathway for C type lectins. *Immunity* **22,** 507–517 (2005).
150. Gross, O. *et al.* Card9 controls a non-TLR signalling pathway for innate anti-fungal immunity. *Nature* **442,** 651–656 (2006).

151. Underhill, D. M., Rossnagle, E., Lowell, C. A. & Simmons, R. M. Dectin-1 activates Syk tyrosine kinase in a dynamic subset of macrophages for reactive oxygen production. *Blood* **106,** 2543 –2550 (2005).
152. Claudio, E., Brown, K., Park, S., Wang, H. & Siebenlist, U. BAFF-induced NEMO-independent processing of NF-[kappa]B2 in maturing B cells. *Nat Immunol* **3,** 958–965 (2002).
153. Dejardin, E. *et al.* The Lymphotoxin-[beta] Receptor Induces Different Patterns of Gene Expression via Two NF-[kappa]B Pathways. *Immunity* **17,** 525–535 (2002).
154. Brown, G. D. *et al.* Dectin-1 Mediates the Biological Effects of β-Glucans. *The Journal of Experimental Medicine* **197,** 1119 –1124 (2003).
155. Gantner, B. N., Simmons, R. M., Canavera, S. J., Akira, S. & Underhill, D. M. Collaborative Induction of Inflammatory Responses by Dectin-1 and Toll-like Receptor 2. *The Journal of Experimental Medicine* **197,** 1107 –1117 (2003).
156. Sato, K. *et al.* Dectin-2 Is a Pattern Recognition Receptor for Fungi That Couples with the Fc Receptor γ Chain to Induce Innate Immune Responses. *Journal of Biological Chemistry* **281,** 38854 –38866 (2006).
157. Robinson, M. J. *et al.* Dectin-2 is a Syk-coupled pattern recognition receptor crucial for Th17 responses to fungal infection. *The Journal of Experimental Medicine* **206,** 2037 –2051 (2009).
158. Barrett, N. A., Maekawa, A., Rahman, O. M., Austen, K. F. & Kanaoka, Y. Dectin-2 Recognition of House Dust Mite Triggers Cysteinyl Leukotriene Generation by Dendritic Cells. *The Journal of Immunology* **182,** 1119 –1128 (2009).
159. Kirchberger, S. *et al.* Human Rhinoviruses Inhibit the Accessory Function of Dendritic Cells by Inducing Sialoadhesin and B7-H1 Expression. *The Journal of Immunology* **175,** 1145 –1152 (2005).
160. Bax, M. *et al.* Campylobacter jejuni Lipooligosaccharides Modulate Dendritic Cell-Mediated T Cell Polarization in a Sialic Acid Linkage-Dependent Manner. *Infect. Immun.* **79,** 2681–2689 (2011).
161. Kanazawa, N., Tashiro, K. & Miyachi, Y. Signaling and immune regulatory role of the dendritic cell immunoreceptor (DCIR) family lectins: DCIR, DCAR, dectin-2 and BDCA-2. *Immunobiology* **209,** 179–190 (2004).
162. Tjomsland, V. *et al.* Complement Opsonization of HIV-1 Enhances the Uptake by Dendritic Cells and Involves the Endocytic Lectin and Integrin Receptor Families. *PLoS ONE* **6,** e23542 (2011).
163. East, L. & Isacke, C. M. The mannose receptor family. *Biochimica et Biophysica Acta (BBA) - General Subjects* **1572,** 364–386 (2002).
164. Mammen, M., Choi, S.-K. & Whitesides, G. M. Polyvalent Interactions in Biological Systems: Implications for Design and Use of Multivalent Ligands and Inhibitors. *Angewandte Chemie International Edition* **37,** 2754–2794 (1998).
165. Belitsky, J. M., Nelson, A., Hernandez, J. D., Baum, L. G. & Stoddart, J. F. Multivalent interactions between lectins and supramolecular complexes: Galectin-1 and self-assembled pseudopolyrotaxanes. *Chem. Biol.* **14,** 1140–1151 (2007).
166. Marón, L. B. *et al.* LUVs recovered with Chitosan: a new preparation for vaccine delivery. *J Liposome Res* **17,** 155–163 (2007).

167. Kang, M. L. *et al.* Pluronic F127 enhances the effect as an adjuvant of chitosan microspheres in the intranasal delivery of Bordetella bronchiseptica antigens containing dermonecrotoxin. *Vaccine* **25,** 4602–4610 (2007).
168. Aarnoudse, C. A., Bax, M., Sánchez-Hernández, M., García-Vallejo, J. J. & van Kooyk, Y. Glycan modification of the tumor antigen gp100 targets DC-SIGN to enhance dendritic cell induced antigen presentation to T cells. *Int. J. Cancer* **122,** 839–846 (2008).
169. Adams, E. W., Ratner, D. M., Seeberger, P. H. & Hacohen, N. Carbohydrate-mediated targeting of antigen to dendritic cells leads to enhanced presentation of antigen to T cells. *Chembiochem* **9,** 294–303 (2008).
170. Zhou, X. *et al.* Enhance immune response to DNA vaccine based on a novel multicomponent supramolecular assembly. *Biomaterials* **28,** 4684–4692 (2007).
171. Sheng, K.-C. *et al.* Delivery of antigen using a novel mannosylated dendrimer potentiates immunogenicity in vitro and in vivo. *Eur. J. Immunol.* **38,** 424–436 (2008).
172. Lu, Y., Kawakami, S., Yamashita, F. & Hashida, M. Development of an antigen-presenting cell-targeted DNA vaccine against melanoma by mannosylated liposomes. *Biomaterials* **28,** 3255–3262 (2007).
173. Valenzuela, H. F. *et al.* O-glycosylation regulates LNCaP prostate cancer cell susceptibility to apoptosis induced by galectin-1. *Cancer Res.* **67,** 6155–6162 (2007).
174. Sanders, R. W. *et al.* The carbohydrate at asparagine 386 on HIV-1 gp120 is not essential for protein folding and function but is involved in immune evasion. *Retrovirology* **5,** 10 (2008).
175. Lindhorst, T. K. *Essentials of Carbohydrate Chemistry and Biochemistry*. (Wiley-VCH, 2007).
176. Ajit Varki, R. D. C. Essentials of Glycobiology. (2009). at <http://www.ncbi.nlm.nih.gov.www.library.gatech.edu:2048/books/NBK1908/>
177. Cummings, R. D. The repertoire of glycan determinants in the human glycome. *Mol. BioSyst.* **5,** 1087–1104 (2009).
178. Yu, Y. Q., Fournier, J., Gilar, M. & Gebler, J. C. Identification of N-Linked Glycosylation Sites Using Glycoprotein Digestion with Pronase Prior to MALDI Tandem Time-of-Flight Mass Spectrometry. *Analytical Chemistry* **79,** 1731–1738 (2007).
179. Jefcoat, A. M. *et al.* Persistent mucin glycoprotein alterations in equine recurrent airway obstruction. *Am. J. Physiol. Lung Cell Mol. Physiol* **281,** L704–712 (2001).
180. Song, X., Lasanajak, Y., Xia, B., Smith, D. F. & Cummings, R. D. Fluorescent Glycosylamides Produced by Microscale Derivatization of Free Glycans for Natural Glycan Microarrays. *ACS Chemical Biology* **4,** 741–750 (2009).
181. Chong, P. *et al.* A strategy for rational design of fully synthetic glycopeptide conjugate vaccines. *Infect. Immun* **65,** 4918–4925 (1997).
182. Lepenies, B., Yin, J. & Seeberger, P. H. Applications of synthetic carbohydrates to chemical biology. *Current Opinion in Chemical Biology* **In Press, Corrected Proof,**
183. Pavlovic, D. *et al.* Chemically synthesized solid phase oligosaccharide probes for carbohydrate-binding receptors. Interactions of the E-, L- and P-selectins with sialyl-

Le(x) and O-sulphated forms linked to biotin or to polyacrylamide. *J. Immunol. Methods* **264,** 53–58 (2002).
184. Lepenies, B. & Seeberger, P. H. The promise of glycomics, glycan arrays and carbohydrate-based vaccines. *Immunopharmacology and Immunotoxicology* **32,** 196–207 (2010).
185. Diallo, J.-S. *et al.* A high-throughput pharmacoviral approach identifies novel oncolytic virus sensitizers. *Mol. Ther* **18,** 1123–1129 (2010).
186. Flaberg, E. *et al.* High throughput live cell imaging reveals differential inhibition of tumor cell proliferation by human fibroblasts. *Int J Cancer* (2010). doi:10.1002/ijc.25612
187. Acharya, A. P. *et al.* The modulation of dendritic cell integrin binding and activation by RGD-peptide density gradient substrates. *Biomaterials* **31,** 7444–7454 (2010).
188. VanderVen, B. C. *et al.* Development of a novel, cell-based chemical screen to identify inhibitors of intraphagosomal lipolysis in macrophages. *Cytometry A* **77,** 751–760 (2010).
189. Acharya, A. P., Clare-Salzler, M. J. & Keselowsky, B. G. A high-throughput microparticle microarray platform for dendritic cell-targeting vaccines. *Biomaterials* **30,** 4168–4177 (2009).
190. Wiggins, H. & Rappoport, J. An agarose spot assay for chemotactic invasion. *BioTechniques* **48,** 121–124 (2010).
191. Sempere, L. F. *et al.* Fluorescence-based codetection with protein markers reveals distinct cellular compartments for altered MicroRNA expression in solid tumors. *Clin. Cancer Res* **16,** 4246–4255 (2010).
192. Mu, Y. *et al.* Transcriptome and expression profiling analysis revealed changes of multiple signaling pathways involved in immunity in the large yellow croaker during Aeromonas hydrophila infection. *BMC Genomics* **11,** 506 (2010).
193. Zornetzer, G. A. *et al.* Transcriptomic Analysis Reveals a Mechanism for a Prefibrotic Phenotype in STAT1 Knockout Mice during Severe Acute Respiratory Syndrome Coronavirus Infection. *J. Virol* **84,** 11297–11309 (2010).
194. Somboonwiwat, K., Chaikeeratisak, V., Wang, H.-C., Fang Lo, C. & Tassanakajon, A. Proteomic analysis of differentially expressed proteins in Penaeus monodon hemocytes after Vibrio harveyi infection. *Proteome Sci* **8,** 39 (2010).
195. Taylor, J. & Ussher, J. E. Optimized Transduction of Human Monocyte-Derived Dendritic Cells by Recombinant Adeno-Associated Virus Serotype 6 (rAAV6). *Hum Gene Ther* (2010). doi:10.1089/hum.2010.087
196. Bowles, R., Patil, S., Pincas, H. & Sealfon, S. C. Validation of efficient high-throughput plasmid and siRNA transfection of human monocyte-derived dendritic cells without cell maturation. *J Immunol Methods* (2010). doi:10.1016/j.jim.2010.09.028
197. Zhu, J. *et al.* High-throughput screening for TLR3-IFN regulatory factor 3 signaling pathway modulators identifies several antipsychotic drugs as TLR inhibitors. *J. Immunol* **184,** 5768–5776 (2010).
198. Osmond, R. I. W., Das, S. & Crouch, M. F. Development of cell-based assays for cytokine receptor signaling, using an AlphaScreen SureFire assay format. *Anal. Biochem* **403,** 94–101 (2010).

199. Srivastava, N. *et al.* Fully integrated microfluidic platform enabling automated phosphoprofiling of macrophage response. *Anal. Chem* **81,** 3261–3269 (2009).
200. Oyelaran, O., Li, Q., Farnsworth, D. & Gildersleeve, J. C. Microarrays with Varying Carbohydrate Density Reveal Distinct Subpopulations of Serum Antibodies. *Journal of Proteome Research* **8,** 3529–3538 (2009).
201. Tao, S.-C. *et al.* Lectin microarrays identify cell-specific and functionally significant cell surface glycan markers. *Glycobiology* **18,** 761–769 (2008).
202. Blixt, O. *et al.* Sialoside analogue arrays for rapid identification of high affinity siglec ligands. *J. Am. Chem. Soc* **130,** 6680–6681 (2008).
203. Ardeshna, K. M. *et al.* Monocyte-derived dendritic cells do not proliferate and are not susceptible to retroviral transduction. *Br. J. Haematol* **108,** 817–824 (2000).
204. Yoshida, M. & Babensee, J. E. Molecular aspects of microparticle phagocytosis by dendritic cells. *J Biomater Sci Polym Ed* **17,** 893–907 (2006).
205. Zupke, O. *et al.* Preservation of dendritic cell function upon labeling with amino functionalized polymeric nanoparticles. *Biomaterials* **31,** 7086–7095 (2010).
206. Burns, S. *et al.* Maturation of DC is associated with changes in motile characteristics and adherence. *Cell Motil. Cytoskeleton* **57,** 118–132 (2004).
207. Acharya, A. P., Dolgova, N. V., Clare-Salzler, M. J. & Keselowsky, B. G. Adhesive substrate-modulation of adaptive immune responses. *Biomaterials* **29,** 4736–4750 (2008).
208. Jain, S. & Vyas, S. P. Mannosylated Niosomes as Adjuvant-Carrier System for Oral Mucosal Immunization. *Journal of Liposome Research* **16,** 331–345 (2006).
209. Apostolopoulos, V. *et al.* Pilot phase III immunotherapy study in early-stage breast cancer patients using oxidized mannan-MUC1 [ISRCTN71711835]. *Breast Cancer Res* **8,** R27–R27 (2006).
210. Song, X. *et al.* Novel fluorescent glycan microarray strategy reveals ligands for galectins. *Chem. Biol* **16,** 36–47 (2009).
211. Ratner, D. M. *et al.* Probing Protein-Carbohydrate Interactions with Microarrays of Synthetic Oligosaccharides. *ChemBioChem* **5,** 379–383 (2004).
212. Disney, M. D. & Seeberger, P. H. The Use of Carbohydrate Microarrays to Study Carbohydrate-Cell Interactions and to Detect Pathogens. *Chemistry & Biology* **11,** 1701–1707 (2004).
213. Taylor, M. E. & Drickamer, K. Structural insights into what glycan arrays tell us about how glycan-binding proteins interact with their ligands. *Glycobiology* **19,** 1155–1162 (2009).
214. Yeeprae, W., Kawakami, S., Yamashita, F. & Hashida, M. Effect of mannose density on mannose receptor-mediated cellular uptake of mannosylated O/W emulsions by macrophages. *Journal of Controlled Release* **114,** 193–201 (2006).
215. White, K. L., Rades, T., Furneaux, R. H., Tyler, P. C. & Hook, S. Mannosylated liposomes as antigen delivery vehicles for targeting to dendritic cells. *Journal of Pharmacy and Pharmacology* **58,** 729–737 (2006).
216. Fotin-Mleczek, M. *et al.* Messenger RNA-based vaccines with dual activity induce balanced TLR-7 dependent adaptive immune responses and provide antitumor activity. *J. Immunother.* **34,** 1–15 (2011).

217. Zhang, T. *et al.* Generation and characterization of a fusion protein of single-chain fragment variable antibody against hemagglutinin antigen of avian influenza virus and truncated protamine. *Vaccine* **28,** 3949–3955 (2010).
218. Martínez Gómez, J. M. *et al.* A protective allergy vaccine based on CpG- and protamine-containing PLGA microparticles. *Pharm. Res.* **24,** 1927–1935 (2007).
219. Okada, H. Brain tumor immunotherapy with type-1 polarizing strategies. *Ann. N. Y. Acad. Sci.* **1174,** 18–23 (2009).
220. Jun, Y. J. *et al.* A tetra(L-lysine)-grafted poly(organophosphazene) for gene delivery. *Bioorg. Med. Chem. Lett.* **17,** 2975–2978 (2007).
221. Maubant, S., Banissi, C., Beck, S., Chauvat, A. & Carpentier, A. F. Adjuvant properties of Cytosine-phosphate-guanosine oligodeoxynucleotide in combination with various polycations in an ovalbumin-vaccine model. *Nucleic Acid Ther* **21,** 231–240 (2011).
222. Midoux, P., Breuzard, G., Gomez, J. P. & Pichon, C. Polymer-based gene delivery: a current review on the uptake and intracellular trafficking of polyplexes. *Curr Gene Ther* **8,** 335–352 (2008).
223. André, S. *et al.* Phenylenediamine-based bivalent glycocyclophanes: synthesis and analysis of the influence of scaffold rigidity and ligand spacing on lectin binding in cell systems with different glycomic profiles. *Org. Biomol. Chem.* **7,** 4715–4725 (2009).
224. Kou, P. M. & Babensee, J. E. Validation of a high-throughput methodology to assess the effects of biomaterials on dendritic cell phenotype. *Acta Biomaterialia* **6,** 2621–2630 (2010).
225. Qi, C. *et al.* Differential pathways regulating innate and adaptive antitumor immune responses by particulate and soluble yeast-derived β-glucans. *Blood* **117,** 6825 –6836 (2011).
226. Greatrex, B. W. *et al.* The synthesis and immune stimulating action of mannose-capped lysine-based dendrimers. *Tetrahedron* **65,** 2939–2950 (2009).
227. Rughetti, A. *et al.* Recombinant Tumor-Associated MUC1 Glycoprotein Impairs the Differentiation and Function of Dendritic Cells. *The Journal of Immunology* **174,** 7764 –7772 (2005).
228. Carlos, C. A. *et al.* Human Tumor Antigen MUC1 Is Chemotactic for Immature Dendritic Cells and Elicits Maturation but Does Not Promote Th1 Type Immunity. *The Journal of Immunology* **175,** 1628 –1635 (2005).
229. Napoletano, C. *et al.* Tumor-Associated Tn-MUC1 Glycoform Is Internalized through the Macrophage Galactose-Type C-Type Lectin and Delivered to the HLA Class I and II Compartments in Dendritic Cells. *Cancer Research* **67,** 8358 –8367 (2007).
230. Traut, R. R. *et al.* Methyl 4-mercaptobutyrimidate as a cleavable cross-linking reagent and its application to the Escherichia coli 30S ribosome. *Biochemistry* **12,** 3266–3273 (1973).
231. Oda, Y., Nagasu, T. & Chait, B. T. Enrichment analysis of phosphorylated proteins as a tool for probing the phosphoproteome. *Nature Biotechnology* **19,** 379–382 (2001).

232. Fukuda, M. in *Current Protocols in Molecular Biology* (John Wiley & Sons, Inc., 2001). at <http://onlinelibrary.wiley.com/doi/10.1002/0471142727.mb1705s26/abstract>
233. Romani, N. *et al.* Proliferating dendritic cell progenitors in human blood. *J. Exp. Med.* **180,** 83–93 (1994).
234. Manavalan, J. S. *et al.* High expression of ILT3 and ILT4 is a general feature of tolerogenic dendritic cells. *Transplant Immunology* **11,** 245–258 (2003).
235. MacCoubrey, I., Moore, P. & Haugland, R. Quantitative fluorescence measurements of cell viability (cytotoxicity) with a multi-well plate scanner. J. Cell Biol. 111 (no. 5, pt. 2): 58a. MacCoubrey, I.C., Moore, P.L., and Haugland, R.P. 1990. *Journal of Cell Biology* **No. 5, pt.2,** 58a (1990).
236. Geijtenbeek, T. B. H. & Gringhuis, S. I. Signalling through C-type lectin receptors: shaping immune responses. *Nat Rev Immunol* **9,** 465–479 (2009).
237. Li, Q., Anver, M. R., Li, Z., Butcher, D. O. & Gildersleeve, J. C. GalNAc?1-3Gal, a new prognostic marker for cervical cancer. *Int J Cancer* **126,** 459–468 (2010).
238. Oyelaran, O., Li, Q., Farnsworth, D. & Gildersleeve, J. C. Microarrays with Varying Carbohydrate Density Reveal Distinct Subpopulations of Serum Antibodies. *Journal of Proteome Research* **8,** 3529–3538 (2009).
239. Van Die, I. *et al.* The Dendritic Cell–specific C-Type Lectin DC-SIGN Is a Receptor for Schistosoma Mansoni Egg Antigens and Recognizes the Glycan Antigen Lewis X. *Glycobiology* **13,** 471–478 (2003).
240. Hsu, S.-C. *et al.* Functional Interaction of Common Allergens and a C-Type Lectin Receptor, Dendritic Cell-Specific ICAM3-Grabbing Non-Integrin (DC-SIGN), on Human Dendritic Cells. *J. Biol. Chem.* **285,** 7903–7910 (2010).
241. Köhn, M., Benito, J. M., Ortiz Mellet, C., Lindhorst, T. K. & García Fernández, J. M. Functional Evaluation of Carbohydrate-Centred Glycoclusters by Enzyme-Linked Lectin Assay: Ligands for Concanavalin A. *ChemBioChem* **5,** 771–777 (2004).
242. Muckerheide, A., Apple, R. J., Pesce, A. J. & Michael, J. G. Cationization of protein antigens. I. Alteration of immunogenic properties. *J. Immunol.* **138,** 833–837 (1987).
243. Damme, E. J. M. V., Peumans, W. J., Pusztai, A. & Bardocz, S. *Handbook of Plant Lectins: Properties and Biomedical Applications*. (John Wiley & Sons, 1998).
244. Shankar, S. P., Chen, I. I., Keselowsky, B. G., García, A. J. & Babensee, J. E. Profiles of carbohydrate ligands associated with adsorbed proteins on self-assembled monolayers of defined chemistries. *Journal of Biomedical Materials Research Part A* **92A,** 1329–1342 (2010).
245. Cantarero, L. A., Butler, J. E. & Osborne, J. W. The adsorptive characteristics of proteins for polystyrene and their significance in solid-phase imunoassays. *Anal. Biochem.* **105,** 375–382 (1980).
246. Johnson, T. R., McLellan, J. S. & Graham, B. S. Respiratory Syncytial Virus Glycoprotein G Interacts with DC-SIGN and L-SIGN To Activate ERK1 and ERK2. *J Virol* **86,** 1339–1347 (2012).
247. Ribeiro, S. *et al.* Cell-surface carbohydrates of Entamoeba invadens. *Parasitology Research* **83,** 801–805 (1997).
248. Feinberg, H., Castelli, R., Drickamer, K., Seeberger, P. H. & Weis, W. I. Multiple Modes of Binding Enhance the Affinity of DC-SIGN for High Mannose N-Linked

Glycans Found on Viral Glycoproteins. *Journal of Biological Chemistry* **282,** 4202 – 4209 (2007).
249. Chapman, A., Trowbridge, I. S., Hyman, R. & Kornfeld, S. Structure of the lipid-linked oligosaccharides that accumulate in class E Thy-1-negative mutant lymphomas. *Cell* **17,** 509–515 (1979).
250. Chapman, A., Fujimoto, K. & Kornfeld, S. The primary glycosylation defect in class E Thy-1-negative mutant mouse lymphoma cells is an inability to synthesize dolichol-P-mannose. *J. Biol. Chem.* **255,** 4441–4446 (1980).
251. Trowbridge, I. S. & Hyman, R. Abnormal lipid-linked oligosaccharides in class E thy-1-negative mutant lymphomas. *Cell* **17,** 503–508 (1979).
252. Adams, E. W., Ratner, D. M., Seeberger, P. H. & Hacohen, N. Carbohydrate-Mediated Targeting of Antigen to Dendritic Cells Leads to Enhanced Presentation of Antigen to T Cells. *ChemBioChem* **9,** 294–303 (2008).
253. Lee, S. J. *et al.* Mannose Receptor-Mediated Regulation of Serum Glycoprotein Homeostasis. *Science* **295,** 1898 –1901 (2002).
254. Wang, S.-K. *et al.* Targeting the carbohydrates on HIV-1: Interaction of oligomannose dendrons with human monoclonal antibody 2G12 and DC-SIGN. *Proc. Natl. Acad. Sci. U.S.A* **105,** 3690–3695 (2008).
255. Lodowska, J. *et al.* The Chemical Composition of Endotoxin Isolated from Intestinal Strain of Desulfovibrio desulfuricans. *ScientificWorldJournal* **2012,** (2012).
256. Harn, D. A., McDonald, J., Atochina, O. & Da'dara, A. A. Modulation of host immune responses by helminth glycans. *Immunological Reviews* **230,** 247–257 (2009).
257. Dam, T. K. & Brewer, F. C. Maintenance of Cell Surface Glycan Density by Lectin–glycan Interactions: A Homeostatic and Innate Immune Regulatory Mechanism. *Glycobiology* **20,** 1061–1064 (2010).
258. Singh, N., Karim, A., Bates, F., Tirrell, M. & Furusawa, K. Adsorption of end-functionalized polystyrene on model textured surfaces. *Macromolecules* **27,** 2586–2594 (1994).
259. Pellicane, G., Costa, D. & Caccamo, C. Phase coexistence in a DLVO model of globular protein solutions. *J. Phys.: Condens. Matter* **15,** 375 (2003).
260. Zhou, X. *et al.* Controlled release of PEI/DNA complexes from mannose-bearing chitosan microspheres as a potent delivery system to enhance immune response to HBV DNA vaccine. *J Control Release* **121,** 200–207 (2007).
261. Hamdy, S., Haddadi, A., Shayeganpour, A., Samuel, J. & Lavasanifar, A. Activation of Antigen-Specific T Cell-Responses by Mannan-Decorated PLGA Nanoparticles. *Pharmaceutical Research* **28,** 2288–2301 (2011).
262. Li, Y.-P. *et al.* The regulatory role of dendritic cells in the immune tolerance. *Biomed Mater Eng* **16,** S163–170 (2006).
263. Dam, T. K. & Brewer, C. F. Lectins as Pattern Recognition Molecules: The Effects of Epitope Density in Innate Immunity*. *Glycobiology* **20,** 270–279 (2010).
264. Rabinovich, G. A. & Toscano, M. A. Turning 'sweet' on immunity: galectin-glycan interactions in immune tolerance and inflammation. *Nat Rev Immunol* **9,** 338–352 (2009).
265. Albeituni, S. H. & Yan, J. The Effects of β-Glucans on Dendritic Cells and Implications for Cancer Therapy. *Anticancer Agents Med Chem* (2012).

266. Bestman-Smith, J., Gourde, P., Désormeaux, A., Tremblay, M. J. & Bergeron, M. G. Sterically stabilized liposomes bearing anti-HLA-DR antibodies for targeting the primary cellular reservoirs of HIV-1. *Biochimica et Biophysica Acta (BBA) - Biomembranes* **1468,** 161–174 (2000).
267. Faraasen, S. *et al.* Ligand-Specific Targeting of Microspheres to Phagocytes by Surface Modification with Poly(L-Lysine)-Grafted Poly(Ethylene Glycol) Conjugate. *Pharm Res* **20,** 237–246 (2003).
268. Muckerheide, A., Domen, P. L. & Michael, J. G. Cationization of protein antigens. II. Alteration of regulatory properties. *J. Immunol.* **138,** 2800–2804 (1987).
269. Domen, P. L., Muckerheide, A. & Michael, J. G. Cationization of protein antigens. III. Abrogation of oral tolerance. *J. Immunol.* **139,** 3195–3198 (1987).
270. Apple, R. J., Domen, P. L., Muckerheide, A. & Michael, J. G. Cationization of protein antigens. IV. Increased antigen uptake by antigen-presenting cells. *J. Immunol.* **140,** 3290–3295 (1988).
271. Schalkwijk, J., van den Berg, W. B., van de Putte, L. B., Joosten, L. A. & van den Bersselaar, L. Cationization of catalase, peroxidase, and superoxide dismutase. Effect of improved intraarticular retention on experimental arthritis in mice. *J. Clin. Invest.* **76,** 198–205 (1985).
272. Taylor, P. R. *et al.* Dectin-1 is required for ?-glucan recognition and control of fungal infection. *Nat Immunol* **8,** 31–38 (2007).
273. O'Connor, R. S. *et al.* Substrate Rigidity Regulates Human T Cell Activation and Proliferation. *J Immunol* **189,** 1330–1339 (2012).
274. York, A. W., Kirkland, S. E. & McCormick, C. L. Advances in the synthesis of amphiphilic block copolymers via RAFT polymerization: Stimuli-responsive drug and gene delivery. *Advanced Drug Delivery Reviews* **60,** 1018–1036 (2008).
275. Crocker, P. R. & Varki, A. Siglecs, sialic acids and innate immunity. *Trends in Immunology* **22,** 337–342 (2001).
276. Anderson, D. G., Putnam, D., Lavik, E. B., Mahmood, T. A. & Langer, R. Biomaterial microarrays: rapid, microscale screening of polymer-cell interaction. *Biomaterials* **26,** 4892–4897 (2005).
277. Zhang, R., Liberski, A., Sanchez-Martin, R. & Bradley, M. Microarrays of over 2000 hydrogels - Identification of substrates for cellular trapping and thermally triggered release. *Biomaterials* **30,** 6193–6201 (2009).
278. Figdor, C. G. Molecular characterization of dendritic cells operating at the interface of innate or acquired immunity. *Pathol. Biol* **51,** 61–63 (2003).
279. Zou, T., Caton, A. J., Koretzky, G. A. & Kambayashi, T. Dendritic Cells Induce Regulatory T Cell Proliferation through Antigen-Dependent and -Independent Interactions. *J Immunol* **185,** 2790–2799 (2010).
280. Zheng, J., Liu, Y., Lau, Y.-L. & Tu, W. CD40-activated B cells are more potent than immature dendritic cells to induce and expand CD4+ regulatory T cells. *Cell Mol Immunol* **7,** 44–50 (2010).
281. Kubota, N., Ebihara, T., Matsumoto, M., Gando, S. & Seya, T. IL-6 and IFN-[alpha] from dsRNA-stimulated dendritic cells control expansion of regulatory T cells. *Biochemical and Biophysical Research Communications* **391,** 1421–1426 (2010).

282. Chung, D. J. *et al.* Indoleamine 2,3-dioxygenase-expressing mature human monocyte-derived dendritic cells expand potent autologous regulatory T cells. *Blood* **114,** 555–563 (2009).
283. Löb, S. & Königsrainer, A. Role of IDO in Organ Transplantation: Promises and Difficulties. *International Reviews of Immunology* **28,** 185–206 (2009).
284. Gil, M. *et al.* Targeting a Mimotope Vaccine to Activating Fc{gamma} Receptors Empowers Dendritic Cells to Prime Specific CD8+ T Cell Responses in Tumor-Bearing Mice. *J Immunol* **183,** 6808–6818 (2009).
285. Albert, M. L. *et al.* Immature dendritic cells phagocytose apoptotic cells via alphavbeta5 and CD36, and cross-present antigens to cytotoxic T lymphocytes. *J. Exp. Med* **188,** 1359–1368 (1998).
286. Anderson, A. E. *et al.* Differential regulation of naïve and memory CD4+ T cells by alternatively activated dendritic cells. *J. Leukoc. Biol* **84,** 124–133 (2008).
287. Benwell, R. K., Hruska, J. E., Fritsche, K. L. & Lee, D. R. Double stranded RNA-relative to other TLR ligand-activated dendritic cells induce extremely polarized human Th1 responses. *Cellular Immunology* **264,** 119–126 (2010).
288. Sakuraba, A. *et al.* Th1/Th17 Immune Response Is Induced by Mesenteric Lymph Node Dendritic Cells in Crohn's Disease. *Gastroenterology* **137,** 1736–1745 (2009).
289. Cao, D.-Y., Yang, J.-Y., Dou, K.-F., Ma, L. & Teng, Z.-H. [alpha]-Fetoprotein and Interleukin-18 Gene-Modified Dendritic Cells Effectively Stimulate Specific Type-1 CD4- and CD8-Mediated T-Cell Response from Hepatocellular Carcinoma Patients in Vitro. *Human Immunology* **68,** 334–341 (2007).
290. Wells, J. W. *et al.* Semi-allogeneic dendritic cells can induce antigen-specific T-cell activation, which is not enhanced by concurrent alloreactivity. *Cancer Immunol Immunother* **56,** 1861–1873 (2007).
291. Canaday, D. H. *et al.* T-cell hybridomas from HLA-transgenic mice as tools for analysis of human antigen processing. *Journal of Immunological Methods* **281,** 129–142 (2003).
292. Met, Ö., Buus, S. & Claesson, M. H. Peptide-loaded dendritic cells prime and activate MHC-class I-restricted T cells more efficiently than protein-loaded cross-presenting DC. *Cellular Immunology* **222,** 126–133 (2003).
293. Poncet, P., Arock, M. & David, B. MHC class II-dependent activation of CD4+ T cell hybridomas by human mast cells through superantigen presentation. *Journal of Leukocyte Biology* **66,** 105 –112 (1999).
294. Foung, S. K., Sasaki, D. T., Grumet, F. C. & Engleman, E. G. Production of functional human T-T hybridomas in selection medium lacking aminopterin and thymidine. *Proc Natl Acad Sci U S A* **79,** 7484–7488 (1982).
295. Fox, F. E. & Platsoucas, C. D. Human T-T cell hybridomas: development and applications. *Hum. Antibodies Hybridomas* **1,** 3–9 (1990).
296. Janeway, C. A. & Medzhitov, R. Innate immune recognition. *Annu. Rev. Immunol* **20,** 197–216 (2002).
297. Ratner, D. M., Plante, O. J. & Seeberger, P. H. A Linear Synthesis of Branched High-Mannose Oligosaccharides from the HIV-1 Viral Surface Envelope Glycoprotein gp120. *European Journal of Organic Chemistry* **2002,** 826–833 (2002).

298. De Leoz, M. L. A. *et al.* Lacto-N-Tetraose, Fucosylation, and Secretor Status Are Highly Variable in Human Milk Oligosaccharides From Women Delivering Preterm. *J. Proteome Res.* **11,** 4662–4672 (2012).
299. DeBose-Boyd, R., Nyame, A. K. & Cummings, R. D. Schistosoma mansoni:Characterization of an α1–3 Fucosyltransferase in Adult Parasites. *Experimental Parasitology* **82,** 1–10 (1996).
300. Sarrats, A. *et al.* Glycan Characterization of PSA 2-DE Subforms from Serum and Seminal Plasma. *OMICS* **14,** 465–474 (2010).
301. Samsen, A. *et al.* DC-SIGN and SRCL bind glycans of carcinoembryonic antigen (CEA) and CEA-related cell adhesion molecule 1 (CEACAM1): recombinant human glycan-binding receptors as analytical tools. *European Journal of Cell Biology* **89,** 87–94 (2010).
302. Ueda, K. *et al.* Development of serum glycoproteomic profiling technique; simultaneous identification of glycosylation sites and site-specific quantification of glycan structure changes. *Mol. Cell Proteomics* **9,** 1819–1828 (2010).
303. Tateno, H. *et al.* Dual specificity of Langerin to sulfated and mannosylated glycans via a single C-type carbohydrate recognition domain. *J. Biol. Chem* **285,** 6390–6400 (2010).
304. Narimatsu, H. *et al.* A strategy for discovery of cancer glyco-biomarkers in serum using newly developed technologies for glycoproteomics. *FEBS J* **277,** 95–105 (2010).
305. Berk, P. & Korenblat, K. in *Cecil Medicine* (Elsevier, 2008).
306. Omenn, G. S. *et al.* Overview of the HUPO Plasma Proteome Project: results from the pilot phase with 35 collaborating laboratories and multiple analytical groups, generating a core dataset of 3020 proteins and a publicly-available database. *Proteomics* **5,** 3226–3245 (2005).
307. Anderson, N. L. Counting the Proteins in Plasma. *Clin Chem* (2010). doi:10.1373/clinchem.2010.146167
308. Coyne, E., Messmore, H. L., Walenga, J. M., Fareed, J. & Wehrmacher, W. H. Ethylenediaminetetraacetic acid (EDTA) in heparin. *Thromb. Res* **90,** 245–246 (1998).
309. Li, C. *et al.* Pancreatic Cancer Serum Detection Using a Lectin/Glyco-Antibody Array Method. *Journal of Proteome Research* **8,** 483–492 (2009).
310. Patwa, T. H., Zhao, J., Anderson, M. A., Simeone, D. M. & Lubman, D. M. Screening of Glycosylation Patterns in Serum Using Natural Glycoprotein Microarrays and Multi-Lectin Fluorescence Detection. *Analytical Chemistry* **78,** 6411–6421 (2006).
311. Itoh, N. *et al.* Analysis of N-glycan in serum glycoproteins from db/db mice and humans with type 2 diabetes. *Am J Physiol Endocrinol Metab* **293,** E1069–1077 (2007).
312. Ge, G. *et al.* Induction of CD4+ CD25+ Foxp3+ T regulatory cells by dendritic cells derived from ILT3 lentivirus-transduced human CD34+ Cells. *Transplant Immunology* **26,** 19–26 (2012).
313. Penna, G. *et al.* Expression of the inhibitory receptor ILT3 on dendritic cells is dispensable for induction of CD4+Foxp3+ regulatory T cells by 1,25-dihydroxyvitamin D3. *Blood* **106,** 3490–3497 (2005).

314. Norian, L. A. *et al.* Tumor-infiltrating regulatory dendritic cells inhibit CD8+ T cell function via L-arginine metabolism. *Cancer Res* **69,** 3086–3094 (2009).
315. Carlin, A. F. *et al.* Molecular mimicry of host sialylated glycans allows a bacterial pathogen to engage neutrophil Siglec-9 and dampen the innate immune response. *Blood* **113,** 3333–3336 (2009).
316. Yuen, C.-T., Gee, C. K. & Jones, C. High-performance liquid chromatographic profiling of fluorescent labelled N-glycans on glycoproteins. *Biomedical Chromatography* **16,** 247–254 (2002).
317. Xia, B. *et al.* Versatile fluorescent derivatization of glycans for glycomic analysis. *Nat Meth* **2,** 845–850 (2005).
318. Suenaga, T., Schutz, C. & Nakata, T. A real time reaction monitoring using fluorescent dansyl group as a solid-phase leaving group. *Tetrahedron Letters* **44,** 5799–5801 (2003).